Dissertation
submitted to the
Combined Faculties of the Natural Sciences and Mathematics
of the Ruperto-Carola-University of Heidelberg, Germany
for the degree of
Doctor of Natural Sciences

Put forward by
Oskar Till
born in Stockholm, Sweden
Examination date: May 4, 2016

Discrete structures in F-theory compactifications

First referee: Prof. Timo Weigand
Second referee: Prof. Jörg Jäckel

Zusammenfassung

In dieser Doktorarbeit werden die globalen Eigenschaften der F-Theorie auf Calabi-Yau Faserungen untersucht. Dies wird sowohl durch phänomenologische Aspekte als auch das tiefere Verständnis von F-theorie Vakua begründet. Im Folgenden werden Faserungen von elliptischen Kurven und Genus-eins Kurven behandelt. Die globalen geometrischen Charakteristika entstehen aus diskreten und arithmetischen Eigenschaften der Faser. Diese können in Faserungen über eine generische Basis untersucht werden.

Im ersten Teil analysieren wir die Rolle der Torsionsuntergruppe der Mordell-Weil Gruppe von Schnitten in vierdimensionalen Kompaktifizierungen. Es wird gezeigt, wie ein Torsionselement die möglichen Materiendarstellungen der Eichtheorie beschränkt. Dies ist äquivalent zur Entstehung einer nicht-trivialen Fundamentalgruppe der Eichgruppe.

Diskrete Symmetriegruppen treten in der F-Theorie durch Kompaktifizierungen auf Torusfaserungen auf. Die diskrete Gruppe ist in der Feldtheorie eine gebrochene $U(1)$ Symmetrie und der Higgs-Mechanismus entspricht einer Deformation in der Geometrie. Es wird im Detail erklärt, wie die diskrete Symmetriegruppe aus zwei verschiedenen Phasen in der M-Theorie entsteht. Dazu wird die Relation zu den homologischen Torsionsuntergruppen der Mannigfaltigkeit beschrieben. Das letzte Kapitel beschäftigt sich mit einer systematischen Konstruktion von Eichflüssen auf Torusfaserungen. Es wird gezeigt, dass das chirale Spektrum frei von Anomalien ist.

Abstract

In this thesis we study global properties of F-theory compactifications on elliptically and genus-one fibered Calabi-Yau varieties. This is motivated by phenomenological considerations as well as by the need for a deeper understanding of the set of consistent F-theory vacua. The global geometric features arise from discrete and arithmetic structures in the torus fiber and can be studied in detail for fibrations over generic bases.

In the case of elliptic fibrations we study the role of the torsion subgroup of the Mordell-Weil group of sections in four dimensional compactifications. We show how the existence of a torsional section restricts the admissible matter representations in the theory. This is shown to be equivalent to inducing a non-trivial fundamental group of the gauge group.

Compactifying F-theory on genus-one fibrations with multisections gives rise to discrete selection rules. In field theory the discrete symmetry is a broken $U(1)$ symmetry. In the geometry the higgsing corresponds to a conifold transition. We explain in detail the origin of the discrete symmetry from two different M-theory phases and put the result into the context of torsion homology. Finally we systematically construct consistent gauge fluxes on genus-one fibrations and show that these induce an anomaly free chiral spectrum.

Acknowledgements

<div align="right">

Oskar Till
February 2016, Heidelberg

</div>

Contents

Chapter 1

Introduction

The study of fundamental interactions in theoretical as well as experimental physics relies heavily on the notion of a point particle. The fundamental particles of the Standard Model have no detected size and are described as mathematical points. Likewise their interactions are described in terms of sharp vertices where the propagating particles meet. The reason for this description of fundamental particles is that it works exceedingly well. Quantum field theory, the marriage of special relativity and quantum mechanics, has a spectacular history of explaining experimental results and of successful predictions of new particles and phenomena. The inclusion of gauge symmetries leads to the framework of Yang-Mills theory, of which the Standard Model is the front example. With the inclusion of the recently found Higgs particle the Standard Model provides a detailed description of the fundamental interactions that can be tested, in some cases to a very high precision. Despite the success of the Standard Model it can not be a complete description of particle physics. Observables such as particle masses and charges receive quantum corrections which are divergent. Nevertheless these observables may be computed because the Standard Model is renormalisable. Through the technique of renormalisation the infinites can be absorbed and give finite results, i.e renormalised quantitites, which can be compared to measured values. This introduces a cut-off energy up to which the computations are valid and above this scale these calculations can not be trusted. Renormalisation is a tool that allows for the extraction of finite observables up to a certain scale but implies that above that scale we lack an understanding of the physics.

Einstein gravity, which is a classical field theory, also has an associated point quantum, the graviton. Due to the fact that the gravitational coupling is so small compared to the electro-weak and strong coupling constants it is not observed. In any quantum theory of gravity this particle must exist, at least as a first approximation. It is also clear that quantum gravity plays a role in nature since there exist processes in nature where strong gravitational interaction is present at distances so short that a quantum description is needed. The early universe and black hole interiors are maybe the most obvious examples. General relativity is based on the assumption of a smooth spacetime geometry where the gravitational force on matter and radiation arises from the spacetime curvature, which itself is sourced by matter and energy. The incompleteness of general relativity alone can be seen by considering the formation of a black hole. When a massive object collapses under its own gravitational attraction, the Einstein field equations drive the system towards a singularity at the center of the black hole. Thus the result of the collapse of initially well understood conditions is a solution which breaks the basic assumption of a smooth spacetime. At the singularity, where the mass- and energy density approaches infinity, one expects a quantum theory of gravity to take over and to resolve this apparent singularity. However, by approaching a quantum theory of gravity through the framework of quantum field theory one immediately encounters problems with infinities. As opposed to Yang-Mills theory general relativity is not perturbatively renormalisable and correlation functions involving gravitons

have divergences that can not be cancelled by a finite number of counter-terms order by order in perturbation theory.

String theory (e.g [1–5] and references therein) provides an ultra-violet completion of Yang-Mills theory and gravity and does so by leaving the realm of point particles as fundamental entities. In essence string theory is the quantized theory of a one-dimensional string propagating in spacetime. From the beginning general covariance in spacetime and quantum mechanics are included and by demanding a consistent quantization of the string a constrained and also remarkably rich theory is obtained. In particular the quantization implies that the spacetime target space of the superstring[1] has ten dimensions. As the string propagates in spacetime general covariance implies that quantized string modes transform as representations of the spacetime symmetry group. From the spacetime perspective we can hence identify the different modes of the string as scalars, spinors and tensors under the Lorentz group. In the low energy limit the string length is negligible and the string states are the particles of the effective quantum field theory. The introduction of the string as the fundamental object implies that there are two different cases to be considered. A string can be closed, sharing its topology with a circle, or it can be an open interval. Among the modes of the open string there is always a massless spin two excitation which is identified with the graviton. Open strings on the other hand always have a massless vector with gauge symmetry in the spectrum, that is, the building block of Yang-Mills theory. A string theory with open strings necessarily has also closed strings, which makes the unification of Yang-Mills theory and gravity unavoidable. This is contrasted to the incompatibility of Yang-Mills theory and gravity as fundamental descriptions of nature.

In the long wavelength limit of string theory the size of the string cannot be resolved and is effectively described as a point particle. This is expected since any sensible ultra-violet completion must reduce to the well established Standard Model in the limit of low energies. At distances comparable to the string length the point particle description breaks down and the strings are resolved. In this high energy regime correlation functions between particles turn into correlation functions of strings. The world-lines of propagating particles get resolved to world-sheets of propagating strings and the interaction vertices get replaced by smooth surfaces joining the string world-sheets. The foremost consequence of this is that correlation functions of strings are finite and no divergences appear. String theory is thus finite in the ultra-violet limit and provides a completion of particle physics that is valid at all energies.

There are five different formulations of string theory named type I, type IIA, type IIB, heterotic $E_8 \times E_8$ and heterotic $SO(32)$. They are all related through duality transformations. This web of dualities include also the eleven dimensional supergravity, which is the low energy limit of M-theory, an eleven dimensional theory coupled to branes. The five string theories and the 11D supergravity can be seen as different perturbative limits of M-theory. In general the dualities between the different formulations exchange strong and weak coupling. In other words, the perturbative expansion and the fundamental degrees of freedom are not the same in two dual formulations. The strings of any chosen formulation are approximated in the low energy, or long wavelength limit by point particles. The point particle theory corresponding to each string theory formulation is the supergravity with the same name, e.g the ten-dimensional type IIB supegravity. The field content of the supergravity comes from the massless modes of the strings.

The strings propagate in a Lorentzian manifold with ten dimensions. If the theory is to be considered as an ultra-violet completion of particle physics this calls for an explanation. After all we only observe four spacetime dimensions. The connection of string theory to four dimensional particle physics and gravity is made by the concept of compactification. This amounts to solutions of string theory where the target space has the form $M_{1,3} \times X_6$ where $M_{1,3}$ is the Lorentzian manifold in which

---

[1]Supersymmetry on the worldsheet of the string is necessary to have a stable vacuum and fermions in spacetime.

we live and do experiments. X_6 is a compact manifold with six dimensions and as it is compact it has a finite volume. The compactification to four dimensions is the limit in which the volume is negligible from a four-dimensional perspective. The field components along the compact directions are integrated out, leaving an effective theory on $M_{1,3}$. All four-dimensional particles, or fields, have their origin in the ten-dimensional theory, satisfying ten-dimensional equations of motion. The equations of motion for the massless modes take the form of Laplace and Dirac equations and their solutions are classified by the topology of the compact space X_6. For a fixed topology of X_6 there are generally many deformations of the geometry. These are parametrised by the components of the metric of X_6 and appear as parameters (scalar vacuum expectation values) of the effective theory in four dimensions. This means that a compactification on X_6 allows for the study of a large class of quantum field theories sharing the features dictated by the topology. The scalar deformations do moreover appear as massless scalars after compactification, and a potential that gives them masses has to be generated. This is the problem of moduli stabilization, which we will not comment further on in this thesis.

This thesis is devoted to the study of a framework of compactifications called F-theory [6–8]. These compactifications interpolate between type IIB string theory with branes, weakly coupled heterotic $E_8 \times E_8$ theory and M-theory. In this thesis we will discuss F-theory and its relation to type IIB string theory and M-theory. F-theory compactifications are attractive from a number of viewpoints and we mention here a few on which we will elaborate in the following. First, from the perspective of type IIB theory F-theory is the generalisation to any value of the string coupling. By geometrising the type IIB compactification data a much larger set of solutions can be studied, including features that do not appear in perturbative type IIB string theory. Secondly, the geometrization of the type IIB data has computational virtues. F-theory compactifications can be studied with powerful mathematical methods from complex algebraic geometry. This way complicated dynamical type IIB systems can be analysed by comparably simple geometric and topological calculations. In many cases special software is available and can be utilized to a high degree. Finally we mention here that F-theory models can be studied at a high degree of generality. The details of the F-theory background geometry implies that large families of effective gauge theories can be studied without specifying all free parameters. F-theory is thus well suited for adressing questions about generic features of gauge theories that come from string compactifications.

In type IIB string theory four dimensional gauge theories are constructed by supplementing the compactification with so called D-branes. They are higher dimensional analogues of strings which wrap submanifolds of the spacetime. Open strings end on the branes and are the source of gauge bosons in type IIB string theory. In the perturbative theory classical gauge groups can be constructed this way. On the other hand, no exceptional Lie groups can arise from perturbative D-branes. By leaving the weakly coupled regime new objects appear which are generalisations of the fundamental string and the D-branes. F-theory is a framework in which all types of branes are treated on equal footing and is in this way the generalisation of type IIB to any value of the string coupling.

F-theory can also be defined through the eleven-dimensional M-theory. To obtain a four-dimensional theory M-theory is compactified on an eight-dimensional manifold which results in a three-dimensional gauge theory. Through what is called the F-theory limit one of the compact directions is decompactified and a four dimensional gauge theory is obtained. In M-theory there are no open strings and instead the gauge bosons and matter states arise from M2-branes that wrap different submanifolds in the compactification geometry. From this point of view F-theory models are a subset of all M-theory compactifications, i.e they correspond to the manifolds that allow for the F-theory limit to be taken. The four dimensional theory obtained from M-theory is dual to the IIB compactification with branes. This is of great importance, as F-theory models that correspond to strongly coupled type IIB theory can be studied through M-theory.

The study of F-theory compactifications is centered around the complex geometry of Calabi-Yau manifolds. As these are complex spaces they are of even real dimension and a multitude of examples can be constructed with suitable topologies. By representing the Calabi-Yau manifolds as hypersurfaces in toric varieties powerful tools and theorems from algebraic geometry apply and allow for computations of geometric and topological data. The same mathematical tools apply for the compactification geometry, regardless of whether the corresponding type IIB model is at weak coupling. It follows that F-theory compactifications are not only in principle the strong coupling generalisation of type IIB theory, but also in practical model building.

Here we also remark that the correspondence between geometry and gauge theory in F-theory is a fascinating and beautiful one. The mathematics of F-theory compactifications has its origins in number theory, complex algebraic geometry and singularity theory. The introduction of F-theory as the strong coupling limit of type IIB string theory is a geometrisation of a modular symmetry in the underlying string theory. Since the introduction of F-theory the understanding of this geometry has developed, and with an ever increasing level of detail and abstraction the correspondence between geometry and gauge theories in various dimensions unveils.

Throughout this thesis we will study numerous explicit geometries. Constructing an F-theory model typically starts by choosing a representation of a smooth Calabi-Yau manifold embedded in an ambient toric variety. By carefully modifying the geometry one introduces singularities as a particular limit of the smooth space. As we will go through in detail in the next chapter the singularities are associated to the gauge theory data of the compactification. The gauge algebra, matter representation content and Yukawa couplings all arise from the singularity structure and can be explicitly computed. By compactifying F-theory on Calabi-Yau manifolds of 4, 6, 8 and 10 real dimensions one obtains gauge theories in 8, 6, 4 and 2 dimensions respectively. These gauge theories are all coupled to gravity and have an ultra-violet completion in string/M-theory. Importantly, when compactifying F-theory on a Calabi-Yau manifold one obtains not only one gauge theory with a certain gauge symmetry and matter spectrum but a large family of theories. The deformations of the Calabi-Yau that preserve the topology and singularity structure are all parameters of the effective gauge theory. Therefore one can use F-theory to study generic properties of gauge theories with certain specified characteristics.

The geometric origin of the gauge theory data and the underlying string theory makes F-theory interesting from a model building perspective, for example in grand unified theories (GUTs). The problem of doublet-triplet splitting of the unified Higgs field and how to break the GUT symmetry to the Standard Model gauge group are not easy to solve in field theory. By embedding the GUT model into an F-theory compactification solutions to these problems can be searched for in a geometric way. Doublet-triplet splitting can in this case be adressed in the geometric origin of the Higgs field and the breaking of $SU(5)$ to the Standard Model gauge group has a topological solution through the introduction of gauge flux.

The main problem of $SU(5)$ GUT models is proton decay operators. In a pure $SU(5)$ GUT model there are dimension four operators that make the proton unstable unless supressed or forbidden. One way to solve this problem is by introducing a selection rule, an abelian continuous or discrete symmetry. The matter fields are charged under this symmetry such that the proton decay operators are forbidden. Non-abelian gauge symmetries in F-theory have been understood for a long time and are related to local geometric data in the compactification. These can be studied even in the absence of a full global description of the compactification geometry. Additional $U(1)$ symmetries on the other hand have their origin in global geometric properties, and for this reason they were only studied and understood in detail more recently. Discrete symmetries are related to $U(1)$ symmetries and the subject of some of the most recent developments in F-theory.

This thesis is concerned with global geometric properties of F-theory compactifications. More

specifically the discrete and arithmetic properties of tori and elliptic curves, which are essential ingredients in any F-theory background. The global structure of gauge theories i.e the topology of the gauge group is determined by certain rational points on the elliptic curve. The study of such rational points is an important subject in number theory and algebraic geometry and we can put this theory in the context of gauge theory. The gauge algebra does not alone determine the global topology of the actual gauge group. By considering so called torsional rational points of the elliptic curve we determine the gauge group corresponding to the gauge algebra induced by the singularities. At the same time we show how the matter spectrum restricts to the irreducible representations that transform under the full gauge group.

The study of discrete symmetries in F-theory was initiated recently by the discovery that F-theory can be compactified on a wider class of manifolds than previously considered. This new class of geometries gives rise to discrete symmetries in the effective field theory upon compactification. In string theory discrete symmetries always arise as broken gauge symmetries. By considering a pair of F-theory models, one with a discrete $\mathbb{Z}_2$ symmetry and one with a $U(1)$ gauge symmetry we show the geometric manifestation of the spontaneous symmetry breaking as a geometric deformation. This involves subtle details in the relation between M-theory in, say, three dimensions and F-theory in four dimensions. Depending on how the geometric deformation is performed different M-theory compactifications arise, which however share the same F-theory limit. In string theory compactifications discrete symmetries are known to correspond to topological invariants known as torsion homology groups. We explain in this thesis the link between torsion homology and discrete symmetries in F-theory.

All models and examples studied in the work underlying this thesis are compact and global Calabi-Yau manifolds represented as hypersurfaces in toric varieties. By use of the software packages SAGE and `Singular` computations of all relevant topological data can be performed. This is done in full generality, valid for large topological classes of geometries. The results hence apply to families of gauge theories rather than single examples.

This thesis is organised as follows: In chapter 2 we introduce F-theory from the type IIB perspective. The need for a consistent and controlled description of the theory when the string coupling grows leads us to F-theory as a geometrisation of the symmetries and the states in type IIB string theory. To understand the geometry we introduce tori, elliptic curves and fibrations of these. Since singularities play a central role in F-theory we turn to describe singularities of tori and torus fibrations. With the background geometry in place we introduce the duality of F-theory with M-theory and describe how gauge symmetries, charged massless matter and couplings have their origin in the structure of the fibration. Finally we introduce fluxes in F-theory compactification which are necessary for, among other things, a chiral matter spectrum.

In chapter 3 we discuss the difference between gauge algebra and gauge symmetry in F-theory [9]. The main object of study in this chapter is the torsion subgroup of the Mordell-Weil group. We show how the presence of an element in this subgroup affects the matter spectrum of the model. All possible matter states in the representations of a Lie algebra are summarized in the weight lattice of the algebra. Mordell-Weil torsion makes this lattice coarser, projecting out all states which are not in representations also of the gauge group. The general theory is exemplified through a number explicit fibrations where the gauge symmetry and the matter content are studied in detail.

In chapter 4 we study F-theory on genus-one fibrations. We show [10] how an F-theory compactification on a genus-one fibration with a bisection results in a four dimensional theory with a $\mathbb{Z}_2$ selection rule. Central in the analysis is the conifold transition, which relates the genus-one fibration to an F-theory model with an extra $U(1)$ gauge symmetry. We show how the discrete symmetry is the remnant of this $U(1)$ symmetry after higgsing by a field with charge 2. The higgsing in field theory is a geometric deformation in F-theory. We pay extra attention to the details of the lift from

M-theory in three dimensions to F-theory in four dimensions. We find that there are two different conifold transitions resulting in two different M-theory compactifications, and how these two theories have the same four-dimensional limit. The relation to torsion homology is demonstrated in detail [11]. The discrete symmetry as a selection rule is demonstrated through explicit models with an additional $SU(5)$ gauge group. Indeed all geometrically realised Yukawa couplings are shown to be singlets under the $\mathbb{Z}_2$ symmetry.

In chapter 5 we study fluxes in F-theory models with discrete symmetries [12]. We generalise the consistency conditions for fluxes from elliptic fibrations to genus-one fibrations. In the model with $SU(5) \times Z_2$ symmetry from chapter 4 we then put the consistency conditions to test. By systematically constructing all gauge fluxes in the genus-one fibration we show that the fluxes obeying the consistency conditions induce an anomaly free chiral spectrum. Furthermore, by constructing all gauge fluxes also in the model with $U(1)$ symmetry we show how the fluxes rearrange in the conifold transition so that the anomalies vanish and the so called D3 tadpole does not change. Any flux solutions has to be properly quantized and we show how the properly quantized fluxes imply the vanishing of the discrete gauge anomalies.

Finally, in chapter 6 we summarise the results and discuss possible further directions of research.

Chapter 2

Physics and geometry of F-theory

To understand F-theory and how the gauge theory data it encodes arise from strings it is instructive to start with type IIB string theory with branes. We take the IIB supergravity as the starting point, and before introducing anything else we just consider the bosonic bulk fields.

The low energy limit of type IIB string theory is type IIB supergravity, where the field content is given by the massless modes of the IIB string. At first we consider the bulk fields coming from closed strings only and later we look at the open string sector and the branes. The fields from the NS-NS sector are the dilaton ϕ, the Kalb-Ramond two-form B_2 with field strength H_3 and the metric tensor field g. In addition there are the Ramond-Ramond form fields; the scalar C_0, and the ascending C_2 and C_4 fields. For each RR field, the corresponding field strength is denoted $F_{n+1} = dC_n$ and by Hodge duality with respect to the background metric $F_{10-n} = \star F_n$. In units where the string length $l_s = 2\pi\sqrt{\alpha'}$ is set to one the bosonic part of the lagrangian can be written [1] as

$$\mathcal{L} = \sqrt{-g}R - \frac{1}{2(\mathrm{Im}\tau)^2}d\tau \wedge \star d\bar{\tau} + \frac{1}{\mathrm{Im}\tau}G_3 \wedge \star d\bar{G}_3 + \frac{1}{2}\tilde{F}_5 \wedge \star\tilde{F}_5 + C_4 \wedge H_3 \wedge F_3 \tag{2.0.1}$$

for $G_3 = F_3 - \tau H_3$ and $\tilde{F}_5 = \star\tilde{F}_5 = F_5 - \frac{1}{2}C_2 \wedge H_3 + \frac{1}{2}B_2 \wedge F_3$. The two real scalar fields are combined into the complex scalar

$$\tau = C_0 + ie^{-\phi}. \tag{2.0.2}$$

The string coupling g_s is generated dynamically in string theory, as the expectation value $\langle e^\phi \rangle$, and thus the field τ may be regarded as a complexification of the string coupling. The classical theory has an $SL(2,\mathbb{R})$ symmetry, under which τ and the 2-form fields transform as

$$\tau \mapsto \frac{a\tau + b}{c\tau + d} \qquad \begin{pmatrix} C_2 \\ B_2 \end{pmatrix} \mapsto M \begin{pmatrix} C_2 \\ B_2 \end{pmatrix} = \begin{pmatrix} aC_2 + bB_2 \\ cC_2 + dB_2 \end{pmatrix} \tag{2.0.3}$$

and where $det\, M = ad - bc = 1$. In the quantized theory, this symmetry is broken to the $SL(2,\mathbb{Z})$ subgroup [13]. This can be seen by taking brane instantons into account. The $D(-1)$ instanton contribution to the partition function comes with a factor of $exp(2\pi i\tau)$. Invariance of this term under the $SL(2,\mathbb{R})$ transformation $\tau \mapsto \tau + b$ restricts b to an integer, implying that the symmetry is broken to $SL(2,\mathbb{Z})$. In type IIB there is also a parity symmetry which is generated by

$$(-1)^{F_L}\Omega \tag{2.0.4}$$

where F_L is the left-moving fermion number and Ω is the world-sheet parity. It acts on the bosonic fields as the $SL(2,\mathbb{Z})$ transformation

$$-\mathrm{id} = \begin{pmatrix} -1 & 0 \\ 0 & -1 \end{pmatrix}. \tag{2.0.5}$$

9
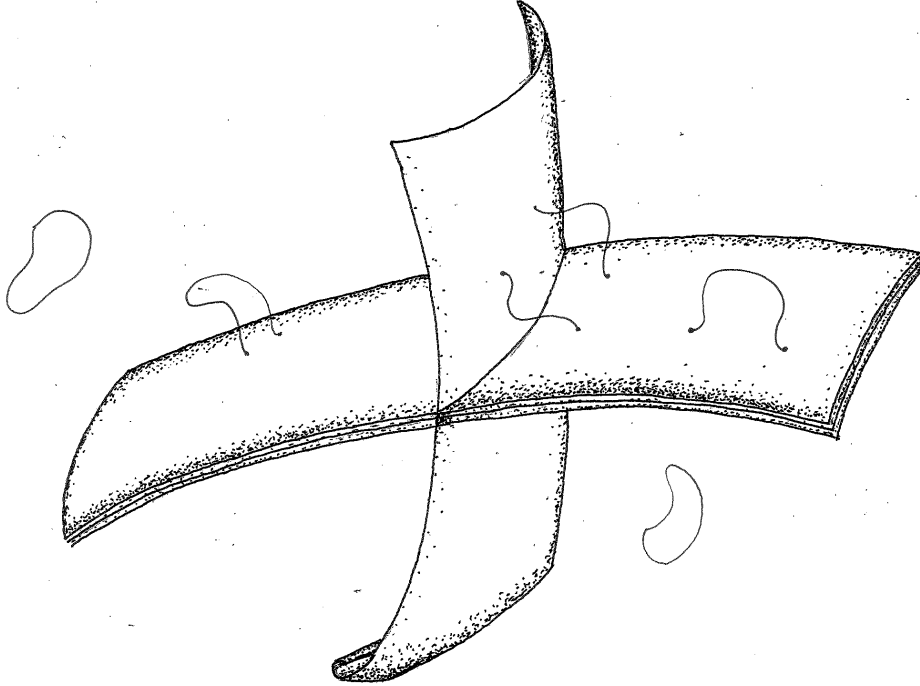
Figure 2.1: Gauge bosons arise from open strings propagating along a stack of branes. Strings strechting between two stacks give rise to charged states that become massless at the intersection of the branes.

Branes in string theory and field theory

Branes are extended, dynamical objects present in type II string theories and M-theory. In the low-energy perspective the branes are solutions of the supergravity theory, generalizing black hole solutions in four dimensions. The supergravity solutions are not only solutions for the metric g but include in general non-trivial profiles for the axio-dilaton τ and the form fields.

From the string theory perspective branes are submanifolds of the ten-dimensional background geometry on which open string modes are localised. In type II string theories boundary conditions have to be included for the embedding of the open strings in the target space. The Dirichlet boundary conditions specify a submanifold in spacetime on which open strings can end, or along which the open string states can propagate. A Dp-brane is such a submanifold where p is the number of spatial dimensions along the brane. In type IIB string theory, with which we will be concerned here, there are brane solutions for all odd p. This matches the RR field sector, as the even rank form fields C_{p+1} can be coupled to, i.e integrated over, the $p + 1$ dimensional world volumes of Dp branes.

As the open strings propagate only along the world-volume of the brane the modes of this string give rise to fields localised on the brane. The massless spectrum of the open string contains a vector field, and any massless vector field is a $U(1)$ gauge field [14]. For the single brane there is therefore a $U(1)$ gauge theory localized on the world-volume of the brane. For N parallel branes there are $U(1)$ vectors along each brane, and also open strings stretching between the branes. These give rise to massive vector states as their mass is proportional to the minimal length of the string. The IIB open string is oriented, and thus the number of vectors are N^2, which is the dimension of the adjoint representation of $U(N)$. However, at this point we only have the Cartan subgroup $U(1)^N$, since the states between the branes, corresponding to the W bosons of $U(N)$, are massive. Putting the N branes on top of each other the 'off-diagonal' vector states becomes massless and fill out the full adjoint of

$U(N)$, and there is a $U(N)$ gauge theory localized at the stack of branes[1].

Consider now a stack of $M+N$ branes on top of each other. The gauge group is $U(M+N)$ of the super-Yang-Mills theory on the stack. By rotating M branes we get two stacks of branes intersecting along a submanifold of one lower dimension, see fig. 2.1. The dimension of the adjoint representation may be rearranged as

$$(M+N)^2 \to M^2 + N^2 + 2MN \tag{2.0.6}$$

indicating the branching rule

$$ad_{U(M+N)} \to ad_{U(M)} + ad_{U(N)} + (M, \bar{N}) + (\bar{M}, N). \tag{2.0.7}$$

In this example the two brane stacks supports two gauge theories, with gauge groups $U(M)$ and $U(N)$, and they are coupled via bifundamental matter representations. The massless matter states arise at the intersection locus, where the constraint on the string length vanishes. As the matter string states stretch between the two stacks they are charged under both gauge groups. Including brane solutions in the supergravity amounts to coupling the gravity theory to localised gauge theories. In this case the action has to be supplemented by terms which are restricted to the world-volume D_p of the branes. Among these terms are the electric couplings

$$q_p \int_{\mathrm{D}p} C_{p+1} \tag{2.0.8}$$

of the RR fields to the brane. q_p denotes the brane charge. In particular, the field C_8 of type IIB theory couples electrically to the 8 dimensional world-volume of a D7-brane via the term

$$\mathcal{L} \supset \int_{D7} C_8 \tag{2.0.9}$$

and thus magnetically to the scalar C_0, since $dC_8 = \star dC_0$. The $D7$ brane is of special interest here since its spatial codimension equals two, and we can think of the branes as points on a two-dimensional surface transversal to the branes. Integrating dC_0 along a closed loop around the brane in the transversal space defines the magnetic charge of the brane, and introduces a monodromy on C_0, and subsequently on τ. Travelling around a brane the axiodilaton transforms as

$$\tau \to \tau + 1, \tag{2.0.10}$$

picking up one unit of magnetic charge (normalized to one). Encircling more than one brane will pick up more units of brane charge to the monodromy. This would lead to an unacceptable multivaluedness of the axio-dilaton, if it were not for the $SL(2, \mathbb{Z})$ symmetry of the theory. The action of this symmetry on the axio-dilation is through a linear fractional transformation (2.0.3), and any such transformation can be obtained by composition of the two generators

$$\begin{aligned} T &: \tau \mapsto \tau + 1 \\ S &: \tau \mapsto -\frac{1}{\tau}. \end{aligned} \tag{2.0.11}$$

The monodromy action by encircling a $D7$ brane is just a T-transformation. The T-generator acts only on the real part of the axiodilaton, leaving the string coupling untouched. The S-transformation on the other hand 'inverts' τ, and exchange strong and weak coupling. A weakly coupled type IIB model, is a setting where all monodromies are generated by T-transformations. We also note that the monodromy around a 7-brane transforms not only τ, but the background of two-form fields as well, as given in (2.0.3).

---

[1]In the string world-sheet theory, the open string end points carry Chan-Paton charges. In this language it can be shown rigorously how the massless vectors transform in the adjoint of $U(N)$.

7-branes at any coupling

We have seen that the perturbative $D7$ brane induces a monodromy transformation

$$\tau \to \tau + n \tag{2.0.12}$$

on the axiodilaton, with n the number of $D7$ branes on top of each other. This transformation is generated only by the T-generator of $SL(2, \mathbb{Z})$, and it is natural to ask about monodromies involving the S-generator of the modular group. Let us go back to the perturbative string in type IIB theory, and the relation to the modular transformations. The fundamental string, $F1$, couples electrically to the Kalb-Ramond field B_2 in the Polyakov action. There is also the $D1$ string ($D1$ brane), which couples electrically to the C_2 field, by integration the 2-form over the world sheet of the $D1$. Now, the B_2 and C_2 fields transform in a $SL(2, \mathbb{Z})$ doublet, as in (2.0.3) and the modular group rotates the field solutions into each other. A (p, q) string is defined as an one-dimensional object with p units of B_2 charge, and q units of C_2 charge. The fundamental string is a $(1, 0)$ string in this notation, and the $D1$ string a $(0, 1)$ string. In perturbative type IIB theory, there are only $(1, 0)$ strings as fundamental degrees of freedom (the $D1$ is a non-pertubative object). Away from the weak coupling limit, not restricting to T-monodromies, we define a (p, q) 7-brane as a hypersurface on which a (p, q) string can end. If all the branes are of the same (p, q) type, it is possible to choose a new $SL(2, \mathbb{Z})$ frame, in which all branes are $D7$ branes. However, if there are different types of (p, q) branes, not all of them can be described as perturbative $D7$ branes, and in this case they are called mutually non-local.

The element of the modular group which transforms a fundamental string into a (p, q)-string is $g_{p,q} = \begin{pmatrix} p & r \\ q & s \end{pmatrix}$. Using this matrix, one may represent the monodromy action of a general (p, q)-brane on the background as

$$M_{p,q} = g_{p,q} M_{1,0} g_{p,q}^{-1} = \begin{pmatrix} 1 - pq & p^2 \\ -q^2 & 1 + pq \end{pmatrix} \tag{2.0.13}$$

where $M_{1,0} = \begin{pmatrix} 1 & 1 \\ 0 & 1 \end{pmatrix}$ is a representative of the T-generator.

By allowing for the most general monodromies around 7-branes, we leave the weakly coupled IIB regime. This non-perturbative region of moduli space is populated by more general (p, q)-branes and allows for physics which cannot be described in the perturbative type IIB theory. One example is the occurence of exceptional gauge groups. F-theory is a framework which elegantly puts all monodromy effects and the gauge theory data into a geometric framework.

2.1   Fibrations for F-theory compactifications

In this section we review the geometric ingredients of an F-theory model. The identification of the axio-dilation with the complex structure of an auxiliary torus is the foundation of F-theory. Therefore we start by describing the torus and its relation to the modular symmetry group. We introduce the arithmetic of elliptic curves and the Mordell-Weil group of rational points. Then we move on to study families of tori corresponding to non-trivial axio-dilaton profiles. For further background on F-theory and compactifications we mention [13, 15, 16].

2.1.1   Tori and elliptic curves

Before describing the fibration structure of F-theory compactifications, we take some time to discuss a single fiber. A torus T^2, or a genus one complex curve in the language of Riemann surfaces, is topologically the product of two circles. The topological circle may be described as the quotient $\mathbb{R}/\mathbb{Z}$
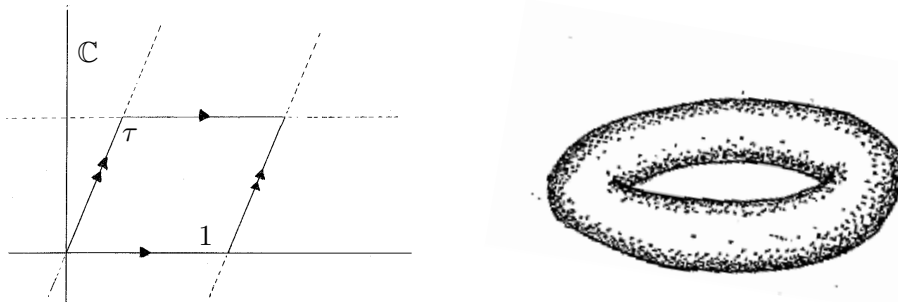
Figure 2.2: The torus T^2 as the quotient of $\mathbb{C}$ by the lattice generated by 1 and τ.

of the real line by a one-dimensional lattice. The real numbers modulo integer translations effectively roll up the real line to a circle. The torus is the product of two such circles, and thus $T^2 \approx \mathbb{R}^2/\Lambda$, where Λ is a two-dimensional lattice. This is the well known construction of the flat torus by identifying opposite sides of a parallellogram (see fig. 2.2). Treating the torus as a complex surface has the virtue of working in an algebraically closed field. We will be studying properties of special points on the torus, and the finding and counting of such points is facilitated by using complex equations. Furthermore, the tori will be embedded in higher-dimensional complex varieties, in which the compatibility of complex coordinates and the metric are dictated by the effective particle theories in four dimensions. In the complex setting the torus is given as the quotient

$$T^2 \approx \frac{\mathbb{C}}{\Lambda} \tag{2.1.1}$$

where Λ is a lattice isomorphic to $\mathbb{Z} \oplus i\mathbb{Z}$, and generated by any two complex numbers not lying on the same complex line. By rescaling and rotating the coordinates the generators of Λ can be taken to be 1 and $\tau \in \mathbb{C}$ (see fig. 2.2). The complex number τ is commonly referred to as the complex structure modulus of the torus. The freedom of changing the basis for the lattice implies that there is a modular action on the complex structure

$$\tau \mapsto \frac{a\tau + b}{c\tau + d}, \quad a, b, c, d \in \mathbb{Z}, \quad ad - bc = 1\,. \tag{2.1.2}$$

The linear fractional transformation preserves the lattice, and thus the torus itself. These transformations acting on the upper half plane generate the modular group, often denoted Γ. It is isomorphic to the projective special linear group $PSL(2, \mathbb{Z})$ of linear transformations, with unit determinant and modulo the parity action $M \to -M$ that puts each matrix and its negative in the same equivalence class [2]. In other words, the modular group acts on the moduli space of the flat torus. The modular group is generated by two elements,

$$T : \tau \mapsto \tau + 1, \qquad S : \tau \mapsto -\frac{1}{\tau} \tag{2.1.3}$$

obeying two relations, and has the presentation $\Gamma = \langle S, T | S^2 = \mathrm{id}, (ST)^3 = \mathrm{id} \rangle$ [17]. From the generators one can see that any τ can be mapped to a point in the fundamental region (see fig. 2.2) $\mathcal{F} : \{\tau | \, Im\,\tau > 0, |\tau| \geq 1, -\frac{1}{2} \leq Re\,\tau \leq \frac{1}{2}\}$, whose interior values of τ correspond to distinct tori. As a quotient of the complex plane, the torus inherits the addition of complex numbers as an operation on points on the torus. We will describe this more closely in the following.

---

[2]This $\mathbb{Z}_2$ parity is identified with the type IIB parity in (2.0.4)

Representation as a hypersurface

The representation of the complex torus as a hypersurface may be derived from considerations of what functions can be constructed on the torus. Any function on the torus has to be doubly periodic,

$$f(\zeta) = f(\zeta + 1) = f(\zeta + \tau), \quad \zeta \in \mathbb{C} \tag{2.1.4}$$

in order to be well defined on the quotient space. Since the torus is a compact space, any holomorphic function on the torus will be a constant, and the non-trivial functions will be the meromorphic ones. The Weierstrass elliptic function

$$\wp(\zeta; \tau) = \frac{1}{\zeta^2} + \sum_{w \in \Lambda \backslash (0,0)} \frac{1}{(\zeta - w)^2} - \frac{1}{w^2} \tag{2.1.5}$$

is the unique [17] complex function with a double pole at each lattice point. It is a theorem [17] that any meromorphic function on the torus is a rational expression in $\wp$ and its first derivative $\wp'$. By comparing the series expansions the equation

$$(\wp')^2 = 4\wp^3 + f\wp + g \tag{2.1.6}$$

is shown to hold for certain functions (Eisenstein series) $f(\tau)$ and $g(\tau)$. By identifying $x \leftrightarrow \wp$, $y \leftrightarrow \wp'$ one obtains the equation[3]

$$y^2 = x^3 + fx + g \tag{2.1.7}$$

which is traditionally called an elliptic equation, or an elliptic curve [4]. This equation constitutes a double cover of the complex plane, branched at four points: the three zeros of the cubic in x, and a 'point at infinity'. If we add this point, performing a one-point compactification of $\mathbb{C}^2$ the expression (2.1.7) is the inhomogeneous form of the so called Weierstrass equation

$$P_W = y^2 - x^3 - fxz^4 - gz^6 = 0 \tag{2.1.8}$$

in the weighted projective space $\mathbb{P}_{2,3,1}$ with homogeneous coordinates $[x : y : z]$. The coefficients f and g may a priori be valued in any field K and the elliptic curve is often denoted $E(K)$. The map between the two descriptions of the torus is given by the Weierstrass equation and a point $\zeta \in \mathbb{C}/\Lambda$ maps as

$$\zeta \mapsto [\wp(\zeta) : \wp'(\zeta) : 1], \tag{2.1.9}$$

a point lying on the torus embedded in $\mathbb{P}_{2,3,1}$ [5]. The 'point at infinity' is given by $[1 : 1 : 0]$, and this point is the image of any lattice point in Λ, in particular the origin of $\mathbb{C}$, and is commonly referred to as the zero-point of the curve.

The smoothness of the hypersurface equation amounts to having a well defined gradient at every point on the curve. In other words, the tangent space dimension are not allowed to jump in dimension at any point. In practice we check that the system

$$\begin{aligned} P_W &= 0 \\ dP_W &= 0 \end{aligned} \tag{2.1.10}$$

has no solution, and in this case the hypersurface is smooth. Singularities, or solutions to the above equations, occur if two or more zeroes of the equation comes together. This is controlled by the

---

[3]For convenience and adopting to the standard in F-theory literature we are changing normalization such that the prefactor of x^3 disappears

[4]This name is due to the occurrence of this y as a function of x in the integrand when computing arclengths of ellipses.

[5]By a different homogenization the Weierstrass equation may be taken as a hypersurface in a projective space with other weight assignments e.g. as a cubic equation in $\mathbb{P}^2$

discriminant Δ, which vanishes *iff* the equation has multiple zeroes. For (2.1.8) the discriminant takes the form

$$\Delta = 4f^3 + 27g^2 \tag{2.1.11}$$

and will play a central role in the following chapters. The link between the description of the torus as a quotient by the lattice $\Lambda = \langle 1, \tau \rangle$ and the Weierstrass equation is provided by the Klein j-invariant, or the j-function

$$j(\tau) = q^{-1} + 744 + 196884q + \dots \qquad q = e^{2\pi i \tau}, \tag{2.1.12}$$

which may be expressed in terms of the coefficients f and g of the Weierstrass equation. In this case

$$j(\tau) = 4 \cdot 24^3 \frac{f^3}{\Delta}. \tag{2.1.13}$$

The j-function is the unique modular invariant bijection from the fundamental region $\mathcal{F}$ to the Riemann sphere, and as seen above it diverges when the elliptic curve develops a singularity. More specifically, when $j \to \infty$ the argument $\tau \to i\infty$. This behaviour of τ is exactly what happens when approaching a $D7$-brane in type IIB string theory. Hence, the zeroes of the discriminant in an F-theory model correspond to branes in the dual type IIB theory. The details of this correspondence will be elaborated upon in what follows.

Rational points and the Mordell-Weil group

A rational point on an elliptic curve is a point whose coordinates $[x : y : z]$ are given by a rational expression in the underlying field K. The zero-point is an example of a rational point, and generically no other rational points exist. However, for certain forms of f and g more rational solutions to the equation (2.1.8) may exist, and this set of rational points forms a group. The map (2.1.9) is in fact an isomorphism, and as such preserving the addition of complex numbers as [17]

$$\zeta + \eta \mapsto [\wp(\zeta + \eta) : \wp'(\zeta + \eta) : 1]. \tag{2.1.14}$$

The set of rational points on the elliptic curve with this addition law is called the Mordell-Weil group. The Mordell-Weil theorem asserts that this group is finitely generated when K is a number field, *i.e.* a finite extension of the rational numbers. In this case,

$$E(K) = \mathbb{Z}^r \oplus \mathbb{Z}_{k_1} \oplus \dots \oplus \mathbb{Z}_{k_n}. \tag{2.1.15}$$

The rank r of this group is the number of generators of the free subgroup and the finite part is called the torsion subgroup $E(K)_{\text{tors}}$. A theorem by Mazur states that for a curve over the rational numbers, the torsion subgroup $E(\mathbb{Q})_{\text{tors}}$ is either $\mathbb{Z}_k$ for $k = 1, \dots, 10, 12$ or $\mathbb{Z}_2 \oplus \mathbb{Z}_k$ for $k = 2, 4, 6, 8$. The converse statement also holds, *i.e.* all possibilities are realised.

2.1.2 Elliptic fibrations

The equation which describes the elliptic curve as a surface in an ambient projective space may be generalized to an equation describing a fibration. Take $\mathcal{B}$ to be a complex manifold. In four dimensional F-theory compactifications $\mathcal{B}$ is a compact Kähler 3-fold. By taking the coefficents of (2.1.8) to be dependent on the coordinates b on $\mathcal{B}$ we get an elliptic curve over each point of the base $\mathcal{B}$. In the Weierstrass representation we have

$$y^2 - x^3 - f(b)xz^4 - g(b)z^6 = 0 \qquad b \in \mathcal{B} \tag{2.1.16}$$

describing an elliptic curve over each point of $\mathcal{B}$. For f and g constant, the fibration is trivial, describing the product space $\mathcal{B} \times E$. The fibration Y is a hypersurface in the ambient space X given by fibering $\mathbb{P}_{2,3,1}$ over $\mathcal{B}$. The divisor $Z : \{z = 0\}$ in the ambient space intersects each fiber in a point, which is the zero-point of the fiber. Globally this defines the zero-section of the fibration, which is an embedding of the base into the fibration. A non-trivial fibration corresponds to non-constant f and g. These can not be holomorphic functions, since the base is compact and on a compact space the only holomorphic functions are the constant functions. To get a non-trivial fibration, we need to take the coefficients to be meromorphic functions on each local patch of $\mathcal{B}$. Globally they are sections of some line bundle. For the hypersurface equation to be well defined with respect to the line bundle scaling it has to be homogeneous, not only with respect to the projective action of $\mathbb{P}_{2,3,1}$, but also with respect to the introduced line bundle $\mathcal{L}$. A choice for scaling assignments leaving the zero section holomorphic is to take x as a section[6] of $\mathcal{L}^2$, y as section of $\mathcal{L}^3$, f a section of $\mathcal{L}^4$ and g a section of $\mathcal{L}^6$. In compactifications to four dimensions that preserve $\mathcal{N} = 1$ supersymmetry, the fibration has to be a Calabi-Yau four-fold and thus the first Chern class must vanish. Denoting by $[\mathcal{L}]$ the divisor class of the line bundle $\mathcal{L}$, one may compute the total Chern class of the fibration by the adjunction formula

$$c(Y) = \frac{c(X)}{c(P_W)} = \frac{c(\mathcal{B})(1 + [x])(1 + [y])(1 + [z])}{1 + 6[\mathcal{L}] + 6[z]} \tag{2.1.17}$$

where the denominator is the Chern class of the hypersurface, which is a divisor in the ambient space and the divisor class is given by the power of the occuring sections i.e $[gz^6] = 6[\mathcal{L}] + 6D_z$. There is only one independent divisor in $\mathbb{P}_{2,3,1}$, analogous to the hyperplane class in ordinary projective space, and thus $[x] = 2[z] + 2[\mathcal{L}]$ and $[y] = 3[z] + 3[\mathcal{L}]$. Expanding (2.1.17) to first order gives

$$c_1(Y) = c_1(\mathcal{B}) - [\mathcal{L}] \tag{2.1.18}$$

which forces $[\mathcal{L}] = c_1(\mathcal{B}) = [\bar{K}_{\mathcal{B}}]$, the class of the anti-canonical bundle on $\mathcal{B}$

Another way to see the Weierstrass equation arise is by using the properties of line bundles on elliptic curves. On an elliptic curve E there is the distinguished zero-point P, which is a divisor on the elliptic curve E. Let $L = \mathcal{O}(P)$ be the dual line bundle on E. It has degree one. For any line bundle on E with $deg\, L > 0$ it holds that $deg\, L = dim\, H^0(L)$, i.e the number of independent sections equals the degree of the bundle. We assume here that this is the case. Furthermore the degree of the n:th power of a linebundle is n times the degree of the bundle itself. Lets now consider the sections of L and its powers. $H^0(L)$ is generated by a single section, which we may call z, $H^0(L^2)$ has two sections; z^2 and another independent one, called x. $H^0(L^3)$ is generated by three sections; we can construct z^3 and xz, and we denote the last one by y. Out of x, y and z the four sections in $H^0(L^4)$ and the five sections in $H^0(L^5)$ can be constructed. The interesting case is at degree 6, since $H^0(L^6)$ has six independent sections but we can construct seven sections: y^2, xyz, yz^3, x^3, x^2z^2, xz^4 and z^6. Hence they have to obey a relation, usually written as

$$y^2 + a_1xyz + a_3yz^3 = x^3 + a_2x^2z^2 + a_4xz^4 + a_6z^6 \tag{2.1.19}$$

for some coeffcient sections a_i. The unity coefficient of the y^2 and x^3 terms ensures that $Z : \{z = 0\}$ intersected with the equation describes the distinguished point holomorphically. If the function field K on $\mathcal{B}$ has not characteristic 2 or 3, the square on the left hand side and the cube on the right hand side may be completed, arriving at the Weierstrass equation $y^2 = x^3 + fxz^4 + gz^6$. The equation (2.1.19) is usually referred to as the Tate form, or in the literature sometimes also as the Weierstrass form. Since x, y and z has line bundle scalings 2,3 and 1 respectively, the above equation can be consistently identified with a degree 6 hypersurface in $\mathbb{P}_{2,3,1}$. By adjunction we may compute the first Chern class

$$c_1(E) = c_1(\mathbb{P}_{2,3,1}) - 6[z] = [x] + [y] + [z] - 6[z] = 0 \tag{2.1.20}$$

---

[6]Exponents of line bundles are always tensor products e.g $\mathcal{L}^2 = \mathcal{L} \otimes \mathcal{L}$.

of this degree 6 hypersurface in $\mathbb{P}_{2,3,1}$ and since the weights of the ambient space add upp to the degree of the hypersurface the first Chern class vanishes. This confirms that (2.1.19) (and also (2.1.8)) describes a compact Calabi-Yau 1-fold, i.e a torus. Taking the coefficents a_i to be sections of some line bundle on a compact base and imposing the Calabi-Yau condition on the fibered manifold, we are led to taking x and y to transform under this line bundle as well.

Note that this method may be used to construct other representations of elliptic curves, with different ambient spaces and even elliptic fibrations as complete intersections of two or more equations. For example, if the elliptic curve has two rational points P and Q, we can repeat the above construction for the line bundle $\mathcal{O}(P+Q)$, and this will lead to a representation of the elliptic curve as a degree four hypersurface in $\mathbb{P}_{1,1,2}$ [18]. This is one example of the fact that the Weierstrass form is not the only way to describe the elliptic fibration as a hypersurface. Any equation, or set of equations whose zero locus defines an elliptic curve will do. One equation may make a certain geometric property easy to analyse, while obscuring others. Any elliptic equation may be brought into Weierstrass form through a birational transformation [7], while going from the Weierstrass form to e.g the Tate representation is not always possible. A useful tool to study in particular higher-dimensional examples of elliptic fibrations is toric geometry. In toric geometry an elliptic curve may be realized as a hypersurface or a complete intersection in an ambient toric variety. The possible realizations of tori as hypersurfaces are classified by the 16 reflexive polygons in two dimensions, see e.g [19]. The associated toric ambient spaces are $\mathbb{P}_{1,1,2}^2$, $\mathbb{P}^1 \times \mathbb{P}^1$, $\mathbb{P}^2$ or blow-ups thereof.

Depending on the choice of ambient toric variety, the most general hypersurface equation in this space has different features. Out of the 16 reflexive polygons 13 have extra rational sections which arise from ambient toric divisors, giving a Mordell-Weil rank of at least one [20]. Three of the 16 polygons admit torsional sections given as the intersection of an ambient toric divisor with the elliptic curve. According to the enumeration of polygons in [19], the elliptic curves in the ambient spaces defined by polygon 13, 15 and 16 have toric Mordell-Weil groups $\mathbb{Z}_2$, $\mathbb{Z} \oplus \mathbb{Z}_2$ and $\mathbb{Z}_3$, respectively [20] (see also [21]). In the later chapters we will study fibrations where the form of the hypersurface equation is chosen to make relevant geometric aspects as lucid as possible.

Rational sections

In this section, we give a brief review of the Mordell-Weil group of a family of elliptic curves. We describe how meromorphic sections naturally come with a group structure. This is a classic topic in mathematics and for more extensive treatments see *e.g.* [17,22]. In chapter 3 we comment in particular on the finite part of this group, the part associated to torsional sections.

An elliptic fibration X over a base manifold $\mathcal{B}$ comes with a holomorphic projection map $\pi : X \to \mathcal{B}$. Since the fibration locally takes the form $E \times U \subset \mathcal{B}$, a choice of projection is $\pi(p, b) = b$, for $p \in E$ and $b \in \mathcal{B}$. The generic fiber is given by $\pi^{-1}(b)$. A rational section is a meromorphic map $\sigma : \mathcal{B} \to X$, such that $\pi \circ \sigma = \mathrm{id}_{\mathcal{B}}$ [8]. In the Weierstrass form the section determines $x = x(f, g)$ and $y = y(f, g)$ as meromorphic functions of the coefficient functions $f(b), g(b)$ over each local patch on $\mathcal{B}$. For the generic fiber $\pi^{-1}(b)$ this solution determines a point on the fiber, as depicted in fig. 2.3. Since the rational section intersects each smooth fiber in a point we have that $\sigma(\mathcal{B})$ defines an embedding of the base $\mathcal{B}$ into the elliptic fibration. A holomorphic section intersects each fiber in a single point while a rational section may wrap irreducible fiber components over loci in the base where the fiber degenerates.

A rational section assigns a rational point on the fiber for every generic point in the base. For any

---

[7]A birational transformation is rational in both the ambient projective coordinates and the function field on the base.

[8]If σ is a holomorphic map, then it is called a holomorphic section.
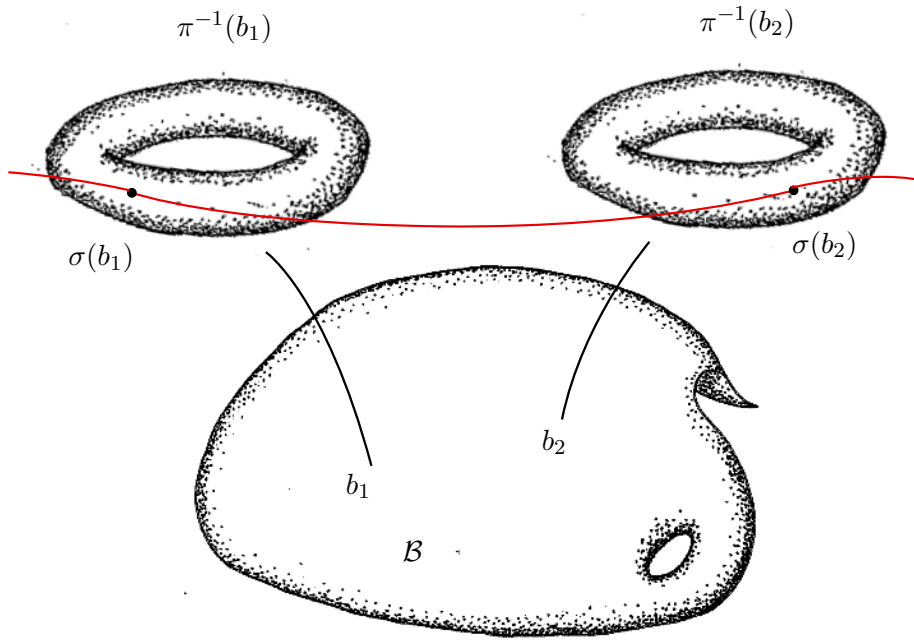
Figure 2.3: An elliptic fibration with projection π. The rational section σ defines a rational point $\sigma(b_i)$ on each generic fiber. Here the fibers $\pi^{-1}(b_i)$ over two points in the base $\mathcal{B}$ are depicted.

fixed point b the rational points are elements of the Mordell-Weil group of the elliptic fiber $\pi^{-1}(b)$. We can now extend the notion of Mordell-Weil group to elliptic fibrations. The zero point gets promoted to the zero section, which in (2.1.16) is given by the intersection of the ambient divisor $Z : \{z = 0\}$ with the hypersurface. Rational points becomes rational sections and the group law is defined fiberwise. Abstractly, we are shifting from considering an elliptic curve over a number field, to an elliptic curve over a function field (in the case of compact $\mathcal{B}$ the field of meromorphic sections of line bundles on $\mathcal{B}$). Note that the zero-section does not serve as one of the generators of the group. In particular, the Mordell-Weil group is trivial when the zero section is the only section of the fibration, and extra rational sections are needed to have a non-trivial group.

The Mordell-Weil theorem for function fields was proven by Lang and Neron [23] and states that the Mordell-Weil group of an elliptic fibration is finitely generated, unless the fibration is birationally equivalent to the trivial fibration $E \times \mathcal{B}$. For most physically interesting settings, which are dual to IIB models with 7-branes, the fibration is non-trivial and the theorem applies.

Determining the Mordell-Weil group for elliptic curves over number fields, or even the rationals $\mathbb{Q}$, is an old and often hard problem in number theory. For certain elliptic surfaces the possible groups $E(K)$ have been classified analogously to the Mazur theorem for elliptic curves. For instance, for a rational elliptic surface the non-trivial possibilities for the Mordell-Weil group are

$$
\begin{array}{lll}
\mathbb{Z}^r \ (1 \le r \le 8), & \mathbb{Z}^r \oplus \mathbb{Z}_2 \ (1 \le r \le 4), & \mathbb{Z}^r \oplus \mathbb{Z}_3 \ (1 \le r \le 2), \\
\mathbb{Z}^r \oplus \mathbb{Z}_2 \oplus \mathbb{Z}_2 \ (1 \le r \le 2), & \mathbb{Z} \oplus \mathbb{Z}_4, & \mathbb{Z}_2 \oplus \mathbb{Z}_4, \\
\mathbb{Z}_2 \oplus \mathbb{Z}_2, & \mathbb{Z}_3 \oplus \mathbb{Z}_3, & \mathbb{Z}_k \ (2 \le k \le 6)
\end{array} \tag{2.1.21}
$$

and in particular the Mordell-Weil group for any rational elliptic surface is torsion-free if its rank is greater than 4 [24]. The general situation for other elliptic surfaces such as elliptically fibered K3 manifolds and for higher-dimensional fibrations, *e.g.* three- and fourfolds, is not as well understood and classifications only exist in special cases such as [25]. However, in the case of elliptic fibrations realized as hypersurfaces in toric varieties there are well-understood cases, where the rational sections

arise from the ambient toric variety. In these cases, geometries with low rank Mordell-Weil group, and small torsion subgroups can be studied in generic settings, as presented in detail in chapter 3.

The Shioda map

An important ingredient in F-theory is the correspondence between rational sections and certain divisor classes on the fibration, more precisely elements of the Néron-Severi group of divisors modulo algebraic equivalence. Any rational section defines a codimension one object embedded into the fibration. As it is rational, it transforms as a section of a line bundle, or in other words, it is a divisor in the Calabi-Yau n-fold. Note that the Néron-Severi group coincides with the Picard group of divisors modulo linear equivalence for spaces with vanishing first cohomology group, which is the situation of relevance throughout this thesis.[9] Let E be a general fiber of π and σ_0 the zero section. Each divisor D on X can be restricted to a divisor $D|_E$ on E which has a specific degree $D \cdot E$. For example, sections restrict to divisors of degree 1. Now for an arbitrary divisor D, the linear combination $D - (D \cdot E)\sigma_0$ restricts to a divisor of degree 0 on E. But the set of divisors of degree 0 on E is just E itself.

In this way, we get a surjective homomorphism of groups

$$\psi : NS(X) \to E(K) \tag{2.1.22}$$

which sends $[D]$ to the K-valued point of E determined by restricting the divisor $D - (D \cdot E)\sigma_0$ to E. (It is surjective because every element of $E(K)$ arises from a rational section σ.) The kernel of this homomorphism is generated by the zero section and by divisors whose restriction to the general fiber E is trivial.

Since the group homomorphism (2.1.22) is surjective, there is an injective homomorphism in the other direction after tensoring with $\mathbb{Q}$. In the case of elliptic surfaces, Shioda [26] introduced such a homomorphism with a specific additional property, which was extended in [27, 28] to elliptic fibrations of arbitrary dimension. Let $\mathcal{T}$ denote the subgroup of $NS(\hat{X})$ generated by the zero-section $[\sigma_0]$, the resolution divisors F_i, and divisors of the form $\pi^{-1}(\delta)$ for $\delta \in NS(\mathcal{B})$ For the smooth elliptic fourfold $\hat{X}_4$ obtained by a flat resolution of X_4, the Shioda map

$$\varphi : E(K) \to NS(\hat{X}_4) \otimes \mathbb{Q} \tag{2.1.23}$$

satisfies the property that $\langle \varphi(\sigma), T \rangle = 0$ for any divisor $T \in \mathcal{T}$, where the pairing $\langle \, , \, \rangle$ is the *height pairing*

$$\langle D_1, D_2 \rangle := \pi(D_1 \cap D_2), \tag{2.1.24}$$

which projects the intersection of two divisors to the base. It is well defined modulo linear equivalence, and so defines a pairing on the Néron-Severi group. For example, given any section in an elliptic fibration its divisor class S defines an element $S - Z$ of the Mordell-Weil group and we have

$$\varphi(S - Z) = S - Z - \pi^{-1}(\delta) + \sum l_i F_i \tag{2.1.25}$$

for some divisor δ on $\mathcal{B}$ and some rational numbers $l_i \in \mathbb{Q}$, which is constructed so that for every $T \in \mathcal{T}$ we have

$$\pi \left(T \cap (S - Z - \pi^{-1}(\delta) + \sum l_i F_i) \right) \tag{2.1.26}$$

is linearly equivalent to zero on the base $\mathcal{B}$. The Shioda map will be frequently used in this thesis and the corresponding physics will be reviewed in section 2.5.1.
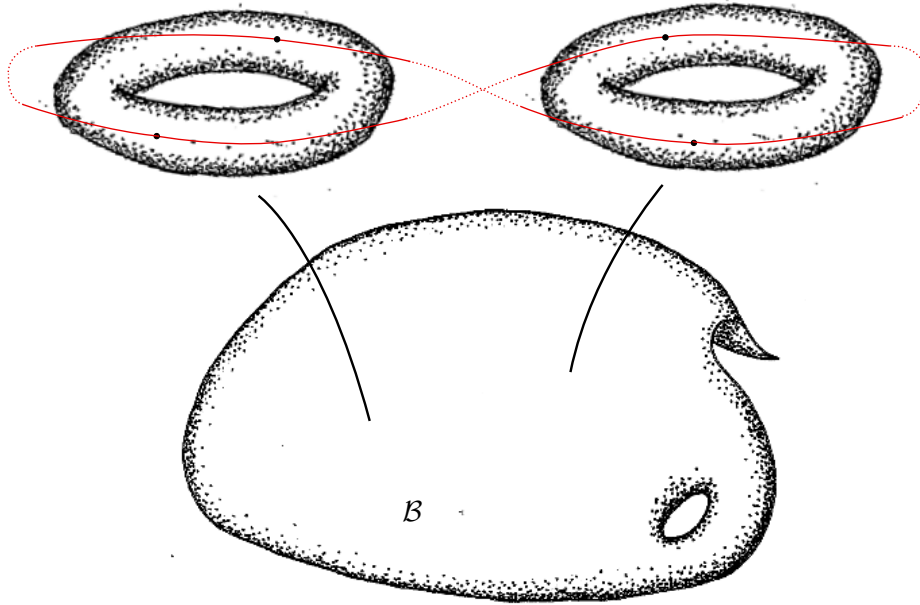
Figure 2.4: A genus-one fibration over the base $\mathcal{B}$. The bisection (in red) intersect each generic fiber in two points, and these are interchanged by monodromy over the base.

2.1.3   Genus-one fibrations

Up to this point we have studied elliptic curves and elliptic fibrations as a mean to geometrize the axiodilaton τ and the monodromy action of $SL(2, \mathbb{Z})$ on the axiodilaton and the 2-form fields of type IIB theory. In more abstract terms we want to specify an axio-dilaton profile τ and a representation of

$$\pi_1(\mathcal{B} - \Delta) \to SL(2, \mathbb{Z}). \tag{2.1.27}$$

The monodromy action on the type IIB fields corresponds to assigning an $SL(2, \mathbb{Z})$ transformation to each closed path around the degeneration loci $\Delta \subset \mathcal{B}$. One may therefore consider a fibration of tori, where the generic fiber has no distinguished zero point, but otherwise shares the defining τ profile and monodromy behaviour [29]. By having local descriptions of τ and (B_2, C_2) in patches over $\mathcal{B}$ the global model is obtained by gluing the patches with $SL(2, \mathbb{Z})$ transformations. In going from an elliptic fibration to a genus-one fibration one allows for translations along the fiber in the maps between patches. This does not preserve the zero-section. In this case the description of each fiber is a quotient of the complex plane by an affine lattice, which has no origin but still is doubly periodic with periods 1 and τ. The fibrations are called genus-one fibrations, as the generic fiber is a genus-one curve, not an elliptic curve which has a distinguished zero point. These fibrations can be constructed explicitly and studied in much the same way as elliptic fibrations as we will see in detail in chapter 4 and 5.

A genus-one fibration has no zero-section, but it can have one or more n-sections, or multi-sections. A section intersects the generic fiber in a point, while an n-section intersect the generic fiber in n points. Globally an n-section constitutes a n-fold cover of the base $\mathcal{B}$, embedded into the fibration. Locally, the n intersection points are distinguishable, and 'look' as n sections meeting the fiber. Globally

---

[9]For a Calabi-Yau manifold $H^1(X)$ is trivial. For this reason, we will systematically restrict our notation to refer to the Néron-Severi group rather than the Picard group.

these n points are interchanged, and are non-trivially glued up to one object, see fig. 2.4 One can think about genus-one fibrations not as a special case, but as more general geometries that admit a description in terms of fibered tori. In the cases where the genus-one fibration has at least one rational section it is an elliptic fibration.

To any genus-one fibration there is a related elliptic fibration called the Jacobian fibration $J(X)$. The genus-one fibration and the Jacobian share the same τ and discriminant Δ. As the Jacobian fibration is an elliptic fibration it has a zero section, and a representation as a Weierstrass equation. However, the Jacobian $J(X)$ may have singularities which cannot be resolved while keeping the Calabi-Yau condition. This holds in particular for smooth and Calabi-Yau genus-one fibrations. There might exist several genus-one fibrations that share the same Jacobian fibration. The number of fibrations with the same $J(X)$, up to isomorphisms are counted by the Tate-Shafarevic group [29]. An elliptic fibration is the trivial element of the Tate-Shafarevic group, while the genus-one fibrations are the non-trivial elements. In the case of the bisection fibration the Tate Shafarevic group is $\mathbb{Z}_2$, with the identity element the Jacobian fibration and the other element represented by the genus-one fibration.

2.2 Singular fibers

The gauge theory data in an F-theory compactification is encoded in the degeneration of the fiber. For an elliptic curve in Weierstrass form, with fixed values of the coefficients f and g it may be singular or smooth depending on whether the discriminant vanishes or not. For an elliptic fibration the singularity structure is more interesting, where the singularity may arise along loci of different codimension. Since the roots of the elliptic equation generally are distinct, the fiber over a generic point of the base is smooth.

The duality of M-theory and F-theory relies on the compactification of the 11 dimensional theory on the elliptic Calabi-Yau. This is very hard to do in the case of a singular geometry, where one does not have control over the homology, i.e all cycles along which the fields reduce. If however, the singular geometry can be described as a degenerate limit of a smooth manifold the reduction is more tractable. There has been some work on F-theory on singular geometries [30] without resolution of deformation, which we do not treat in more detail here.

2.2.1 Singularities in general

The following two sections briefly introduce the desingularization of a hypersurface. Understanding singularities as limits of smooth spaces follows two main paths, called deformation and resolution, or blow-up.

Deformation

The deformation of a singularity is a continous transformation. It is a parametrization of a family of smooth spaces, where the singular geometry appears as a limit in the introduced parameter. Here we illustrate the deformation through the following simple example for a real hypersurface. Consider the quadric equation

$$x^2 + y^2 - z^2 = 0, \quad (x, y, z) \in \mathbb{R}^3 \tag{2.2.1}$$

This describes a double cone, seen in fig 2.5, where the two 'tips' meet in a singular point at the origin. Indeed, at this point on the hypersurface the gradient vanishes as in (2.1.10). The hypersurface equation can be deformed to

$$x^2 + y^2 - z^2 = \alpha^2 \tag{2.2.2}$$
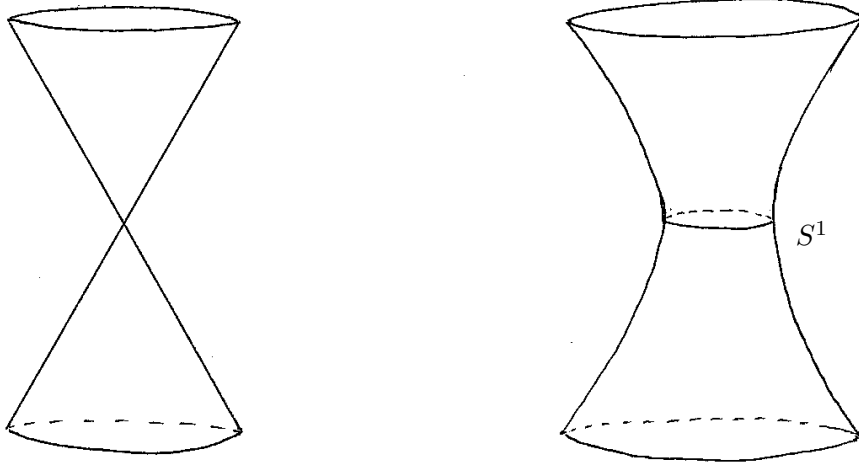
Figure 2.5: The deformation of a conic singularity. The the singularity is seen as the limit where the radius of the circle S^1 goes to zero.

by the introduction of a continuous parameter α, such that the singularity appears in the $\alpha \to 0$ limit. This is the equation of a hyperboloid, which asymptotes to the singular cone far away from the origin. Around the 'waist' of the hyperboloid there is a circle S^1, whose radius is parametrized by α. In the singular limit the size $Vol(S^1)$ of this non-trivial 1-cycle goes to zero, and is referred to as a collapsing cycle. In other words, we may regard the singularity as the result of contracting a non-trivial cycle on the manifold. In this case, the geometry is a two real dimensional surface, and the collapsing cycle is one dimensional. For deformation of singularities this illustrates the general result that the collapsing cycle is always an element of the middle homology group $H_{dim(X)/2}(X)$.

Blow-up

The blow up resolution is the other way to desingularize a space. In this scheme the singular locus is cut out, and replaced by a cycle in a way that make the total space smooth. We take the elliptic curve

$$P = -y^2 + x^3 + ax^2z^2 \quad a \in \mathbb{C} \tag{2.2.3}$$

as an example. a is a constant and this hypersurface defines an elliptic curve embedded in $\mathbb{P}_{2,3,1}$. As in (2.1.16) the ambient space divisor $Z : \{z = 0\}$ intersects the hypersurface in a point, which is a divisor on the elliptic curve. This equation is singular at $(x, y) = (0, 0)$ because $(x = 0, y = 0, z \neq 0)$ is a solution to the equations

$$P = 0, \quad dP = x(3x + 2az^2)\,dx - 2y\,dy + 2ax^2z\,dz = 0\,. \tag{2.2.4}$$

We desingularize this equation by an ambient space blow-up. By introducing a new ambient coordinate s, and a new scaling relation $(x, y, s) \sim (\lambda x, \lambda y, \lambda^{-1}s)$ the dimension of the ambient space does not change. The blow-up transformation is

$$(x, y) \to (sx, sy) \tag{2.2.5}$$

under which the hypersurface

$$P \to s^2(-y^2 + sx^3 + ax^2z^2)\,. \tag{2.2.6}$$

The solution $s = 0$ to above equation is discarded in what is called the proper transform

$$\tilde{P} = -y^2 + sx^3 + ax^2z^2 \tag{2.2.7}$$
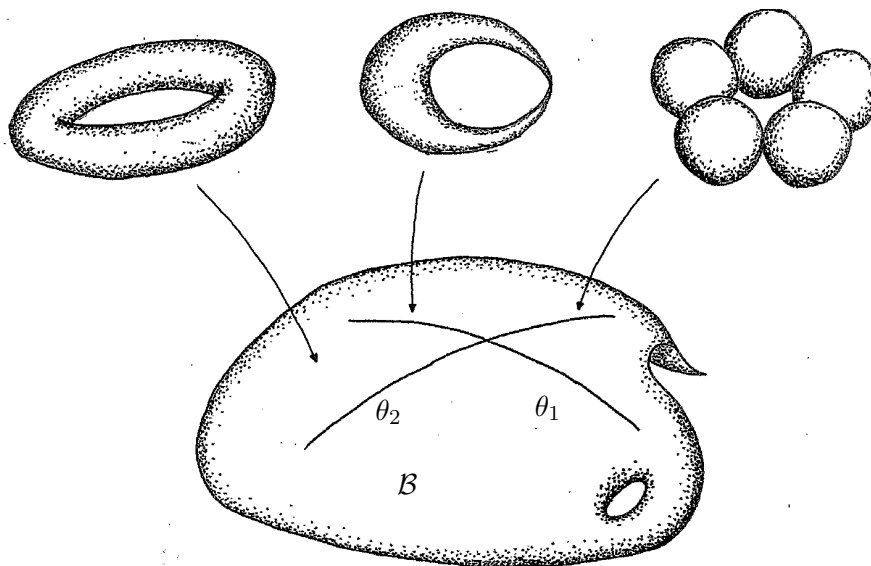
Figure 2.6: Some features of an F-theory fibration. Over a generic point on the base the fiber is a smooth genus-one curve (left). Over certain loci θ_1 in the base the fiber degenerates (middle). By resolving the singularity over θ_2 the fiber becomes a tree of curves, intersection as the Dynkin diagram of an affine Lie algebra, in this case $\mathfrak{su}(5)$.

since setting s to zero in (2.2.5) takes us back to the singularity at $x = 0$ and $y = 0$. The ambient space now has the toric representation

$$
\begin{array}{cccc}
x & y & z & s \\
\hline
2 & 3 & 1 & 0 \\
0 & 1 & 1 & -1
\end{array}
\tag{2.2.8}
$$

and the Stanley-Reisner ideal is $\{xy, sz\}$, which means that neither x and y nor s and z can vanish simultaneously, see e.g [31]. We see now that the singularity at $x = y = 0$ is 'cut out' by the Stanley-Reisner ideal. Using also the second generator of the SR-ideal one can check that

$$
\tilde{P} = 0 \quad d\tilde{P} = x(3xs + 2az^2)\,dx - 2y\,dy + 2ax^2z\,dz + 3xs^2\,ds = 0
\tag{2.2.9}
$$

has no solutions and thus $\tilde{P} = 0$ is a smooth hypersurface. The zero-point at $z = 0$ remains unaltered, and in addition there is a new point on the elliptic curve given by $s = 0$. This point is called the exceptional divisor of the blow-up. Importantly it is always a divisor, i.e a complex codimension one object. For a hypersurface of any dimension the blow-up results in one or more exceptional divisors. In this case only one blow-up was needed to make the hypersurface smooth and there is only one exceptional divisor. If the hypersurface is not smooth after the blow-up, a sequence of blow-ups can be performed, each introducing a new exceptional divisor and eventually reaching the smooth case. The exceptional divisors have a certain intersection pattern, which can be used to identify and classify the possible singularities. In the next section we review this for the case of elliptic fibrations.

2.2.2 Singularities in elliptic fibrations

The singularities of the elliptic fibration are found by analysing the discriminant, as introduced in (2.1.11) for the single elliptic curve. The discriminant of the fibration takes the same form

$$
\Delta \sim 4f(b)^3 + 27g(b)^2
\tag{2.2.10}
$$
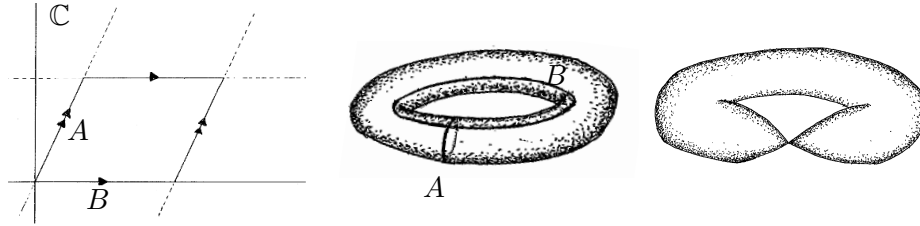
Figure 2.7: A singularity in the torus fiber arise when a 1-cycle collapses. On the right the singular fiber resulting from a shrinking A-cycle.

but in this case it varies over the base manifold. If the discriminant vanishes at some sublocus of $\mathcal{B}$, then the fiber will become singular over this locus. The singular fiber arising can be described by the collapse of a 1-cycle in the fiber. Note that this applies to a single fiber, or a fiber over a sublocus. For Calabi-Yau manifolds, there is are globally defined 1-cycles as the Hodge numbers $h^{1,0}(X) = h^{0,1}(X)$ vanish. The type of singularity depends on the collapsing 1-cycle, and we will describe how to determine the degeneration of the fibration in the following. Furthermore, since the discriminant varies over $\mathcal{B}$, which for 4-dimensional compactifications is a complex 3-fold, the degeneration can occur at loci of different codimension. These have very different physical interpretations, and will be treated separately in the following.

Singularity types of the elliptic fiber

The elliptic fiber $E(K)$, over a fixed and generic point on the base, has first homology group $H_1(T^2) \approx \mathbb{Z}^2$. The generators of this group are usually called the A-cycle and the B-cycle as in fig. 2.7. We choose the orientation so that the intersection number $A \cdot B = 1$. If either of these cycles collapses to a point the torus pinches, developing a singularity. More generally, any element $pA + qB \in H_1(T^2)$ may collapse, i.e $Vol(pA + qB) \to 0$ giving rise to a certain singularity type. By construction, see fig. 2.7, the modular group acts on the 1-cycles of the torus, and for an elliptic fibration there is a relation between the singularity type and the $SL(2, \mathbb{Z})$ monodromy action on the first homology group. The relation is given by the Picard-Lefschetz monodromy formula [32]

$$\eta \mapsto \eta - (\eta \cdot \gamma)\gamma \tag{2.2.11}$$

which gives the monodromy action on a 1-cycle η when encircling a codimension one locus, where the cycle γ collapses. Parametrizing $\eta = \begin{pmatrix} a \\ b \end{pmatrix}$ and the collapsing cycle $\gamma = \begin{pmatrix} p \\ q \end{pmatrix}$ the intersection form is $\eta \cdot \gamma = aq - bp$ and the monodromy action may be written

$$\begin{pmatrix} a \\ b \end{pmatrix} \mapsto \begin{pmatrix} a \\ b \end{pmatrix} - (aq - bp) \begin{pmatrix} p \\ q \end{pmatrix} = \begin{pmatrix} 1 - pq & p^2 \\ -q^2 & 1 + pq \end{pmatrix} \begin{pmatrix} a \\ b \end{pmatrix} \tag{2.2.12}$$

and we can take the monodromy to be defined by the matrix on the right hand side. This is the $SL(2, \mathbb{Z})$ action on the backgound fields induced by the (p, q) 7-brane in (2.0.13). Recall that the presentation of the modular group in terms of the generators is $\langle T, S | S^2 = (ST)^3 = \text{id} \rangle$ and the quadratic and cubic constraints reduce the possible monodromies to a few classes, up to change of $SL(2, \mathbb{Z})$-frame. The monodromies associated with the different singularity types are given in (2.2.13).

In the F-theory fibration one may therefore identify the 7-branes in type IIB string theory by finding the singularity type over the codimension one locus in the base $\mathcal{B}$ where the degeneration occurs. The 1-cycles of the fiber do however exist only locally, and it is often not practical to find the monodromy action this way. Luckily, the singularity type can be found also from the hypersurface representation of the fibration, due to the work by Kodaira [33].
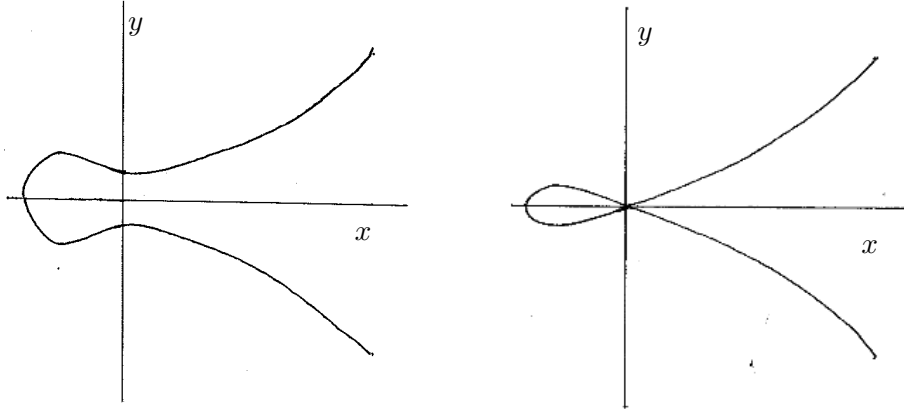
Figure 2.8: A real projection of an elliptic curve, restricting to real x and y in the Weierstrass model. On the left a smooth curve and on the right a singular one.

In the Weierstrass form, the type of singularity is encoded in the vanishing order of the coefficients f, g and the discriminant Δ at the locus of the singularity. For elliptic surfaces, that is elliptic fibrations over one dimensional bases, Kodaira classified all possible degenerations as rational double points (RDP)[10]. These are singularities occuring as self-intersections of the elliptic curve, depicted in fig. 2.8. In this case, at a point b_0 in the base where the fiber becomes singular, the discriminant will vanish to some polynomial order in the local base coordinate b_0. A point on a one dimensional base is a divisor, here denoted D. In other words, at D the discriminant $\Delta \sim b_0^n \tilde{\Delta}$. Furthermore, the coefficient sections f and g may also have vanishing orders at this point. By analysing the possible combinations of vanishing orders the singularities were classified in [33]. In the following table we present the result, and supplement the monodromy action corresponding to each singularity.

$ord(f)\|_D$	$ord(g)\|_D$	$ord(\Delta)\|_D$	Kodaira type	Singularity	Monodromy
≥ 0	≥ 0	0	I_0	$-$	$\begin{pmatrix} 1 & 0 \\ 0 & 1 \end{pmatrix}$
0	0	1	I_1	$-$	$\begin{pmatrix} 1 & 1 \\ 0 & 1 \end{pmatrix}$
0	0	2	I_2	A_1	$\begin{pmatrix} 1 & 2 \\ 0 & 1 \end{pmatrix}$
0	0	m	I_m	A_{m-1}	$\begin{pmatrix} 1 & m \\ 0 & 1 \end{pmatrix}$
≥ 1	1	2	II	$-$	$\begin{pmatrix} 1 & 1 \\ -1 & 0 \end{pmatrix}$
1	≥ 2	3	III	A_1	$\begin{pmatrix} 0 & 1 \\ -1 & 0 \end{pmatrix}$
≥ 2	2	4	IV	A_2	$\begin{pmatrix} 0 & 1 \\ -1 & -1 \end{pmatrix}$
≥ 2	≥ 3	6	I_0^*	D_4	$-\begin{pmatrix} 1 & 0 \\ 0 & 1 \end{pmatrix}$
2	3	$6+n$	$I_n^*, n \geq 1$	D_{4+n}	$-\begin{pmatrix} 1 & n \\ 0 & 1 \end{pmatrix}$
≥ 3	4	8	IV^*	E_6	$\begin{pmatrix} -1 & -1 \\ 1 & 0 \end{pmatrix}$
3	≥ 5	9	III^*	E_7	$\begin{pmatrix} 0 & -1 \\ 1 & 0 \end{pmatrix}$
≥ 4	5	10	II^*	E_8	$\begin{pmatrix} 0 & -1 \\ 1 & 1 \end{pmatrix}$
≥ 4	≥ 6	≥ 12	$non-minimal$	$not\ a\ RDP$	$-$

(2.2.13)

---

[10]A rational double point, du Val singularity or a simple surface singularity is an isolated singularity of a complex surface whose resolution consist of a tree of smooth rational curves.
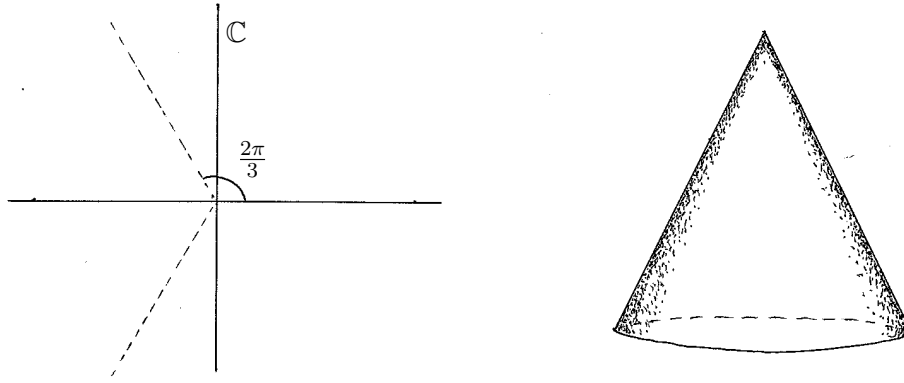
Figure 2.9: A conic singularity as a quotient of $\mathbb{C}$ by a discrete rotation. Here the example of a $\mathbb{Z}_3$ subgroup of all rotations of the complex plane is depicted.

The first line in (2.2.13) is the trivial case, where the fiber is smooth over the divisor D. In the I_1 and II cases the fiber is singular but the fibration remains smooth. This is analogous to describing a sphere S^2 as a fibration of a circle S^1 over an interval, where the circle contracts to a point at the interval endpoints. In this case the fibre S^1 degenerates over the endpoints, but the fibration is smooth. The following lines are the descendent cases of degeneration types. The fourth column is the notation Kodaira used and the fifth column the notation as an ADE classification. The final column contains the $SL(2, \mathbb{Z})$ monodromy action induced by the collapsing 1-cycle.

The ADE classification of the degeneration of the elliptic fiber over divisors in the base is a beautiful correspondence, which underlies the appearence of gauge symmetries in F-theory. These rational double point singularities are also known as du Val singularities. They can be understood in several ways, and here we'll briefly describe them first in terms of a local description of the singularity and second through the resolution by a series of blow-ups.

Locally the elliptic surface at a smooth point is diffeomorphic to an open set in $\mathbb{C}^2$. By quotienting $\mathbb{C}^2$ by the action of a discrete symmetry group singularities can arise, and the du Val singularities all have a quotient description. An analogous example is the quotient of $\mathbb{C}$ by a rotation of $2\pi/n$ rotation around the origin, making a cone with the singularity at the tip (fig. 2.9). The discrete group in this example is the $\mathbb{Z}_n$ subgroup of $U(1)$ group of rotations of $\mathbb{C}$. In the case of $\mathbb{C}^2$ the rotation acts by $SL(2, \mathbb{C})$, or equivalently by $SU(2)$ on the doublet of the complex coordinates. Hence we may construct singularities locally through quotients by discrete subgroups of $SU(2)$. These are visualized as the subgroups of the $SO(3) \subset SU(2)$ rotations of the sphere S^2. The discrete subgroups are the rotation groups of the platonic solids, viewed as point sets on the sphere. These groups are the polyhedral binary groups, including the $\mathbb{Z}_n$ symmetry of n equidistant points along the equator of S^2. In the following table the ADE singularities are presented as quotients $\mathbb{C}^2/G$ and the local form of the hypersurface equation is given

Type	G	Equation	
A_n	$\mathbb{Z}_{n+1}$	$x^2 + y^2 + z^{n+1}$	
D_n	Binary dihedral $BD_{4(n-2)}$	$x^2 z + y^2 + z^{n-1}$	
E_6	Binary tetrahedral	$x^3 + y^2 + z^4$	(2.2.14)
E_7	Binary octahedral	$x^3 + y^2 + xz^3$	
E_8	Binary icosahedral	$x^3 + y^2 + z^5$	

One may also approach the classification of singularity types through the resolution via blow-ups. Depending on the singularity type, one or more blow-ups is required to achieve a smooth space. The
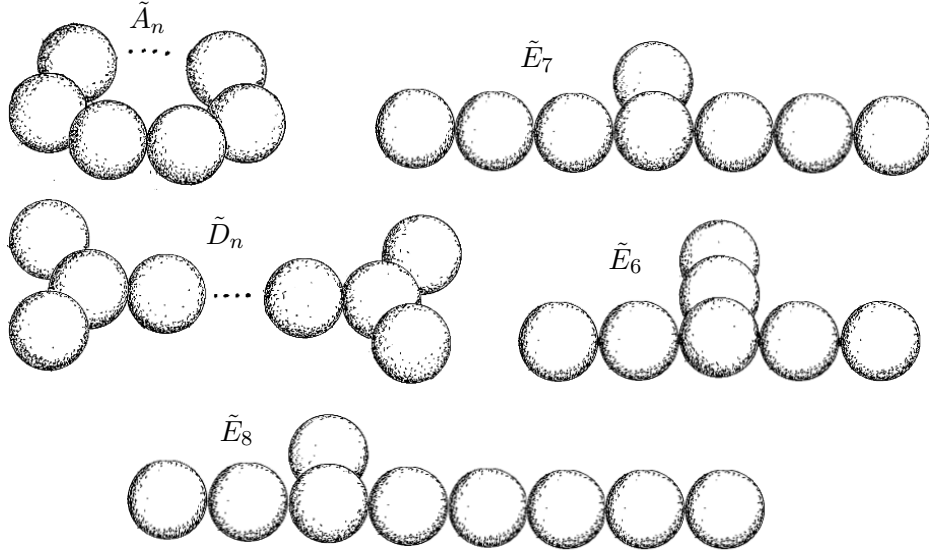
Figure 2.10: The trees of intersecting curves $\mathbb{P}^1_i$ in the fiber take the form of affine Dynkin diagrams of ADE type. The resolved fibers are fibered over the divisor θ in the base where the singularity sits.

resolution introduces a new set of divisors in the elliptic fibration, and one may ask what happens to the topological invariants of the geometry in the resolution process. For purposes of F-theory models preserving $\mathcal{N} = 1$ supersymmetry the Calabi-Yau condition $c_1(X) = 0$ must hold also after the resolution. The resolutions preserving the first Chern class are called crepant resolutions [11]. Each blow-up introduces an exceptional divisor, in the case of an elliptic surface X exceptional curves. The intersection number of two such divisors is defined as

$$F_i \cdot F_j = \int_X \eta_i \wedge \eta_j \equiv -C_{ij} \qquad (2.2.15)$$

where η_i is the Poincare dual of the divisor D_i. The right hand side is referred to as the intersection form. By the resolution of a certain singularity, the singular point is replaced by a tree of divisors, and it is observed that the tree takes the form of an affine Dynkin diagram of ADE type, see fig. 2.10. The correspondence between the resolved geometry and the ADE Lie algebras is stated as[12]

$$\{Intersection\ form\ of\ exceptional\ divisors\} \leftrightarrow \{Cartan\ matrix\ of\ ADE\ Lie\ algebra\}. \qquad (2.2.16)$$

For elliptic surfaces with vanishing canonical class, i.e elliptic K3 surfaces the singularities which admit crepant resolutions are precisely of ADE type [34]. For four-fold fibrations there is no intersection number between two divisors and the above intersection form generalizes to

$$\int_{X_4} F_i \wedge F_j \wedge \pi^* D_a \wedge \pi^* D_b = -C_{ij} \int_{\mathcal{B}} \theta \wedge D_a \wedge D_b \qquad (2.2.17)$$

where $D_{a,b}$ are any two divisors on the base, and $\theta \subset \mathcal{B}$ is the divisor over which the singularity sits. In the case of fibrations of higher dimension, e.g Calabi-Yau threefolds and fourfolds the Kodaira classification still holds for singularities in codimension one in the base, with the addition of the possible monodromy action on the resolution divisors when moving along the divisor in the base. This monodromy makes for the possibility of non-simply laced gauge algebras. For singularities in higher codimension, the list of possibilities grows and a general classification is not completed. On the other hand, when realising elliptic fibrations as hypersurfaces in toric varieties, the crepant resolution is often easy to construct. And when a resolution is found, the intersection form of the resolution divisors is explicitly constructed.

---

[11]As opposed to resolutions introducing a discrepancy in the canonical class, a term coined by M. Reid

[12]The self-intersection numbers are negative, so the intersection form is the negative of the Cartan matrix

2.2.3   Summarizing the divisor classes

We have seen that divisors originating from the fiber in the resolved fibration $\hat{X}$ come from two sources; rational sections and resolution divisors. In the case of a genus-one fibration the rational sections are exchanged for the multi-section classes. We here assume that the singularities in the fibration X can be resolved such that $\hat{X}$ is smooth and flat, i.e all the fibers are one-dimensional. The resolution divisors F_i are $\mathbb{P}^1$ fibrations over the codimension one loci w in $\mathcal{B}$ where the singularity was located. In addition there can be divisor classes D_a coming from the base, which by pullback give rise to divisors $\pi^* D_a$ on the full fibration. For any elliptic n-fold, the Neron-Severi group of divisors modulo algebraic equivalence, is given by the class of the zero section, the classes of the generators of the Mordell-Weil group, by resolution divisors and divisors pulled back from the base [27]. Algebraic equivalence is a finer equivalence relation than linear equivalence of divisors, or homological equivalence of cycles. In this thesis we will for simplicity use the coarser equivalences of divisors or homology cycles when appropriate. In other words, for an elliptic fibration the rank of the Neron-Severi group

$$\text{rank } NS(\hat{X}) = 1 + \text{rank } NS(\mathcal{B}) + \text{rank } E(K) + \sum_{w \in \Delta} (n_w - 1), \qquad (2.2.18)$$

where n_w is the number of irreducible fiber components over w which is a factor of the discriminant Δ. The resolved fiber consists of the original component plus the components introduced by the blow-up. This makes $n_w - 1$ the number of resolution divisors. The first term corresponds to the zero section. In the case of a genus-one fibration, no zero section and no Mordell-Weil group are present. The formula will then get modified by exchanging the corresponding terms by the multi-section classes. Recall that $\mathcal{T}$ is the subgroup of $NS(\hat{X})$ generated by the zero-section $[\sigma_0]$, the resolution divisors F_i, and divisors of the form $\pi^{-1}(\delta)$ for $\delta \in NS(\mathcal{B})$. The divisors on $\hat{X}$ are thus generated by the classes in $\mathcal{T}$ and the divisor classes $S_i - Z = [\sigma_i] - [\sigma_0]$ from the free generators of $E(K)$.

We note here that the divisor class $R - Z = [\sigma_r] - [\sigma_0] \in NS(\hat{X})$ associated with a torsional section σ_r has the property that $k(R - Z)$ can be expressed in terms of the generators of $\mathcal{T}$, where k is the order of the torsional element of the Mordell-Weil group. It follows that $R - Z$ can be expressed in terms of these generators using $\mathbb{Q}$-coefficients. The Neron-Severi group is thus torsion-free, since the image of a torsion section can be expressed in terms of only non-torsional objects. This is crucial for the analysis in chapter 3. As described in the next section, this expression for $R - Z$ is closely related to the so-called Shioda map [26], [27, 28]. This is in line with the result for elliptic surfaces in [35], where a trivial class on the hypersurface is obtained by adding a certain rational linear combination of resolution divisors to $R - Z$.

2.3   The Sen limit, or how to reconstruct type IIB string theory

We introduced F-theory by considering first weakly coupled type IIB string theory. The notion of general (p, q) 7-branes as the objects that source all possible $SL(2, \mathbb{Z})$ monodromies arise when leaving the weak coupling limit and F-theory incorporates this full set of possibilities in the fibration structure. Given an F-theory geometry one may ask how to recover the type IIB description, when the string coupling goes to zero. This is the weak coupling limit of F-theory and was introduced by Sen in [36], and therefore referred to as the Sen limit. By a certain parametrization of the fibration, the Sen limit restricts all monodromies to the T-type monodromy induced by $D7$ branes, and at the same time reproduces the orientifold involution of perturbative type IIB string theory.

When the string coupling $g_s = \langle \exp(\phi) \rangle$ goes to zero, the axiodilation vev $\langle \tau \rangle = \langle C_0 \rangle + i g_s^{-1}$ approaches $i\infty$. In this limit C_0 is negligible, and the expansion (2.1.12) of the j-function is dominated

by the first term

$$j(\tau) \sim e^{-2\pi i \tau} . \qquad (2.3.1)$$

Large values of the j-function correspond to large $\operatorname{Im} \tau$, which means small string coupling. In the following we show how Sen's parametrization allows for large $j(\tau)$ almost everywhere on the base. For ϵ a constant the rewriting

$$\begin{aligned} f &= -3h^2 + \epsilon\eta \\ g &= -2h^3 + \epsilon h\eta + \epsilon^2\chi \end{aligned} \qquad (2.3.2)$$

of the Weierstrass coefficients makes the leading terms cancel in the discriminant $\Delta = 4f^3 + 27g^2$. The h, η and χ are sections of $\bar{K}_{\mathcal{B}}^2$, $\bar{K}_{\mathcal{B}}^4$ and $\bar{K}_{\mathcal{B}}^6$ respectively. For any fixed and non-zero value of ϵ there is no loss of generality since η and χ span all the values of f and g. If the fibration is given in Tate form (2.1.19), the Sen limit amounts to replacing

$$a_3 \to \epsilon a_3, \qquad a_4 \to \epsilon a_4, \qquad a_6 \to \epsilon^2 a_6 . \qquad (2.3.3)$$

For the Weierstrass coefficients as above the j-function takes the form

$$j(\tau) \sim \frac{(\epsilon\eta - 3h^2)^3}{\Delta} \qquad (2.3.4)$$

and the discriminant factors as

$$\Delta \sim \epsilon^2 h^2 (\eta^2 + 12h\chi) + \mathcal{O}(\epsilon^3) . \qquad (2.3.5)$$

Hence, for small values of ϵ the zero loci of the discriminant are found at

$$h = 0, \qquad \text{and} \qquad \eta^2 + 12h\chi = 0 \qquad (2.3.6)$$

in the base. As $\epsilon \to 0$ the j-function takes large values in all regions except where the nominator in (2.3.4) goes to zero, i.e where $|h| \sim \sqrt{|\epsilon|}$. Inspecting the discriminant, we see that the coupling remains weak, except for the locus where $h = 0$. The monodromies around these loci can be computed using the weak coupling assumption [36]. Around the locus $\eta^2 + 12h\chi = 0$ the monodromy is of T-type, or $SL(2, \mathbb{Z})$ conjugate to T. This is the monodromy induced by a single $D7$ brane. If this zero locus has multiplicity n, the monodromy is T^n. Around $h = 0$ the monodromy can be shown to be $-T^{-4}$, which is the monodromy induced by the orientifold $O7$-plane in type IIB theory [36]. We collect the results in the following table:

Locus	Monodromy	Type IIB solution
$h = 0$	$-T^{-4}$	$O7$ plane
$\eta^2 + 12h\chi = 0$	T	$D7$ brane.

$$(2.3.7)$$

In the discriminant the $O7$ locus at $h = 0$ appears as the factor h^2. Thus, when leaving the $\epsilon \to 0$ limit this factor will split into two parts, each describing a non-perturbative 7-brane such that the joint monodromy, when encircling both 7-branes is $-T^{-4}$. The F-theory description of the $O7$-plane is thus a bound state of non-perturbative branes which can be resolved at finite coupling.

By identifying the zero locus of h as the $O7$ plane it is possible to describe the Calabi-Yau threefold from which the IIB orientifold is derived. The $O7$ plane is the fixed locus of an $\mathbb{Z}_2$ action and the manifold M which is described by the equation

$$\xi^2 = h \qquad (2.3.8)$$

is the simplest realization of a hypersurface with a involution σ and a fixed point set at $h = 0$. The $\mathbb{Z}_2$ involution

$$\sigma : \xi \mapsto -\xi \qquad (2.3.9)$$

and since h is a section of $\bar{K}_{\mathcal{B}}^2$ the new coordinate ξ transforms as a section of $\bar{K}_{\mathcal{B}}$. M is a double cover of the base $\mathcal{B}$ of the F-theory elliptic fibration. M is a hypersurface in an ambient space with total Chern class $c(B)(1 + [\bar{K}_{\mathcal{B}}])$, since ξ transforms under the anticanonical bundle. The hypersurface is of second order with respect to this class and by adjunction we have that

$$c_1(M) = c_1(B) + c_1(\bar{K}_{\mathcal{B}}) - 2c_1(\bar{K}_{\mathcal{B}}) = 0 \qquad (2.3.10)$$

and thus $\xi^2 = h$ describes a Calabi-Yau manifold. The F-theory description utilizes the modular symmetry of the elliptic fiber, and not the full $SL(2, \mathbb{Z})$ symmetry of type IIB. In (2.0.4) we saw that the action of the left-handed fermion index and the worldsheet parity $(-1)^{F_L}\Omega$ gets quotiented out in the F-theory description. Together with the orientifold involution the Sen limit gives a description of

$$\text{Type IIB on } M/(-1)^{F_L} \cdot \Omega \cdot \sigma \,. \qquad (2.3.11)$$

There are many more F-theory compactifications on elliptic $(n + 1)$-folds than weakly coupled type IIB compactifications on n-folds. In general it is impossible to find a parametrisation of the form in (2.3.2) while keeping the full singularity structure of the fibration. If one insists on writing the Weierstrass coefficients f and g as Sen suggested, one is forced to tune the complex structure moduli, so that a weak coupling limit can be achieved. This amounts to finding an analogue of (2.3.3) and can be very involved. In this case strong coupling effects such as exceptional gauge symmetries and non-perturbative couplings disappear. However, by constructing F-theory models with classical gauge groups which can be realised as brane stacks with orientifold planes, it might be possible to take the Sen limit, and recovering the type IIB branes and compactification geometry. We note here that there exist other versions of weak coupling limits [37]. These have other explicit forms or achieve a constant j-function as opposed to a large-valued j-function. Finally we also note that the limit $\epsilon \to 0$ in the Sen parametrisation renders the fibration singular. To avoid this conceptual problem the so called stable Sen limit was introduced [38], wherein the singularity gets resolved.

2.4 Defining F-theory through the duality with M-theory

Approaching F-theory through type IIB string theory provides a lot of intuition about the four dimensional gauge theory. Symmetries and physical degrees of freedom are often straightforward to evaluate through knowledge about the physics of brane stacks in string theory. It also provides a description of type IIB theory when the coupling is not weak. However, when the string coupling is not weak, and there is no Sen limit available there is a need for another way of defining what F-theory is. The question is, what is F-theory on any elliptically fibered Calabi-Yau variety? By using the T-duality between type IIB and type IIA string theory, and that the strong coupling limit of type IIA theory is the eleven dimensional M-theory a better definition of F-theory is available. In this chapter we review this construction, and use it to describe the physics of elliptic fibrations with singularities in different codimensions.

2.4.1 The F-theory limit

When the string coupling gets large the weakly coupled type IIA supergravity has a dual description. By identifying the string coupling with the radius of a new circular physical dimension the strong coupling limit is the unique eleven dimensional supergravity. This duality lifts at high energies to

a duality between type IIA string theory and a eleven dimensional theory called M-theory. Weakly coupled IIA theory is equivalent to strongly coupled M-theory, and vice versa. The strong coupling limit amounts to infinite radius of the M-theory circle which decompactify to a eleven dimensional theory.

The pure 11D supergravity has a simple spectrum. It consists of the eleven dimensional metric g and a 3-form gauge field C_3 together with the gravitino. This theory is coupled to the two dimensional M2 and five dimensional M5 branes, which origin from the strings and branes in IIA string theory. When compactifying M-theory, these branes may wrap submanifolds and give rise to massive states. The mass of these states are proportional to the volume of the wrapped cycles, and in the compactification limit additional massless states appear.

Four dimensional compactifications of M-theory with $\mathcal{N} = 1$ supersymmetry are obtained by vacuum solutions of the form $M_4 \times X_7$, where X_7 is a real 7-manifold with one covariantly preserved spinor, taking the role of the conserved supercharge. A compact and real Ricci flat 7-fold with a covariantly constant spinor is known as a G_2-manifold as the holonomy group acting on the tangent bundle is G_2. Although the basic principles of these compactifications are known very little model building has been done with G_2 manifolds. [13] This is mainly due to technical obstacles. Until recently, very few explicit constructions of G_2 manifolds were known. Also, since 7-manifolds cannot be complex there is no use of holomorphic quantities or the powerful techniques from algebraic geometry over algebraically closed fields. However, if we compactify M-theory on an elliptically fibered Calabi-Yau manifold all these mathematical tools become available, and we can discuss F-theory from a M-theory point of view.

Compactifying M-theory on a elliptic Calabi-Yau fourfold gives a $\mathcal{N} = 2$ gauge theory in three dimensions. This theory has four conserved supercharges. In what is called the F-theory limit, this three dimensional theory gets lifted to four dimensions by decompactifying along one of the 1-cycles of the fiber torus. This preserves all supercharges and they rearrange into one single Dirac spinor in four dimensions, hence a $\mathcal{N} = 1$ gauge theory. Lets review the F-theory limit in a little more detail for a compactification on a Calabi-Yau fourfold, for a closer treatment see [13]. Locally the homology basis of the torus fiber T^2, the A-cycle and the B-cycle have radii R_A and R_B. In the F-theory limit the fiber volume $\mathrm{Vol}(T^2)$ goes to zero. The first step of the limit amounts to identifying the M-theory circle with one of the fiber cycles, say the A-cycle. By taking $R_A \to 0$ a weakly coupled type IIA theory is obtained. In the second step a T-duality transformation is performed along the B-cycle, giving a type IIB theory on the dual circle woth radius $\tilde{R}_B = \frac{l_s^2}{R_B}$. In the compactification limit $R_B \to 0$ and the dual circle decompactifies and the three dimensional theory turns into a four dimensional theory. Note here that one of the big dimensions has its origin in one of the torus dimensions. This is the opposite of the case when we introduced F-theory through type IIB string theory, where the fiber direction are just a tool, geometrizing the $SL(2, \mathbb{Z})$ symmetry. Note also, that T-dualizing the weakly coupled type IIA theory gives a type IIB theory which is generally not weakly coupled, agreeing with our previous discussion of F-theory as the generalization of type IIB theory to any coupling.

Through the F-theory limit any elliptic, or genus-one fibration defines an F-theory model. Some of these fibrations will have a perturbative type IIB, or a perturbative heterotic formulation but the vast majority have neither. Using M-theory however gives a definition of what we mean by F-theory when the geometry have no immediate interpretation in terms of branes or heterotic bundles.

---

[13]Recent progress [39–41] might bring new interest in G_2 compactifications.

2.5   Gauge theory data from geometry

Having introduced the definition of F-theory through M-theory we are ready to describe the four dimensional gauge theory in terms of the fibration of the F-theory geometry. First we discuss gauge symmetries, abelian and non-abelian ones, and then turn to charged matter and Yukawa couplings. The treatment of global properties of the gauge theory as well as discrete symmetries will be left for the following chapters.

2.5.1   Abelian gauge symmetries

In the sequel we denote by G the non-abelian part of the gauge group of an F-theory compactification on an elliptically fibered Calabi-Yau 4-fold Y_4 over the base manifold $\mathcal{B}$ and denote its Cartan subgroup by H. Let us assume that the singularities of Y_4 responsible for the appearance of a non-abelian gauge group G in codimension-one admit a crepant resolution $\hat{Y}_4$. Expanding the M-theory 3-form C_3 as $C_3 = \sum_i A_i \wedge F_i$ with F_i the resolution divisors gives rise to the Cartan $U(1)$ gauge fields A_i. Therefore the resolution divisors F_i span the coroot lattice $Q^\vee$ of the Cartan subalgebra $\mathfrak{h}$.

We recall that the divisors originating from the fiber in an F-theory compactification are either the classes of rational sections or resolution divisors. In this chapter we discuss the physics of the rational sections. If σ is a rational section it defines a divisor on the elliptic fibration. The Poincaré dual of the divisor class $[\sigma]$ is a two-form $w \in H^{1,1}(X)$. We denote by x the local coordinates of the compact manifold X, and y is the position in the Minkowski three-space $M^{1,2}$ factor of the M-theory background. Any solution for the three-form field can be expanded in the homology if the compact space, each homology class beeing represented by a unique harmonic form. Hence we can write

$$C_3 = A^i(y) \wedge w_i(x) + \dots \tag{2.5.1}$$

and we see that any harmonic two-form w_i give rise to a corresponding 1-form A^i in the three-dimensional field theory. This one form field has a $U(1)$ gauge symmetry which descends from the gauge transformation $C_3 \to C_3 + d\Lambda_2$ in the eleven dimensional theory. In other words, it is a $U(1)$ gauge field. In three dimensions any rational section correspond to a $U(1)$ gauge field. Note especially that the existence of abelian gauge symmetry is a global property of the fibration. It does not refer to special loci in the base and in particular not to the codimension one singularity structure. In order to have a $U(1)$ gauge field in four dimensions the three dimensional one form must lift to a one form in four dimension. Not all rational sections will give rise to extra $U(1)$ gauge group factors. One will be of another nature. This is because lifting the three dimensional theory to four dimensions is done on a circle. In one limit this circle goes to zero radius and we have a three dimensional theory. In the other limit the circle grows to infinite size, and the gauge theory is four dimensional. This is analogous to the classical Kaluza-Klein theory, where gravity in $n + 1$ dimensions is compactified on a circle, and gives rise to gravity plus electromagnetism in n dimensions. The extra one form is the gravi-photon and has its origin in the metric. This will happen also in the F-theory limit, and one of the abelian gauge fields in three dimensions will correspond to the gravi-photon, or the Kaluza-Klein (KK) $U(1)$ gauge field.

The Shioda map in F-theory

The Mordell-Weil group, as introduced previously in this chapter is not generated by all independent rational sections. The zero-section σ_0, being the trivial element of $E(K)$, is not a generator, and a generating set of the Mordell-Weil group can be taken to be

$$\{\sigma_i - \sigma_0\} \tag{2.5.2}$$

for all $\sigma_i \neq \sigma_0$. The rank of this group is the number of rational sections in addition to the zero section. Each section gives rise to a divisor class. The Shioda map is a homomorphism

$$\varphi : E(K) \to NS(X) \otimes \mathbb{Q} \tag{2.5.3}$$

from the Mordell-Weil group to the Neron-Severi group of all divisors, where the linear combinations are taken with rational coefficients. Explicitly the Shioda map takes

$$\varphi(\sigma) \equiv W = [\sigma] - [\sigma_0] - \pi^{-1}(\delta) + \sum l_i F_i \,, l_i \in \mathbb{Q} \tag{2.5.4}$$

where δ is a divisor on $\mathcal{B}$ and the F_i are resolution divisors. The coefficients l_i and the class δ are determined by demanding that the intersection numbers

$$\int_X W \wedge Z \wedge D_a \wedge D_b,$$
$$\int_X W \wedge D_a \wedge D_b \wedge D_c, \tag{2.5.5}$$
$$\int_X W \wedge F_i \wedge D_a \wedge D_b$$

vanish for all D_i, which are divisor classes pullbacked from $\mathcal{B}$. This is just the statement made below (2.1.23), that the image of the Shioda map has zero pairing with all divisors in $\mathcal{T}$. The first two conditions are often referred to as the *one leg in the fiber condition* and ensure that the divisor W do not lie completely in the base or fill up the full fiber, respectively. Intuitively we want the divisor class, or equivalently the two-form w to have support along only one of the fiber dimensions, since only one of them decompactifies in the F-theory limit. The three dimensional gauge field then lifts to a four dimensional field along this direction. The third condition expresses that W is orthogonal to the resolution divisors F_i, which define the Cartan $U(1)$ generators in the case where there are non-abelian gauge factors coming from codimensions one singularities. The combination $W \wedge D_a$ in (2.5.5) is a so called vertical flux in $H^{2,2}(X)$. This can achieve any vacuum expectation value, which can be used to engineer a chiral spectrum. If the one-leg condition is not fulfilled, this vacuum expectation value breaks Lorentz invariance in four dimensions. Furthermore, if the last condition is not fulfilled, this flux will break the gauge group. The discussion on valid fluxes is treated in more detail in section 2.6 and in chapter 5.

2.5.2 Non-abelian gauge symmetries

Lets turn to the next class of fibral divisors in an elliptic, or genus-one fibration. The resolution divisors F_i of a codimension one singularity are localized, as opposed to the sections responsible for abelian gauge groups. If θ denotes the divisor class in the base, over which the fiber degenerates and the irreducible fiber components are the curves $\mathbb{P}^1_i$ then

$$\mathbb{P}^1_i \hookrightarrow F_i \to \theta \tag{2.5.6}$$

are the resolution divisors. Each is given by the fibration of one irreducible curve along over the divisor θ in the base. We have seen that singularities in the F-theory geometry correspond to branes in the type IIB theory. The gauge bosons origin from open string states, confined along the world-volume of the branes. In F-theory and in particular the M-theory description of F-theory the gauge bosons arise from M2 branes wrapping the irreducible fiber components over these loci in the base. As in the open string case, these states are localized, as the resolution divisors are fibrations over the very same loci. In the compactification limit, the volume of the resolution divisors goes to zero, and as

the masses of the wrapped brane states are proportional to the cycle volume these become massless vectors. To construct all gauge bosons in the adjoint representation we have to consider two cases. As in the case of an abelian group factor, the resolution divisors F_i are dual to harmonic two-forms w_i, and expanding

$$C_3 = A_i \wedge w_i + \cdots \tag{2.5.7}$$

gives rise to one form fields A_i. This gives the Cartan elements of the non-abelian gauge group. To fill out the full adjoint representation of the gauge group, that is the off-diagonal elements one must also take into account states from branes wrapping more than one fiber component. In the $SU(n)$ case there are $n-1$ Cartan $U(1)$'s from the resolution divisors. In addition the $M2$ branes can wrap chains

$$S_{ij} = \mathbb{P}_i \cup \mathbb{P}_{i+1} \cup ... \cup \mathbb{P}_j, \ i \le j \tag{2.5.8}$$

of adjacent fiber components over θ. Taking both orientations into account this gives $n^2 - n$ different states corresponding to the off-diagonal W bosons of the $SU(n)$. Together thy form the $n^2 - 1$ dimensional adjoint representation [13]. This logic can be repeated and reproduces the adjoint states of also the D and E-type Lie groups.

2.5.3   Charged matter representations

At codimension two loci in the base, where two of the discriminant factors meet, the degeneration of the fiber generally enhances. We can illustrate this through the following toy model, which is not an elliptic fibration. Consider the non-compact hypersurface

$$x^2 + y^2 = b_1^m b_2^n \tag{2.5.9}$$

in an ambient space $\mathbb{C}^2 \times \mathcal{B}$. Here x and y are coordinates of the first factor, playing the role of fiber coordinates, and b_i are some functions on the base $\mathcal{B}$. At the codimension one loci in the base where $b_1 = 0$ and $b_2 = 0$, the hypersurface is singular, and the singularity type is A_{m-1} and A_{n-1} respectively. If this were an F-theory background, the gauge group would be $SU(m) \times SU(n)$. At the codimension two locus where $b_1 = b_2 = 0$, we can write the hypersurface as $x^2 + y^2 = b_1^{m+n}$, and the singularity type enhances to A_{m+n-1}. This is reminiscent of the discussion of brane stacks around (2.0.7) and we can think about this enhanced singularity as the breaking of a larger gauge group. From this viewpoint we think about the larger $SU(m+n)$ gauge factor as the starting point, and when the codimension two locus factors into two codimension one loci we obtain two gauge group factors. By branching the adjoint representation into $ad(SU(m)) \oplus ad(SU(n))$ one get also two bifundamental representations, which host matter states charged under the gauge group.

In type IIB string theory these extra charged matter states are due to open strings between different brane stacks, see fig. 2.1. In the F-theory language we recall that the fibration is smooth, and that all singularites are resolved. This implies that over the enhancement loci in the base, there are more fiber components. In explicit examples one find that one or more irreducible curves in the fiber over $\{b_1 = 0\}$ factors, or become reducible when $b_2 = 0$. The wrapping of M2 branes on these extra curves gives rise to states which are localized and charged under the gauge factors that meet.

The representations in which the charged matter transform can be obtained directly from the geometry. The above case makes use of the local enhancement, and branching rules. This does not always work, and one must check explicitly what states appear and how the transform. The world-volume action of the M2 brane contains the term

$$\int_{Vol(M2)} C_3 \tag{2.5.10}$$

analogous to the world line action $q \int A_\mu dx^\mu$ for a particle with charge q under a $U(1)$ gauge field A. Let C be a curve in $\mathcal{B}$ over which some fiber component split. We denote by $\mathbb{P}^1_k$ the split curve in the fiber, which is fibered over C. Using the expansion (2.5.7) we get from a M2 brane wrapping this split curve

$$\int_{C \times \mathbb{P}^1_k} A^i \wedge w_i = \int_{\mathbb{P}^1_k} w_i \int_C A^i \equiv (\mu_i)_k \int_C A^i \,. \tag{2.5.11}$$

The two forms w_i are dual to the resolution divisors F_i. The last term is the world-line action of the charged particled and the prefactor is the intersection numbers of the split curves with the divisors so we write

$$(\mu_i)_k = F_i \cdot \mathbb{P}^1_k \tag{2.5.12}$$

in homology. These numbers are interpreted as the charges with respect to the diagonal $U(1)$'s A_i of the non-abelian gauge group. These intersection numbers are thus the eigenvalues of the Cartan generators F_i, i.e the weights of the representation in which the state transform [42]. This way the charged matter representations are defined directly through the geometry, without referring to the brane analogy and can be effectively computed in explicit models.

Note here, that obtaining the weights of the representations as topological intersection numbers relies on the intersection pairing between curves and divisors. This applies also away from non-abelian degeneration loci. In the case of abelian symmetries the charged matter appear as new fiber components over a codimension two locus which does not lie in a non-abelian divisor in $\mathcal{B}$. Recall that the existence of an extra rational section is equivalent to an extra rational solution to the Weierstrass equation. This implies, for a fully resolved model, that the hypersurface equation factors over a codimension two locus. We can take the so called $U(1)$ restricted model as an example. This is the Tate model, restricted to the part of the moduli space where the coefficient section a_6 vanishes identically. This introduces a codimension two singularity which is resolved by a blow-up in the ambient space. This gives a ambient divisor class $S : \{s = 0\}$, which restricts to an extra fiber component over the locus in the base where the singularity appear. The resolved form [31] is

$$sy^2 + a_1 sxyz + a_3 yz^3 = s^2 x^3 + a_2 sx^2 z^2 + a_4 xz^4 \tag{2.5.13}$$

and at the locus in $\mathcal{B}$ where $\{a_3 = a_4 = 0\}$ it factorizes as

$$s(y^2 - sx^3 + a_1 xyz - a_2 x^2 z^2) = 0 \,. \tag{2.5.14}$$

Each of the two factors above defines an irreducible fiber component, topologically equivalent to a sphere, denoted $\mathbb{P}^1_i$ for $i = 1, 2$. The $U(1)$ charges of the states coming from wrapping an $M2$ brane on these curves are given by the intersection number

$$W \cdot [\mathbb{P}^1_i] \tag{2.5.15}$$

of the Shioda map W of the extra section and the class of the fiber component. This type of computation will occur frequently in the following chapters, for different hypersurface equations and for more than one matter curve in the base. Note also that singularity enhancement does not only occur at the intersection of two different codimension one loci, but can also appear as self-intersection loci of a single divisor in the base.

2.5.4 Yukawa couplings

To have interaction terms, or Yukawa couplings between the matter fields we must go to codimension three in the base $\mathcal{B}$, or in the fourfold X. A codimension three locus in the base is a point, and is

referred to as a Yukawa point in this case. Since the charged matter is localized along curves in the base, the interaction terms are only possible where two or more such curves meet. Again we can use the type IIB intuition, using a setup with three stacks of branes. Generically they intersect along three matter curves, which meet in a point. Localized matter propagating along the curves may meet, or interact at the intersection point. To obtain a interaction term in the four dimensional field theory, the three fields has to form a gauge singlet.

In the F-theory fibration the Yukawa point is the intersection point of matter curves. Each matter curve has its corresponding singularity, or in the resolved model, its particular tree of intersecting irreducible curves in the fiber. Over the point where the matter curves meet, there is a further enhancement of the singularity. In the smooth geometry this means that further curves in the fiber split by further factorization of the hypersurface equation over this point. In the simplest case the curve $\mathbb{P}^1_{R_a}$, which gives rise to a state in the representation R_a of the gauge group split into the homological sum $\mathbb{P}^1_{R_b} + \mathbb{P}^1_{R_c}$. Branes wrapping these two curves give rise to charged matter states in representations R_b and R_c respectively. If the states in the three representations can be combined into a gauge singlet then this is a coupling in the four dimensional theory. In general the matter states correspond to sums of the fiber components, and arise from branes wrapping multiple irreducible curves. To find gauge singlets from the geometry one can however use that fact the the full fiber class is uncharged under the gauge groups. The homological sum of all fiber components, including multiplicities, is the class of the full fiber which has zero charge with respect to both the abelian and non-abelian Cartan generators. Therefore, if one can arrange the fiber components into three groups, the homological sum of each group of curves correspond to a state in a certain representation, and these three states form a gauge singlet since the total charge is zero. In homology [43] this is the statement that the sum of the three curve classes associated with weights is trivial modulo the fiber class. It follows that there is a 3-chain Γ whose boundary consist of these curves i.e

$$\partial\Gamma = \sum_a [C_{R_a}] \tag{2.5.16}$$

where $[C_{R_a}] = [\sum n_i \mathbb{P}^1_i]$ for fiber components $\mathbb{P}^1_i$ with multiplicities n_i. This three-chain can be thought of as the equivalent of a Feynman rule vertex for the $M2$ brane states.

2.6   Fluxes in F-theory

In addition to the background geometry of a four-dimensional F-theory compactification, specifying the metric g, there is a freedom in the choice of vacuum expectation value for the field strength $G_4 = dC_3$. For F-theory model building the G_4 flux is essential as it is the source of chirality in the matter spectrum, can be used for gauge symmetry breaking in GUT models and has to be included for moduli stabilization [14]. In the following we briefly review the background on F-theory fluxes and their properties. Extra focus will be put on the transversality condition to provide a foundation for the developments presented in 5.

By considering M-theory on a Calabi-Yau fourfold it was shown [44] that in order to have a solution to the supersymmetric equations of motion that the form of the G_4 flux is restricted. The only non-trivial flux solution is of cohomology type $(2,2)$, i.e an element of $H^{2,2}(X)$. Second, the flux solution must be primitive in the sense of Lefschetz decomposition. For J the Kähler form of the fourfold

$$\int_X G_4 \wedge J \wedge D = 0 \tag{2.6.1}$$

---

[14]This is to a large extent an open problem in F-theory.

must hold for any two-form class D on X. This is usally stated shortly as $G_4 \wedge J = 0$. In addition the flux has to be properly quantized [45], which can be stated as

$$G_4 + \frac{c_2(X)}{2} \in H^4(X, \mathbb{Z}) \cap H^{2,2}(X_4) \tag{2.6.2}$$

in the case of M-theory on a Calabi-Yau fourfold. $c_2(X)$ is the second Chern class of the the tangent bundle of X [15]. For smooth elliptic fibrations the second Chern class is always even [46, 47], and thus the flux is integral. Odd second Chern classes are only due to effects from (resolved) singularities, and if this is the case a non-trivial flux solution has to exist in order to satisfy (2.6.2). We will comment more on the quantization condition in relation to discrete anomalies in chapter 5.

The 7-brane charges in F-theory is entirely encoded in the singularities. The charges of 3-branes and 5-branes in type IIB other the other hand are induced by the flux configuration. The D3 brane is especially interesting as it is an $SL(2, \mathbb{Z})$ invariant. This is seens as it couples electrically to the 4-form field C_4 which is a $SL(2, \mathbb{Z})$ singlet. The net D3 charge is the difference of number of D3 branes and anti-D3 branes and is given by

$$n_{D3} = \frac{\chi(X_4)}{24} - \frac{1}{2} \int_{X_4} G_4 \wedge G_4. \tag{2.6.3}$$

This relation is known as the D3-tadpole condition. As seen there are two sources for D3 charge. The first term is the Euler number of the fourfold, $\chi(X_4) = \int_{X_4} c_4(X_4)$ and sums up curvature contributions to n_{D3}. The second term is the flux-induced tadpole. If n_{D3} is negative, there is a net number of anti-D3 branes and gives a possibly unstable vacuum with broken supersymmetry. Thus, the amount of flux that can be introduced is limit from above by the Euler number.

2.6.1 The transversality condition

In an F-theory compactification some symmetries are generally desired to survive the F-theory limit. In particular for model building the four dimensional Lorentz symmetry is to be respected, and the carefully constructed gauge symmetries from the fibration as well. Introducing an arbitrary G_4 flux of the right type will generally break some or all of these symmetries. The solutions to the flux transversality conditions which we introduce here are precisely the flux configurations that respect the Lorentz and gauge symmetries in four dimensions. We will only consider fluxes on elliptic fibrations here, as consistent flux solutions on genus-one fibrations is the main result which underlies chapter 5.

Recall that in the F-theory limit relies on a T-duality transformation along one of the 1-cycles of the fiber. This compact direction grows to one of the macroscopic spatial directions in four dimensions. One immediate consequence is that care must be taken when introducing fluxes [44, 48]. Since the flux is a tensor quantity Lorentz invariance in four dimensions forbids fluxes with non-trivial vacuum expectation value along the circle along which the T-dualization is performed [49]. More precisely, the G_4 flux must have *one leg in the fiber* to meet this requirement. Indeed, in [49] it was shown that a flux with zero or two legs along the fiber maps to the self-dual 5-form flux F_5 in type IIB string theory. In this case the vacuum expectation value extends along the non-compact directions and breaks Lorentz invariance. The remaining possibility is a flux with one (real) leg in the fiber. These solutions do not lie completely in the base, nor do they fill the two fiber directions. For the elliptically fibered 4-fold

$$\pi : X_4 \to \mathcal{B} \tag{2.6.4}$$

---

[15]For M-theory on a general spin 8-manifold, the second Chern class is replaced by the first Pontryagin class.

with projection π this transversality condition [49] is usually expressed in slightly more formal terms as follows: By definition, an elliptic fibration has a zero section $\sigma^{(0)} : \mathcal{B} \to X_4$ which defines an embedding of the base $\mathcal{B}$ as a divisor $\sigma^{(0)}(\mathcal{B})$ into X_4,

$$\iota_\sigma : \sigma^{(0)}(\mathcal{B}) \hookrightarrow X_4. \tag{2.6.5}$$

For an elliptic fibration with a Mordell-Weil group of non-zero rank, i.e in the presence of several independent sections the choice of zero-section is not unique [50, 51]. However the different choices of identity element in the Mordell-Weil group all asymptote to the same effective theory in the F-theory limit.

Let us assume that one particular section is chosen as our zero-section and with Z we denote its homology class. For simplicity we assume the zero-section to be holomorphic, but this is not necessary [50, 52]. If the zero section is meromorphic it may wrap fiber components in codimension two. In this case it is possible to take a linear combination with base divisors that have intersection number one with all fibers, effectively acting as a holomorphic section. From the perspective of the 3-dimensional M-theory effective action, Z generates a $U(1)$ gauge group which is to be identified with the Kaluza-Klein $U(1)$ obtained by reducing the 4-dimensional F-theory compactification along a circle S^1 (see section 2.4.1, and for a recent discussion in the language of 3-dimensional supergravity [53]).

As discussed above the effective action light charged matter states arise from M2-branes wrapping suitable fibral curves [54–57]. This includes both the non-Cartan vector bosons and extra charged localised matter. More precisely, each component field $\Psi(y, z)$ of an $\mathcal{N} = 1$ multiplet of the 4-dimensional F-theory action decomposes, upon circle reduction to three dimensions, to a zero mode plus a full tower of Kaluza-Klein (KK) excitations $\Psi(y, z) = \sum_{n \in \mathbb{Z}} \psi_n(y) e^{inz}$. As before, y denotes external coordinates in the 3-dimensional M-theory vacuum and z is the KK-circle coordinate. The $U(1)$ charge of the higher KK states is given by the intersection number $n = \int_{C_n} Z$ of the zero-section and C_n, the fibral curve wrapped by the M2-brane associated with state $\psi_n(y)$. Since Z is a section, it has intersection number $+1$ with a generic non-degenerate fiber. This is still true for split fibers in higher codimension, but not all components of the fiber will intersect Z. The zero mode ψ_0, which has zero $U(1)_{KK}$ charge thus arise from M2-branes wrapping a fibral curve C_0 with vanishing intersection with the zero-section Z. As Z has intersection number one with the full fiber $\mathfrak{f}$ the ascending KK state of $U(1)_{KK}$ charge n is then created by an M2-brane wrapping in addition the full elliptic fiber n times such that its associated fibral curve can be written as $C_n = C_0 + n\mathfrak{f}$.

In terms of intersection numbers of (co-)homology classes the transversality condition of [49] takes the form (e.g. [31, 58–61])

$$\int_{X_4} G_4 \wedge Z \wedge \pi^{-1} D_a \overset{!}{=} 0, \tag{2.6.6}$$

$$\int_{X_4} G_4 \wedge \pi^{-1} D_a \wedge \pi^{-1} D_b \overset{!}{=} 0 \tag{2.6.7}$$

for $D_{a,b}$ any divisor classes on the base.[16] The first condition (2.6.6) guarantees that G_4 does not lie completely in the base because the zero section as an embedding of the base ensures that

$$\int_{X_4} G_4 \wedge Z \wedge \pi^{-1} D_a = \int_{\sigma^{(0)}(\mathcal{B})} \iota_\sigma^*(G_4 \wedge \pi^{-1} D_a) \overset{!}{=} 0. \tag{2.6.8}$$

We read this as the vanishing of the net flux through any 4-cycle D_a on the base. The second condition (2.6.7) expresses that the solution cannot have two legs along the fiber. This condition can be rephrased

---

[16]For ease of notation we will oftentimes omit the explicit pull-back symbol through this thesis. From the context it will be clear which divisors comes from the base.

as the constraint that the chiral index of all KK partners equals that of the zero mode. Indeed the intersection $\pi_X^{-1} D_a \cap \pi_X^{-1} D_b$ is a 4-cycle extending along the full fiber over a curve $D_a \cap D_b$ in the base and $\int_{\pi_X^{-1} D_a \cap \pi_X^{-1} D_b} G_4$ computes the chiral index of states associated with M2-branes wrapping the full fiber over $D_a \cap D_b$. The fiber curves associated with the different KK states differ only by a multiple of the fiber class. Hence, if the integral over any 4-cycle of this type vanishes, this guarantees in particular that the multiplicities of the fields ψ_n are the same for all n. This is the field theoretic way of stating the requirement of Lorentz invariance. A discussion along these lines can also be found e.g. in [62, 63].

In models with non-abelian gauge symmetries the Cartan generators correspond to the exceptional divisor classes F_i from the resolution of the singularity. Introducing flux we must in addition demand that

$$\int_{X_4} G_4 \wedge F_i \wedge \pi^{-1} D_a \stackrel{!}{=} 0 \qquad (2.6.9)$$

in order to leave the non-abelian gauge group unbroken in the F-theory limit. Recall from section 2.5.2 that the M2-branes that wrap combinations of the rational fibers $\mathbb{P}_i^1$ of the resolution divisors F_i give rise to non-abelian massless vector bosons in the F-theory limit [54]. Flux configurations that respect (2.6.9) induces no chiral index for the associated gauginos. If all but one of the equations (2.6.9) are satisfied the F-theory gauge group will be broken to the commutant of the associated Cartan generator. This is utilized for example in models with hypercharge GUT breaking [64, 65].

We can now give some examples of fluxes that satisy the transversality conditions. In type IIB theory both the closed and open string sector contributes to the set of possible fluxes [44]. The former case include the H_3 and F_3 fluxes corresponding to the B_2 and C_2 form fields. The second possibility is brane fluxes f from localized one form fields along branes. In F-theory defined through M-theory both kinds of fluxes are unified into G_4. The brane fluxes f arise from so called *vertical* fluxes in F-theory. These fluxes are elements of $H^{1,1}(X_4) \wedge H^{1,1}(X_4) \subset H^{2,2}(X_4)$ and the simplest such flux is of the form $w \wedge f$ where the two form w correspond to a $U(1)$ generator and f is the pullback of a divisor class on the base. Thus the divisor class $[w]$ correspond either to an element in the Mordell-Weil group or to a Cartan generator of a non-abelian gauge group.

The so called Cartan fluxes are of the form $F_i \wedge \pi_X^{-1} D$ for any class D pulled back from the base. Because the holomorphic zero-section intersects precisely the affine node of the Kodaira fiber over a divisor with non-abelian gauge group the condition (2.6.6) is fulfilled by all the Cartan fluxes. Therefore the special case of (2.6.6) for $G_4 = F_i \wedge \pi_X^{-1} D$ is the condition that the KK $U(1)$ is chosen 'orthogonal' to the non-abelian gauge group. If $[w]$ correspond to an element of the Mordell-Weil group the transversality conditions for the flux $w \wedge f$ are identical with the construction of the $U(1)$ generator through the Shioda map. This means that for any F-theory compactification with abelian gauge factors, there are corresponding flux configurations that can be consistently turned on.

The G_4 fluxes that are not wedge products of two-forms are generally hard to describe and write down explicitly. The fourth cohomology groups of elliptically fibered fourfolds are often large, which makes the problem not only technical, but also computationally intensive. In chapter 5 we will construct one example of a flux that cannot be written as a wedge product of $(1,1)$-forms.

Chapter 3

Non-simply connected gauge groups in F-theory

The non-abelian gauge symmetries are directly linked to the codimension one singularities of the F-theory fibration. The resolution divisors are identified with the Cartan generators of the Lie algebra of the gauge group. The field theory in four dimensions has as gauge symmetry a Lie group whose Lie algebra is given by the geometry. This can be ambiguous. For example, if the discriminant factors such that there is a A_1 singularity over a certain locus in the base the gauge algebra is $\mathfrak{su}(2)$. In this case the gauge group can be either $SU(2)$ or $SO(3) \approx SU(2)/\mathbb{Z}_2$, since they share the same Lie algebra. For a pure gauge theory with only local operators there is no difference between these two gauge theories. If non-local operators e.g line operators are included there is however a difference [66]. More striking differences are found when including matter. $SO(3)$ has no spinor representation, while its double cover $SU(2) \approx Spin(3)$ has the two dimensional spinor representation [1]. The Lie group $SU(2)$ is simply connected, $\pi_1(SU(2)) \approx 0$, while $SO(3)$ is a non-simply connected group with $\pi_1(SO(3)) \approx \mathbb{Z}_2$.

Another example is the Standard Model, where all matter representations are invariant under the $\mathbb{Z}_6$ subgroup of the center $\mathbb{Z}_3 \oplus \mathbb{Z}_2 \oplus U(1) \subset SU(3)_c \times SU(2)_L \times U(1)_Y$. This indicates that the gauge group is in fact $(SU(3)_c \times SU(2)_L \times U(1)_Y)/\mathbb{Z}_6$ [67]. This can be put into a GUT perspective. The smallest simple Lie group that contains the Standard Model gauge group is $SU(5)$. Embedding the Standard Model into this unifying group amounts to a choice of a block diagonal form $S(U(3) \times U(2)) \subset SU(5)$ with unit determinant. Group theoretically $S(U(3) \times U(2))$ is isomorphic to $(SU(3) \times SU(2) \times U(1))/\mathbb{Z}_6$, following [68].

The main result in this chapter is that torsion elements in the Mordell-Weil group give rise to four dimensional gauge theories with non-simply connected gauge groups. The first result on this relation [69] considered eight dimensional compactifications. The duality with heterotic string theory was used to show that the torsion subgroup of the Mordell-Weil group is isomorphic to the fundamental group of the gauge group. This was conjectured to hold also in six dimensional F-theory models [57]. The results presented in this chapter gives a constructive method for determining the fundamental group of the gauge group also in any F-theory model, in particular in four dimensional compactifications. In F-theory we do not directly see the difference between one gauge group or a finite quotient thereof, since the singularity only provides information about the Lie algebra. However the matter spectrum will indicate what the possible gauge group of the theory is. If the F-theory model of the above example features a curve in the base over which states in the two dimensional representation are localized, then the gauge group has to be $SU(2)$, since no such representation of $SO(3)$ exist. The theoretical background and the presentation of explicit examples with a non-simply connected gauge group is the

---

[1]Quotienting out the $\mathbb{Z}_2$ center of $Spin(3)$ projects out all half-integer spin representations.

main content of this chapter.

Recall that the Shioda map associates a divisor class to every rational section. For rational sections that generate the free part of the Mordell-Weil group the divisor classes are non-trivial. The Shioda map of a torsion element of the Mordell-Weil group is a trivial divisor on the fibration. By using this fact we construct a divisor class corresponding to an element in the coweight lattice. As such it has integer pairing with any element of the weight lattice or in other words, it has integer intersection numbers with all curves corresponding to matter states. As the Shioda map gives a divisor class as a fractional linear combination of resolution divisors, this integer pairing is non-trivial. The only possible matter representations are the ones which are integrally paired with the new coweight. The center and the fundamental group of the gauge group may be computed from this relation between the weight and the coweight lattices.

This chapter is largely based on [9]. In particular the explicit models presented are the same. Related work include [20, 69, 70]. We first give the general structure and make the connection between torsional sections, divisor classes and the representation theory. The theory is then applied to explicit examples. We study fibrations that has a description as hypersurfaces in toric varieties we consider a number of different models with non-abelian as well as abelian gauge factors. Out of the 16 toric realizations as reflexive polygons three hypersurface equations have non-trivial Mordell-Weil torsion. The Mordell-Weil groups of these fibrations are $\mathbb{Z}_2, \mathbb{Z}_3$ and $\mathbb{Z} \oplus \mathbb{Z}_2$. The first two cases appeared in [69] and the third one can be seen as a restriction of the first one that results in one new rational section. A generic hypersurface equation have no torsion sections [2]. The specialization that ensures the existence of torsion sections also imply that there are a non-abelian singularity in codimension one. In addition, using the classification of toric tops [19, 71] we implement further non-abelian singularities, more intricate matter spectra and show how the new coweight have integral pairing with all weights.

The torsion subgroup of the Mordell-Weil group has also been studied via string junctions and configurations of (p, q)-branes [72]. As the paper [69] this approach is also eight-dimensional and reproduces the classification of Mordell-Weil lattices for elliptic surfaces [24]. Subsequent work addressed the same problem for elliptic threefolds [73]. In this thesis we will not comment further on this approach.

3.1 Torsional sections and divisor classes

Throughout this chapter we consider a singular elliptic fourfold Y_4 and its crepant resolution $\hat{Y}_4$. Lets start by considering the divisor class R of a torsional meromorphic section $[\sigma_r]$ of order k. The corresponding generator of the Mordell-Weil group is $\sigma_r - \sigma_0$ such that $R - Z$ is a generator of the torsional part of the Mordell-Weil group of $\hat{Y}_4$. In section 2.2.3 we saw that the image of a torsion element under the Shioda map is trivial, since the Neron-Severi group is torsion-free. The divisor class of a torsion section is not independent and hence it exists some linear combination of resolution divisors F_i such that

$$\Sigma := R - Z - \pi^{-1}(\delta) + \frac{1}{k} \sum a_i F_i \qquad \text{with} \quad a_i \in \mathbb{Z} \tag{3.1.1}$$

is trivial in $NS(\hat{Y}_4) \otimes \mathbb{Q}$ and thus in particular in $H^2(\hat{Y}_4, \mathbb{R})$. Indeed, as described in section 2.2.3, it is guaranteed that $R - Z$ can be expressed as a linear combination with $\mathbb{Q}$ coefficients of the generators of $\mathcal{T}$, the subgroup of $NS(\hat{Y}_4)$ generated by $[\sigma_0]$, the resolution divisors F_i and $\pi^{-1}(\delta)$ for some divisor class δ on $\mathcal{B}$. Thus, $R - Z$ minus this linear combination is trivial in $NS(\hat{Y}_4) \otimes \mathbb{Q}$. By constructing

---

[2]One may view the toric constructions as realizing the most general form *with* this prescribed Mordell-Weil group.

the Shioda map one obtain a specific such linear combination of the form (2.1.25) as

$$\varphi(R - Z) = R - Z - \pi^{-1}(\delta) + \sum_i l_i F_i. \tag{3.1.2}$$

The rational numbers l_i are in fact of the form $\frac{a_i}{k}$ with $a_i \in \mathbb{Z}$. Since φ is a homomorphism, $\varphi(k(\sigma_r - \sigma_0)) = k(R - Z - \pi^{-1}(\delta) + \sum_i l_i F_i)$ and this must be trivial in $NS(\hat{Y}_4) \otimes \mathbb{Q}$ because $\sigma_r - \sigma_0$ is k-torsion. The homomorphism φ map identify the identity elements of respective groups and thus $R - Z - \pi^{-1}(\delta) + \sum_i l_i F_i$ is trivial in $NS(\hat{Y}_4) \otimes \mathbb{Q}$, as claimed above.

In our examples $\hat{Y}_4$ is given by a hypersurface equation in an ambient toric variety. In these fibrations the class $-k\Sigma$ turns out to be a toric divisor on the toric ambient space which does not intersect the Calabi-Yau hypersurface $\hat{Y}_4$. Furthermore, in the toric examples we will consider the base divisor δ will be given by $\bar{\mathcal{K}}_{\mathcal{B}}$, the anti-canonical divisor of $\mathcal{B}$. If the hypersurface equation is homogeneous with respect to further line bundle classes on $\mathcal{B}$ our examples generalize correspondingly.

Since $[\Sigma]$ is trivial as an element of $H^2(\hat{Y}_4, \mathbb{R})$, it does not define an extra $U(1)$ generator as would be the case if σ_r were a non-torsional rational section. Since discrete symmetries in string theory arise as broken gauge symmetries we do not see $\mathbb{Z}_k$ symmetry factors arising from torsion sections. The origin of discrete symmetry factors is treated in detail in the next chapter. We may use the triviality of Σ in $NS(\hat{Y}_4) \otimes \mathbb{Q}$ to define the class

$$\Xi_k \equiv R - Z - \pi^{-1}(\delta) = -\frac{1}{k} \sum_i a_i F_i, \quad a_i \in \mathbb{Z}, \tag{3.1.3}$$

which defines an element in $H^2(\hat{Y}_4, \mathbb{Z})$. The left hand side is by construction valued in the integer cohomology and thus the right hand side is integral as well, though the form suggests otherwise. In the explicit examples we will see that the pairing of this divisor class with all matter curves is indeed integer.

At a first glance one may guess that the k-torsional section in the elliptic fibration induces a k-torsional element in $H^2(\hat{Y}_4, \mathbb{Z})$. The fibrations with Mordell-Weil torsion always come with codimension one singularities which have to be resolved. The resolution divisors F_i provide an obstruction to having torsion in cohomology. Indeed, from (3.1.3) we see that while the class $[\Xi_k]$ is not torsion in the cohomology $H^{1,1}_{\mathbb{Z}}(\hat{Y}_4) = H^2(\hat{Y}_4, \mathbb{Z}) \cap H^{1,1}(\hat{Y}_4)$, it does represent a k-torsional element in the quotient cohomology $H^{1,1}_{\mathbb{Z}}(\hat{Y}_4)/\langle [F_i] \rangle_{\mathbb{Z}}$ of classes modulo integer linear combinations of resolution classes. Namely,

$$k \cdot [\Xi_k] = -\sum_i a_i [F_i] = 0 \mod f \in \langle [F_i] \rangle_{\mathbb{Z}}, \tag{3.1.4}$$

which establishes $[\Xi_k]$ as k-torsion up to resolution divisors. Hence we can think of torsion sections as giving rise to a kind of torsion in (co-)homology, but torsion homology cycles will not play a role when compactifying this theory. In section 3.3.1 we give an intuitive argument of why such a torsional element arise in the elliptic fibrations studied in the examples.

3.2 The global structure of the gauge group in presence of Mordell-Weil torsion

In the previous section we outlined the properties of a torsional section and its associated divisor class. The two main main conclusions is that a torsional element of the Mordell-Weil group does not give rise to a independent divisor class nor to torsion in homology. Hence we do not have an extra $U(1)$ symmetry nor a discrete $\mathbb{Z}_k$ selection rule [74] in the four dimensional compactification. By analyzing

the representation theory we will put the torsional section into the context of the lift from the gauge algebra to the gauge group. This determines the global structure of the gauge group and implies restrictions on the matter spectrum.

The non-abelian gauge algebra $\mathfrak{g}$ in an F-theory compactification on $\hat{Y}_4$ is dictated entirely by the resolved fibers in codimension one. The algebra $\mathfrak{g}$ governs the local behaviour of the gauge group G and can be defined through a linear expansion around the identity element of G. The global structure of G can generally not be obtained only by the knowledge of the algebra. When the algebra and the representation content are known, then G can be obtained and we will outline this theory in this section.

For any state in a representation of $\mathfrak{g}$ there is a corresponding weight vector, see e.g [75, 76] [Slansky] for background on the representation theory of Lie groups and algebras. Each component of this vector are the eigenvalues of the Cartan generators acting on the state. Thus, a n-dimensional representation can be seen as a certain collection of n weight vectors, or shortly: weights. All weights in all representations of $\mathfrak{g}$ that occur lie in the weight lattice Λ. The root lattice $Q \subset \Lambda$ is the smallest sublattice of Λ that contains the weights in the adjoint representation. It is spanned by the simple roots. Both these lattices have dual lattices $\Lambda^\vee$ and $Q^\vee \subset \Lambda^\vee$ containing the coweights and coroots respectively. Any element of the coweight lattice is, by definition, integrally paired with an element of the weight lattice through the non-degenerate form (scalar product)

$$\Lambda^\vee \times \Lambda \to \mathbb{Z}. \tag{3.2.1}$$

Obtaining the representation content of an F-theory model relies on the identification of curves and divisors with elements in Λ and $\Lambda^\vee$. The integral pairing is provided by the homological intersection number between suitable classes. The divisors F_i correspond to the generators of the Cartan subalgebra $\mathfrak{h}$ of $\mathfrak{g}$. The Cartan generators, or equivalently the resolution divisors, span the coroot lattice $Q^\vee = \langle F_i \rangle_{\mathbb{Z}}$. As the coroots lie in $\Lambda^\vee$ they are integrally paired with the weights in any representation. Recall that the localised charged massless matter states in representation ρ of the full gauge group G arise from M2-branes wrapping suitable fiber components $\mathbb{P}^1_\rho$ over codimension-two loci on $\mathcal{B}$. The fiber components in question can be identified with the weights of the representation ρ. The intersection number $F_i \cdot \mathbb{P}^1_\rho$ is the i:th component of the weight λ_ρ identified with the matter state.

The global structure of the gauge group is encoded in the representation data encoded in the weight and root lattices. For definiteness we consider in the following a semi-simple Lie group G. For such G it holds [75, 76] that

$$\pi_1(G) \approx \frac{\Lambda^\vee}{Q^\vee}. \tag{3.2.2}$$

Since the fundamental group is given in relative terms, i.e comparing the 'fineness' of two lattices it will be useful to compare G to its *universal cover* G_0. They share the same Lie algebra $\mathfrak{g}$ and the coweight lattice of G_0 is by definition $\Lambda_0^\vee \approx \langle F_i \rangle_{\mathbb{Z}}$. The dual weight lattice Λ_0 then contains all information about the representations that occur in a gauge theory with gauge group G_0. Since by assumption $\Lambda_0^\vee = Q^\vee$, the group G_0 is simply-connected.

Now, suppose without lack of generality that the F-theory compactification gives rise to gauge algebra $\mathfrak{g} \oplus \mathfrak{g}'$, for $\mathfrak{g}$ semi-simple and whose Cartan subgroups are spanned by two sets of resolution divisors F_i and F_i'. In the following analysis $\mathfrak{g}'$ and its gauge group G' take a spectator role and are included for generality. We are interested in the structure of the global gauge group $G \times G'$. Suppose furthermore that the Mordell-Weil group has k-torsion and that the class Ξ_k defined in (3.1.3) involves only the Cartan generators F_i of $\mathfrak{g}$, and not the generators F_i' of $\mathfrak{g}'$. The class Ξ_k is integer and therefore its intersection with the split fiber components $\mathbb{P}^1_\rho$ is integer as well. Group theoretically this implies that we can identify Ξ_k with a coweight in $\Lambda^\vee$ since $\mathbb{P}^1_\rho$ correspond to a weight in Λ. Having fractional

Lie algebra	Center of universal covering group
$A_{n \geq 1}$	$\mathbb{Z}_{n+1}$
$B_{n \geq 2}$	$\mathbb{Z}_2$
$C_{n \geq 3}$	$\mathbb{Z}_2$
$D_{2n+1 \geq 4}$	$\mathbb{Z}_4$
$D_{2n \geq 4}$	$\mathbb{Z}_2 \oplus \mathbb{Z}_2$
E_6	$\mathbb{Z}_3$
E_7	$\mathbb{Z}_2$
E_8	-
F_4	-
G_2	-

Table 3.2.1: Simple Lie algebras and the center of their universal covering groups.

coefficients in $\frac{1}{k}\mathbb{Z}$ with respect to the F_i, the class Ξ_k corresponds to an element in the coweight lattice $\Lambda^\vee$ which is finer (by order k) compared to the sublattice $\Lambda_0^\vee = \langle F_i \rangle_\mathbb{Z}$ spanned by the F_i alone. Therefore the fundamental group $\pi_1(G) \approx \frac{\Lambda^\vee}{Q^\vee}$ has a $\mathbb{Z}_k$ component, compared to the first fundamental group of G_0 and thus we have a non-simply connected gauge group. The universal covering group G_0 is simply connected and therefore the gauge group $G \times G'$ in such an F-theory compactification with Mordell-Weil torsion $\mathbb{Z}_k$ has as first fundamental group

$$\pi_1(G) \times \pi_1(G') = \mathbb{Z}_k \times \pi_1(G'). \tag{3.2.3}$$

By comparing what order the coroot sublattice is in the coweight lattice we see that Mordell-Weil torsion affect the topology of the gauge group. By comparing the root and the weight lattices we will see that the possible representations get restricted at the same time. Introducing the coweight Ξ_k refines the coweight lattice. To preserve the integer pairing (3.2.1) the weight lattice Λ is forced to be coarser compared to the weight lattice Λ_0, which is the dual of $\Lambda_0^\vee$. The possible weights become a subset of all weights that would be possible on the basis of the Lie algebra alone. In the F-theory fibration the only realized fiber components which are identified with weights have integer pairing with the class of Ξ_k. Considering the maximal weight lattice Λ_0 there are many representations whose weight vectors do not pair integrally with Ξ_k, and are therefore 'forbidden'. No matter representations are actively removed from the spectrum, since they did not appear in the first place. Rather, by comparing to more generic fibrations, without torsional sections one observe that certain representations, which are otherwise present and expected, are not realized in the geometry.

The statement about a courser weight lattice can be coined in terms of the center Z_G of the gauge group G. The center Z_G is the subgroup of G that commute with all elements in G. For a semi-simple Lie group G the center is given by [75, 76]

$$Z_G \approx \frac{\Lambda}{Q}. \tag{3.2.4}$$

where the root lattice $Q \subset \Lambda$. In Table 3.2.1 a list of the centers of the universal covering groups of the simple Lie algebras is given. Geometrically Q is spanned by the fiber components associated with the adjoint representation of G localised in codimension one. To have a reference point, let us again consider the universal cover group G_0 introduced above with center Z_{G_0}. Since Mordell-Weil torsion $\mathbb{Z}_k$ renders Λ coarser by a factor of $\mathbb{Z}_k$ compared to Λ_0, the center of G is smaller by the same amount,

$$Z_G = Z_{G_0}/\mathbb{Z}_k. \tag{3.2.5}$$

Importantly, this means that $\mathbb{Z}_k$ be equal to, or a subgroup of the center of G_0, which constrains the possible gauge algebra $\mathfrak{g}$ that can possibly be realized. By contrast, any extra spectator Lie algebra $\mathfrak{g}'$ whose generators do not enter Ξ_k is unconstrained. For example, if the Mordell-Weil torsion is $\mathbb{Z}_2$, then a gauge algebra $\mathfrak{g} = \mathfrak{su}(k)$ is possible only for $k = 2n$. We will see examples of this when constructing explicit F-theory fibrations with torsion in the Mordell-Weil group. In particular in section 3.3.5 we comment more on this general result. Accounting for the change of the center, the total gauge group is given by

$$G_0/\mathbb{Z}_k \times G'. \tag{3.2.6}$$

This can be directly understood in terms of the construction of our coweight element Ξ_k in (3.1.3). The exponential map lifts an element of $\mathfrak{g}$ to the group G. The exponentiation of Ξ_k generates a $\mathbb{Z}_k$ subgroup of Z_{G_0}. Since Ξ_k has integer pairing with every representation that is present (*i.e.* with every lattice point in the weight lattice Λ, but not with all elements of Λ_0), the corresponding center element (viewed as an element of G_0) acts trivially on every such representation. In effect the actual gauge group is therefore not $G_0 \times G'$, but $G_0/\mathbb{Z}_k \times G'$.

Let's analyze the lifting to the Lie group in a bit more detail. To construct an element in the center of G_0 one exponentiates a linear combination $\Xi = \sum m_i F_i$ of Cartan generators F_i for some, for now arbitrary, coefficients m_i. We denote by ρ_d a d-dimensional representation of $\mathfrak{g}$. Any state $|\lambda^n, \rho_d\rangle$ in the representation ρ_d is labeled by a weight λ^n in the weight system of ρ_d. Letting Ξ act on such a state gives

$$\Xi \cdot |\lambda^n, \rho_d\rangle = \sum_i m_i \lambda_i^n |\lambda^n, \rho_d\rangle, \qquad n = 1, \ldots, d, \qquad i = 1, \ldots, r, \tag{3.2.7}$$

where λ_i^n is the eigenvalue of F_i on this state vector. An element c in the center $Z_{G_0} \in G_0$ commutes with any element in G_0 and can therefore be represented as a multiple of the $d \times d$ unit matrix when acting on the state $|\lambda^n, \rho_d\rangle$, i.e

$$c|_{\rho_d} \cdot |\lambda^n, \rho_d\rangle = a_n \mathbb{1} \cdot |\lambda^n, \rho_d\rangle \tag{3.2.8}$$

for $a_n \in \mathbb{C}$. The matrix c is identified as the exponentiation of Ξ acting on ρ_d if

$$a_n = \exp\left(2\pi i \sum m_i \lambda_i^n\right). \tag{3.2.9}$$

Moreover, for c to lie in a $\mathbb{Z}_k$ subgroup of the center of G_0, c^k acts as $\mathbb{1}$ on any representation ρ_d, or equivalently $(a_n)^k = 1$ for all n. Therefore, if we identify Ξ with the k-fractional linear combination $\Xi_k = -\frac{1}{k}\sum_i a_i F_i$, we see that this does indeed generate a $\mathbb{Z}_k$ subgroup of Z_{G_0}. Moreover, since Ξ_k has integer pairing with all weights in the weight lattice Λ of the actual gauge group G, the element c acts trivially on every such representation. We note here that all results of this section carries over to the general case where the Mordell-Weil group has as torsion subgroup a sum $\mathbb{Z}_{k_1} \oplus \ldots \oplus \mathbb{Z}_{k_n}$ of finite groups.

3.3　Mordell-Weil group $\mathbb{Z}_2$

In the subsequent sections we exemplify the structure of F-theory compactifications on elliptic fibrations with torsional Mordell-Weil group as outlined above. In [69] defining equations for elliptic fibrations with Mordell-Weil group $\mathbb{Z}_k$ for $k = 2, 3, 4, 5, 6$, $\mathbb{Z}_2 \oplus \mathbb{Z}_n$ with $n = 2, 4$ and $\mathbb{Z}_3 \oplus \mathbb{Z}_3$ as hypersurfaces in $\mathbb{P}_{2,3,1}[6]$ fibrations was derived. As it turns out, the restriction of the complex structure moduli of the fibration necessary for the Mordell-Weil group to have torsion induces singularities in the fiber over divisors on the base $\mathcal{B}$. To explicitly analyse these singular loci and their resolution we

focus in this work on the subset of geometries in the list of [69] which can be treated torically as certain hypersurfaces. As noted already, there exist 16 reflexive polygons in two dimensions which describe an elliptic curve as a hypersurface in a toric ambient space. Of these only three admit torsional sections in the Mordell-Weil group as the intersection of a toric divisor with the generic hypersurface defined by the dual polygon. The Mordell-Weil group of these fibrations has already been provided in [20]. As we will show, they correspond to the geometries with Mordell-Weil group $\mathbb{Z}_2$ and $\mathbb{Z}_3$ as well as a further specialisation of the $\mathbb{Z}_2$-model in the list of [69]. For each of these three fibration types we construct a compact model fibered over a generic base $\mathcal{B}$ and analyse in detail the interplay between the torsional sections and the global structure of the gauge group. In addition we implement further non-abelian gauge symmetries by the construction of toric tops [19].

3.3.1 An $SU(2)/\mathbb{Z}_2$-fibration

We begin with the simplest example, which is an elliptic fibration with torsional Mordell-Weil group $\mathbb{Z}_2$.As derived in [69], an elliptic fibration with a $\mathbb{Z}_2$-torsional section admits a representation as the hypersurface $P = 0$ with

$$P = -y^2 - a_1 x\, y\, z + x^3 + a_2\, x^2\, z^2 + a_4\, x\, z^4 \tag{3.3.1}$$

and $[x : y : z]$ fiber coordinates in a $\mathbb{P}_{2,3,1}$-fibration over some base $\mathcal{B}$. To ensure that the variety $P = 0$ satisfies the Calabi-Yau condition the coefficients a_i must be sections of $\bar{\mathcal{K}}_{\mathcal{B}}^i$ with $\bar{\mathcal{K}}_{\mathcal{B}}$ the anti-canonical bundle of the base $\mathcal{B}$. Note that (3.3.1) corresponds to an otherwise generic Tate model with $a_6 \equiv 0$ and $a_3 \equiv 0$. It can therefore be viewed as a further specialisation of the $U(1)$ restricted Tate model, defined in [77] by setting $a_6 \equiv 0$. The latter has Mordell-Weil group $\mathbb{Z}$ and in turn represents a special case of the elliptic fibrations with Mordell-Weil group $\mathbb{Z}$ as described in [18].

Singularity structure and resolution

The elliptic fibration (3.3.1) is easily brought into Weierstrass form with

$$f = a_4 - \frac{1}{3}\left(a_2 + \frac{a_1^2}{4}\right)^2, \quad g = \frac{1}{27}\left(a_2 + \frac{a_1^2}{4}\right)\left(2(a_2 + \frac{a_1^2}{4})^2 - 9a_4\right).$$

From f and g and the discriminant

$$\Delta = \frac{1}{16}a_4^2\left(4\,a_4 - \left(a_2 + \tfrac{1}{4}a_1^2\right)^2\right) \tag{3.3.2}$$

one infers an $\mathfrak{su}(2)$-singularity at $a_4 = 0$. Indeed, the gradient of (3.3.1) in the patch $z \neq 0$,

$$dP = (-a_1\,y + 3\,x^2 + 2\,a_2\,x + a_4)\,dx - (2\,y + a_1\,x)\,dy\ - xy\,d_B\,a_1 + x^2\,d_B\,a_2 + x\,d_B\,a_4\,, \tag{3.3.3}$$

with d_B the total derivative with respect to the base coordinates, vanishes together with the hypersurface equation (3.3.1) for $x = y = a_4 = 0$. The situation is similar to the $U(1)$-restricted model with $a_6 \equiv 0$ but $a_3 \neq 0$ [77], in which, however, the singularity appeared over the curve $\{a_3 = 0\} \cap \{a_4 = 0\}$ on $\mathcal{B}$. Since in (3.3.1) a_3 is set to zero from the very beginning, the $\mathfrak{su}(2)$ locus is promoted to the divisor $\{a_4 = 0\}$. We will come back to this enhancement of the $\mathfrak{u}(1)$ gauge algebra of the $U(1)$ restricted Tate model to $\mathfrak{su}(2)$ by setting $a_3 \equiv 0$ in section 3.4.2.

To resolve the singularity we perform a blow-up in the fiber ambient space

$$x \to s\,x\,, \qquad y \to s\,y\,. \tag{3.3.4}$$
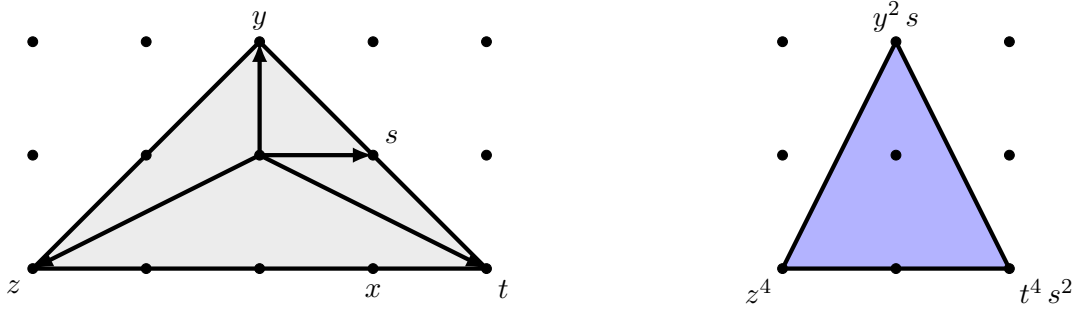
Figure 3.1: Polygon 13 of [19] together with its dual polygon. The coordinate x is blown-down, and not part of the fan.

Since $a_6 \equiv 0$, this does not spoil the Calabi-Yau condition of the hypersurface as one can see from the proper transform of (3.3.1) given by

$$\hat{P} = -y^2\,s - a_1 x\,y\,z\,s + x^3\,s^2 + a_2\,x^2\,z^2\,s + a_4\,x\,z^4\,, \tag{3.3.5}$$

which is checked to be smooth (see [31, 77] for the analogous blow-up if $a_3 \neq 0$). In order to facilitate the description of the $\mathbb{Z}_2$-torsional section it turns out useful to perform a further ambient space blow-up

$$s \to t\,s\,, \qquad x \to t\,x\,, \tag{3.3.6}$$

under which the proper transform of (3.3.5) becomes

$$\hat{P} = -y^2\,s - a_1 x\,y\,z\,s\,t + x^3\,s^2\,t^4 + a_2\,x^2\,z^2\,s\,t^2 + a_4\,x\,z^4. \tag{3.3.7}$$

The Stanley-Reisner ideal after the two blow-ups id obtained from the fan in fig. 3.1 and is generated by

$$\text{SR-i}: \quad \{y\,t,\ y\,x,\ s\,x,\ s\,z,\ t\,z\}\,, \tag{3.3.8}$$

We observe that the divisor $X : \{x = 0\}$ does not intersect the hypersurface which will be crucial in the following. For now it means that x can be set to one in (3.3.7) and we will analyse the fibration $\hat{P} = 0$ with

$$\hat{P} = -y^2\,s - a_1 y\,z\,s\,t + s^2\,t^4 + a_2\,z^2\,s\,t^2 + a_4\,z^4 \tag{3.3.9}$$

over a suitable base $\mathcal{B}$. If $\mathcal{B}$ is 3-dimensional, this defines an elliptically fibered Calabi-Yau 4-fold $\hat{Y}_4$. The weight matrix of the homogeneous coordinates can be taken to be

y	z	s	t	$\sum$
2	1	0	1	4
1	1	2	0	4

$$\tag{3.3.10}$$

and the Stanley-Reisner ideal simplifies to

$$\{y\,t,\ s\,z\}\,. \tag{3.3.11}$$

Note that the weight matrix (3.3.10) coincides with the weight matrix as read off from the toric fan depicted in Figure 3.1, which corresponds to polygon 13 in the list [19] of 16 torically embedded hypersurface elliptic curves. The fibration (3.3.9) with $s \equiv 1$, corresponding to the blow-down of the resolution divisor associated with the $\mathfrak{su}(2)$ singularity over $a_4 = 0$, has been analysed previously in [78] and shown to correspond to an elliptic fibration with restricted $SL(2,\mathbb{Z})$ monodromy. We will analyze this relation in more detail in section 3.3.5.

Figure 3.2: To the left we depict the factorised fiber over the base locus $a_4 = 0$; the purple $\mathbb{P}^1$ indicates the $s = 0$ part while the grey $\mathbb{P}^1$ is the second irreducible part of the elliptic curve. To the right the fiber over the base locus $a_4 = \frac{1}{4}(a_2 + \frac{1}{4}a_1^2)^2$ is shown. The multiplicity is one, and the fiber is singular. The blue and green crosses indicate the specified points $z = 0$ and the $\mathbb{Z}_2$-point $t = 0$ of the elliptic curve, respectively.

The advantage of passing to the hypersurface representation (3.3.9) is that the $\mathbb{Z}_2$-torsional point on the elliptic fiber is now explictly given by the intersection of the fiber with the toric divisor

$$T : t = 0. \tag{3.3.12}$$

This can be checked via the group law on the elliptic curve. We will henceforth denote T as the $\mathbb{Z}_2$ section of the fibration. The holomorphic zero-section is given by $Z : z = 0$.

To study the geometry further we note that the fibration restricted to the $\mathfrak{su}(2)$-sublocus $\{a_4 = 0\}$ in the discriminant (3.3.2) factorises as

$$\hat{P}|_{a_4=0} = s\left(-y^2 - a_1\,y\,z\,t + \left(s\,t^4 + a_2\,z^2\,t^2\right)\right). \tag{3.3.13}$$

The resolution divisor $S : s = 0$ is a $\mathbb{P}^1$-fibration over the locus $\{a_4 = 0\}$ on $\mathcal{B}$ as the coordinate s is just a toric ambient space coordinate. The other irreducible component of (3.3.13) is quadratic in y and must therefore be studied in more detail. Note first that this component does not intersect the $\mathbb{Z}_2$ section T, but only the holomorphic zero-section Z. Since z and t cannot both vanish along it, we can go to the patch where y and s can vanish simultaneously. Here the second factor of (3.3.13) becomes

$$y^2 + a_1\,y - (s + a_2) = 0. \tag{3.3.14}$$

The discriminant of this quadratic equation is a linear function in s so that we find one branching point in the s-plane. Since the point at '$s = \infty$' ($z = 0$) is also single valued, we can take the branch-cut from $s = -(\frac{1}{4}a_1^2 + a_2)$ to infinity. Gluing the two $\mathbb{P}^1$s viewed as compactified complex planes along the branch-cut, we obtain again a $\mathbb{P}^1$. The two irreducible parts of (3.3.13) intersect each other in two points, as can be seen from (3.3.14). The factorised fiber over the base divisor $\{a_4 = 0\}$ is depicted on the left in Figure 3.2. Over the zero set of the second factor of the discriminant (3.3.2),

$$4\,a_4 - (a_2 + \tfrac{1}{4}a_1^2)^2 = 0, \tag{3.3.15}$$

we analyse the fiber structure by substituting (3.3.15) into (3.3.9). This gives the hypersurface equation

$$\hat{P}|_{(\ldots=0)} = -y^2\,s - a_1\,y\,z\,s\,t + s^2\,t^4 + a_2\,z^2\,s\,t^2 + \tfrac{1}{4}(a_2 + \tfrac{1}{4}a_1^2)^2\,z^4\,.$$

To determine the fiber type, we can go to the patch where y and z are allowed to vanish simultaneously. We set $s = 1$ since the divisor $\{s = 0\}$ does not intersect the elliptic curve away from $\{a_4 = 0\}$ and

complete the square as

$$
\begin{aligned}
y^2 + a_1\, y\, z &= 1 + a_2\, z^2 + \tfrac{1}{4}(a_2 + \tfrac{1}{4}a_1^2)^2\, z^4 \\
\Rightarrow (y + \frac{1}{2}a_1\, z)^2 &= 1 + (a_2 + \tfrac{1}{4}a_1^2)\, z^2 + \tfrac{1}{4}(a_2 + a_1^2)^2\, z^4 \\
\Rightarrow (y + \frac{1}{2}a_1\, z)^2 &= \left(1 + \tfrac{1}{2}(a_2 + \tfrac{1}{4}a_1^2)\, z^2\right)^2 \\
\Rightarrow \left(y + \frac{1}{2}a_1\, z - 1 - \tfrac{1}{2}(a_2 + \tfrac{1}{4}a_1^2)\, z^2 \right) &\left(y + \frac{1}{2}a_1\, z + 1 + \tfrac{1}{2}(a_2 + \tfrac{1}{4}a_1^2)\, z^2 \right) = 0\,.
\end{aligned}
$$

Therefore, it appears as if the elliptic curve factorises into two rational curves. However, these two $\mathbb{P}^1$s are equivalent as follows from the second row of the weight matrix (3.3.10) because the equivalence relation $(y, z) \sim (-y, -z)$ is left over after setting s to one[3]. Thus the fiber is just a single rational curve; moreover, it has a singular point, cf. Figure 3.2, at $y = -\frac{1}{2}a_1 z$, $s = -\frac{1}{8}(a_1^2 + 4a_2)z^2$ (and $t = 1$ due to the Stanley-Reisner ideal), where the gradient along the fiber coordinates vanishes even though the fibration as such is non-singular. Thus the fiber is of Kodaira-type I_1, and the locus (3.3.15) does not give rise to any further gauge symmetry.

Interestingly, apart from the codimension-one splitting of the fiber over $\{a_4 = 0\}$ no further degeneration of the fiber occurs in higher codimension. In particular, the fiber over the intersection curve $\{a_4 = 0\} \cap \{a_2 + \frac{1}{4}a_1^2 = 0\}$ of the two components of the discriminant does not factorise further. This can be understood by considering the vanishing of f and g along that locus: f vanishes to order 1, g vanishes to order 2 and the discriminant Δ consequently to order 3, giving a Kodaira fiber of type III. This type of fiber has two components just like the familiar A_1-fiber, but they are tangent to each other rather than meeting at two distinct points, and there is no enhancement or matter (consistent with [79, 80]). This is remarkable because naively one might have expected an enhancement from A_1 to A_2 at the intersection of the A_1-locus with the I_1-component of the discriminant and thus localised massless matter in the fundamental of $\mathfrak{su}(2)$. The absence of this enhancement and the associated fundamental representation is a typical property of fibrations with torsional Mordell-Weil group. To summarize, the fibration (3.3.1) gives rise to an F-theory compactification with gauge algebra $\mathfrak{su}(2)$ and no localised charged matter.

Torsional divisors and free quotient

The absence of charged localized matter in the fundamental representation is a consequence of the $\mathbb{Z}_2$ Mordell-Weil group and the resulting global structure of the gauge group. To see this let us first exemplify how the torsional Mordell-Weil group of the elliptic fiber induces a torsional element in $H^{1,1}(\hat{Y}_4, \mathbb{Z})$ modulo the integer lattice spanned by the resolution divisors. In the present model with gauge algebra $\mathfrak{g} = \mathfrak{su}(2)$ the lattice of resolution divisors is simply $\langle S \rangle_{\mathbb{Z}}$. To find the element Σ_2 of the form (3.1.1) we make an Ansatz and demand that (2.1.26) be satisfied. In the present situation this amounts to demanding that Σ_2 have 'one leg in the fiber' and that it be orthogonal to the exceptional divisor S, in the sense that for all $\omega_4 \in H^4(B)$ and $\omega_2 \in H^2(B)$

$$
\int_{\hat{Y}_4} \Sigma_2 \wedge Z \wedge \pi^*\omega_4 = \int_{\hat{Y}_4} \Sigma_2 \wedge \pi^*\omega_2 \wedge \pi^*\omega_4 = \int_{\hat{Y}_4} \Sigma_2 \wedge S \wedge \pi^*\omega_4 = 0. \tag{3.3.16}
$$

This uniquely determines

$$
\Sigma_2 = T - Z - \bar{\mathcal{K}} + \frac{1}{2}S \tag{3.3.17}
$$

---

[3]This can also be seen from the N-lattice polygon of Figure 3.1 because y and z do not span the lattice. The patch where y and z are allowed to vanish simultaneously is, therefore, $\mathbb{C}^2/\mathbb{Z}_2$ and not $\mathbb{C}^2$ as one would naïvely think.

with $\bar{\mathcal{K}} = \pi^{-1}\bar{\mathcal{K}}_{\mathcal{B}}$. This element is in fact trivial in $H^2(\hat{Y}_4, \mathbb{R})$. Indeed, recall that the fibration $\hat{Y}_4$ is described as the hypersurface (3.3.7) in an ambient toric space. Consider the toric divisor $X : \{x = 0\}$ in this ambient space. Its class is

$$X = 2Z - S - 2T + 2\bar{\mathcal{K}} = -2\Sigma_2. \tag{3.3.18}$$

However, as discussed, X does not intersect the hypersurface $\hat{Y}_4$ and therefore its class is trivial on the hypersurface. Thus also Σ_2 is trivial in $H^{1,1}(\hat{Y}_4, \mathbb{R})$. This implies that

$$\Xi_2 := T - Z - \bar{\mathcal{K}} = -\frac{1}{2}S, \tag{3.3.19}$$

thereby identifying Ξ_2 as 2-torsion in $H^{1,1}(\hat{Y}_4, \mathbb{Z})/\langle S\rangle_{\mathbb{Z}}$.

According to the discussion in section 3.1, associated with Ξ_2 is an extra coweight defined over $\frac{1}{2}\mathbb{Z}$. Thus, to preserve the pairing with the weights, the weight lattice is forced to be coarser. In particular the representation $\mathbf{2}$ of $\mathfrak{su}(2)$ cannot be present in this model as its weight would have half-integer pairing with the fractional coweight $\Xi_2 = -\frac{1}{2}S$, in contradiction with the fact that $T - Z - \bar{\mathcal{K}}$ is manifestly integer. This is the deeper reason behind the absence of a fundamental representation at the intersection of the $\mathfrak{su}(2)$-divisor $\{a_4 = 0\}$ with the second discriminant component. The gauge group of the model is thus

$$G = SU(2)/\mathbb{Z}_2 \tag{3.3.20}$$

with $\pi_1(G) = \mathbb{Z}_2$.

One can give an intuitive geometric explanation for the appearance of the 2-torsion element Ξ_2 in $H^{1,1}(\hat{Y}_4, \mathbb{Z})/\langle S\rangle_{\mathbb{Z}}$ as follows: Restrict the elliptically fibered Calabi-Yau $\hat{Y}_4$ over $\mathcal{B}$ given by the hypersurface equation (3.3.7) to $\mathcal{B}\backslash\{a_4 = 0\}$. As will be discussed momentarily, the resulting space $\hat{Y}_4'$ is a free $\mathbb{Z}_2$ quotient,

$$\hat{Y}_4' = \widetilde{\hat{Y}_4'}/\mathbb{Z}_2, \tag{3.3.21}$$

with $\widetilde{\hat{Y}_4'}$ an elliptic fibration over $\mathcal{B}\backslash\{a_4 = 0\}$. Correspondingly

$$\pi_1(\hat{Y}_4') \supset \mathbb{Z}_2, \tag{3.3.22}$$

where additional discrete torsion pieces may arise if $\pi_1(\mathcal{B}\backslash\{a_4 = 0\})$ is non-trivial. Since the resolution divisor S is fibered over $\{a_4 = 0\}$ this is in agreement with the appearance of a torsional element in $H^{1,1}(\hat{Y}_4, \mathbb{Z})/\langle S\rangle_{\mathbb{Z}}$.

The relation (3.3.21) can be seen as follows: Consider the fibration over a generic locus on the base $\mathcal{B}$ where $a_4 \neq 0$. Since the resolution divisor $s = 0$ intersects the fiber only over $\{a_4 = 0\}$ we can set s to one away from that locus. Then (3.3.9) becomes

$$y^2 + a_1 y z t = t^4 + a_2 z^2 t^2 + a_4 z^4 . \tag{3.3.23}$$

This is a special $\mathbb{P}_{1,1,2}[4]$ fibration with homogeneous coordinates $[t : z : y]$, which in addition to the equivalence relation $(t, z, y) \sim (\lambda t, \lambda z, \lambda^2 y)$ enjoys a further $\mathbb{Z}_2$ identification

$$t \sim -t, \qquad y \sim -y. \tag{3.3.24}$$

In fact, the most generic $\mathbb{P}_{1,1,2}[4]$ representation of an elliptic curve contains the nine terms

$$y^2, \, t^4, \, z^4, \, z^2 t^2, \, yzt; \qquad yt^2, \, yz^2, \, zt^3, \, tz^3. \tag{3.3.25}$$
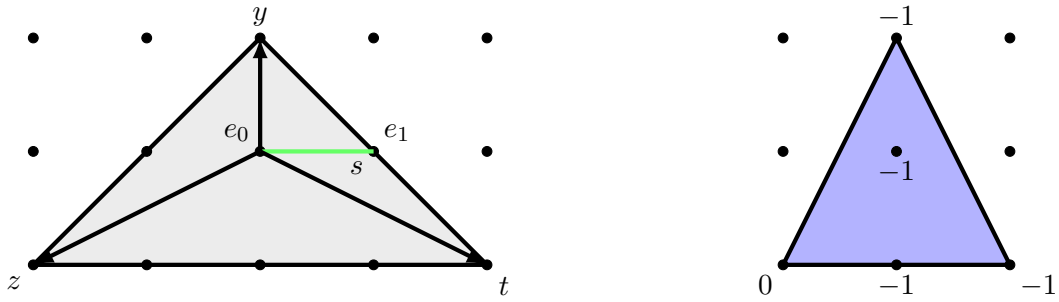
Figure 3.3: On the lefthand side the only possible $\mathfrak{su}(2)$-top over polygon 13 of [19] is depicted. The green color indicates the layer at height one, containing the nodes e_0 and e_1. On the righthand side we give the dual top, bounded from below by the values z_{min}, shown next to the nodes.

Precisely the first five terms present in (3.3.23) are compatible with the $\mathbb{Z}_2$ identification (3.3.24). Note that by a coordinate redefinition we can set $a_1 \equiv 0$, thereby arriving at the special $\mathbb{P}_{1,1,2}[4]$-fibration that goes by the name of the Légendre family. In any case, we can view (3.3.23) as the result of starting with a $\mathbb{P}_{1,1,2}[4]$ fibration described by the hypersurface equation

$$y^2 + a_1 y\, z\, t = t^4 + a_2 z^2\, t^2 + a_4\, z^4 + c_1\, y\, t^2 + c_2\, y\, z^2 + c_3\, z\, t^3 + c_4\, t\, z^3, \tag{3.3.26}$$

enforcing the $\mathbb{Z}_2$ symmetry by setting $c_i \equiv 0$ (we call the resulting space $\widetilde{Y_4'}$) and then quotienting by this $\mathbb{Z}_2$ symmetry. The fact that $\hat{Y}_4'$ is really the quotient of $\widetilde{Y_4'}$ by (3.3.24) is automatically implemented by the toric description because the dual polyhedron exclusively contains monomials invariant under (3.3.24). Importantly, the $\mathbb{Z}_2$ acts freely as the fixed point sets $\{t = y = 0\}$ and $\{z = y = 0\}$ do not lie on $\hat{Y}_4'$ due to the Stanely-Reisner ideal. Note that the role of this $\mathbb{Z}_2$ quotient symmetry was stressed already in [78] albeit in a slightly different context.

This description makes the existence of discrete one-cycles on $\hat{Y}_4'$ manifest: Consider the locus $z = 0$ on (3.3.23). On $\widetilde{Y_4'}$ it is given by $y = \pm 1$, where we have used the scaling of $\mathbb{P}_{1,1,2}$ to set $t = 1$ since t and z cannot simultaneously vanish as a consequence of the Stanely-Reisner ideal. A path from $y = -1$ to $y = +1$ on the double cover $\widetilde{Y_4'}$ corresponds to a non-contractible closed loop on $\hat{Y}_4'$. This loop is torsional as going along it twice is contractible again.

The existence of a torsion one-cycle implies also a torsion six-cycle because in general

$$\mathrm{Tor}_p(Y) \simeq \mathrm{Tor}_{D-p-1}(Y) \tag{3.3.27}$$

with D the real dimension of Y. This picture has relied on setting $s = 1$ and is thus really valid away from the locus $a_4 = 0$. Therefore all we can conclude is the existence of a 2-torsion element in $H^{1,1}(\hat{Y}_4, \mathbb{Z})/\langle S \rangle_{\mathbb{Z}}$.

3.3.2   An $(SU(2) \times SU(2))/\mathbb{Z}_2$-fibration

The analysis so far has treated all coefficients a_i appearing in (3.3.1) as maximally generic. We now further restrict the coefficients a_i defining the $\mathbb{Z}_2$-torsional fibration in its singular form (3.3.1) or its resolution (3.3.9) such as to create additional non-abelian singularities in the fiber. A special class of such restrictions corresponds to specializations $a_i \to a_{i,j} w^j$ with $W : \{w = 0\}$ a base divisor and $a_{i,j}$ *generic*. Since the fibration (3.3.1) is in global Tate form, the possible enhancements one can obtain via such specialisations can be conveniently determined via Tate's algorithm [79–81] as summarized *e.g.* in table 2 of [81]. Another advantage of this class of enhancements is that the corresponding

fibrations can be treated torically. Indeed, the possible enhancements of type $a_i \to a_{i,j} w^j$ with generic $a_{i,j}$ which admit a crepant resolution are classified by the tops construction [71, 82], which provides both the possible vanishing patterns $a_{i,j}$ (coinciding with Tate's algorithm) and the toric resolution. For a detailed account of how to read off the vanishing orders from the toric data of a top in the present context we also refer to [83].

From the classification of tops by Bouchard and Skarke [19] for the 16 hypersurface elliptic fibrations, we note that the only tops possible for the fiber (3.3.7) correspond to singularity type A_{2n+1} for $n \geq 0$, C_n and D_{2n+4} for $n \geq 1$, B_3 and E_7. This is indeed in agreement with an analysis via Tate's algorithm as a consequence of $a_3 \equiv 0$ and $a_6 \equiv 0$. The associated gauge algebras have the property that their universal cover groups have a center with a $\mathbb{Z}_2$-subgroup. Indeed, as we will exemplify below, in all models of this type the Mordell-Weil torsion $\mathbb{Z}_2$ will be identified with this $\mathbb{Z}_2$-subgroup of the center.

To verify this pattern explicitly we begin with an A_1 top, corresponding to an affine $\mathfrak{su}(2)$-type fiber over a divisor $W : w = 0$ on $\mathcal{B}$. There is, in fact, only one possible A_1 top over this polygon, see Figure 3.3. The singular version of the associated fibration is obtained by replacing in (3.3.1) a_4 by $a_{4,1}w$. The discriminant of this fibration,

$$\Delta \sim w^2 a_{4,1}^2 \big((a_1^2 - 4a_2)^2 - 64w a_{4,1}\big), \tag{3.3.28}$$

reflects the gauge algebra $\mathfrak{su}(2) \oplus \mathfrak{su}(2)$.

The toric resolution of this fibration is described by the hypersurface equation

$$\hat{P} = sy^2 + a_1 styz - e_1 s^2 t^4 - a_2 st^2 z^2 - a_{4,1} e_0 z^4 \,, \tag{3.3.29}$$

corresponding to the reflexive pair in Figure 3.3 (again after scaling x to one, since X does not intersect the hypersurface). For definiteness we choose a triangulation with Stanley-Reisner ideal

$$\{sz, tz, ty, e_0 s, e_1 z\}. \tag{3.3.30}$$

The extra $\mathfrak{su}(2)$-fiber is found over $W : \{w = 0\}$ with $\pi^* w = e_0 e_1$. Indeed, over W the two fiber components $\mathbb{P}_0^1$ and $\mathbb{P}_1^1$ are given by the intersection of the ambient divisors $E_0 : \{e_0 = 0\}$ and $E_1 : \{e_1 = 0\}$ with the hypersurface equation and two generic divisors in the base,

$$\mathbb{P}_i^1 = E_i \cap \hat{P}|_{e_i=0} \cap D_a \cap D_b, \qquad i = 0, 1. \tag{3.3.31}$$

They intersect as the affine $\mathfrak{su}(2)$ Dynkin diagram.

The discriminant also suggests three codimension-two enhancement loci, at $W \cap \{a_{4,1} = 0\}$, $W \cap \{a_1^2 = 4a_2\}$ and $\{a_{4,1} = 0\} \cap \{a_1^2 = 4a_2\}$. Splitting of fiber components only occurs over the first one[4], where $\mathbb{P}_1^1$ factors into the two components

$$\mathbb{P}_{1s}^1 \;\; = \;\; E_1 \cap \{s = 0\} \cap \{a_{4,1} = 0\} \cap D_a \cap D_b, \tag{3.3.32}$$

$$\mathbb{P}_{1A}^1 \;\; = \;\; E_1 \cap (y + \tfrac{1}{2}a_1 t \pm t\sqrt{\tfrac{a_1^2}{4} - a_2})(y + \tfrac{1}{2}a_1 t \mp t\sqrt{\tfrac{a_1^2}{4} - a_2}) = 0\} \cap \{a_{4,1} = 0\} \cap D_a \cap D_b.$$

Note that the two factors in brackets appearing in $\mathbb{P}_{1A}^1$ get exchanged when the sign of the square root changes across a branch cut on $\mathcal{B}$ so that $\mathbb{P}_{1A}^1$ really describes a single $\mathbb{P}^1$. The weight

$$\mathbb{P}_{1A}^1 \cdot (E_1, S) = (-1, 1) \tag{3.3.33}$$

---

[4]The other two loci are completely analogous to the curve $\{a_4 = 0\} \cap \{a_1^2 = 4a_2\}$ analysed in the previous section, where no splitting of the fiber was found despite an enhancement of the vanishing order of the discriminant.

is in the weight system of the $(\mathbf{2}, \mathbf{2})$ of $\mathfrak{su}(2) \oplus \mathfrak{su}(2)$. This implies massless matter in the $(\mathbf{2}, \mathbf{2})$ representation over $W \cap \{a_{4,1} = 0\}$. Again, no fundamental matter $(\mathbf{1}, \mathbf{2})$ or $(\mathbf{2}, \mathbf{1})$ is found.

Our derivation of the extra coweight induced by the torsional section $T : \{t = 0\}$ is only mildly modified by the extra $\mathfrak{su}(2)$ singularity compared to the previous section. The Shioda map Σ_2 of T takes the form

$$\Sigma_2 = T - Z - \bar{\mathcal{K}} + \frac{1}{2}(S + E_1), \tag{3.3.34}$$

which is trivial on the hypersurface since the divisor class

$$X = 2Z - S - 2T + 2\bar{\mathcal{K}} - E_1 \tag{3.3.35}$$

does not intersect (3.3.29) due to the Stanley-Reisner ideal. The extra coweight is associated with the class

$$\Xi_2 \equiv T - Z - \bar{\mathcal{K}} = -\frac{1}{2}(S + E_1), \tag{3.3.36}$$

which is torsion in $H^{1,1}(\hat{Y}_4, \mathbb{Z})/\langle S, E_1 \rangle_{\mathbb{Z}}$ and manifestly integral on the split curves over $W \cap \{a_{4,1} = 0\}$. This explains why the bifundamental representation is indeed present, whereas fundamental representations of the form $(\mathbf{1}, \mathbf{2})$ or $(\mathbf{2}, \mathbf{1})$, which for group theoretic reasons would have fractional pairing with the coweight Ξ_2, are not possible.

This refinement of the coweight lattice makes the gauge group non-simply connected and the gauge group is

$$G = \frac{SU(2) \times SU(2)}{\mathbb{Z}_2}. \tag{3.3.37}$$

An example of this type was also given in [84].
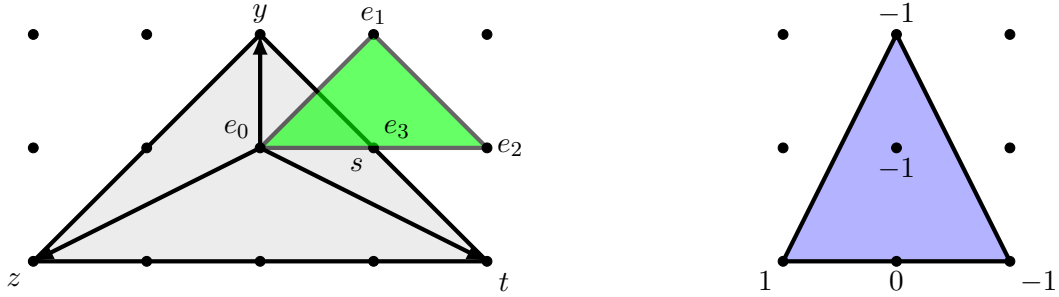
Figure 3.4: The lefthand side shows an $\mathfrak{su}(4)$-top over polygon 13 of [19]. The green layer contains the points at height one. On the righthand side we depict the dual top, bounded from below by the values z_{min}, shown next to the nodes.

3.3.3 An $(SU(4) \times SU(2))/\mathbb{Z}_2$-fibration

In this section we consider the next example in the A-series [19], corresponding to an affine $\mathfrak{su}(4)$-type fiber. This construction yields the unique top of Figure 3.4 associated with the hypersurface equation

$$\hat{P} = -y^2 s\, e_1 - a_1\, y\, z\, s\, t + s^2\, t^4\, e_2^2\, e_3 + a_{2,1}\, z^2\, s\, t^2\, e_0\, e_2\, e_3 + a_{4,2}\, z^4\, e_0^2\, e_3. \tag{3.3.38}$$

The pullback of the projection of the fibration obeys $e_0 e_1 e_2 e_3 = \pi^* w$, defining an affine $\mathfrak{su}(4)$ fiber over $W : \{w = 0\}$ in the base. From one of the 16 triangulations of this top we obtain the Stanley-Reisner ideal

SR-i : $\{y\, t,\ y\, e_0,\ y\, e_2,\ y\, e_3,\ s\, z,\ s\, e_0,\ s\, e_2,\ s\, e_3,\ z\, e_2,\ z\, e_3,\ e_0\, e_2,\ t\, z\, e_1,\ t\, e_0\, e_1,\ t\, e_1\, e_3\}. \tag{3.3.39}$

The three exceptional divisors e_1, e_2, e_3 and the part of the original fiber e_0 are all fibered over $\{w = 0\}$ with fiber components

$$\mathbb{P}^1_i = \{E_i\} \cap \{\hat{P}|_{e_i=0} = 0\} \cap D_a \cap D_b \quad i = 0, \ldots, 3. \tag{3.3.40}$$

The explicit equations are provided in appendix A.1. The irreducible fiber components intersect like the nodes of the affine Dynkin diagram of $\mathfrak{su}(4)$ type. This is also seen in Figure 3.4, where the upper layer reproduces this structure by construction. To analyze the localised charged matter we infer from the discriminant of (3.3.38),

$$\Delta = 16 \, w^4 \, a_{4,2}^2 \left(\left(4 \, w \, a_{2,1} + a_1^2 \right)^2 - 64 \, w^2 \, a_{4,2} \right), \tag{3.3.41}$$

the codimension-two enhancement loci[5]

$$\{w = a_{4,2} = 0\} \qquad \text{and} \qquad \{w = a_1 = 0\}. \tag{3.3.42}$$

The factorization properties of the fiber components (see appendix A.1) identify the split curves in the fiber. At $\{w = a_{4,2} = 0\}$ the component $\mathbb{P}^1_1$ splits into three components, whose intersection numbers with the exceptional divisors from the $\mathfrak{su}(4)$ and $\mathfrak{su}(2)$ singularities are

$$\begin{aligned}
\mathbb{P}^1_{e_1=s=0} \cdot (E_1, E_2, E_3) &= (0, 0, 0), & \mathbb{P}^1_{e_1=s=0} \cdot (S) &= (-2), \\
\mathbb{P}^1_{e_1=t=0} \cdot (E_1, E_2, E_3) &= (-1, 1, 0), & \mathbb{P}^1_{e_1=t=0} \cdot (S) &= (1), \\
\mathbb{P}^1_{e_1=R1=0} \cdot (E_1, E_2, E_3) &= (-1, 0, 0), & \mathbb{P}^1_{e_1=R1=0} \cdot (S) &= (1),
\end{aligned} \tag{3.3.43}$$

respectively. The $(-1, 1, 0)$ and $(-1, 0, 0)$ are weights in the fundamental of $\mathfrak{su}(4)$ and from the right column we find the weights of the fundamental representation of $\mathfrak{su}(2)$ (which is the same as the anti-fundamental). Indeed the full weight system is reproduced by taking linear combinations of fibral curves. Hence the charged matter at this locus transforms in representation $(\mathbf{4}, \mathbf{2})$ of $\mathfrak{su}(4) \oplus \mathfrak{su}(2)$.

Over $\{w = a_1 = 0\}$ the relevant intersections are

$$\begin{aligned}
\mathbb{P}^1_{e_1=e_3=0} \cdot (E_1, E_2, E_3) &= (0, 1, -2), & \mathbb{P}^1_{e_1=e_3=0} \cdot (S) &= (0), \\
\mathbb{P}^1_{e_1=R2_1=0} \cdot (E_1, E_2, E_3) &= (-1, 0, 1), & \mathbb{P}^1_{e_1=R2_1=0} \cdot (S) &= (0), \\
\mathbb{P}^1_{e_1=R2_2=0} \cdot (E_1, E_2, E_3) &= (-1, 0, 1), & \mathbb{P}^1_{e_1=R2_2=0} \cdot (S) &= (0),
\end{aligned} \tag{3.3.44}$$

where $(-1, 0, 1)$ is one of the weights in the $\mathbf{6}$-representation of $\mathfrak{su}(4)$. States originating from these curves are uncharged under $\mathfrak{su}(2)$. This is as expected since this locus is away from the $\mathfrak{su}(2)$ divisor $\{a_{4,2} = 0\}$. The following table summarizes the matter spectrum:

Top over polygon 13: $\mathfrak{su}(4) \times \mathfrak{su}(2)$

Locus	Charged matter	
$w \cap a_{4,2}$	$(\mathbf{4}, \mathbf{2})$	(3.3.45)
$w \cap a_1$	$(\mathbf{6}, \mathbf{1})$	

Again we stress the absence of fundamental representations. The Shioda-type Ansatz for the toric divisor class T yields

$$\Sigma_2 = T - Z - \bar{\mathcal{K}} + \frac{1}{2}\left(S + E_1 + 2E_2 + E_3\right), \tag{3.3.46}$$

which for the same reasons as before turns out to be trivial in $H^{1,1}(Y_4, \mathbb{R})$. The coweight element

$$\Xi_2 = T - Z - \bar{\mathcal{K}} = -\frac{1}{2}(S + E_1 + 2E_2 + E_3), \tag{3.3.47}$$

[5]All other enhancement loci as read off from the discriminant do not correspond to an extra fiber splitting.
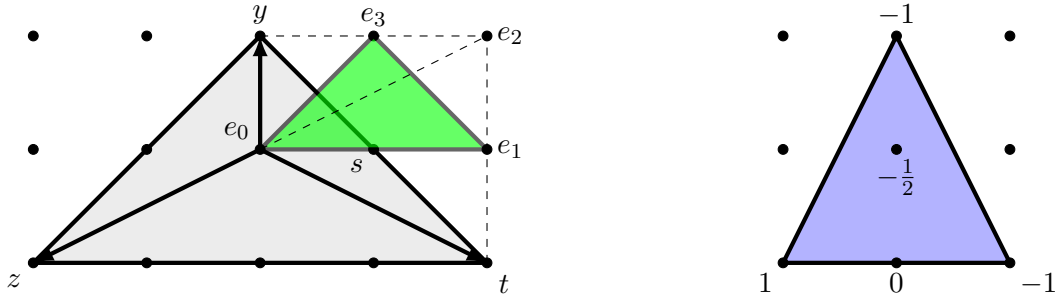
Figure 3.5: The lefthand side shows the unique B_3-top over polygon 13 of [19]. The green layer contains the points at height one and the node labelled e_2 is at height two. On the right side we depict the dual top, bounded from below by the values z_{min}, shown next to the nodes.

which is 2-torsion in $H^{1,1}(\hat{Y}_4, \mathbb{Z})/\langle S, E_1, E_2, E_3\rangle_{\mathbb{Z}}$, forces the weight lattice to be coarser in order to preserve the integer pairing of coweights and weights. Indeed, the intersection of Ξ_2 with all split curves corresponding to weights of the matter representations is integer, and representations such as $(\mathbf{4}, 1)$ or $(1, \mathbf{2})$ which would violate this integral pairing are absent. This identifies the global gauge group as

$$G = \frac{SU(4) \times SU(2)}{\mathbb{Z}_2}. \tag{3.3.48}$$

3.3.4   A $(Spin(7) \times SU(2))/\mathbb{Z}_2$-fibration

Keeping the same ambient fiber space as in previous section, we now consider a top corresponding to the non-simply laced Lie algebra B_3. The top is constructed uniquely from the classification [19] and the corresponding hypersurface equation is

$$\hat{P} = e_1^2 s^2 t^4 + e_3 s y^2 + a_1 e_0 e_1 e_2 e_3 s t y z + a_2 e_0 e_1 s t^2 z^2 + a_4 e_0^2 z^4. \tag{3.3.49}$$

Having a node at $z = 2$ in the top defines the divisor $W = \{w = 0\}$ in the base with $\pi^* w = e_0 e_1 e_2^2 e_3$ and gives multiplicity 2 to the corresponding curve $\mathbb{P}_2^1$ in the fiber over W. The occurrence of the multiplicity of the node in the projection to the base is crucial to make W scale under the scaling relations coming from the $z \geq 1$ layers of the top. The affine B_3 Dynkin diagram is read off along the edges at $z \geq 1$ of the top in Figure 3.5. The non-simply laced structure of this algebra is reflected in the fact that the intersection of the ambient divisor E_3 with the hypersurface

$$E_3 \cap \hat{P}|_{e_3=0} \cap D_a \cap D_b, \qquad D_{a,b} \subset \mathcal{B} \tag{3.3.50}$$

gives rise to two curves. These are described by the factorization

$$\{e_3 = 0\} \cap \{s^2 + a_2 e_0 s + a_4 e_0^2 = 0\} \qquad \Leftrightarrow$$
$$\{e_3 = 0\} \cap \{(s + \frac{1}{2} a_2 e_0 \pm e_0 \sqrt{\frac{a_2^2}{4} - a_4})(s + \frac{1}{2} a_2 e_0 \mp e_0 \sqrt{\frac{a_2^2}{4} - a_4}) = 0\}. \tag{3.3.51}$$

The two factors on the righthand side give rise to the curves $\mathbb{P}_{3\pm}^1$ and they get exchanged when the signs of the square roots shift upon travelling along W in the base. As a check, the negative of the Cartan matrix C_{ij} of B_3 is reproduced as the intersection numbers

$$E_i \cdot (\mathbb{P}_0^1, \mathbb{P}_1^1, \mathbb{P}_2^1, \mathbb{P}_{3\pm}^1)_j = -C_{ij}. \tag{3.3.52}$$

By analyzing the codimension-two loci, we find only one curve in $\mathcal{B}$ over which the fiber degenerates further. This happens over $W \cap \{a_4 = 0\}$ and by calculating the charges of the split fiber components weights in the weight system of the $(\mathbf{8}, \mathbf{2})$ of $\mathfrak{so}(7) \oplus \mathfrak{su}(2)$ are found, where $\mathbf{8}$ is the spinor representation. By using that the toric divisor X does not restrict to the hypersurface the Shioda map of the torsional section gives a class

$$\Xi_2 \equiv T - Z - \bar{\mathcal{K}} = -\frac{1}{2}(S + 2E_1 + 2E_2 + E_3) \tag{3.3.53}$$

with integer intersection with all fiber components over the matter curve. Consistently with the appearance of the representation $(\mathbf{8}, \mathbf{2})$ of $\mathfrak{so}(7) \oplus \mathfrak{su}(2)$ the gauge group is

$$G = \frac{Spin(7) \times SU(2)}{\mathbb{Z}_2}, \tag{3.3.54}$$

where the $\mathbb{Z}_2$ is the common center of $Spin(7)$ and $SU(2)$ and $\pi_1(G) = \mathbb{Z}_2$. Even though not realized in this geometry, all representations $(\mathbf{8}, \mathbf{R_e})$ for $\mathbf{R}_e$ an even-dimensional representation of $SU(2)$ would also be allowed, and also the representations $(\mathbf{7}, \mathbf{R_o})$ for $\mathbf{R}_o$ an odd-dimensional representation of $SU(2)$.

3.3.5 Generalisation to $Sp(n)/\mathbb{Z}_2$, $SU(2n)/\mathbb{Z}_2$, $Spin(4n)/\mathbb{Z}_2$, Type IIB limit and restricted monodromies

The toric enhancements described in the previous sections involved the specialization $a_4 \to a_{4,n}w^n$ for $W : \{w = 0\}$ some divisor different from the A_1-locus $\{a_4 = 0\}$. Clearly one can also identify w with a_4, thereby producing a single gauge group factor. According to the general discussion, this single group factor will be strongly constrained by the requirement that the universal cover gauge group G_0 contain a $\mathbb{Z}_2$-subgroup in its center.

Indeed, if $\bar{\mathcal{K}}_{\mathcal{B}}^{4/n}$ exists as a line bundle with non-trivial sections, we can simply factorise

$$a_4 = (\tilde{a}_4)^n \tag{3.3.55}$$

with $\tilde{a}_4 \in H^0(\mathcal{B}, \bar{\mathcal{K}}_{\mathcal{B}}^{4/n})$. Since the analysis of the singular geometry and its resolution has been exemplified in detail in the previous sections, we content ourselves with determining the resulting gauge groups by application of Tate's algorithm [79, 81] without explicitly constructing the resolution. For generic a_2, Tate's algorithm in the form of table 2 of [81] indicates that the fiber over $\tilde{a}_4 = 0$ is of Kodaira type I_{2n}^{ns}, with the superscript denoting the *non-split* type. The associated gauge algebra is the rank n Lie algebra $\mathfrak{sp}(n)$ (with the convention that $\mathfrak{sp}(1) \simeq \mathfrak{su}(2)$). This identifies the gauge group as

$$G = \frac{Sp(n)}{\mathbb{Z}_2}. \tag{3.3.56}$$

As described in subsection 3.3.1, if $n = 1$ the global structure of G makes extra massless representations along the curve $\{\tilde{a}_4 = 0\} \cap \{\frac{1}{4}a_1^2 + a_2 = 0\}$ impossible; this is no longer true for $n \geq 2$. Indeed, in this case Tate's algorithm predicts, as described in detail in [80], for the fiber type over this curve Kodaira type I_{2n-4}^{*s} (with the superscript standing for *split* type), corresponding to gauge algebra $\mathfrak{so}(4n)$. From the branching rule of the adjoint of $SO(4n)$ along $SO(4n) \to SU(2n) \times U(1) \to Sp(n) \times U(1)$ one deduces matter in the 2-index antisymmetric representation of $Sp(n)$ of dimension $2n^2 - n - 1$ along $\{\tilde{a}_4 = 0\} \cap \{\frac{1}{4}a_1^2 + a_2 = 0\}$ (see in particular Table 9 of [80]). This is compatible with the gauge group $G = Sp(n)/\mathbb{Z}_2$.

Next, one can engineer a gauge algebra $\mathfrak{su}(2n)$ by factoring $a_4 = (\tilde{a}_4)^n$ and in addition restricting $a_2 = a_{2,1}\tilde{a}_4$ for suitable $a_{2,1} \in H^0(\mathcal{B}, \bar{\mathcal{K}}_{\mathcal{B}}^{2-4/n})$ (if existent). In this case the gauge group is

$$G = \frac{SU(2n)}{\mathbb{Z}_2}, \qquad n \geq 2. \tag{3.3.57}$$

Note that the Mordell-Weil torsion group $\mathbb{Z}_2$ appears here as a proper subgroup of the center $\mathbb{Z}_{2n}$ of the universal cover $G_0 = SU(2n)$. The same argument as above predicts massless matter in the antisymmetric representation of $SU(2n)$ localised on the curve $\{\tilde{a}_4 = 0\} \cap \{a_1 = 0\}$. The appearance of this matter distinguishes $G = SU(2n)/\mathbb{Z}_2$ as realized here from $SU(2n)/\mathbb{Z}_{2n}$. The possibility that the Mordell-Weil torsion appears as a proper subgroup of the center of the universal cover G_0 had previously been noted in eight-dimensional F-theory compactifications on K3 in [69, 85].

The only remaining chain of enhancements of this type which is possible according to Tate's algorithm leads to gauge algebra $\mathfrak{so}(4n)$ with $n \geq 4$ and corresponds to $a_4 = (\tilde{a}_4)^n$, $a_2 = a_{2,1}\tilde{a}_4$ and $a_1 = a_{1,1}\tilde{a}_4$. The restriction to $n \geq 4$ comes about as a necessary condition for a section $a_1 \in H^0(\mathcal{B}, \bar{\mathcal{K}}_{\mathcal{B}}^{1-4/n})$ to exist. According to the analysis in [80] we expect matter in the vector representation along the curve $\{\tilde{a}_4 = 0\} \cap \{a_{2,1} = 0\}$. Note that the universal cover group $G_0 = Spin(4n)$ has center $\mathbb{Z}_2 \times \mathbb{Z}_2$. The appearance of the vector representation (but not the spinor) is in perfect agreement with the gauge group being

$$G = \frac{Spin(4n)}{\mathbb{Z}_2} = SO(4n), \qquad n \geq 4. \tag{3.3.58}$$

The observed pattern has a natural interpretation in the weak coupling Type IIB orientifold limit. This Sen limit [36] is realized as the limit $\epsilon \to 0$ after rescaling $a_3 \to \epsilon\, a_3$, $a_4 \to \epsilon\, a_4$, $a_6 \to \epsilon^2\, a_6$ [86]. The discriminant locus can be brought into the form

$$\Delta \simeq \epsilon^2 h^2 (\eta^2 - h\chi) + \mathcal{O}(\epsilon^3), \tag{3.3.59}$$

and the Type IIB Calabi-Yau

$$X_{IIB} : \xi^2 = h \tag{3.3.60}$$

is a double cover of the F-theory base $\mathcal{B}$ branched over the orientifold plane localised at $h = 0$. The orientifold action on X_{IIB} acts as $\xi \to -\xi$. The locus $\eta^2 - h\chi = 0$ on $\mathcal{B}$ and its uplift to the Calabi-Yau double cover X_{IIB} represents the D7-brane locus. In the configuration at hand, due to the restriction $a_3 \equiv 0$ and $a_6 \equiv 0$, one finds

$$h = -\frac{1}{12}(a_1^2 + 4a_2), \qquad \chi = 0, \qquad \eta = a_4 = (\tilde{a}_4)^n. \tag{3.3.61}$$

For generic a_2 the D7-brane system is given by a stack of D7-branes on the uplift of the divisor $\{a_4 = 0\}$ to the double cover X_{IIB}; since this locus is invariant under the orientifold projection, the D7-brane stack supports gauge algebra $\mathfrak{sp}(n)$. The antisymmetric matter appears at the intersection with the O7-plane at $h = 0$. If $a_2 = a_{2,1}\tilde{a}_4$, then the analysis of [87] shows that the D7-branes wrap a divisor on the Calabi-Yau double cover which is not mapped to itself under the orientifold action. Its corresponding non-abelian gauge algebra is therefore indeed $\mathfrak{su}(n)$ with antisymmetric matter at the intersection of the D7-brane stack with its image on top of the O7-plane. For completeness, note that the further specialization $a_1 = a_{1,1}\tilde{a}_4$, corresponding to the $Spin(4n)/\mathbb{Z}_2$ series in F-theory, has an ill-defined weak-coupling limit with two O7-planes intersecting over a curve of conifold singularities.

Apart from reproducing the F-theory predictions, this weak coupling analysis exemplifies how the global structure of the gauge group in the Type IIB limit can be understood from the specific D7-brane

configuration and the absence (or presence) of certain matter representations. In the situation under consideration, what changes the gauge group from $Sp(n)$ or $SU(2n)$ to $Sp(n)/\mathbb{Z}_2$ and $SU(2n)/\mathbb{Z}_2$ is that in the discriminant (3.3.59) no extra single D7-brane arises in addition to the non-abelian brane stack at $\{\tilde{a}_4 = 0\}$; if present the intersection curve of such a brane with the D7-brane stack would lead to matter in the fundamental representation of $Sp(n)$ or $SU(2n)$ and thus change the global structure of the gauge group.

Finally, let us point out that the elliptic fibration (3.3.9) with $s \equiv 1$, *i.e.* the singular model corresponding to the blow-down of the A_1-fiber at $\{a_4 = 0\}$, was considered in [78] from a related, but slightly different perspective: In this work it was shown that this class of elliptic fibrations does not exhaust the full $SL(2, \mathbb{Z})$ monodromy group, but only the subgroup $\Gamma_0(2) \subset SL(2, \mathbb{Z})$.[6] In fact, restricted $\Gamma_0(k)$-monodromy is a consequence of the existence of an order k point on the elliptic fiber [78], which, in the language of our analysis, is equivalent to Mordell-Weil k-torsion. There are a number of geometric consequences of this [17]. For example, the modular curve $\mathfrak{h}/\Gamma_0(2)$ has *two* "cusp" points at which $j = \infty$, corresponding to the two irreducible factors a_4 and $\left(4a_4 - (a_2 + \frac{1}{4}a_1^2)^2\right)$ of the discriminant (3.3.2). As we have seen in examples, it is the factor a_4 which vanishes when the corresponding gauge group factor is related to $\mathbb{Z}_2$ torsion. By contrast, one can in principle also engineer additional gauge group factors by factorising $\left(4a_4 - (a_2 + \frac{1}{4}a_1^2)^2\right)$ without factorising a_4 as such. Such non-toric enhancements would lead to what we called the 'spectator' gauge group G' in section 3.2 and which is unconstrained by the $\mathbb{Z}_2$ torsion. Indeed, while all gauge algebras that can be engineered torically are easily checked to lead to Kodaira monodromies contained in $\Gamma_0(2)$, this set does not exhaust the list of $\Gamma_0(2)$-compatible singularities (*e.g.* it misses A_{2k} - see appendix B of [78]). Such algebras would have to come from a non-toric enhancement involving the second factor of the discriminant. We will see an example of an abelian spectator group $G' = U(1)$ in the next section.

3.4 Mordell-Weil group $\mathbb{Z} \oplus \mathbb{Z}_2$

3.4.1   An $(SU(2) \times SU(2))/\mathbb{Z}_2 \times U(1)$ fibration

The generic elliptic fibration with $\mathbb{Z}_2$-torsional Mordell-Weil group admits an interesting specialization such as to enhance the Mordell-Weil group to $\mathbb{Z}_2 \oplus \mathbb{Z}$. As it turns out the generator of the free part of the Mordell-Weil group can be described again very conveniently as a toric section.

In fact, the specialization we have in mind gives rise to the second of the three elliptic fibrations realized as hypersurfaces in a toric ambient space with Mordell-Weil torsion [20]. The fiber is defined by the reflexive pair in Figure 3.6, which corresponds to polygon 15 and its dual in the classification of [19]. The associated elliptic curve is the vanishing locus of a biquadric in a blow-up of $\mathbb{P}^1 \times \mathbb{P}^1$. The hypersurface equation defined via the dual polygon is

$$\hat{P} = cd^2v^2w^2 + c^2du^2v^2 + \gamma_1 cduvwz + \gamma_2 dw^2z^2 + \delta_2 cu^2z^2, \qquad (3.4.1)$$

where we have set the coefficients of the first two terms to one since they are sections of the trivial bundle over the base[7]. The coefficients γ_i and δ_i are sections of $\bar{\mathcal{K}}^i$. A choice for the scaling relations

---

[6]Recall that $\Gamma_0(k)$ is defined as the subgroup of $SL(2, \mathbb{Z})$-matrices $\begin{pmatrix} a & b \\ c & d \end{pmatrix}$ with $c \equiv 0 \mod k$.

[7]If we had chosen a fibration such that these two coefficients are sections of non-trivial bundles, $z = 0$ would not be a holomorphic section but a birational one.
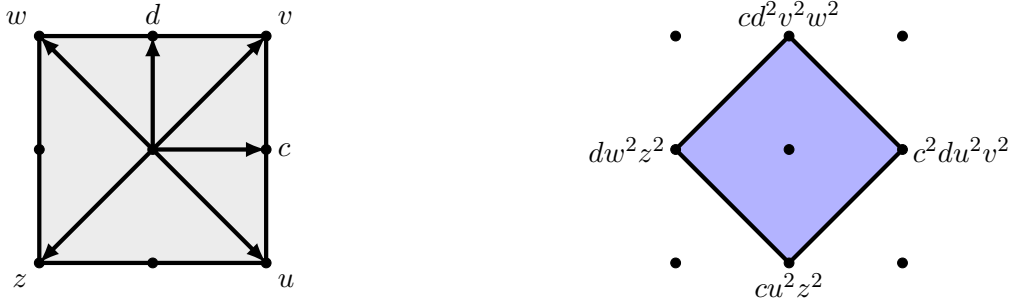
Figure 3.6: Polygon 15 of [19] together with its dual polygon.

of the fiber coordinates is

u	v	w	z	c	d	$\sum$
1	0	1	0	0	0	2
0	1	0	1	0	0	2
0	0	0	1	1	1	3
0	0	1	1	2	0	4

$$(3.4.2)$$

which is consistent with the degree of homogeneity of (3.4.1). The Stanley-Reisner ideal of the toric ambient space of the fiber takes the form $\{uv, uw, ud, vz, zc, zd, wc, cd, vw\}$.

The biquadric (3.4.1) can be brought into Weierstrass form, where it can be compared with the Weierstrass model associated with the fibration (3.3.1) analysed in the previous section. This identifies

$$a_1 = \gamma_1\,, \qquad a_2 = -(\gamma_2 + \delta_2)\,, \qquad a_4 = \gamma_2\delta_2\,, \qquad (3.4.3)$$

where a_i are the coefficients of the generic $\mathbb{Z}_2$-torsion fibration (3.3.1). As we will show, the result of this specialization of a_2 and a_4 is the enhancement of the Mordell-Weil group from $\mathbb{Z}_2$ to $\mathbb{Z}_2 \oplus \mathbb{Z}$ (as computed previously in [20]) and the appearance of an extra $\mathfrak{su}(2)$ factor.

To analyse the non-abelian sector, we first note that the discriminant of equation (3.4.1) takes the form

$$\Delta \sim \gamma_2^2\delta_2^2[\gamma_1^4 - 8\gamma_1^2(\gamma_2 + \delta_2) + 16(\gamma_2 - \delta_2)^2]. \qquad (3.4.4)$$

Together with the Weierstrass functions f and g of the associated Weierstrass model this suggests an A_1 singularity at $\{\gamma_2 = 0\}$ and $\{\delta_2 = 0\}$ respectively. Indeed, the hypersurface equation factorises over these loci as

$$\begin{aligned} \{\gamma_2 = 0\}: &\quad c\left(cdu^2v^2 + d^2v^2w^2 + \gamma_1 duvwz + \delta_2 u^2z^2\right), \\ \{\delta_2 = 0\}: &\quad d\left(cdv^2w^2 + c^2u^2v^2 + \gamma_1 cuvwz + \gamma_2 w^2z^2\right), \end{aligned} \qquad (3.4.5)$$

and we identify the irreducible components $\mathbb{P}_c^1$ and $\mathbb{P}_d^1$ as the restriction to the fiber of the resolution divisors $C : \{c = 0\}$ and $D : \{d = 0\}$ of these singularities.

On general grounds [20,21], the intersection of the toric divisors $U : \{u = 0\}$, $V : \{v = 0\}$, $W : \{w = 0\}$, $Z : \{z = 0\}$ with the hypersurface give rise to sections of the fibration, not all of which are independent. Since $Z : \{z = 0\}$ is a holomorphic section we choose it as the zero-section. Then, the Mordell-Weil group is generated by differences of sections $U - Z$, $V - Z$, $W - Z$, which are not all independent. Let us first consider the Shioda map for the section $U : \{u = 0\}$. Requiring, as usual, one leg in the fiber as well as orthogonality with the exceptional divisors gives

$$W_U = 2(U - Z - \bar{\mathcal{K}}) + C\,, \qquad (3.4.6)$$

which is unique up to an overall normalization, here chosen such as to arrive at integer charges below. We take this non-trivial element W_U as the generator of the free part of the Mordell-Weil group, and physically identify it with the generator of the associated, suitably normalized $U(1)$ part of the gauge group.

On the other hand, the intersection of the section $V : \{v = 0\}$ with the elliptic curve describes a 2-torsion point, as noted already in [20]. The Shioda map for $V : \{v = 0\}$ yields the element

$$\Sigma_2 = V - Z - \bar{\mathcal{K}} + \frac{1}{2}(C + D). \tag{3.4.7}$$

However, V is not an independent toric divisor class, but may be expressed as

$$V = Z + \bar{\mathcal{K}} - \frac{1}{2}(C + D), \tag{3.4.8}$$

which makes Σ_2 a trivial class. Since the model we consider here is a restriction of the model with just a $\mathbb{Z}_2$ section we have the analogous situation that Σ_2 is given by a divisor in the ambient space which restricts to a trivial class on the hypersurface. The integer class

$$\Xi_2 \equiv V - Z - \bar{\mathcal{K}} = \frac{1}{2}(C + D) \tag{3.4.9}$$

is 2-torsion in $H^{1,1}(\hat{Y}_4, \mathbb{Z})$ modulo resolution classes and to be identified with a coweight element momentarily.

Having established the gauge algebra $\mathfrak{su}(2) \oplus \mathfrak{su}(2) \oplus \mathfrak{u}(1)$ we turn to the matter representations in codimension 2. From the discriminant (3.4.4) the three potential enhancement loci which could host matter charged under the non-abelian gauge groups are identified as

$$\{\gamma_2 = \delta_2 = 0\}, \quad \{\gamma_1 = \gamma_2 = 0\}, \quad \{\gamma_1 = \delta_2 = 0\}. \tag{3.4.10}$$

At the loci $\{\gamma_1 = \gamma_2 = 0\}$ and $\{\gamma_1 = \delta_2 = 0\}$, which would naively give rise to fundamental matter, the equation does not factorize further, and hence no extra matter is found there. But at the locus $\{\gamma_2 = \delta_2 = 0\}$ the equation factorizes as

$$cdv \underbrace{(cu^2v + dvw^2 + \gamma_1 uwz)}_{R}, \tag{3.4.11}$$

where the curves $\mathbb{P}^1_c$, $\mathbb{P}^1_d$, $\mathbb{P}^1_v$ and the last component $\mathbb{P}^1_R$ intersect as the affine A_3 Dynkin diagram. We calculate the charges of the split component $\mathbb{P}^1_{v=0}$ as

$$\mathbb{P}^1_{v=0} \cdot (C, D) = (1, 1), \tag{3.4.12}$$

giving the highest weights of the bifundamental $(\mathbf{2}, \mathbf{2})$. By acting on this with the respective roots the entire $(\mathbf{2}, \mathbf{2})$ is reproduced. With the normalization (3.4.6) the $U(1)$ charge of this state is

$$W_U \cdot \mathbb{P}^1_{v=0} = 1. \tag{3.4.13}$$

Extra massless matter is localized at the singlet curve $\{\gamma_2 = \delta_2\} \cap \{\gamma_1 = 0\}$. This is an I_2 locus over which the hypersurface equation factorizes as

$$(cu^2 + dw^2)(cdv^2 + \delta_2 z^2), \tag{3.4.14}$$

and we denote the fiber components by $\mathbb{P}^1_-$ and $\mathbb{P}^1_+$ respectively. These have zero intersection with the Cartan divisors C, D (and are thus invariant also under the center of the gauge group) and their $U(1)$-charges are computed as

$$W_U \cdot \mathbb{P}^1_\pm = \pm 2. \tag{3.4.15}$$

Hence we find a representation $(\mathbf{1}, \mathbf{1})_{\pm 2}$ with respect to $\mathfrak{su}(2)_C \oplus \mathfrak{su}(2)_D \oplus U(1)$.

At the intersection points $\gamma_1 = \gamma_2 = \delta_2 = 0$ of the two matter curves the fiber type changes to form a non-affine Dynkin diagram of D_4. This is because the component $(cu^2 v + dvw^2 + \gamma_1 uwz)_R$ in the fiber over the curve $\{\gamma_2 = \delta_2 = 0\}$ splits off a factor of v as $\gamma_1 = 0$, corresponding to a factorisation

$$c \, d \, v^2 \, (cu^2 + dw^2). \tag{3.4.16}$$

At those points a Yukawa coupling $(\mathbf{2}, \mathbf{2})_1 \, (\mathbf{2}, \mathbf{2})_1 \, (\mathbf{1}, \mathbf{1})_{-2}$ is localised.

As is manifest, the divisor Ξ_2 has integer pairing with all split curves associated with the representations $(\mathbf{2}, \mathbf{2})_1$ and $(\mathbf{1}, \mathbf{1})_{\pm 2}$ and is therefore identified with a coweight. With coefficients in $\frac{1}{2}\mathbb{Z}$ the coweight lattice is made finer by this extra coweight, and only weights in representations integer paired with Ξ_2 are allowed. Again this is the reason for the absence of for example a fundamental representation at the loci $\{\gamma_1 = \gamma_2 = 0\}$ and $\{\gamma_1 = \delta_2 = 0\}$. Note that the expression for Σ_2 does not include a term proportional to the $U(1)$-generator W_U, but only the generators C and D of the $\mathfrak{su}(2)_C \oplus \mathfrak{su}(2)_D$ Cartan $U(1)$s. In particular, integrality of the pairing of Ξ_2 does therefore not constrain the allowed $U(1)$ charges, but only the non-abelian part of the representation. We conclude that the gauge group is

$$G = \frac{SU(2)_C \times SU(2)_D}{\mathbb{Z}_2} \times U(1), \tag{3.4.17}$$

whose first fundamental group $\pi_1(G) = \mathbb{Z} \oplus \mathbb{Z}_2$ coincides with the Mordell-Weil group as expected.

3.4.2   A chain of fibrations via Higgsing

The elliptic fibrations described in sections 3.3.1, 3.3.2 and 3.4.1 can be viewed as a successive specialization of a Tate model

$$P = y^2 - x^3 + a_1 xyz + a_2 x^2 z^2 + a_3 yz^3 + a_4 xz^4 + a_6 z^6, \tag{3.4.18}$$

which for generic $a_i \in H^0(\mathcal{B}, \bar{\mathcal{K}}^i)$ has trivial Mordell-Weil and gauge group. If $a_6 \equiv 0$, the fibration corresponds to a $U(1)$ restricted Tate model [77] with Mordell-Weil group $\mathbb{Z}$, gauge group $G = U(1)$ and a massless singlet $\mathbf{1}_{\pm 1}$ localized at the curve $\{a_3 = 0\} \cap \{a_4 = 0\}$. The extra section degenerates to a $\mathbb{P}^1$ over this matter curve [59, 77, 87]. From this, one reaches the fibration (3.3.1) with Mordell-Weil group $\mathbb{Z}_2$ and $G = SU(2)/\mathbb{Z}_2$ by setting in addition $a_3 \equiv 0$. This promotes the $U(1)$ generator of the $U(1)$ restricted model to the $\mathfrak{su}(2)$ Cartan generator, which is $\mathbb{P}^1$ fibered over the $\mathfrak{su}(2)$-divisor $\{a_4 = 0\}$. Since the $U(1)$ restricted model has only one type of charged singlet, which becomes part of the $\mathfrak{su}(2)$ adjoint multiplet, the specialization to $a_3 \equiv 0$ does not give rise to any extra matter states. This way the gauge group $G = SU(2)/\mathbb{Z}_2$ could in fact have been anticipated even without any knowledge of the torsional Mordell-Weil group. The reverse process corresponds to the Higgsing of $G = SU(2)/\mathbb{Z}_2$ to $U(1)$ via a Higgs in the adjoint of $SU(2)$, more precisely the component with zero Cartan charge.

A further factorisation $a_4 = a_{4,1} w$ enhances, as described, the gauge group to $G = (SU(2) \times SU(2))/\mathbb{Z}_2$ (cf. 3.3.29) without changing the Mordell-Weil group. Finally, if $w \in H^0(\mathcal{B}, \bar{\mathcal{K}}^2)$, specialising in addition to $a_2 = -(w + a_{4,1})$ enhances the Mordell-Weil group to $\mathbb{Z}_2 \oplus \mathbb{Z}$ and the gauge group to $G = (SU(2) \times SU(2))/\mathbb{Z}_2 \times U(1)$ - see (3.4.3) with $\gamma_2 = a_{4,1}$ and $\delta_2 = w$. The reversed chain of Higgsing thus relates all these fibrations as

$$\frac{SU(2) \times SU(2)}{\mathbb{Z}_2} \times U(1) \to \frac{SU(2) \times SU(2)}{\mathbb{Z}_2} \to \frac{SU(2)}{\mathbb{Z}_2} \to U(1) \to \emptyset. \tag{3.4.19}$$

Figure 3.7: To the left a $\mathfrak{su}(4)$ top over polygon 15 of [19]. The green layer contains the points at height one. To the right the dual top, bounded from below by the values z_{min} shown next to the nodes.

Note that the fibration (3.3.29) with $G = (SU(2) \times SU(2))/\mathbb{Z}_2$ can be shown to coincide with a model that was recently considered in [84]. In this paper, a different chain of Higgsing was considered which takes the form

$$\frac{SU(2) \times SU(2)}{\mathbb{Z}_2} \to SU(2) \to U(1) \to \mathbb{Z}_2. \tag{3.4.20}$$

The chain (3.4.19) is a specialization of the deformations involved in (3.4.20). In particular, the fibration with Mordell-Weil group $\mathbb{Z}$ and $G = U(1)$ reached in (3.4.20) is described as a special $\mathbb{P}_{1,1,2}[4]$-fibration [18] and can in general not be represented as a global Tate model. However, a specialization of this family of fibrations corresponds to the $U(1)$ restricted Tate model appearing in (3.4.19). The endpoint of the Higgsing process (3.4.20) with gauge group $\mathbb{Z}_2$ is a genus-one fibration [29] which is not an elliptic fibration. The absence of a $\mathbb{Z}_2$ remnant in the last step in our chain (3.4.19) can be viewed as a consequence of the division by the $\mathbb{Z}_2$ center in the $G = SU(2)/\mathbb{Z}_2$ model.

3.4.3 An $(SU(4) \times SU(2) \times SU(2))/\mathbb{Z}_2 \times U(1)$ fibration

We now exemplify the implementation of a further non-abelian singularity by constructing a top. According to the classification in [19] the only A-type singularities admissible over this polygon are A_{3+2n}, in agreement with Tate's algorithm. We consider here the $A_3 = \mathfrak{su}(4)$ case, with a unique top corresponding to the dual on the righthand side in Figure 3.7. The hypersurface equation is given by

$$\hat{P} = e_2 e_3 c^2 du^2 v^2 + e_1 e_2 cd^2 v^2 w^2 + \gamma_1 cduvwz + \gamma_2 e_0 e_1 dw^2 z^2 + \delta_2 e_0 e_3 cu^2 z^2 \tag{3.4.21}$$

with discriminant

$$\Delta \sim \varpi^4 \gamma_2^2 \delta_2^2 \left[\gamma_1^4 - 8\varpi \gamma_1^2 (\delta_2 + \gamma_2) + 16\varpi^2 (\gamma_2 - \delta_2)^2 \right] \tag{3.4.22}$$

for $\pi^* \varpi = e_0 e_1 e_2 e_3$. We see that imposing the factorization

$$\gamma_1 \to \gamma_1, \quad \gamma_2 \to \varpi \gamma_2, \quad \delta_2 \to \varpi \delta_2 \tag{3.4.23}$$

on the coefficients of (3.4.1) gives the same behaviour as the top construction. This pattern is just the standard factorisation deduced by the Tate algorithm. For the chosen triangulation of this top we obtain a Stanley-Reisner ideal generated by

$$\{uv, uw, ud, vz, zc, zd, wc, cd, vw,$$
$$ce_0, de_0, ve_0, ce_1, ue_1, ze_1, de_2, we_2, ze_2, ce_3, de_3, ve_3, we_3, ze_3, e_1 e_3, ue_0 e_2\}.$$

In addition to the A_1 singularities, with resolution divisors C and D, we have a fiber degeneration over $\{\varpi = 0\}$ with irreducible components

$$\mathbb{P}_i^1 = \{E_i\} \cap \{\hat{P}|_{e_i=0} = 0\} \cap D_a \cap D_b \quad i = 0, \ldots, 3, \tag{3.4.24}$$

where D_a and D_b are some generic divisors in $\mathcal{B}$. These are intersecting as the affine $\mathfrak{su}(4)$ Dynkin diagram, as can be read off from the top in Figure 3.7. For the explicit expressions we refer to appendix A.2. The $U(1)$-generator from the previous section gets corrected by the exceptional divisors from the extra $\mathfrak{su}(4)$ locus and takes the form

$$W_U = 4(U - Z - \bar{\mathcal{K}}) + 2C + E_1 + 2E_2 + 3E_3. \tag{3.4.25}$$

The normalization is chosen such as to give integer charges of all matter states. In the same way we get additional contributions to the Shioda map Σ_2 of the torsion section, which is a trivial class since V can be written as the linear combination

$$V = Z + \bar{\mathcal{K}} - \frac{1}{2}(C + D + E_1 + 2E_2 + E_3). \tag{3.4.26}$$

We identify with the new coweight the integer class

$$\Xi_2 \equiv V - Z - \bar{\mathcal{K}} = \frac{1}{2}(C + D + E_1 + 2E_2 + E_3), \tag{3.4.27}$$

which is 2-torsion in $H^{1,1}(\hat{Y}_4, \mathbb{Z})$ modulo resolution classes. Repeating the analysis of the previous section we find that the extra coweight class Ξ_2 is independent of the $U(1)$-generator.

In what follows we compute the additional charged matter representations localized at codimension-two loci in the base, *i.e.* the matter curves that lie in the $\mathfrak{su}(4)$ divisor $\{\varpi = 0\}$. The full equations are omitted here and are found appendix A.2. By inspection of the discriminant (3.4.22) the potential enhancement loci are

$$\{\varpi = \gamma_1 = 0\}, \quad \{\varpi = \gamma_2 = 0\}, \quad \{\varpi = \delta_2 = 0\}, \tag{3.4.28}$$

in addition to the curves considered in the previous section. At $\{\varpi = \gamma_1 = 0\}$ the fiber components $\mathbb{P}_0^1$ and $\mathbb{P}_2^1$ split and the total fiber has the intersection structure of the affine D_4 Dynkin diagram. The weights of the split curves are

$$\begin{aligned}
\mathbb{P}_{e_0=e_2=0}^1 \cdot (E_1, E_2, E_3) &= (1, -1, 1), & \mathbb{P}_{e_0=e_2=0}^1 \cdot (C, D) &= (0, 0), \\
\mathbb{P}_{e_0=e_3u^2+e_1w^2=0}^1 \cdot (E_1, E_2, E_3) &= (0, 1, 0), & \mathbb{P}_{e_0=e_3u^2+e_1w^2=0}^1 \cdot (C, D) &= (0, 0), \\
\mathbb{P}_{e_2=\gamma_2e_1+\delta_2e_3cu^2=0}^1, \cdot (E_1, E_2, E_3) &= (0, -1, 0), & \mathbb{P}_{e_2=\gamma_2e_1+\delta_2e_3cu^2=0}^1 \cdot (C, D) &= (0, 0).
\end{aligned} \tag{3.4.29}$$

The $(0, 1, 0)$ is the highest weight of the $\mathbf{6}$ of $\mathfrak{su}(4)$. Including the $U(1)$ charges we therefore find the representation $(\mathbf{6}, \mathbf{1}, \mathbf{1})_2 + c.c.$.

At $\{\varpi = \gamma_2 = 0\}$ the curve $\mathbb{P}_2^1$ splits into three components and the full fiber has the structure of an affine A_5 Dynkin diagram. We expect to find matter charged under the $\mathfrak{su}(4)$ and the $\mathfrak{su}(2)_C$ factors along this curve in the base. Indeed the split curves have charges

$$\begin{aligned}
\mathbb{P}_{e_2=c=0}^1 \cdot (E_1, E_2, E_3) &= (0, 0, 0), & \mathbb{P}_{e_2=c=0}^1 \cdot (C, D) &= (-2, 0), \\
\mathbb{P}_{e_2=u=0}^1 \cdot (E_1, E_2, E_3) &= (0, -1, 1), & \mathbb{P}_{e_2=u=0}^1 \cdot (C, D) &= (1, 0), \\
\mathbb{P}_{e_2=\gamma_1v+\delta_2e_0e_3u=0}^1 \cdot (E_1, E_2, E_3) &= (1, -1, 0), & \mathbb{P}_{e_2=\gamma_1v+\delta_2e_0e_3u=0}^1 \cdot (C, D) &= (1, 0),
\end{aligned} \tag{3.4.30}$$

where the $(0, -1, 1)$ and the $(1, -1, 0)$ are weights in the fundamentals $\mathbf{4}$ and $\bar{\mathbf{4}}$ respectively. Including the $U(1)$ charges we have the $(\mathbf{4}, \mathbf{2}, \mathbf{1})_1 + c.c.$ along this matter curve.

Along $\varpi = \delta_2 = 0$ the configuration is completely analogous to that along $\varpi = \gamma_2 = 0$ and gives rise to massless matter in representation $(\mathbf{4}, \mathbf{1}, \mathbf{2})_1 + c.c.$. The massless matter spectrum is summarized in the following table:

Top over polygon 15: $\mathfrak{su}(4) \times \mathfrak{su}(2)_C \times \mathfrak{su}(2)_D \times U(1)$

Locus	*Charged matter*
$\gamma_1 \cap \{\gamma_2 = \delta_2\}$	$(\mathbf{1}, \mathbf{1}, \mathbf{1})_4$, $(\mathbf{1}, \mathbf{1}, \mathbf{1})_{-4}$
$\gamma_2 \cap \delta_2$	$(\mathbf{1}, \mathbf{2}, \mathbf{2})_2$, $(\mathbf{1}, \mathbf{2}, \mathbf{2})_{-2}$
$\varpi \cap \gamma_1$	$(\mathbf{6}, \mathbf{1}, \mathbf{1})_2$, $(\mathbf{6}, \mathbf{1}, \mathbf{1})_{-2}$
$\varpi \cap \gamma_2$	$(\mathbf{4}, \mathbf{2}, \mathbf{1})_1$, $(\bar{\mathbf{4}}, \mathbf{2}, \mathbf{1})_{-1}$
$\varpi \cap \delta_2$	$(\mathbf{4}, \mathbf{1}, \mathbf{2})_1$, $(\bar{\mathbf{4}}, \mathbf{1}, \mathbf{2})_{-1}$

$$(3.4.31)$$

It is confirmed that the coweight element Ξ_2 is integer-valued on all split curves responsible for the matter representations. We finally conclude that the gauge group is

$$\frac{SU(4) \times SU(2)_C \times SU(2)_D}{\mathbb{Z}_2} \times U(1) \, . \tag{3.4.32}$$

3.5 Mordell-Weil group $\mathbb{Z}_3$

As a further illustration we now analyze elliptic fibrations with $\mathbb{Z}_3$ torsional Mordell-Weil group. The general form of such fibrations was derived in [69]. As we will show this fibration allows for a toric representation, which in fact coincides with the last of the 3 reflexive pairs of polygons admitting a torsional Mordell-Weil group [20]. The fan is given by the 16th reflexive polygon in the enumeration by [19]. We first present the toric representation of this fibration, its singularity structure and impose further non-abelian degenerations of the fiber to analyse the resulting matter spectrum and global structure of the gauge group.

3.5.1 An $SU(3)/\mathbb{Z}_3$-fibration

The generic form of an elliptic fibration with a $\mathbb{Z}_3$-section is given by the vanishing locus of the hypersurface equation [69]

$$P = y^2 + a_1 xyz + a_3 yz^3 - x^3 \tag{3.5.1}$$

in weighted projective space $\mathbb{P}_{[2,3,1]}$. Such fibrations therefore fit again into the class of global Tate models, but with $a_6 \equiv 0$ and in addition $a_2 \equiv 0$ and $a_4 \equiv 0$. The equivalent Weierstrass model is defined by

$$f = \frac{1}{2} a_1 a_3 - \frac{1}{48} a_1^4 \, , \qquad g = \frac{1}{4} a_3^2 + \frac{1}{864} a_1^6 - \frac{1}{24} a_1^3 a_3 \tag{3.5.2}$$

with discriminant

$$\Delta = \frac{1}{16} a_3^3 (27 a_3 - a_1^3) \, . \tag{3.5.3}$$

The vanishing order of Δ at $\{a_3 = 0\}$, where neither f nor g vanish, signals an A_2-singularity over this locus. The singularity at $x = y = a_3 = 0$ is resolved by two blow-ups

$$(x, y) \to (sx, sy), \qquad (s, y) \to (qs, qy) \tag{3.5.4}$$

with proper transform

$$\hat{P} = sq^2 y^2 + a_1 qsxyz + a_3 yz^3 - qs^2 x^3 \tag{3.5.5}$$
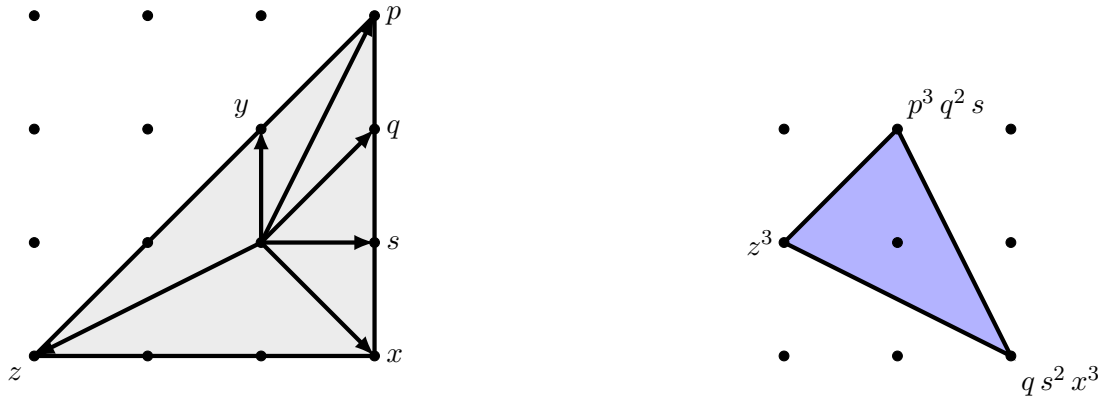
Figure 3.8: Polygon 16 of [19] together with its dual polygon. The coordinate y is scaled to one and does not contribute to the monomials.

as the resulting equation. The Stanley-Reisner ideal after these two blow-ups is $\{qx, qy, qz, xy, sz\}$ (see Fig 3.8). The hypersurface equation (3.5.1) has an equivalent toric description as a generic hypersurface which makes the vanishing of the coefficients a_2, a_4 and a_6 manifest. To see this we perform yet another blow-up by

$$q \to pq, \qquad y \to py, \tag{3.5.6}$$

under which the proper transform of equation (3.5.5) is

$$\hat{P} = sp^3q^2y^2 + a_1pqsxyz + a_3yz^3 - qs^2x^3. \tag{3.5.7}$$

The Stanley-Reisner ideal now extends to $\{sz, qz, pz, xy, sy, qy, ps, px, qx\}$ and implies that the locus $\{y = 0\}$ does not intersect the hypersurface any more. Hence we can use one scaling relation to set $y = 1$. After this step we arrive at the hypersurface equation

$$\hat{P} = p^3q^2s + a_1pqsxz + a_3z^3 - qs^2x^3 \tag{3.5.8}$$

defined in the ambient space with scaling relations

x	z	s	q	p	$\sum$
1	1	0	0	1	3
1	2	0	3	0	6
0	1	1	1	0	3

(3.5.9)

and SR ideal $\{sz, qz, px, ps, qx\}$. A blow-down of this fibration was also considered in [78], where it was shown that the structure group of the elliptic fibration is the subgroup $\Gamma_0(3)$ of $SL(2, \mathbb{Z})$. As we will see, the structure of admissible gauge groups is in agreement with the appearance of such restricted monodromy.

Over the locus $\{a_3 = 0\}$ the hypersurface equation (3.5.8) factors as

$$\hat{P}|_{a_3=0} = qs(p^3q - sx^3 - a_1pxz) \tag{3.5.10}$$

with three irreducible factors. The intersection pattern of the irreducible parts of the fiber, denoted by $\mathbb{P}^1_s$, $\mathbb{P}^1_q$ and $\mathbb{P}^1_{eq}$, is shown in Fig. 3.9. The two resolution divisors $Q : \{q = 0\}$ and $S : \{s = 0\}$ are $\mathbb{P}^1$-fibrations over $\{a_3 = 0\}$ and are associated with the two Cartan generators of $\mathfrak{su}(3)$.

The vanishing order of the discriminant increases by 1 on the curve $\{a_3 = 0\} \cap \{a_1 = 0\}$, naively suggesting an enhancement of the singularity type from A_2 to A_3 and thus localised matter in the
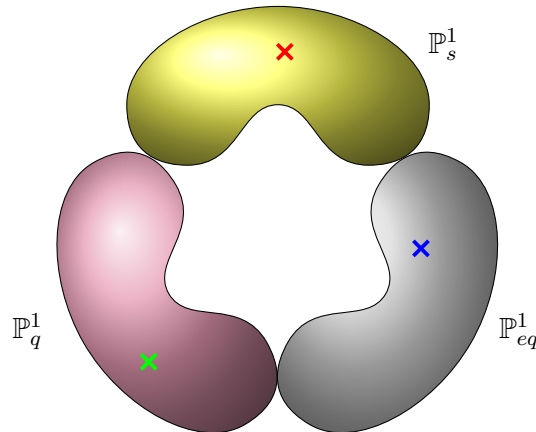
Figure 3.9: The factorised fiber over the base locus $a_3 = 0$; The blue cross indicates the zero point $z = 0$ and the green and red crosses indicates the points $p = 0$ and $x = 0$, respectively.

fundamental **3** of $\mathfrak{su}(3)$. In actuality, however, no higher degeneration of the fiber structure occurs over this curve because none of the three components in (3.5.10) factorises further. This can be seen directly by considering the Weierstrass coefficients f and g (3.5.2): along $\{a_3 = 0\} \cap \{a_1 = 0\}$, each coefficient vanishes to order 2, which implies that the Kodaira type of the degenerate fibers is type IV. This is very similar to the familiar A_2, except that the three components of the fibers meet in a single point rather than meeting pairwise at three different points. There is no enhancement or matter (consistent with [79, 80]). The absence of the fundamental representation, which would be expected to be present in generic fibrations with $\mathfrak{su}(3)$ gauge algebra, will be understood momentarily from the global structure of the gauge group.

The toric Mordell-Weil group is generated by the differences $P - Z$ or $X - Z$ with P, X, Z corresponding to the vertices of polygon 16 [20] with coordinates as in Fig. 3.8. Using the SR-ideal, we conclude that each of these sections intersects only one of the $\mathbb{P}^1$'s, and each $\mathbb{P}^1$ intersects only one of the sections.

The divisor class $Y : \{y = 0\}$ does not intersect the hypersurface and may be expressed as

$$Y = 3Z - S - 2Q - 3P + 3\bar{\mathcal{K}}. \tag{3.5.11}$$

Hence we can define the integer class

$$\Xi_3 \equiv P - Z - \bar{\mathcal{K}} = -\frac{1}{3}(S + 2Q) \tag{3.5.12}$$

associated with a new coweight. Any weight of a charged matter representation has to have integer pairing with Ξ_3, making the weight lattice an order three coarser lattice. In particular, this forbids the fundamental representation of $SU(3)$, in agreement with our findings above. Note also that the fundamental representation would be transforming under the center $\mathbb{Z}_3$ of $SU(3)$. Thus the gauge group is $SU(3)/\mathbb{Z}_3$. Note that the specialization $a_3 = (\tilde{a}_3)^n$, if admissible, modifies the gauge group to

$$G = SU(3n)/\mathbb{Z}_3, \tag{3.5.13}$$

corresponding to a fiber structure of split Kodaira type I_{3n}^s. For $n = 2$, the fiber over the curve $\{\tilde{a}_3 = 0\} \cap \{a_1 = 0\}$ degenerates further to Kodaira type IV^*, as reflected in the vanishing orders $(3, 4, 8)$ of (f, g, Δ) in the Weierstrass model. This signals an enhancement of the singularity type from $A_5 \simeq \mathfrak{su}(6)$ to E_6. From the branching rules of the adjoint representation of E_6 under the
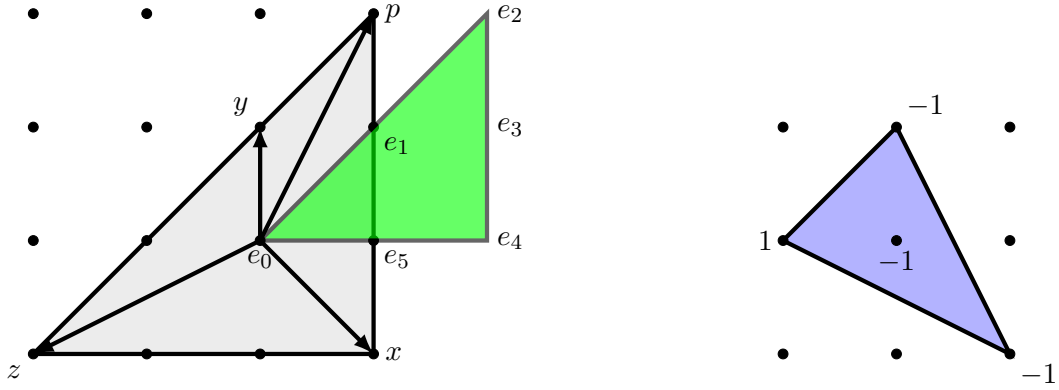
Figure 3.10: The $\mathfrak{su}(6)$ top over polygon 16 is shown to the left. The green layer contains the points at height one. The right side defines the dual top, bounded from below by the values z_{min} shown next to the nodes.

decomposition to $\mathfrak{su}(6)$ one infers massless matter in the triple-antisymmetric representation **20** of $\mathfrak{su}(6)$, in agreement with the gauge group $SU(6)/\mathbb{Z}_3$. However, for $n \geq 3$ the Kodaira type fiber over $\{\tilde{a}_3 = 0\} \cap \{a_1 = 0\}$ is beyond E_8 according to Kodaira's list. This means that no crepant resolution of the fibration exists whenever the locus $\{\tilde{a}_3 = 0\} \cap \{a_1 = 0\}$ is non-trivial, and F-theory on such spaces is ill-defined. This complication does not arise for eight-dimensional F-theory compactifications on K3, where the codimension-one loci are points on the base $\mathcal{B} = \mathbb{P}^1$ and thus no problematic enhancement of this type arises. Indeed, the case $n = 6$ corresponds to the $SU(18)/\mathbb{Z}_3$ model presented in equ. (5.4) of [85] for F-theory on a K3 surface.

Finally, let us note that the F-theory model does not possess a well-defined weak coupling Type IIB limit, at least not of the usual type à la Sen: Since $a_2 \equiv 0$ (in addition to $a_4 \equiv 0$ and $a_6 \equiv 0$), the quantity h defining the Type IIB Calabi-Yau X_{IIB} as the hypersurface $\xi^2 = h$ factorises, $h = -\frac{1}{12}a_1^2$. Thus the locus $\xi = 0 = a_1$ is singular.

3.5.2   An $(SU(6) \times SU(3))/\mathbb{Z}_3$-fibration

To further illustrate this relation between the $\mathbb{Z}_3$ Mordell-Weil group and the global structure of the gauge group we implement an additional non-abelian fiber degeneration in codimension-one. This results in an F-theory compactification with a richer matter spectrum. As we will see, only matter representations occur which are compatible with the extra coweight induced by the torsion generator of the Mordell-Weil group. To implement an extra non-Abelian singularity in the hypersurface (3.5.8) we construct a top. According to the classification in [19] the only possible tops encoding A-type degenerations are the affine A_2, A_5, A_8 etc. Here we construct the single top corresponding to the affine A_5, realizing an $\mathfrak{su}(6)$ theory along a divisor in the base. The hypersurface equation in the ambient space defined by the top is now given by

$$\hat{P} = e_1 e_2^2 e_3 p^3 q^2 s + a_1 pqsxz + a_3 e_0^2 e_1 e_5 z^3 - e_3 e_4^2 e_5 qs^2 x^3, \tag{3.5.14}$$

where the coefficients of the monomials are chosen to match (3.5.8). The discriminant takes the form

$$\Delta \sim w^6 a_3^3 (a_1^3 - 27w^2 a_3), \tag{3.5.15}$$

where $\pi^* w = e_0 e_1 e_2 e_3 e_4 e_5$ defines the $\mathfrak{su}(6)$-divisor as $W : \{w = 0\}$ in the base $\mathcal{B}$. For the chosen triangulation of the top we obtain the Stanley-Reisner ideal

$$\{ps, px, qx, qz, sz, pe_3, pe_4, pe_5, qe_0, qe_1, qe_3, qe_4, qe_5, ze_1, ze_2, ze_3, ze_4, ze_5,$$
$$se_0, se_1, se_3, se_4, se_5, xe_1, xe_0 e_3, xe_3 e_5, e_0 e_2, e_0 e_4, e_1 e_4, e_1 e_5, e_2 e_4, e_2 e_5\}. \tag{3.5.16}$$

In addition to the A_2 singularity with resolution divisors S and Q one finds a fiber degeneration over $W : \{w = 0\}$ with irreducible components

$$\mathbb{P}^1_i = \{E_i\} \cap \{P_W|_{e_i=0} = 0\} \cap D_a \cap D_b \quad i = 0, \ldots, 5, \tag{3.5.17}$$

where D_a and D_b are some generic divisors in $\mathcal{B}$. These are intersecting as the affine A_5 Dynkin diagram as can also be read off from the top in Figure 3.10. For the explicit expressions we refer to appendix A.3.

We next compute the charged matter representations at enhancement loci in codimension-two. By inspection of the discriminant (3.5.15) we see that there are three potentially interesting loci,

$$\{w = a_1 = 0\}, \qquad \{w = a_3 = 0\} \qquad \text{and} \qquad \{a_1 = a_3 = 0\}. \tag{3.5.18}$$

The locus $\{a_1 = a_3 = 0\}$, despite the increased vanishing order of Δ, does not give rise any massless matter, as discussed already in the previous section. Thus, no massless states in representation $(\mathbf{1}, \mathbf{3})$ of $\mathfrak{su}(6) \oplus \mathfrak{su}(3)$ exist. The enhancement over the remaining two loci is determined by calculating the factorization of the fiber components over these loci. The explicit equations are presented in appendix A.3.

At $\{w = a_1 = 0\}$ the fiber components $\mathbb{P}^1_0$ and $\mathbb{P}^1_3$ factorize, resulting in six distinct fiber components. They intersect as the *non-affine* E_6 Dynkin diagram. The weights at this locus are obtained by computing the intersection numbers of the split fiber components with the resolution divisors E_i and S, Q of the $\mathfrak{su}(6)$ and $\mathfrak{su}(3)$ singularities, respectively. As an example we consider the split curves arising from $\mathbb{P}^1_0$ and compute the weights

$$\begin{aligned}
\mathbb{P}^1_{e_0=e_3=0} \cdot (E_1, E_2, E_3, E_4, E_5) &= (1, 0, -1, 0, 1), & \mathbb{P}^1_{e_0=e_3=0} \cdot (S, Q) &= (0, 0), \\
\mathbb{P}^1_{e_0=e_1p^3+e_5x^3=0} \cdot (E_1, E_2, E_3, E_4, E_5) &= (0, 0, 1, 0, 0), & \mathbb{P}^1_{e_0=e_1p^3+e_5x^3=0} \cdot (S, Q) &= (0, 0),
\end{aligned} \tag{3.5.19}$$

which are in the $(\mathbf{20}, \mathbf{1})$ of $\mathfrak{su}(6) \oplus \mathfrak{su}(3)$.

Over $\{w = a_3 = 0\}$ the component $\mathbb{P}^1_3$ factorizes. This results in 9 distinct curves, intersecting as the affine $\mathfrak{su}(9)$ Dynkin diagram. We compute the charges

$$\begin{aligned}
\mathbb{P}^1_{e_2=x=0} \cdot (E_1, E_2, E_3, E_4, E_5) &= (0, -1, 1, 0, 0), & \mathbb{P}^1_{e_2=x=0} \cdot (S, Q) &= (1, 0), \\
\mathbb{P}^1_{e_2=a_1p+e_3sx^2=0} \cdot (E_1, E_2, E_3, E_4, E_5) &= (1, -1, 0, 0, 0), & \mathbb{P}^1_{e_2=a_1p+e_3sx^2=0} \cdot (S, Q) &= (0, 1),
\end{aligned} \tag{3.5.20}$$

recognizing the $(0, -1, 1, 0, 0)$ and $(1, -1, 0, 0, 0)$ as a weight of the $\mathbf{6}$ and $\bar{\mathbf{6}}$ of $\mathfrak{su}(6)$, respectively. Taking into account also the $\mathbf{3}$ and $\bar{\mathbf{3}}$ weights of $\mathfrak{su}(3)$ on the right one deduces along $\{w = a_3 = 0\}$ matter in the bifundamental $(\mathbf{6}, \mathbf{3})$ (plus its conjugate).
The matter spectrum is summarized in the following table:

Top over polygon 16: $\mathfrak{su}(6) \times \mathfrak{su}(3)$

Locus	Charged matter	
$w \cap a_3$	$(\mathbf{6}, \mathbf{3}), (\bar{\mathbf{6}}, \bar{\mathbf{3}})$	(3.5.21)
$w \cap a_1$	$(\mathbf{20}, \mathbf{1})$	

Finally we remark that the fibration is non-flat at the codimension-three points $w = a_1 = a_3 = 0$, where one of the defining equations of the fiber components vanishes identically. This is precisely the intersection locus of the matter curves supporting the $(\mathbf{6}, \mathbf{3})$ and $(\mathbf{20}, \mathbf{1})$ representations. The severe degeneration of the fibration at this locus reflects the fact no triple Yukawa coupling can be constructed out of the $\mathbf{20}$ (antisymmetric in three indices) together with the $\mathbf{6}$ and the $\bar{\mathbf{6}}$. Thus, in order to make sense out of F-theory compactified on the associated Calabi-Yau 4-fold the matter

curves in question must not meet, which is a strong constraint on the base space $\mathcal{B}$. This constraint does not arise for F-theory on lower-dimensional Calabi-Yau n-folds.

We are now in a position to discuss the global structure of the gauge group. The Shioda-type map for the generator of the $\mathbb{Z}_3$-torsional Mordell-Weil group reads

$$\Sigma_3 = P - Z - \bar{\mathcal{K}} + \frac{1}{3}\left(S + 2Q + 2E_1 + 4E_2 + 3E_3 + 2E_4 + E_5\right) \tag{3.5.22}$$

with $\bar{\mathcal{K}} = \pi^*\bar{\mathcal{K}}_\mathcal{B}$. Here $P = \{p = 0\}$, whose intersection with the fiber is the $\mathbb{Z}_3$ torsion point. From the $\mathfrak{su}(6)$ top we infer that the toric divisor class $\{y = 0\}$ in the ambient space is expressed as

$$Y = 3Z - S - 2Q - 3P + 3\bar{\mathcal{K}} - 2E_1 - 4E_2 - 3E_3 - 2E_4 - E_5\,. \tag{3.5.23}$$

We thus see that

$$-3\Sigma_3 = Y \tag{3.5.24}$$

and Y does not intersect the hypersurface. Hence Σ_3 is trivial in $H^{1,1}(Y_4, \mathbb{R})$ and

$$\Xi_3 \equiv P - Z - \bar{\mathcal{K}} = -\frac{1}{3}\left(S + 2Q + 2E_1 + 4E_2 + 3E_3 + 2E_4 + E_5\right)\,. \tag{3.5.25}$$

Again, $P - Z - \bar{\mathcal{K}}$ is a 3-torsion element of $H^{1,1}(\hat{Y}_4, \mathbb{Z})/\langle F_i \rangle_\mathbb{Z}$ for $\langle F_i \rangle_\mathbb{Z}$ the lattice spanned by all the exceptional divisors. Furthermore, it is easy to check that Ξ_3 has integer intersection with all weights computed computed above. Due to the refinement of the coweight lattice the gauge group for this model is thus

$$G = \frac{SU(6) \times SU(3)}{\mathbb{Z}_3} \tag{3.5.26}$$

with $\pi_1(G) = \mathbb{Z}_3$. The correspondingly coarser weight lattice implies that the center Λ/Q of the gauge group is trivial.

3.6   Summary

In this chapter we have studied F-theory compactifications on elliptic fibrations with torsional Mordell-Weil group. While non-torsional rational sections give rise to massless $U(1)$ gauge symmetries, the torsional subgroup affects the global structure of the gauge group. In general, the gauge group is of the form $G \times G'$, where G is affected by the Mordell-Weil torsion and G' is a spectator with respect to torsion elements which can be trivial. The presence of $\mathbb{Z}_k$-torsional sections guarantees the existence of a k-fractional linear combination of resolution divisors associated with the Cartan generators of G which has integer intersection number with every fiber component. We have showed how to identify this linear combination with an element of the coweight lattice of G, which is rendered finer by a factor k compared to the universal cover G_0 of G. This enhances the first fundamental group of G by $\mathbb{Z}_k$ with respect to to G_0. It follows that the gauge group is non-simply connected.

The spectrum of allowed matter representations is constrained to the extent that only those elements in the weight lattice are allowed which have an integer pairing with the coweights associated with the Mordell-Weil torsion. This makes the weight lattice coarser than expected as the coweight is k-fractional by construction. The points of the weight lattice that remains correspond precisely to the states that are not only representations of the algebra, but also of the non-simply connected gauge group. An equivalent way of putting this is that the torsional subgroup $\mathbb{Z}_{k_1} \oplus \ldots \oplus \mathbb{Z}_{k_n}$ of the Mordell-Weil group can be identified with a subgroup of the center of the universal cover group G_0, and the gauge group of the F-theory compactification is $G_0/(\mathbb{Z}_{k_1} \oplus \ldots \oplus \mathbb{Z}_{k_n}) \times G'$. Importantly the

torsional Mordell-Weil group has no particular effect on the structure of the Yukawa couplings between the matter states as such, which is encoded in the fiber type in codimension-three. Contrary to naive expectations, torsional section are not responsible for *e.g.* discrete selection rules in the effective action of an F-theory compactification.

We have exemplified this picture for elliptic fibrations with torsional Mordell-Weil group $\mathbb{Z}_2$ and $\mathbb{Z}_3$, whose defining equation had already been presented in [69]. These fibrations can be analysed torically as hypersurfaces in toric ambient spaces, and, as we have seen, coincide with two out of the 16 possible hypersurface torus fibrations, whose Mordell-Weil group has been computed also in [20]. The third possible hypersurface elliptic fibration with Mordell-Weil group $\mathbb{Z} \oplus \mathbb{Z}_2$ [20], is shown to be complex structure specialization of the $\mathbb{Z}_2$-model. All these fibrations are related to a special class of elliptic fibrations with Mordell-Weil group $\mathbb{Z}$ [77] by a chain of (un)Higgsings.

An interesting next step would be to study also fibrations with Mordell-Weil group $\mathbb{Z}_4$ and higher. The defining Tate model for examples of such fibrations has been given in [69]. It would be interesting to express these fibrations as complete intersections (as opposed to hypersurfaces) or even determinantal varieties and to study their properties at the same level of detail as achieved for the hypersurface models in this article. An example of particular interest would be the realisation of an Standard Model gauge symmetry in a fibration with a $\mathbb{Z}_6$ torsion section. The matter spectrum of such a model would be expected to agree with that of the standard model.

An exciting aspect of gauge theories with non-simply connected gauge groups is the physics of non-local operators such as the spectrum of dyonic Wilson line operators. As studied *e.g.* in [66], the spectrum of such dyonic operators depends on the weight lattice of the gauge group G and of its Langlands dual G^*. As we have seen, the weight lattice Λ of an F-theory compactification on an elliptic fibration is intimately related to the geometry of torsional sections. It would be interesting to investigate further the relation between torsional sections, the spectrum of dyonic Wilson line operators and the global structure of the gauge group in F-theory.

Chapter 4

Discrete symmetries and F-theory on genus-one fibrations

In F-theory the framework for geometric realisations of gauge symmetries is by now well understood. Already in the original work [6–8] it was outlined how non-abelian gauge symmetries and charged matter representations appear in the four dimensional quantum field theory. More recently the global structure of elliptic fibrations and the link between the free Mordell-Weil group and abelian gauge groups have been worked out [18, 20, 31, 52, 59, 61–63, 70, 77, 83, 84, 88–100]. On the other hand, the realisation of discrete symmetries from the F-theory fibration was only recently understood, with the work by the author and collaborators [10,11] and the parallell work in [70,101]. Until only recently [29] all work on F-theory, both model building and phenomenology as well as more conceptual work and the study of string dualities has been done under the assumption of an elliptically fibered compactification manifold. Relaxing the requirement of having a distinguished zero-section enlargens the set of possible F-theory vacua to incorporate also genus-one fibrations, introduced in section 2.1.3.

In this chapter we analyse four dimensional F-theory models with discrete symmetries. In string theory all discrete symmetries have to arise as broken continuous symmetries [102]. As in the case of abelian gauge symmetries, the presence of a discrete symmetry restricts the operator spectrum of the theory, in particular the Yukawa couplings in four dimensions. A discrete symmetry has however no associated propagating degrees of freedom. Recent work on discrete symmetries in string theory is e.g [103–111]. With this as the starting point the simplest case of a discrete symmetry is a $\mathbb{Z}_k$ subgroup of an abelian gauge group. In field theory such a discrete remnant of a $U(1)$ symmetry appears by higgsing with a field which has charge k under this group. In other words, if the higgs field is invariant only under a $\mathbb{Z}_k$ subgroup of the $U(1)$, then this subgroup remains unbroken[1]. By constructing a pair of F-theory fibrations we show the geometric manifestation of this higgsing as a conifold transition between an elliptic fibration and a genus-one fibration. Having the explicit transition between the two geometries, where the elliptic fibration is well understood, we carefully map out the physics associated with the genus-one fibration and how the discrete symmetry and the matter state charges can be understood geometrically.

We will start by studying the model considered in [18], which is the most general form of an elliptic fibration over $\mathcal{B}$ with a Mordell-Weil group of rank one. This implies, as we have seen, an extra $U(1)$ gauge group in four dimensions. This model has two charged matter representations residing over codimension-two loci in the base. Over these loci Kodaira I_2 fibers are found [18] and M2 branes

---

[1]For recent work studying the Higgsing of abelian symmetries in smooth heterotic string models see [112–114]. The Higgsing of non-abelian gauge symmetries in F-theory compactifications via deformations has been described in detail in [115,116].

wrapping the fiber components give rise to matter charged under the $U(1)$ gauge group. The matter fields, denoted $\mathbf{1}_1$ and $\mathbf{1}_2$ have charge one and two under the $U(1)$ symmetry, respectively. Via a conifold transition this model is related to a generic quartic equation in $\mathbb{P}_{1,1,2}$ and this hypersurface equation describes a genus-one fibration over the same base $\mathcal{B}$. The genus-one fibration has no zero section, but a bisection and has an associated Jacobian fibration described by a Weierstrass model. The Jacobian fibration is singular and does not admit a crepant resolution. The genus-one fibration is however smooth and admits a full analysis of the fiber structure in all codimensions and subsequently the corresponding physics. In [84] the conifold transition was given an interpretation in terms of the Higgsing by giving the field $\mathbf{1}_2$ a vev which breaks the $U(1)$ to a $\mathbb{Z}_2$ discrete group. In this work [84] the fibration was studied over explicit complex two-dimensional bases which means that the field theories was studied in six dimensions. The same fibration, slightly generalized, was also studied in [117]. In the next section the details of these two fibrations, and the linking conifold transition is presented.

In this chapter, which is based on the papers [10, 11] we will study a genus-one fibration with a bisection. We show in detail how the $\mathbb{Z}_2$ discrete group arise from the geometry of four dimensional F-theory compactifications. The analysis is very general as we consider fibrations over generic three-fold bases. In addition to the discrete group $\mathbb{Z}_2$ we implement a further non-abelian gauge symmetry. In the explicit examples, first studied in [10], we consider two different embeddings of the GUT symmetry $SU(5)$. Constructing four dimensional models differs in several ways from the previously studied six dimensional compactifications. The first is that in the four-dimensional models there are Yukawa couplings between the charged fields. These arise at points of codimension three in the base where the matter curves meet. In the presence of the $SU(5)$ singularity we have five types of couplings between the singlet, the fundamental and the anti-symmetric $SU(5)$ representations: $\mathbf{\bar{5}\,\bar{5}\,10}$, $\mathbf{5\,10\,10}$, $\mathbf{1\,\bar{5}\,5}$, $\mathbf{1\,10\,\overline{10}}$, $\mathbf{1\,1\,1}$. The elliptic fibration with the massless $U(1)$ symmetry has already been studied in the presence of an additional $SU(5)$ singularity in [83], wherein it was shown that all the possible couplings which are singlets w.r.t the $U(1)$ group appear in the geometry. When higgsing the four dimensional theory with the field $\mathbf{1}_2$ two main effects are expected. The first is that one expects the selection rules governing the presence of a coupling to be modified from the $U(1)$ charge to a $\mathbb{Z}_2$ charge. In other words, the Yukawa couplings should be singlets with respect to the discete symmetry instead of the abelian gauge symmetry. The second is that some fields can gain a mass from operators of the type $\mathbf{1\,\bar{5}\,5}$, $\mathbf{1\,10\,\overline{10}}$, $\mathbf{1\,1\,1}$ which involve the $SU(5)$ singlet which obtains a vacuum expectation value. The geometric manifestation of these effects are the main results of this chapter. We will show how the conifold transition leads to a recombination of the matter curves that host charged matter coupled to the Higgs field. This would correspond to a rearrangement and splitting of the 7-branes in a type IIB compactification. It follows that the massless matter spectrum change and that the couplings after the transition respect not the abelian gauge symmetry, but the discrete $\mathbb{Z}_2$ subgroup. A third important difference is that in four dimensions also G_4 flux has to be considered as part of the compactification. In the conifold transition this is not only a possibility, but a necessity. The discussion of fluxes in F-theory on genus-one fibrations is the subject of chapter 5.

To give a complementary picture we also study the four dimensional theory, and its reduction to three dimensions on the M-theory circle. The state $\mathbf{1}_2$ gives rise to a tower of Kaluza-Klein (KK) modes when put on this circle. Here we observe that the Higgs field responsible for the deformation of the geometry is to be identified with a specific mode in this reduction. Identifying the relevant KK mode in the geometry enables us to further support and extend the field theory picture suggested in [84,117]. The four dimensional field theory is of course an important motivation for this work. Developing the technical tools and the understanding of genus-one fibrations allows us to implement discrete gauge symmetries relevant for string theory phenomenology. Indeed, the particular geometries studied in this chapter, being grand unified theories with a remnant discrete gauge symmetry, are interesting starting points for model building. E.g the model in section 4.7 has a remnant $\mathbb{Z}_2$ symmetry which

	u	v	w	s
$\bar{\mathcal{K}}$	·	1	2	·
b_2	·	-1	-1	·
U	1	1	2	·
S	·	1	1	1

Table 4.1.1: Divisor classes and coordinates of the fiber ambient space, with $\mathcal{K}$ the canonical bundle of the base $\mathcal{B}$ and b_2 the line bundle defined by the divisor class $[b_2]$ on $\mathcal{B}$.

can be identified with the R-parity of the Minimal Supersymmetric Standard Model (MSSM).

String compactifications on geometries with torsional homology cycles are known to give rise to discrete symmetries. In section 4.5 we put torsion homology in the context of F-theory on genus-one fibrations. Crucial here is that to the genus-one fibration with a bisection there are two different phases of M-theory that share the same F-theory limit. The genus-one fibration has no torsion in homology, but in the associated Jacobian fibration torsional cycles appear in the deformation. We show in detail how these cycles appear in the conifold transition and how the $\mathbb{Z}_2$ torsion subgroup is linked to the bisection.

4.1 An elliptic fibration with $U(1)$ gauge symmetry

We will start by considering the fibration considered in [18], which is the most general form of an elliptic fibration supporting two sections: the zero section and an additional section which is associated to a massless $U(1)$ gauge symmetry. In other words the Mordell-Weil group has rank one. The elliptic fiber is given by the hypersurface equation

$$P_1 := sw^2 + b_0 s^2 u^2 w + b_1 suvw + b_2 v^2 w + c_0 s^3 u^4 + c_1 s^2 u^3 v + c_2 su^2 v^2 + c_3 uv^3 = 0 \qquad (4.1.1)$$

for b_i and c_i sections of suitable line bundles on $\mathcal{B}$ chosen such that the total fibration is Calabi-Yau[2]. The ambient coordinates $[u : v : w : s]$ are subject to the scaling relations

$$(u, v, w, s) \simeq (\lambda u, \lambda \mu v, \lambda^2 \mu w, \mu s), \quad \mu, \lambda \in \mathbb{C}^* \qquad (4.1.2)$$

and the Stanley-Reisner ideal is generated by $\{uw, vs\}$. This ambient toric variety corresponds to the fan given by polygon 6 in the enumeration of [19] and the monomials of the hypersurface equation are given by the dual polygon. As in the previous chapter we adopt their enumeration of the reflexive polygons since we are applying their construction and classification of toric tops in section 4.6 and 4.7. For (4.1.1) to describe a Calabi-Yau fibration b_1 has to transform as a section of the canonical bundle $\bar{\mathcal{K}}$ on the base. For this hypersurface this does not determine all coefficient sections, but one has the freedom to introduce a scaling under one more line bundle $\mathcal{L}$ on $\mathcal{B}$. We make the choice to parametrise this line bundle by the divisor class of the section b_2 i.e the first Chern class $c_1(\mathcal{L}) = [b_2]$. The scaling relations of the fiber coordinates is summarised in Table (4.1.1). The coefficients b_i and c_i transform as sections of line bundles on $\mathcal{B}$ whose first Chern classes are displayed in Table 4.1.2. This ambient fiber space can be thought of as the blow-up of the point $u = w = 0$ in the projective space $\mathbb{P}_{1,1,2}$ where $S : \{s = 0\}$ is the exceptional divisor. Note especially that this resolution is performed in the ambient space, and the exceptional divisor is a toric divisor in $\mathrm{Bl}^1\mathbb{P}_{1,1,2}$, not on the hypersurface. If we take (4.1.1) and set $s \equiv 1$, which is a reversal of the resolution or a 'blow down', we obtain the

---

[2]In a common notation this fibration is referred to as a $\mathrm{Bl}^1\mathbb{P}_{1,1,2}[4]$-fibration over $\mathcal{B}$. This is read as a general degree four hypersurface in the ambient space given by one blow-up of $\mathbb{P}_{1,1,2}$, fibered over $\mathcal{B}$.

b_0	b_1	b_2	c_0	c_1	c_2	c_3	c_4
$2\bar{\mathcal{K}} - b_2$	$\bar{\mathcal{K}}$	b_2	$4\bar{\mathcal{K}} - 2b_2$	$3\bar{\mathcal{K}} - b_2$	$2\bar{\mathcal{K}}$	$\bar{\mathcal{K}} + b_2$	$2b_2$

Table 4.1.2: Classes of the coefficients entering (4.1.1).

polynomial of a non-generic quartic in $\mathbb{P}_{1,1,2}$. The conifold transition amounts to the deformation of the blow-down to a generic quartic, which will be described in the next section.

The fibration (4.1.1) has a family of conifold singularities over the curve in the base where $b_2 = c_3 = 0$. Restricting the hypersurface equation to this locus reveals the singular point on the fiber at $u = w = 0$. The appearance of this curve of singularities is a consequence of the non-generic form of the hypersurface as a quartic in $\mathbb{P}_{1,1,2}$ i.e the abscence of a monomial term $c_4 v^4$ which would be present in the general case. At the same time this implies the appearance of two independent sections in the singular model, which generate a Mordell-Weil group of rank one,

$$\text{Sec}_1 : [u : v : w] = [0 : 1 : -b_2], \qquad \text{Sec}_2 : [u : v : w] = [0 : 1 : 0]. \tag{4.1.3}$$

The section Sec_1 intersects the conifold points over the curve $b_2 = c_3 = 0$. After the blow-up resolution of this conifold point, $u \to u\,s, w \to w\,s$, Sec_1 is replaced by the resolution divisor $S : \{s = 0\}$, whose intersection with the hypersurface defines a rational section. As we have taken U and S as the basis for the ambient divisor classes we can identify the holomorphic zero-section of the fibration (4.1.1) with the intersection of U with the fibration.[3] The image of the extra rational section under the Shioda map is

$$\text{w} = S - U - \bar{\mathcal{K}} - [b_2], \tag{4.1.4}$$

and is the generator of a $U(1)$ gauge symmetry in F-theory compactifications on the elliptic fibration. The details of this geometry were given in [18] for a generic base space $\mathcal{B}$ of complex dimension two. Here we are interested in the conifold transition as a higgsing in four dimensional field theory and the resulting discrete selection rule. Hence we extend this analysis to base spaces $\mathcal{B}$ of complex dimension three. This adds to the work [18] a more complicated structure of the matter curves (as opposed to matter points) on $\mathcal{B}$ and their intersection at Yukawa points in codimension three on $\mathcal{B}$.

Over codimension-two loci in the base in this fibration Kodaira I_2 fibers are found [18] giving rise to matter charged under the $U(1)$ gauge group. There are two types of such splittings which means there are two types of matter fields, $\mathbf{1}_1$ and $\mathbf{1}_2$, with the subscript denoting their charge, which reside over two distinct loci in the base. We have chosen the notation $\mathbf{1}$ since these matter states will remain singlets under the $SU(5)$ gauge group introduced later. By inspection of (4.1.1) one finds one factorisation over the codimension-two locus

$$C_1 : (b_2, c_3), \tag{4.1.5}$$

written in the ideal notation. The subvariety corresponding to this ideal is the conifold curve $b_2 = c_3 = 0$ mentioned above. Over C_1 the fiber factorises into

$$P_1|_{C_1} = s\,(w^2 + b_0 s\,u^2\,w + b_1\,u\,v\,w + c_0\,s^2\,u^4 + c_1\,s\,u^3\,v + c_2\,u^2\,v^2). \tag{4.1.6}$$

The two factors define two rational curves $\mathbb{P}^1_s$ and $\mathbb{P}^1_{\text{res.}}$ intersecting as the affine $SU(2)$ Dynkin diagram. As seen from the factorisation the rational section S degenerates over C_1, where it wraps the entire fiber component $\mathbb{P}^1_s$. This is an example of the behaviour of a rational section, as opposed to a holomorphic

---

[3]We will sometimes use the rational section and the corresponding ambient divisor class interchangably. It is always the case that the divisor class restricts to the class of the section on the hypersurface.

fiber over C_1 fiber over C_2

Figure 4.1: The fiber structure over the singlet curves C_1 and C_2. Blue denotes the section S and green the section U.

one. M2-branes wrapping the fiber component $\mathbb{P}^1_{\text{res.}}$ yield states with charge $q = \int_{\mathbb{P}^1_{\text{res.}}} \text{w} = +2$ since the section S intersects $\mathbb{P}^1_{\text{res.}}$ in two points and the section U intersects the fiber only in one point on $\mathbb{P}^1_s$, cf. Figure 4.1. The charged matter localized along C_1 is the state $\mathbf{1}_2$ and its conjugate. The specific intersection numbers with the fiber curves becomes important in section 4.3, where we provide more details on the interpretation of M2-branes wrapped on the distinct fiber components. As found in [18], the fiber can also factorise into two components none of which is wrapped by the section S. As this I_2 fiber exist without reference to the extra section it will exist also in the singular blow-down of (4.1.1) corresponding to $s \equiv 1$. To find the locus in $\mathcal{B}$ over which the I_2 fiber appears one completes the square in w and writes the hypersurface equation as

$$P_1 = \left[w + \frac{1}{2}(b_0 u^2 + b_1 uv + b_2 v^2) \right]^2$$
$$+ (c_0 - \frac{1}{4}b_0^2)u^4 + (c_1 - \frac{1}{2}b_0 b_1)u^3 v + (c_2 - \frac{1}{2}b_0 b_2 - \frac{1}{4}b_1^2)u^2 v^2 + (c_3 - \frac{1}{2}b_1 b_2)uv^3 - \frac{1}{4}b_2^2 v^4.$$
$$(4.1.7)$$

The equation factorises if the polynomial in u and v in the second line is a perfect square. By making an Ansatz of the form $(Au^2 + Buv + Cv^2)^2$ one obtain five equations, three of which determine the coefficients A, B and C in terms of the b_i and c_i. The remaining two equations takes the form

$$- c_1 b_2^4 + b_1 b_2^3 c_2 + b_0 b_2^3 c_3 - b_1^2 b_2^2 c_3 - 2b_2^2 c_2 c_3 + 3b_1 b_2 c_3^2 - 2c_3^3 = 0,$$
$$- c_3^2 b_0^2 + b_1 b_2 b_0^2 c_3 - b_1 b_2^2 b_0 c_1 + b_2^2 c_1^2 + b_1^2 b_2^2 c_0 - 4b_1 b_2 c_0 c_3 + 4c_0 c_3^2 = 0.$$
$$(4.1.8)$$

These two polynomials generate an ideal of the polynomial ring $\mathbb{C}[b_i, c_i]$ over $\mathcal{B}$ whose vanishing locus defines a variety on $\mathcal{B}$ with a complicated substructure. The individual irreducible components of (4.1.8) are found by decomposing the ideal into prime ideals. The prime ideals define varieties of different codimension in $\mathbb{C}[b_i, c_i]$ and the components relevant for the matter spectrum are singled out as the codimension-two loci. The solutions for A and B in the Ansatz above are rational in b_i and c_i. In particular b_2 and $2c_3 - b_1 b_2$ appear as denominators and thus the factorization is valid away from the vanishing locus of these two polynomials which define the ideal $(b_2, 2c_3 - b_1 b_2)$. As the ideal $(b_2, 2c_3 - b_1 b_2) = (b_2, c_3)$ we see that this new I_2 locus in the base is well defined away from the curve C_1 hosting the $\mathbf{1}_2$ state. The method of prime ideal decomposition was used in [63,93] (see also [118]) to determine the irreducible singlet curves in an analogous fibration with Mordell-Weil group of rank two [52,63,83,92] (see [70,94] for an analysis in this spirit of, among other things, the singlet locus of even more general fibrations).

By using `Singular` [119], a software package for polynomial algebra we can analyse the locus (4.1.8) in detail. By taking the saturation of C_1 in (4.1.8), i.e the ideal obtained by factoring out all powers of C_1 in (4.1.8), we find that it does not split into further components. Hence we can take this new ideal to define our I_2 locus, without any complications coming from poles at C_1 in the
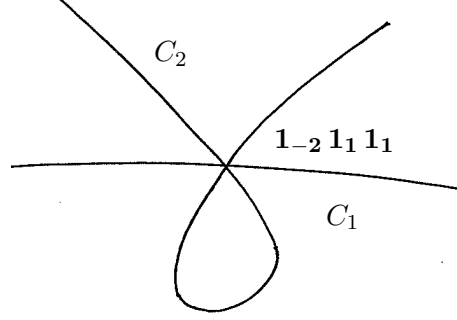
Figure 4.2: The singlet curves and the Yukawa coupling in codimension three.

factorization. The only component of (4.1.8) is

$$C_2 : \{\text{An ideal with 15 generators}\}, \tag{4.1.9}$$

which is of codimension two despite the large number of generators. Thus the generators do not intersect transversally. The explicit form is given in (B.2.1) in the appendix. One can furthermore, with the aid of `Singular`, show that the curve C_2 is singular along a sublocus, a point of self-intersection to be discussed in more detail momentarily. By construction, the fiber over C_2 splits into homologous $\mathbb{P}^1$s. The charges of the corresponding states are the intersection numbers ± 1 with the $U(1)$ generator. Thus, along C_2 the matter states $\mathbf{1}_{\pm 1}$ are localised.

The two singlet curves intersect in codimension three on $\mathcal{B}$, i.e. at points. The singular locus of C_2 coincides with the intersection point $C_1 \cap C_2$ and by prime decomposition the complicated structure of C_2 reduce to

$$C_1 \cap C_2 : (b_2, c_3, b_1^2 c_0 - b_0 b_1 c_1 + b_0^2 c_2 + c_1^2 - 4c_0 c_2). \tag{4.1.10}$$

By restricting the hypersurface to this point the fiber factors into three rational curves

$$P|_{C_1 \cap C_2} = s \left(\tilde{w}^2 - \left(\frac{u}{\sqrt{b_1^2 - 4c_2}} [(c_1 - \frac{1}{2} b_0 b_1) su + 2(c_2 - \frac{1}{4} b_1^2) v] \right)^2 \right) \tag{4.1.11}$$

intersecting as the affine $SU(3)$ Dynkin diagram. The first factor defines the curve $\mathbb{P}_s^1$, with $U(1)$ charge -2, and the second factor is the difference of two squares which defines two curves, each with charge 1. This confirms the presence of the Yukawa coupling $\mathbf{1}_{-2} \mathbf{1}_1 \mathbf{1}_1 + c.c$ at this point. Note that the non-meromorphic prefactor $(b_1^2 - 4c_2)^{-1/2}$ presents no difficulty as it evaluates to a number at this point and no monodromy can occur.

4.2 A genus-one fibration with $\mathbb{Z}_2$ symmetry

In the previous section we saw how the appearance of a rank-one Mordell-Weil group and thus the presence of a $U(1)$ gauge group factor in F-theory fibrations of the form (4.1.1) is a consequence of the non-generic form of the hypersurface equation in which the potential quartic term $c_4 v^4$ is missing. From here on we treat the abscence of this term as the restriction to a sublocus of the complex structure moduli space where c_4 vanishes identically. By starting with the blow-down of s in (4.1.1) and moving away from the $c_4 \equiv 0$ locus in moduli space one is effectively turning on this quartic term. The resulting generic quartic equation in $\mathbb{P}_{1,1,2}$ describes a smooth genus-one fibration and is given by the hypersurface equation

$$P_2 = w^2 + b_0 u^2 w + b_1 uvw + b_2 v^2 w + c_0 u^4 + c_1 u^3 v + c_2 u^2 v^2 + c_3 uv^3 + c_4 v^4 = 0 \tag{4.2.1}$$

in a $\mathbb{P}_{1,1,2}$ fibration over $\mathcal{B}$. The scaling relations of u, v, w as well as the classes of b_i and c_i are the same as in section 4.1. This model was first discussed in [29,84] as an example of a genus-one fibration with a bi-section (see also [117]). The intersection of U with the generic fiber consists of two points, as seen by the factorization

$$P_2|_{u=0} = \left(w + \frac{1}{2}\left(b_2 + \sqrt{b_2^2 - 4\,c_4} \right) v^2 \right) \left(w + \frac{1}{2}\left(b_2 - \sqrt{b_2^2 - 4\,c_4} \right) v^2 \right). \tag{4.2.2}$$

As $c_4 \neq 0$ these two points are the two branches of the square root $\sqrt{b_2^2 - 4\,c_4}$, and moving over the branch cut in the base exchanges these two points. Globally this means that the two intersection points cannot be separated, and the intersection of U with the hypersurface defines the class of a bisection. Over each local patch in $\mathcal{B}$ the generic fiber is intersected in two points, as in fig. 2.4. In the limit $c_4 \to 0$, the square roots disappear and the bisection splits into the two rational sections in (4.1.3). One is the zero-section in the $U(1)$ model in the previous section, the other is the extra rational section, given by S upon resolution.

The singularity at (b_2, c_3) in the previously discussed $U(1)$ model is not present in this genus-one fibration, due to the deformation term. There is however still a codimension two locus over which the fiber factorises [29,84]. This locus is found in the same way as around (4.1.8) by making an Ansatz for the factorisation. This follows the analysis as in [84] but as we are considering fibrations over three-fold bases we need to take some extra care in finding the matter curve. Completing the square in w yields

$$P_2 = \tilde{w}^2 + a_0 u^4 + a_1 u^3 v + a_2 u^2 v^2 + a_3 u^2 v^2 + a_4 v^4 \tag{4.2.3}$$

with $\tilde{w} = w + \frac{1}{2}(b_0 u^2 + b_1 uv + b_2 v^2)$ and the shifted coefficients

$$a_0 = -c_0 + \frac{1}{4}b_0^2, \qquad a_1 = -c_1 + \frac{1}{2}b_0 b_1, \tag{4.2.4}$$

$$a_2 = -c_2 + \frac{1}{2}b_0 b_2 + \frac{1}{4}b_1^2, \qquad a_3 = -c_3 + \frac{1}{2}b_1 b_2, \qquad a_4 = -c_4 + \frac{1}{4}b_2^2. \tag{4.2.5}$$

There are two cases to consider: If $a_4 \neq 0$ we can make the ansatz [84]

$$P_2 = \tilde{w}^2 - a_4(Au^2 + Buv + v^2)^2 = (\tilde{w} - \sqrt{a_4}(Au^2 + Buv + v^2))(\tilde{w} + \sqrt{a_4}(Au^2 + Buv + v^2)). \tag{4.2.6}$$

By comparing this ansatz to the original equation P_2 one finds a solution for A and B as [84]

$$A = \frac{4a_2 a_4 - a_3^2}{8a_4^2}, \qquad B = \frac{a_3}{2a_4} \tag{4.2.7}$$

and in addition two constraints $p_1 = p_2 = 0$ for

$$\begin{aligned}
p_1 =\,& b_2^6 c_0 - b_1^2 b_2^3 c_4 b_0 + b_1 b_2^4 c_3 b_0 - b_2^5 c_2 b_0 + b_2^4 c_4 b_0^2 + b_1^4 c_4^2 - 2b_1^3 b_2 c_4 c_3 + b_1^2 b_2^2 c_3^2 + 2b_1^2 b_2^2 c_4 c_2 + \\
& - 2b_1 b_2^3 c_3 c_2 + b_2^4 c_2^2 - 12b_2^4 c_4 c_0 + 4b_1^2 b_2 c_4^2 b_0 - 4b_1 b_2^2 c_4 c_3 b_0 - b_2^3 c_3^2 b_0 + 8b_2^3 c_4 c_2 b_0 + \\
& - 8b_2^2 c_4^2 b_0^2 + 2b_1^2 c_4 c_3^2 - 2b_1 b_2 c_3^3 - 8b_1^2 c_4^2 c_2 + 8b_1 b_2 c_4 c_3 c_2 + 2b_2^2 c_3^2 c_2 - 8b_2^2 c_4 c_2^2 + \\
& + 48b_2^2 c_4^2 c_0 + 4b_2 c_4 c_3^2 b_0 - 16b_2 c_4^2 c_2 b_0 + 16c_4^3 b_0^2 + c_3^4 - 8c_4 c_3^2 c_2 + 16c_4^2 c_2^2 - 64c_4^3 c_0\,,
\end{aligned} \tag{4.2.8}$$

$$\begin{aligned}
p_2 =\,& -\frac{1}{2}b_1^3 b_2 c_4 + \frac{1}{2}b_1^2 b_2^2 c_3 - \frac{1}{2}b_1 b_2^3 c_2 + \frac{1}{2}b_2^4 c_1 + b_1 b_2^2 c_4 b_0 - \frac{1}{2}b_2^3 c_3 b_0 + b_1^2 c_4 c_3 + \\
& - \frac{3}{2}b_1 b_2 c_3^2 + 2b_1 b_2 c_4 c_2 + b_2^2 c_3 c_2 - 4b_2^2 c_4 c_1 - 4b_1 c_4^2 b_0 + 2b_2 c_4 c_3 b_0 + c_3^3 - 4c_4 c_3 c_2 + 8c_4^2 c_1\,.
\end{aligned}$$

This shows that the factorisation (4.2.6) occurs over the variety defined by

$$\tilde{C}_1 = \{p_1 = 0\} \cap \{p_2 = 0\} - \{a_4 = 0\} \cap \{p_1 = 0\} \cap \{p_2 = 0\}\,, \tag{4.2.9}$$

where the subset of the solution over which $a_4 = 0$ is subtracted. One can show that $a_4 = 0$ implies $a_3 = 0$ when $\{p_1 = 0\} \cap \{p_2 = 0\}$. For base spaces of dimension two, as analysed in [84], this is the complete I_2 locus. Here we consider three-dimensional bases and hence the case $a_4 = 0$ must also be taken into account. For $a_4 = 0$, the above ansatz for the factorisation is not valid. Let us assume that $a_0 \neq 0$ and instead make the ansatz

$$P_2|_{a_4=0} = \tilde{w}^2 - a_0(u^2 + Duv)^2 = (\tilde{w} + \sqrt{a_0}u(u + Dv))(\tilde{w} - \sqrt{a_0}u(u + Dv)). \tag{4.2.10}$$

Expanding and comparing coefficients identifies the solution

$$D = \frac{a_1}{2\,a_0} \tag{4.2.11}$$

and gives two more constraints $a_3 = a_1^2 - 4a_2a_0 = 0$. For a generic base $\mathcal{B}$ and a generic choice of sections b_i, c_i we note that the assumption $a_0 \neq 0$ holds at $\{a_4 = 0\} \cap \{a_3 = 0\} \cap \{a_1^2 - 4a_2a_0 = 0\}$. Thus the above factorisation (4.2.10) is valid at the codimension-three loci

$$\tilde{C}_2 = \{a_4 = 0\} \cap \{a_3 = 0\} \cap \{a_1^2 - 4a_2a_0 = 0\}. \tag{4.2.12}$$

Summarizing the two cases the I_2 type fiber factorisation occurs over the locus

$$C = \tilde{C}_1 \cup \tilde{C}_2. \tag{4.2.13}$$

It turns out that this locus C has a representation as the vanishing locus of a prime ideal. This ideal is found by taking the saturation of the ideal generated by p_1 and p_2 with respect to (a_3, a_4). This representation of C may be decomposed into 16 prime ideal factors presented in (B.2.2) in the appendix. The codimension two curve is hence described as the non-transversal intersection of 16 polynomials on the base. One can show that the points $\tilde{C}_2$ all lie on the variety defined by this prime ideal and are indeed the only loci on $p_1 \cap p_2$ for which $a_4 = 0$. Importantly, we can use our representation of C in terms of prime ideals to show that C defines an irreducible, smooth curve on $\mathcal{B}$. This is the locus where the fiber is of I_2-type, over which the matter states are localised.

M2-branes wrapping either of the two fiber components over C give rise, in the F-theory limit, to massless singlet states. Due to the absence of sections, it is not possible to define a $U(1)$ generator w as in equation (4.1.4). There is not even a zero section in this fibration, and there is no notion of a Mordell-Weil group. As explained above, S and the zero-section are 'glued' together into the bi-section U which intersects the fiber class in two points. Only when c_4 vanishes, the two points can be globally distinguished. By global monodromy effects these two points are interchanged over the base $\mathcal{B}$ [29] and there is no possibility to globally single one of the points out. Nonetheless it is possible to define a $\mathbb{Z}_2$-charge of the singlet states with respect to the bisection U. By setting $u = 0$ in (4.2.8) one can confirm that the divisor class U intersects each of the two split fiber components over the locus $\tilde{C}_1$ in a single point given by

$$u = 0, \qquad w = \pm\frac{1}{\sqrt{b_2^2 - 4c_4}}v^2, \tag{4.2.14}$$

respectively. Since $a_4 = b_2^2 - 4c_4$ does no vanish along $\tilde{C}_1$ these two points are well-defined, and are not identified through the scaling relation in $\mathbb{P}_{1,1,2}$. By approaching the points in the codimension three locus $\tilde{C}_2$, the two intersection points of the bisection coincide not only with each other but also with one of the intersection points of the rational lines of the I_2 fiber. That the two points come together is the expected behaviour of the monodromy of the two points $u = 0$ around this codimension-three locus on $\mathcal{B}$. As pointed out in [29],this behaviour prevents us from defining a well-defined $U(1)$ charge. If we would take the difference of the two points, as in the Shioda map, the charge would change

sign when going around the the point in C. This observation leads to a better guess, if we instead take the sum of the points this combination is even, or invariant, under the monodromy and this sign ambiguity is solved. In order for the two states that come from the two different $\mathbb{P}^1$s of the I_2 fiber to have conjugate charges we can only take the charges modulo two. The interpretation of this behaviour is that the intersection of the bi-section U with the rational lines of the fiber is a $\mathbb{Z}_2$ quantum number. In section 4.6.2 we will study this model with additional non-abelian gauge symmetry, and confirm that the $\mathbb{Z}_2$ charge of all matter states is consistent with the couplings and thus the discrete symmetry acts as a selection rule in four dimensions.

4.3 The field theory picture

In this section, we discuss the interpretation of the geometry from a field theory perspective. These results [10, 11] extend considerably the work [84] in which the field theory was also discussed. In particular we show how the discrete symmetry arises in one of the two M-theory phases, while absent in the other. In the M-theory/F-theory duality the geometry that we discuss can be understood in terms of the four-dimensional field theory associated to the F-theory compactification. We start by considering the elliptic compactification with an extra $U(1)$ gauge group and later study the higgsing of this theory. The three dimensional M-theory compactification is obtained by a circle reduction of the four dimensional F-theory model on a three dimensional Lorentzian manifold $M_{1,2}$ times a circle S^1. We will take a three dimensional perspective, and include not only the zero-modes on the circle, but also the KK modes. In particular we are interested in the three dimensional $U(1)$ gauge fields corresponding to $U(1)_0$ and $U(1)_1$. The $U(1)_0$ is the graviphoton originating from the metric along the S^1 and is called the KK $U(1)$. The second gauge factor, $U(1)_1$, is the three dimensional vector coming from the zero mode (along the circle) of the $U(1)$ in four dimensions which has its origin in the additional rational section. The fourth components of the four-dimensional vectors become scalars, denoted ξ_0 and ξ_1 in the three-dimensional theory. The first scalar is the metric component parametrising the volume of the compactification circle and its vev $\langle \xi_0 \rangle = 1/R$ where R is the circle radius. The second scalar is the component of the four dimensional gauge vector A^1_{4D} along the S^1 and is related to the Wilson line as $\xi_1 = \int_{S^1} A^1_{4D}$. The shift symmetry $\xi_1 \to \xi_1 + 1/R$ from the periodicity of the Wilson line is a large gauge symmetry.

To probe the theory we introduce a couple of matter fields in the four dimensional gauge theory Ψ^1 and Ψ^2. The superscript denotes the $U(1)$ charge in four dimensions. Upon compactification to three dimensions these fields give rise to a KK tower

$$\Psi^i_n = \sum_{n=-\infty}^{n=+\infty} \psi^i_n e^{2\pi i n y} \tag{4.3.1}$$

of three dimensional fields ψ^i_n. Here y is the coordinate along the circle S^1. The masses of the ψ^i_n are given by $m_n = \left| \frac{n}{R} \right|$ as long as the vev $\langle \xi_1 \rangle$ vanishes. In this case only the zero modes remain massless. For any non-zero n there are two fields of the same mass, corresponding to the modes $\pm n$. By turning on a vev for ξ_1 or equivalently, moving on the Coulomb branch, the mass formula changes to

$$m^q_n = \left| q \langle \xi_1 \rangle + \frac{n}{R} \right| \;, \tag{4.3.2}$$

as seen by reducing the $U(1)$ covariant derivative. Here q denotes the charge with respect to the gauge field A^1_{4D}. By recalling that $\langle \xi_0 \rangle = 1/R$, and that the KK level n is the $U(1)_0$ charge we see that the two terms on the right in have the same structure. By turning on a vev for ξ_1 the zero mode is not massless anymore. The masses of the two modes at the first KK level cease to be degenerate. One of
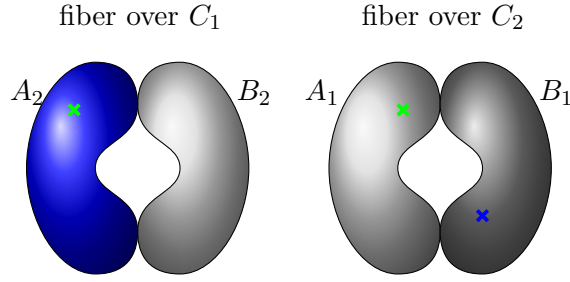
Figure 4.3: The fiber structure over the singlet curves C_1 and C_2 taken from [10] with blue denoting the section S and green the section U.

them becomes lighter and the other heavier. As $\xi_1 \to \frac{1}{qR}$ the lighter one becomes massless, and takes the role of the zero mode, all the other modes rearrange such that the KK tower is the same as for $\xi_1 = 0$.[4]

We will now explain how this field theory picture is manifest in the F-theory geometry. The states ψ_n^1 and ψ_n^2 are associated to membranes wrapping certain components of the fiber over the C_1 and C_2 loci in (4.1.5) and (4.1.9). We are considering the resolved fibration (4.1.1) with the two sections represented by the classes U and S. Both sections give rise to a $U(1)$ gauge field in three dimensions, and we denote them by $U(1)_U$ and $U(1)_S$. The zero-section is identified with the graviphoton and the Shioda map gives the second gauge factor. In the field theory notation above this reads

$$U(1)_0 = U(1)_U , \qquad U(1)_1 = U(1)_S - U(1)_U . \tag{4.3.3}$$

Recall that the charges of the matter states are computed by integrating the M2 action over the components of the fiber that they wrap. As we saw in section 4.1 the intersection of U and S with the split fiber components is different. Here we denote the irreducible fiber components by A_i and B_i, with A and B beeing the two curves in the fiber. Over the double-charged locus C_1 the component A_2 is wrapped by the section S, which is also the component intersected by U in a point. Over the single-charged locus C_2 the curve A_1 is the component intersected by U and B_1 the component intersected by S. This situation is depicted in Figure 4.3. The charges of the states wrapping them are simply given by the appropriate intersection numbers with the sections. In terms of $U(1)_0$ and $U(1)_1$ this gives the charges of

$$\begin{aligned} Q\left(M_{A_2}\right) &= (1,-2) , \\ Q\left(M_{B_2}\right) &= (0,2) , \\ Q\left(M_{A_1}\right) &= (1,-1) , \\ Q\left(M_{B_1}\right) &= (0,1) . \end{aligned} \tag{4.3.4}$$

Here, for instance, M_{A_1} denotes the state wrapping the A_1-cycle over the curve C_2 with the single-charged states. For each of the states there will also be anti-M2 states of opposite charge wrapping the same fiber components which will form their (four-dimensional $N = 2$) superpartners. When we now turn to discussion of the Higgs mechanism, the higgsing is to be performed along the D-flat direction, where the states and their partners have equal vacuum expectation values.

The higgsing that we are interested in corresponds to giving a vacuum expectation value to a state on the doubly-charged curve C_1. This corresponds to a geometric deformation of the $\text{Bl}^1\mathbb{P}_{1,1,2}$

---

[4]Note that for a field of charge q it is sufficient to shift $\xi_1 \to \xi_1 + \frac{1}{qR}$. One consequence of this is that, if we have also a state of charge one say, then there are q different vacua for the charge one state which are all equivalent from the charge q state perspective. In particular in a background where the state of charge q obtains a VEV there are q different vacua for the charge one state. This can also be thought of in terms of the spectrum of Wilson line operators in the four-dimensional theory that are not gauge equivalent, see for example [102].

	A_2	B_2	A_1	B_1
S	-1	2	0	1
U	1	0	1	0
$S+U$	0	2	1	1
$S-U$	-2	2	-1	1

Table 4.3.1: $U(1)$ charges of M2-branes wrapping fiber components in M-theory compactified on P_1.

model with two sections. Importantly, the deformation occurs *after* first blowing down the divisor S, which corresponds to shrinking the curve A_2 over the double-charged locus. The conifold transition is a transition over the singularity, where the blow-down renders the Calabi-Yau singular, and the deformation by the term $c_4 v^4$ in the conifold transition gives a new fibration which is smooth. The Higgs field in the field theory comes from the massless spectrum of the F-theory compactification. Therefore, the Higgs must be the massless state after the blow-down, i.e. it is the state M_{A_2} as its mass goes to zero when the curve A_2 collapses. We see that this state has charge 1 under $U(1)_0$ and therefore it is a first excited KK state, or at level one in (4.3.1). The fact that the vev is given to a KK state was first shown in [117] and in particular this was shown to recover the appropriate Chern-Simons terms. From the geometric perspective it is clear that the higgsed field is massless since it corresponds to a deformation mode of the geometry, or in other words, a flat direction in the moduli space. More general discussions of the importance of Kaluza-Klein modes in F/M-theory duality are found in [50,52]. From the charges we can also read off the remaining massless combination of three-dimensional $U(1)$'s which remains after Higgsing. This is precisely the linear combination

$$U(1)_{\text{massless}} = 2U(1)_0 + U(1)_1 \tag{4.3.5}$$

of gauge fields under which the state M_{A_2} is uncharged and hence the vev do not break this $U(1)$. This combination is precisely the one found in [117], based on the geometric data in an explicit conifold transition between explicit example geometries. From the field theory perspective we see why the massless $U(1)$ in three dimensions must be given by this specific combination. The reason why the same combination is found in [117] over explicitly chosen base manifolds is that it only depends on the fiber and is independent of $\mathcal{B}$.

The fact that the higgsed state is not the zero mode in the Kaluza-Klein expansion is, although maybe surprising, in perfect match with the field theory discussion we have presented. As long as the vacuum expectation value of ξ_1 is chosen to be $\langle \xi_1 \rangle = \frac{1}{2R}$, in which case the mass (4.3) vanishes. By fixing this point on the Coulomb branch of $U(1)_1$ implies that the fiber over the single charge locus C_2 to be resolved. This is because the states from wrapping A_1 and B_1 are both massive, and the mass of charged matter states is, as we recall, due to the volume of the fiber component. This is in nice agreement with the geometry since the fibration is smooth by construction and the fiber over C_2 is resolved in the first place. Moreover, the mass of the two states is seen to be equal for this specific vev of $\langle \xi_1 \rangle$ and both $M(A_1)$ and $M(B_1)$ have mass $m = 1/2R$. This implies that the volume, i.e the area of the two fiber components is equal, as required by the presence of a multi-section, which was pointed out in [84].

Since the Higgs state has charge 2 we expect two vacua [102] in the three-dimensional theory after the Higgsing. Indeed, as seen below (4.3) the periodicity of the Wilson line ξ_1 is reduced by a factor of q^{-1}. If this was the only field it has no further implication, but in presence of the field of charge one there are now two equivalence classes of solutions. The geometric reason for the two solutions lie in the blow-down to the singular fibration. For the conifold transition outlined above we considered the blow-down realised by setting $s \equiv 1$. The singular quartic hypersurface in $\mathbb{P}_{1,1,2}$ arise as the curve
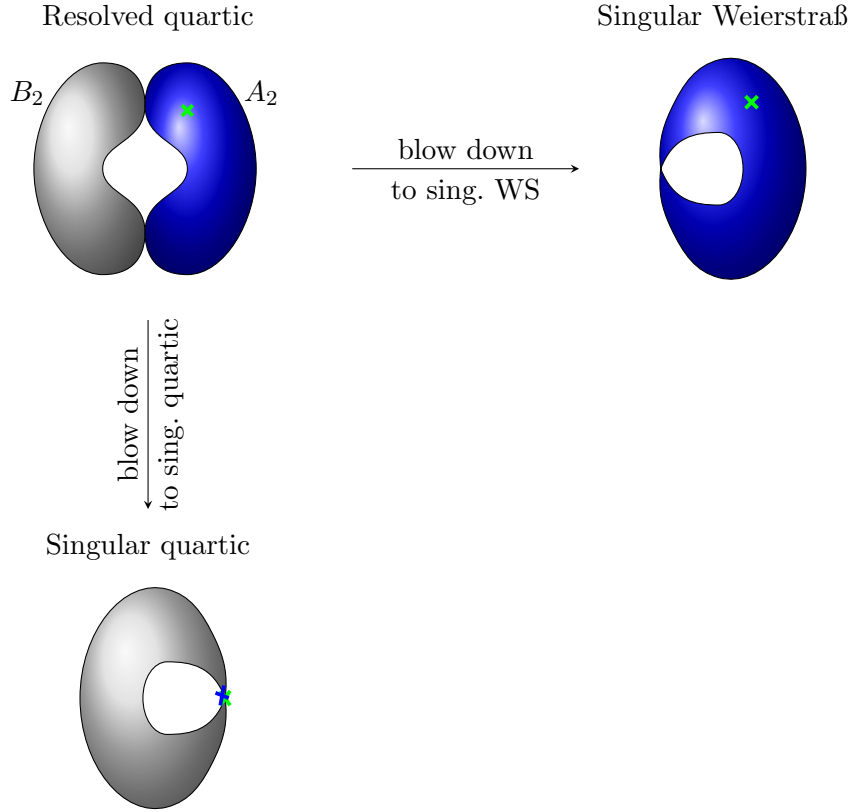
Figure 4.4: The fiber over the charge-two locus C_1. As in Figure 4.1, blue denotes the section, in the resolved model identified with S, and green the section U.

A_2 collapses. The other possibility is the collapse of B_2, as depicted in Fig 4.4. By constructing the Jacobian form, through a birational transformation into the Weierstrass form one find that the fibration is singular both at the charge two locus C_1 and the singly charged curve C_2[5]. To study this vacuum we first identify the M2 brane states that is massless. Over C_2 it is the curve B_1 that shrinks to zero size, as it is not intersected by the zero-section. Over C_2 the component B_2 is the collapsing cycle. This is shown by mapping the singular Weierstrass model back to a $\mathrm{Bl}^1\mathbb{P}_{1,1,2}$ fibration which, crucially, corresponds to a different blow-down than in the model previously considered. In particular the cycle B_2 shrinks to zero size in this blow-down.

We can therefore identify the massless states as coming from M_{B_2} and M_{B_1}. Both these states are massless only at the origin $\langle \xi_1 \rangle = 0$ of the Coulomb branch. By giving a vev to the Higgs state M_{B_2} fixes the point on the Coulomb branch where M_{B_1} is massless. This is equivalent to the vanishing volume of B_1, and thus at this point the singly charged locus is not resolved. This is the manifestation of the statement that the Jacobian fibration of the deformed geometry does not admit a Kähler resolution [29]. We point out that in the two vacua, or geometrically in the $\mathbb{P}_{1,1,2}$ fibration and its Jacobian, the Higgs fields are two different fields. In one case it is M_{B_2} and in the other case M_{A_2} and they are modes at different KK levels. Since the higgsing is by different fields in the two cases, the two vacua we are discussing are two different Higgs branches in the three dimensional theory, coming from a four dimensional theory on a circle. The general picture is that a Higgs field of charge n in four dimensions leads to n three dimensional vacua, each associated to one of the n KK modes. The geometric manifestation of the n vacua is n different blow-downs to a singular fibration. These n three

---

[5]If we turn off the doubly-charged locus C_1, e.g by choosing a base in which the intersection of b_2 and c_3 is zero, we reach the $U(1)$-restricted model studied in [77, 89], in which the singly-charged locus has been analysed in detail.

dimensional vacua are physically distinct, and are not mere reformulations of the same physics.

4.4 The symmetry group in three and four dimensions

In the four dimensional F-theory limit the remaining symmetry group after the Higgsing is $\mathbb{Z}_2$. In three dimensions there are however different gauge groups in the two physically distinct higgsings in the $\mathbb{P}_{1,1,2}$ fibration and in the Jacobian fibration. In the Jacobian the Higgs field $M(B_2)$ has charges $(0,2)$ and therefore the gauge group is broken as $U(1)_0 \times U(1)_1 \to U(1)_0 \times \mathbb{Z}_2$. The Higgs is not charged under the KK $U(1)$ which is therefore unbroken. In the $\mathbb{P}_{1,1,2}$ fibration the Higgs state $M(A_2)$ has charges $(1, -2)$. As we have seen this higgsing breaks one $U(1)$ while the linear combination of $U(1)$'s under which the Higgs is uncharged remains unbroken. By changing the basis for the two $U(1)$ generators appropriately the breaking is seen to be $U(1)_0 \times U(1)_1 \to U(1)_2$ and there is no discrete gauge group remnant, cf. appendix B.1. This further shows how the two three-dimensional vacua are physically distinct.

In the second case where there is no discrete symmetry the Higgs has charge one under $U(1)_U$ i.e it is a first excited KK mode. This implies that the background has a vacuum expectation value for the Higgs which is spatially varying along the circle. This mixes the geometric action on the wavefunctions associated to translations along the circle with the internal gauge symmetry. Since it is a first excited KK mode but has charge 2 under the four dimensional $U(1)_{S-U}$ the remaining symmetry

$$U(1)_2 = U(1)_{S+U} = U(1)_{S-U} + 2U(1)_U \tag{4.4.1}$$

corresponds to moving at twice the rate along the circle as along the internal $U(1)$. In particular it means that the $\mathbb{Z}_2$ subgroup of $U(1)_{S-U}$ corresponding to a shift in phase by π takes us a full path around the circle, i.e acts trivially. The $\mathbb{Z}_2$ is therefore actually a three dimensional symmetry and becomes a subgroup of the remnant three dimensional symmetry $U(1)_{S+U}$ constructed from $U(1)_U$ and the zero mode of $U(1)_{S-U}$.

This picture of Higgsing has a nice reformulation in terms of a Stückelberg mechanism. The usual map is to write the Higgs field as a modulus and a phase, $\phi = he^{ic}$, the phase part being associated with an axion c. Now since the Higgs has a first KK mode profile it depends on the circle coordinate y as e^{iy}, which implies a linear profile for the axion field. The field therefore has an associated flux when integrated over the circle. This matches the observation in [120] (see also [101, 117]) that the F-theory T-dual perspective to the M-theory geometry should be a fluxed reduction over a circle. The flux then breaks the KK $U(1)_U$ while the fact that the Higgs has charge 2 under the four dimensional $U(1)_{S-U}$ means that the axion couples to it with coefficient 2 and (linearly) breaks it. The resulting three-dimensional $U(1)$ is then the combination that remains of the zero mode of $U(1)_{S-U}$ and $U(1)_U$ as discussed above.

It remains to show how the four-dimensional $\mathbb{Z}_2$ symmetry emerges from the three-dimensional $U(1)$ symmetry. To understand this we consider the states in the theory. Before the gauge symmetry breaking there is a tower of KK states associated to the circle reduction. In the M-theory compactification the KK number n corresponds to the wrapping number of the M2-brane on the full fiber. In order to uplift a three-dimensional field to a four-dimensional one we need the full set of KK states to recreate the four dimensional field. The KK modes span the full set of harmonic functions when expanding the wavefunction of the four-dimensional field in the fourth dimension, which is the decompactification of the circular dimension. Since the KK $U(1)$ is a section of the singular $\mathbb{P}_{1,1,2}$ fibration it intersects the fiber in a point, and for each full fiber wrapping the KK number is increased by one, eventually filling the full KK tower. After the higgsing, i.e the deformation there is no zero section nor an extra section and the surviving symmetry is $U(1)_2 = 2U(1)_0 + U(1)_1$. From (4.3.3) we see

that this combination corresponds to $U(1)_U + U(1)_S$ which correspond to the class $U + S$ before the deformation. By deforming this sum becomes the bisection of the genus-one fibration. The wrapping number of the full fiber by the bisection is now 2, and the KK number increase in steps of two. We see from (4.3.4) that the $U(1)_2$ charges of the singly charged states $M(A_1)$ and $M(B_1)$ are odd. Since the KK numbers differ by two, the full Kaluza-Klein tower of these singly charged states have only odd KK numbers. When uplifting this expansion of odd KK modes to four dimensions the four dimensional field will be odd under a reflection parity in the fourth direction. This is an effective $\mathbb{Z}_2$ symmetry in four dimensions, as any odd number of fields will integrate to zero. The same $\mathbb{Z}_2$ symmetry seen from the perspective of the singular Weierstrass model will be discussed in the next chapter.

4.5   Torsion homology and genus one fibrations

In this section we discuss the appearance of a $\mathbb{Z}_2$ symmetry in four dimensions from the singular Weierstrass form we introduced in the previous section. We will show how torsional homology cycles appear in the geometry and explain the relation to the discrete symmetry in the F-theory limit. To put torsion homology cycles into the perspective of string compactifications we turn briefly to type IIA compactifications on a Calabi-Yau 3-fold X_3. Here the appearance of a closed string Ramond-Ramond (RR) $\mathbb{Z}_k$ symmetry is in one-to-one correspondence with the existence of torsional (co)homology groups on X_3 [74]. Since there are no propagating degrees of freedom associated with a discrete symmetry, the 'smoking gun' for a $\mathbb{Z}_k$ symmetry in four-dimensional field theory is matter charged under the symmetry. In this case the existence of $\mathbb{Z}_k$ charged particles and strings [102]. In field theory these arise a priori as operators describing the associated probe particles and strings. In a UV completion including gravity all such operators are conjectured to be realized as physical objects [102]. In compactifications of type IIA string theory these $\mathbb{Z}_k$ charged particles and strings are due to wrapped D2- and D4-branes along k-torsional 2- and 3-cycles. By definition, k copies of such k-torsional cycles are homologically trivial and thus k copies of the $\mathbb{Z}_k$ charged particles and strings are uncharged and can thus decay [74]. Furthermore, the existence of such torsional 2- and 3-cycles implies also torsional cocycles in cohomology. In particular the existence of a torsional 3-form α which by definition satisfies

$$d\mathrm{w} = k\,\alpha \tag{4.5.1}$$

for some 2-form w. The type IIA 3-form C_3 in the RR sector can be decomposed as $C_3 = A \wedge \mathrm{w} + \dots$ gives rise to a massive $U(1)$ gauge potential A. Because it aquires a mass the gauge symmetry group is in fact broken to $\mathbb{Z}_k$. The effective action in four dimensions features precisely this discrete symmetry. To summarize, a closed string $\mathbb{Z}_k$ symmetry in type IIA on X_3 manifests itself geometrically in the fact that [74]

$$\begin{aligned}
\mathrm{Tor}H_2(X_3, \mathbb{Z}) &\simeq \mathrm{Tor}H_3(X_3, \mathbb{Z}) = \mathbb{Z}_k, \\
\mathrm{Tor}H^3(X_3, \mathbb{Z}) &\simeq \mathrm{Tor}H^4(X_3, \mathbb{Z}) = \mathbb{Z}_k.
\end{aligned} \tag{4.5.2}$$

Because of the duality between type IIA theory and M-theory one expect that torsion homology has a role to play also in F-theory compactifications. Until our work [11] the question on how this comes about was not answered. The reason for this was that the genus-one fibrations studied [10, 29, 70, 84, 101, 117] all had homology groups with trivial torsion subgroups [121]. In this section we present the link between torsion cycles and discrete symmetries in F-theory by discussing both the field theory and the associated fibration. For concreteness we will stick to the example of a $\mathbb{Z}_2$ symmetry and to the quartic hypersurface in $\mathbb{P}_{1,1,2}$ which is genus-one fibered with a bisection. The conclusions however extend immediately to larger discrete symmetry groups.

As we have seen, a $\mathbb{Z}_2$ symmetry in the effective action of F-theory compactified to $2n$ large dimensions is related to a pair of fibrations: the hypersurface P_2 and the Jacobian P_W. These
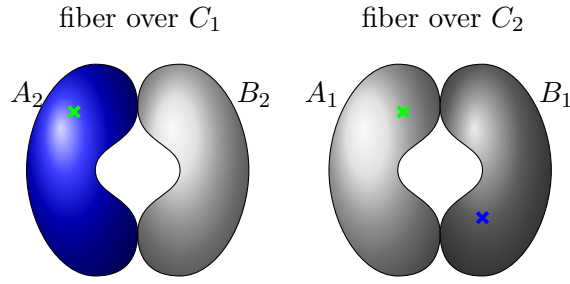
Figure 4.5: The fiber structure over the singlet curves C_1 and C_2 taken from [10] with blue denoting the section S and green the section U.

are both fibrations over a base $\mathcal{B}$ of complex dimension $5 - n$. The fibration P_2 is the genus-one fibration given by a general quartic in $\mathbb{P}_{1,1,2}$ [29]. P_W is the singular Jacobian fibration of P_2 whose Weierstrass form has a zero-section, but also terminal singularities. The number of distinct fibrations, or isomorphism classes of fibrations that share the same Jacobian fibration is counted by the Tate-Shafarevic group, and the $\mathbb{Z}_k$ symmetry in the F-theory compactification on a genus-one fibration is related to k equivalence classes of fibrations [84]. In our $\mathbb{Z}_2$ example the two classes in the Tate-Shafarevic group is the trivial element, the Jacobian fibration P_W itself, and a representative of the second element is P_2. The two fibrations give rise to one and the same F-theory compactification in $2n$ dimensions, but the M-theory compactifications to $2n - 1$ dimensions are different, as we already have seen in previous section. By taking into account that the Higgs vacuum expectation value can vary along the compactification circle we put our results into the context of F/M-theory duality for genus-one fibrations where a flux is introduced on the circle in the F-theory limit [101, 117, 120]. For simplicity we will mostly consider the case $n = 3$ which correspond to a six dimensional F-theory compactification, and compactifications of M-theory to five dimensions[6]. This means that matter is localised at points in the base $\mathcal{B}_2$, and that there are no Yukawa points realized at codimension three loci. We are interested in torsion cycles and the F-theory limit here and not in discrete selection rules, which we will discuss in the $SU(5)$ examples in the following sections.

4.5.1 Torsion from the Weierstrass fibration

The Jacobian fibration associated with the fibration P_2 [29, 84] has the non-generic Weierstrass representation

$$P_W = y^2 - x^3 - fxz^4 - gz^6 \tag{4.5.3}$$

with $[x : y : z]$ homogeneous coordinates of $\mathbb{P}_{231}$ and

$$
\begin{aligned}
f &= e_1 e_3 - \frac{1}{3}e_2^2 - 4e_0 e_4, \\
g &= -e_0 e_3^2 + \frac{1}{3}e_1 e_2 e_3 - \frac{2}{27}e_2^3 + \frac{8}{3}e_0 e_2 e_4 - e_1^2 e_4
\end{aligned}
\tag{4.5.4}
$$

for

$$
\begin{aligned}
e_0 &= -c_0 + \frac{1}{4}b_0^2, & e_1 &= -c_1 + \frac{1}{2}b_0 b_1, \\
e_2 &= -c_2 + \frac{1}{2}b_0 b_2 + \frac{1}{4}b_1^2, & e_3 &= -c_3 + \frac{1}{2}b_1 b_2,
\end{aligned}
$$

---

[6]In the end of section 4.5.1 we will comment on the four dimensional case.

$$e_4 \;=\; -c_4 + \frac{1}{4}b_2^2. \tag{4.5.5}$$

While P_2 and P_W have the same discriminant, their fiber structure are different [29]. The Weierstrass model has a holomorphic zero-section, given by the intersection of the ambient divisor $Z : z = 0$ with P_W. Furthermore P_W exhibits non crepant-resolvable I_2-singularities over the specific locus C on $\mathcal{B}$ over which the fiber in P_2 is a smooth I_2 fiber. The Weierstrass model P_W is related via a conifold transition to a smooth fibration $\hat{P}_W$. This resolved model can be identified with the geometry of P_1 in (4.1.1) by mapping the Weierstrass model to a $\mathbb{P}_{112}[4]$-fibration and resolving the latter into a $\text{Bl}^1\mathbb{P}_{112}[4]$-fibration over $\mathcal{B}_2$. The conifold transition occurs as the 2-step process

$$\hat{P}_W \to P_W|_{c_4 \equiv 0} \to P_W. \tag{4.5.6}$$

As pointed out in section 4.3 the crucial difference compared to the transition relating P_1 to P_2 is that now in passing from $\hat{P}_W \to P_W|_{c_4 \equiv 0}$ the fiber component B_2 and, simultaneously, B_1 shrink to zero size. Recall that in the transition $P_1 \to P_2$ it is instead the curve A_2 over C_1 that shrinks. From the intersection numbers in table 4.3.1 we deduce the Kähler cone on $\text{Bl}^1\mathbb{P}_{112}[4]$ relevant for the curves in the fiber. In this choice of basis these are the divisor classes, or $(1,1)$-forms, with positive intersection numbers with all fibral curves. A Kähler form inside this Kähler cone is given by

$$J = t_1\,U + t_2\,(S + U)$$

with t_1, $t_2 > 0$. Integrating this two-form over the curves A_I, A_1, B_2 and B_1 yields

$$\int_{A_2} J = t_1, \quad \int_{B_2} J = 2\,t_2, \quad \int_{A_1} J = t_1 + t_2, \quad \int_{B_1} J = t_2\,.$$

In this way we get a parametrisation of the volumes of the irreducible curves over C_2 and C_1 in terms of t_1 and t_2. The blow-down to the singular quartic P_2 is therefore identified with the limit $t_1 \to 0$, while the blow-down to the singular Weierstrass (4.5.6) corresponds to $t_2 \to 0$. The states that become massless in the second case are M2-branes wrapping B_2 (and also those wrapping B_1). The M2-brane on the vanishing B_2 is the Higgs field which acquires a vev upon deforming the model from $P_W|_{c_4 \equiv 0} \to P_W$. The states associated with B_1 are mere spectators in this process. From table 4.3.1 we see that under $U(1)_U \times U(1)_{S-U}$ the Higgs field has charges $(0, 2)$ and as a result it breaks

$$U(1)_U \times U(1)_{S-U} \to U(1)_U \times \mathbb{Z}_2. \tag{4.5.7}$$

This result does not depend on the chosen basis for the two $U(1)$'s. Any other basis for the charges that preservs the physics has to be related to the chosen one by a unimodular transformation. But a Higgs field which is charged only under one of the $U(1)$s with charge 1 can't be the image of the vector $(0, 2)$ under such a transformation. As the Higgs has charge 2 under one of the $U(1)$'s a compactification of M-theory to five dimensions on P_W does exhibit a $\mathbb{Z}_2$ symmetry. The Weierstrass model has a zero-section which means that under the standard duality to F-theory in six-dimensions the $U(1)_U$ embeds into the six-dimensional diffeomorphism invariance and only the $\mathbb{Z}_2$ symmetry remains. This origin of the discrete $\mathbb{Z}_2$ in F-theory on P_W is contrasted to how the $\mathbb{Z}_2$ arise in the P_2 model.

Since no torsion cycles exist in the P_2 hypersurface we now turn to the geometry P_W. We will show how the torsional cycles appear and that the group of torsion cycles is the discrete symmetry group. To understand this we will analyze in detail the conifold transition from the smooth $\hat{P}_W$ to P_W in more detail. The conifold transition occurs is in line with the well-known general analysis of [122–124] except for some details which has not appeared in the F-theory literature before and which are responsible for the appearance of torsion homology groups.

On $\hat{P}_W$ the locus $C_1 = \{b_2 = 0\} \cap \{c_3 = 0\}$ consists of $N = [b_2] \cdot [c_3]$ points on the base $\mathcal{B}_2$ of the fibration over which the fiber factorises. Let us label the two fiber components by B_2^i and A_2^i with
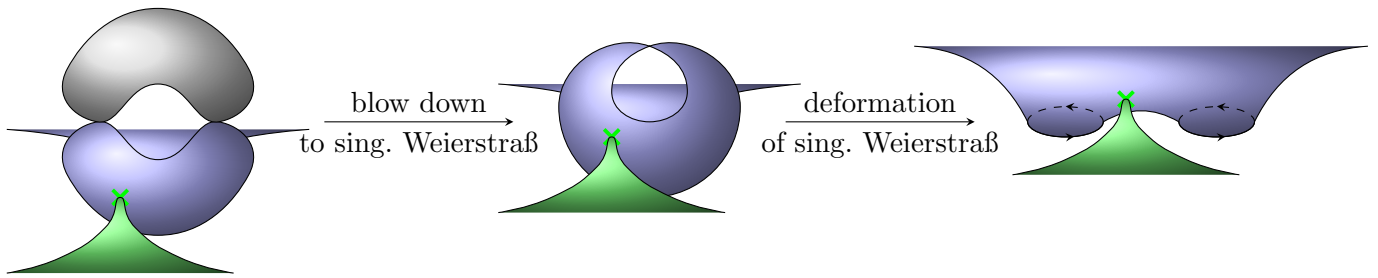
Figure 4.6: Figure showing the boundaries induced after the conifold transition in the Weierstrass hypersurface in $\mathbb{P}_{231}$. The divisor S is denoted in blue and U is denoted in green. After the transition U does not develop a boundary and therefore is associated to the five-dimensional $U(1)_U$ symmetry. On the other hand S develops two boundaries of the same orientation. The sum over all the points B_I^i for *each one* of the two boundaries illustrated gives the torsional 3-cycle associated to the $\mathbb{Z}_2$ symmetry.

$i = 1, \ldots, N$. Due to the fibration structure all B_2^i are homologous to each other. This gives rise to $N - M = N - 1$ homology relations of the form $B_2^1 = B_2^j$ for $j = 2, \ldots, N$. Each of these homology relations is associated with a 3-chain Γ_{1j} such that $\partial \Gamma_{1j} = B_2^1 - B_2^j$ which states the homological equivalence of B_2^1 and B_2^j. In the conifold transition the B_2^i first shrinks to zero size and then, by the deformation they get replaced by 3-spheres S_3^i[7] In [122–124] the general result that the 3-spheres enjoy $M = 1$ homology relations was showed. Hence the number of independent spheres after the deformation is $N - 1$.

At the same time as the B_2^i shrink, also the fiber component B_1 over the locus C_2 shrinks to zero size, but the deformation corresponding to switching on c_4 does not deform the resulting singularities into 3-spheres. This is another incarnation of the statement that on P_W non-crepant resolvable I_2 singularities in the fiber remain. We will comment more on these singularities in the following.

According to the analysis [122–124] of the conifold transition with $M = 1$, there must exist one 'magnetic' 4-cycle which intersects each of the two-spheres B_2^i. This 4-cycle is identified with the divisor S with intersection numbers

$$S \cdot B_2^i = 2. \tag{4.5.8}$$

Indeed, the rational section S wraps the entire fiber A_2^i, and the two intersection points with B_2^i are evident from figure 4.1. Importantly, the other section U does not intersect the B_2^i and therefore, since the B_2^i are fibral curves and there are only two divisor classes coming from the fiber. These are U and S and thus he fibration structure guarantees that no other integer four-cycle exists intersecting the B_2^i. In particular there exists no such divisor with intersection number 1 (as opposed to 2). After shrinking the B_2^i cycles to nodes and deforming them into S_3^i they each induce a boundary on S turning it into a 4-chain. At the intersection points on S the deformation three-spheres are glued in, and as S 'ends' on the S_3^i all the deformation cycles constitute a boundary in homology.

Here we point out a crucial detail of the conifold transition $\hat{P}_W \to P_W$. The divisor S intersects the two-cycles B_2^i at *two* points and so they each induce two boundaries of the same orientation. Thus the precise homological relation obeyed by the S_i^3 is

$$2\,\Gamma = \partial \hat{S}, \qquad \Gamma = \sum_i S_3^i \tag{4.5.9}$$

---

[7]Recall that the deformation of a singularity introduces cycles in the mid homology. Here we are studying complex three-fold fibrations, and hence the new cycles have 3 real dimensions.

where $\hat{S}$ is the 4-chain arising from S in the deformation. This is illustrated in fig. 4.6. The torsional cycle is hence identified with the 3-chain Γ as a $\mathbb{Z}_2$ element of $\mathrm{Tor}H_3(P_W, \mathbb{Z})$. Since the base $\mathcal{B}_2$ is generic no other torsion elements occurs and so

$$\mathrm{Tor}H_3(P_W, \mathbb{Z}) = \mathbb{Z}_2. \tag{4.5.10}$$

We stress that the appearance of the torsion cycle Γ as the boundary of the 4-chain $\hat{S}$ relies on the fact that S intersects each of the shrinking 2-cycles B_2^i. Note that in addition, S also intersects the shrinking fiber component B_1 over C_2 as is evident from table 4.3.1. The singular fibers over C_2 remains after the deformation but it is possible [125] to resolve these singularities after a suitable blow-up in the base $\mathcal{B}_2$. This will replace the former intersection points with S by an even-dimensional cycle and thus does not induce any additional boundaries for the 4-chain $\hat{S}$ which could spoil the argument. Consistently, the general analysis of [125] shows that after resolving the singularities by a blow-up in the base the resulting geometry has non-trivial torsional cohomology.

As we have shown that $\mathrm{Tor}H_3(P_W, \mathbb{Z}) = \mathbb{Z}_2$ the universal coefficient theorem implies that on a smooth manifold also $\mathrm{Tor}H_2(P_W, \mathbb{Z}) = \mathbb{Z}_2$. In order to identify these torsional cycles we study the resolved $\mathrm{Bl}^1\mathbb{P}_{112}[4]$-fibration. Recall that this is the general form of a fibration with rank one Mordell-Weil group. Since we are looking for a torsional 2-cycle we are interested in the homology classes of the fiber components A_1, B_1, A_2 and B_2. Since there are only two homologically independent sections these four fiber components must enjoy certain homology relations. This is because they are fibral curves and hence only intersect the sections S and U. Therefore these intersection numbers, as given in table 4.3.1, determine uniquely their homology classes. In particular we see that in homology $2B_1 = B_2$, which means that there are 3-chains stretching between a point in the set of points C_1 and two points in the set C_2 with a boundary $2B_1 - B_2$. An illustration of this is given in fig. 4.7. Now as we perform the conifold transition over the C_1 loci the B_2 shrink and then are deformed as S^3s and can no longer form boundaries to these 3-chains. Hence, essentially, the remaining 3-chain has boundary $2B_1$ and should be identified with the torsional element. The complication is that before the deformation the blow-down has to be performed and in this both B_2 and B_1 collapses, and as B_1 shrinks the fibration becomes singular over the point set C_2 in $\mathcal{B}_2$.

In order to find the torsional elements on the smooth space, the singularities at C_2 must be resolved. Here we do not perform the resolution explicitly but work under the assumption that a resolution can be found. In this case the full fibration is smooth and the universal coefficient theorem applies. The previously identified torsional 3-cycle implies an element in $\mathrm{Tor}H_2(P_W, \mathbb{Z}) = \mathbb{Z}_2$. In [126] a small resolution of the base was discussed. This resolution is non-Kähler but could be used to identify the torsional cycles. The other way, in terms of a full resolution by a blow-up of the base locus C_2 introduces an exceptional divisor E_2 on the base. This divisor replaces the points C_2 and results in an I_2 fiber over a divisor in the base. This case is analogous to the introduction of $SU(2)$ gauge symmetry by an $SU(2)$ singularity over a divisor. In [125] it was shown that at certain points $\hat{C}_2 \subset E_2$ the fiber type will enhance and give rise to matter charged under this $SU(2)$. In this smooth fibration the torsional 2-cycles would be indentified by 3-chains stretching between the points C_1 and the matter loci $\hat{C}_2$ as before. In an explicit example on would have to check that the blow-up in the base can be performed in a crepant way.

Since we have shown how the non-trivial torsion homology arise in the P_W model we can return to the P_2 fibration and see why the torsion is absent in this case. As in this case the A_2 curve shrinks the divisors S and U both develop a single boundary from each of the A_2^i of opposite orientation, see fig. 4.8. This implies that neither U nor S can be identified with a torsion element. If we take the sum $S + U$ formed by gluing the boundaries together we get a 4-cycle. Note that if we chose to consider the 4-chain corresponding to $S - U$ instead it would indeed have 2 boundaries of the same orientation at each locus, but this would not imply torsion since these boundaries are just the boundaries of S and
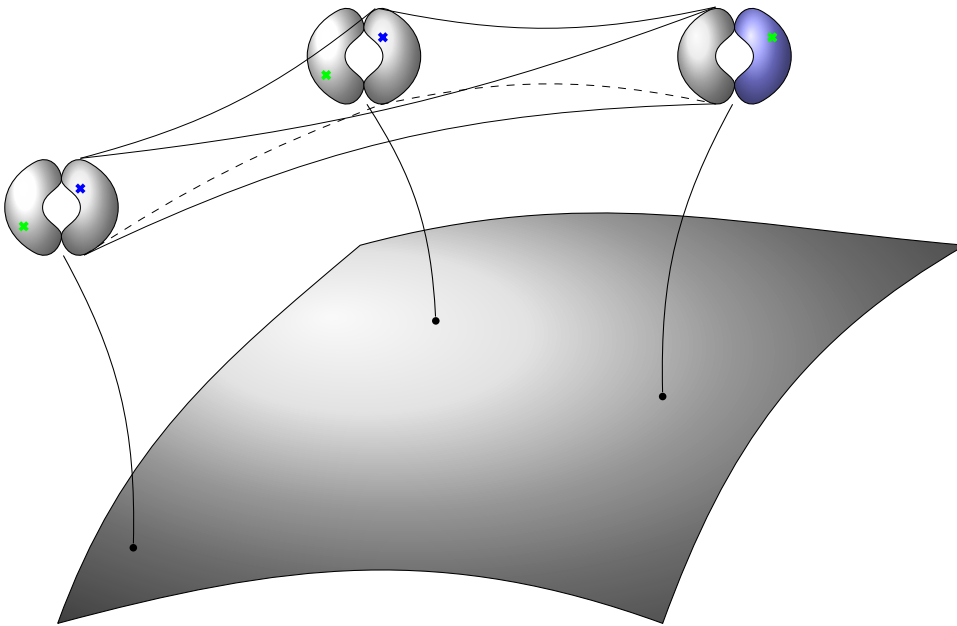
Figure 4.7: Figure showing the 3-chains stretching between a point in the set of points C_1 and two points in the set C_2 in the resolved space. The boundary of the chain is therefore $2B_1 - B_2$. After the deformation the boundary B_2 is lost leaving a chain with a boundary $2B_1$ and thereby identifying B_1 as the torsional 2-cycle.
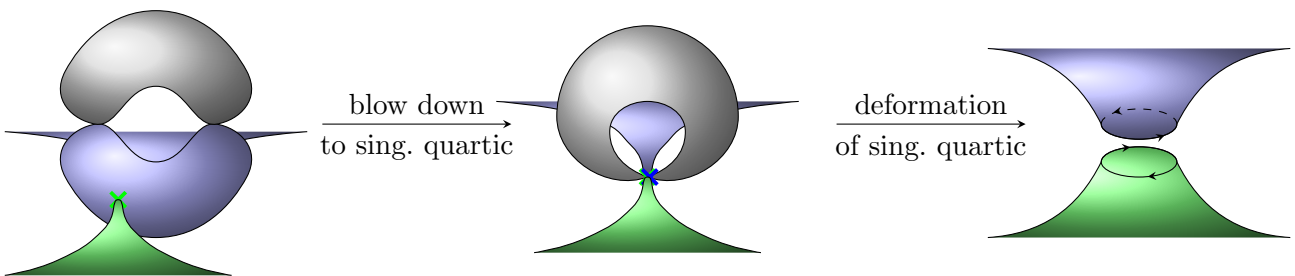
Figure 4.8: Figure showing the boundaries induced after the conifold transition in the quartic hypersurface in $\mathbb{P}_{112}$. The divisors S, denoted in blue, and U, denoted in green, both develop a single boundary from each of the A_2^i of opposite orientation. The two boundaries are then glued together to form the divisor $S + U$ corresponding to the remnant five-dimensional $U(1)$ symmetry.

U, which have 'half' the boundary of $S - U$. Indeed, the analogue of the construction pictured in fig 4.7, but for shrinking A_2 components imply homology relations between the fiber components. But in this case there is no double intersection points and as the A_2^i shrinks it only implies that $A_1 = B_1$ in homology and no any torsion elements.

By Poincaré duality the existence of a $\mathbb{Z}_2$ torsional 3-cycle implies the existence of a 3-form α such that

$$2\,\alpha = d\text{w}. \tag{4.5.11}$$

The 2-form w is not closed and is the Poincaré dual to the 4-chain $\hat{S}$ and can be interpreted as the generator of the $\mathbb{Z}_2$ symmetry. Expanding the M-theory 3-form C_3 as $C_3 = A \wedge \text{w} + \ldots$ gives rise to a massive $U(1)$ gauge field in five spacetime dimensions. This corresponds precisely to the $U(1)_{S-U}$ gauge symmetry which gets broken by the Higgsing (see [88] for a discussion of this mechanism in the context of F-theory).

We now turn to discuss further physical significances of the identified torsional cycles[8]. A gauge theory with a $\mathbb{Z}_2$ symmetry has a set of Wilson line operators [102]. In the case that the matter spectrum contains particles with electric $\mathbb{Z}_2$ charge the line operators can be seen as the corresponding world-lines. In a quantum field theory the Wilson line operators exist even in the absence of the charged particles but in a completion of the gauge theory that include gravity it is conjectured [102] that all possible charges must be populated by physical states, in this case the charged particles. To appreciate how this conjecture is indeed confirmed in our M/F-theoretic setting, consider the five-dimensional effective field theory associated with M-theory compactified on P_W. The Wilson line operators describe the word-line of M2-branes wrapping the identified torsional 2-cycles, which do exist as physical particles, in perfect agreement with the above conjecture. One might wonder if a modification of the geometry would be possible that gives rise to a $\mathbb{Z}_2$ gauge theory without such physical $\mathbb{Z}_2$ charged particles. As we have seen, the torsional 2-cycles wrapped by the associated M2-branes are related to the fibre components over C_2 before the deformation. The class of C_2 depends on the class of the coefficients c_i and b_i defining the Weierstraß model. Recall that these transform as sections of certain line bundles on the base. One might try to exploit the existing freedom in choosing these line bundles to arrange for the cohomology class of the locus C_2 to be trivial, in which case no $\mathbb{Z}_2$ charged states would exist. It is easy to see by direct inspection of the coefficient classes (cf. e.g. Table 1 of [10]), however, that this also removes the Higgs field along C_1 and thus destroys the $\mathbb{Z}_2$ gauge theory in the first place. This is of course in agreement with the universal coefficient theorem which guarantees that $\text{Tor} H_3(P_W, \mathbb{Z}) \simeq \text{Tor} H_2(P_W, \mathbb{Z})$.

In five dimensions, the magnetic dual to an electrically charged particle is a string. In our setting these magnetic objects again exist as physical objects arising from M5-branes wrapping the 4-chain $\hat{D}$. Since $\hat{D}$ has the boundary 2Γ, one can consider a configuration consisting of an M5-brane on the 4-chain $\hat{D}$ together with two M5-branes on Γ. This is the M-theory analogue of the configuration considered before in [124] with the important difference that here the M5-branes on the boundary of $\hat{D}$ give rise to *two* membranes in five dimensions ending on the ('magnetic') string. This again realises the expectations based on the general framework of $\mathbb{Z}_2$ gauge theory described in [102]: In a four-dimensional $\mathbb{Z}_k$ gauge theory, k units of flux tubes (strings) end on a magnetic monopole to turn the full configuration into a stable object, and in five dimensions the strings and magnetic monopoles become membranes and 'magnetic' strings.

---

[8]See [74] for an analogous analysis in four-dimensional Type II compactifications.
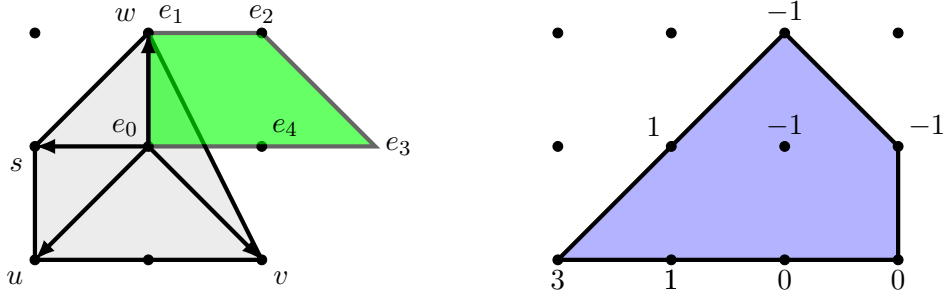
Figure 4.9: $SU(5)$ top 2 over polygon 6 of [19] together with its dual polygon, bounded below by the values z_{min}, shown next to the nodes.

4.6 Models with $SU(5)$ gauge symmetry

In this section we combine the $U(1)$ and $\mathbb{Z}_2$ symmetries studied previously with additional non-abelian gauge symmetry. Due to the appearance of additional charged matter and Yukawa interactions, we will be able to lend further support to the role of the $\mathbb{Z}_2$ symmetry as a discrete selection rule for the couplings of the theory. We present in the following sections the explicit models considered in [10].

We will implement an extra SU(5) gauge theory along a divisor $W : \theta = 0$ on the base $\mathcal{B}$. Among the possible complex structure moduli restrictions giving rise to such a gauge group enhancement, a special class is given by *toric tops* [71, 82]. In this approach the base sections b_i and c_k factorise as $b_i = b_{i,j}\theta^j$ and $c_k = c_{k,l}\theta^l$ for suitable powers j and l and $b_{i,j}$ and $c_{k,l}$ generic. All such consistent configurations for all 16 torus fibrations realised as toric hypersurfaces have been classified in [19], including their corresponding non-abelian gauge symmetries. Using the techniques of [19], one finds that there are five such inequivalent specifications compatible with an $SU(5)$ gauge symmetry along $\theta = 0$ for the $U(1)$ model [20, 83, 92] described in section 4.1. For the $\mathbb{Z}_2$ model of section 4.2 there are three inequivalent tops [20]. But we should note here that the five tops in the $U(1)$ case can be matched by the three tops in the $\mathbb{Z}_2$ case by the additional symmetry of the fiber polygon after removing the point corresponding to the ambient fiber coordinate s.

4.6.1 The $SU(5) \times U(1)$ case

The details of the $SU(5) \times U(1)$ models have already been analysed in [83], cf. appendix B.3, but for the convenience of the reader we will repeat here the derivation of the most important results. We begin with the model described by the second $SU(5)$ top [92] over polygon six in the enumeration by [19], see fig. 4.9. The proper transform of the hypersurface equation after resolution takes the form[9]

$$\begin{aligned}
P_1^{SU(5)} = {}& sw^2e_1e_2 + b_0s^2u^2we_0^2e_1^2e_2e_4 + b_1suvw + b_2v^2we_2e_3^2e_4 \\
& + c_0s^3u^4e_0^4e_1^3e_2e_4^2 + c_1s^2u^3ve_0^2e_1e_4 + c_2su^2v^2e_0e_3e_4 + c_3uv^3e_0e_2e_3^3e_4^2,
\end{aligned} \tag{4.6.1}$$

where to avoid clutter we use b_i and c_k instead of $b_{i,j}$ and $c_{k,l}$ although we really mean the latter when referring to b_i and c_k in the sequel.

Using the hypersurface equation (4.6.1) and the following Stanley-Reisner ideal

$$\text{SR-i}: \quad \{vs, ve_1, ve_2, wu, we_0, we_4, ue_3, se_3, e_0e_3, e_1e_3, ue_1, ue_2, ue_4, se_4, e_1e_4, se_2\}, \tag{4.6.2}$$

---

[9]Note the modified order of the exceptional divisors compared to [83].

which corresponds to one of the phases of the resolution, we can work out the splitting of the fiber along the GUT divisor W. The five fiber components are given by

$$
\begin{aligned}
\mathbb{P}_0^1 &= e_0 \cap b_1 s u v + s e_1 e_2 + b_2 v^2 e_2 e_4\,, & w &= e_3 = 1\,, \\
\mathbb{P}_1^1 &= e_1 \cap b_1 s w + b_2 w e_2 + c_2 s e_0 + c_3 e_0 e_2\,, & u &= v = e_3 = e_4 = 1\,, \\
\mathbb{P}_2^1 &= e_2 \cap b_1 w + c_1 e_0^2 e_1 e_4 + c_2 e_0 e_3 e_4\,, & u &= v = s = 1\,, \qquad (4.6.3) \\
\mathbb{P}_3^1 &= e_3 \cap b_0 w e_2 e_4 + b_1 v w + w^2 e_2 + c_0 e_2 e_4^2 + c_1 v e_4\,, & u &= s = e_0 = e_1 = 1\,, \\
\mathbb{P}_4^1 &= e_4 \cap b_1 v + e_2\,, & u &= w = s = e_1 = 1\,.
\end{aligned}
$$

Due to the additional non-abelian singularity, the divisor (4.1.4) associated with the $U(1)$ symmetry of section 4.1 gets modified by the exceptional divisors E_i of the $SU(5)$. The new $U(1)$ generator, which is uncharged under the non-abelian singularity, is given by

$$
\mathrm{w} = 5(S - U - \bar{\mathcal{K}} - [b_2]) + 4E_1 + 3E_2 + 2E_3 + E_4\,, \qquad (4.6.4)
$$

where the overall normalisation has been chosen such as to render all appearing $U(1)$ charges integer in the sequel.

Matter curves

To obtain the matter curves, we take the hypersurface equation (4.6.1) prior to resolution[10] and calculate from it f and g of its associate Jacobian fibration. From f and g we can calculate the discriminant Δ of the fibration, which agrees with the discriminant of (4.6.1). The divisor $\Delta = 0$ gives the locus of the singular torus fibers. The vanishing order of Δ at that locus relates to the order of the singularity. We expand the discriminant in θ,

$$
\Delta \sim \theta^5 [b_1^4 b_2 (b_1 c_3 - b_2 c_2)(b_1^2 c_0 - b_0 b_1 c_1 + c_1^2) + \mathcal{O}(\theta)]\,, \qquad (4.6.5)
$$

to look for singularity enhancements beyond $SU(5)$ along the GUT divisor. As we can see from the above equation, these lie at

$$
\theta = b_1 = 0\,, \quad \theta = b_2 = 0\,, \quad \theta = (b_1 c_3 - b_2 c_2) = 0\,, \quad \theta = (b_1^2 c_0 - b_0 b_1 c_1 + c_1^2) = 0\,.
$$

At these four curves matter transforming under the $SU(5)$ is localised. To determine the type of matter, one can either explore the vanishing orders of f and g at these curves or directly analyse the characteristics of the resolved fibers over these loci, which is the approach we will take in the following.

Along the curve[11] $\mathcal{C}_{\mathbf{10}_{-2}} = W \cap \{b_1 = 0\}$ the fiber components

$$
\begin{aligned}
\mathbb{P}_0^1 &= e_0 \cap e_2 (s e_1 + b_2 v^2 e_4)\,, \\
\mathbb{P}_2^1 &= e_2 \cap e_0 e_4 (c_1 e_0 e_1 + c_2 e_3)
\end{aligned} \qquad (4.6.6)
$$

factorise and the fiber topology becomes that of the affine $SO(10)$ Dynkin diagram. The intersection numbers of the new effective curves with the divisors E_1 up to E_4 are

$$
\begin{aligned}
\mathbb{P}_{e_0=e_2=0}^1 &\cdot (E_1, E_2, E_3, E_4) = (1, -1, 0, 1)\,, \\
\mathbb{P}_{e_0=se_1+b_2v^2e_4=0}^1 &\cdot (E_1, E_2, E_3, E_4) = (0, 1, 0, 0)\,.
\end{aligned} \qquad (4.6.7)
$$

These intersection vectors are just the $U(1)$-Cartan charges of M2-branes wrapping these $\mathbb{P}^1$s. Therefore, they can be associated with states in the $\overline{\mathbf{10}}$ and $\mathbf{10}$ representation of $SU(5)$, respectively.

---

[10] To obtain the original singular form of (4.6.1) we just have to set e_0 to θ and e_1, e_2, e_3, e_4 to one.

[11] The labeling of the curve will be justified a posteriori.

At the locus $\mathcal{C}_{\mathbf{5}_{-6}} = W \cap \{b_2 = 0\}$ the fiber curve

$$\mathbb{P}_0^1 = e_0 \cap s(b_1 uv + e_1 e_2) \tag{4.6.8}$$

factorises. Calculating again the charges under the exceptional divisors, we find

$$\begin{aligned}
\mathbb{P}_{e_0=s=0}^1 \cdot (E_1, E_2, E_3, E_4) &= (1, 0, 0, 0)\,, \\
\mathbb{P}_{e_0=b_1uv+e_1e_2=0}^1 \cdot (E_1, E_2, E_3, E_4) &= (0, 0, 0, 1)\,,
\end{aligned} \tag{4.6.9}$$

which are the highest weights of the $\mathbf{5}$- and $\bar{\mathbf{5}}$-representation of $SU(5)$.

At the third enhancement locus, $\mathcal{C}_{\mathbf{5}_4} = W \cap \{b_1 c_3 - b_2 c_2 = 0\}$, we find the splitting

$$\mathbb{P}_1^1 = e_1 \cap (c_3 e_2 + c_2 s)(b_1 w + c_2 e_0)/c_2 \tag{4.6.10}$$

when solving for $b_2 = b_1 c_3/c_2$ away from $\{c_2 = 0\}$. The charges under the exceptional divisors reveals again states in the $\bar{\mathbf{5}}$- and the $\mathbf{5}$-representation.

Finally, at the matter curve $\mathcal{C}_{\mathbf{5}_{-1}} = W \cap \{b_1^2 c_0 - b_0 b_1 c_1 + c_1^2 = 0\}$ we find the splitting

$$\mathbb{P}_1^3 = e_3 \cap (b_1 w + c_1 e_4)(b_1^2 v + b_0 b_1 e_2 e_4 - c_1 e_2 e_4)/b_1^2 \tag{4.6.11}$$

when solving for c_0 away from the locus $\{b_1 = 0\}$. These two new states correspond again to the fundamental and anti-fundamental representation of $SU(5)$.

The $U(1)$ charges for the matter states over the four curves $\mathcal{C}_{\mathbf{10}_{-2}}$, $\mathcal{C}_{\mathbf{5}_{-6}}$, $\mathcal{C}_{\mathbf{5}_4}$ and $\mathcal{C}_{\mathbf{5}_{-1}}$ are obtained by intersecting the new effective fiber components with the $U(1)$ generator w given in (4.6.4). The intersection numbers are -2, -6, 4 and -1, respectively, thereby justifying the labeling of the curves. The intersection numbers with the fibral curves corresponding to conjugate states have opposite signs.

Finally, we should note that the structure of $U(1)$ charged singlets is unaffected by the addition of the non-abelian gauge group factor along the divisor W, even though the specific form of the defining equations for the two types of singlet curves may differ slightly compared to the pure $U(1)$ model. To derive the singlet curves we must take into account the appearance of factors of θ in $c_k = c_{k,l}\theta^l$ etc. The structure of the curves and their intersections is unchanged, though. Due to the overall—and arbitrary—normalization factor of 5 in the $U(1)$ generator (4.6.4), the singlets are now of charge $\mathbf{1}_{10}$ and $\mathbf{1}_5$.

Yukawa couplings on W

There are three types of Yukawa points with couplings involving only the states charged under the $SU(5)$. The $\mathbf{10}_{-2}$-curve meets the $\mathbf{5}_4$- and the $\mathbf{5}_{-6}$-curves at $W \cap \{b_1 = 0\} \cap \{b_2 = 0\}$. The fiber enhances to the affine $SO(12)$ diagram at this locus. By grouping the irreducible fiber components one may construct a gauge singlet of states with the coupling $\mathbf{10}_{-2}\,\bar{\mathbf{5}}_6\,\bar{\mathbf{5}}_{-4} + c.c.$

The $\mathbf{10}_{-2}$-curve intersects the $\mathbf{5}_{-1}$-curve at the points $W \cap \{b_1 = 0\} \cap \{c_1 = 0\}$. Over this locus the resolved fiber takes the form of the affine $SO(12)$ diagram. Constructing the gauge singlet identifies the coupling $\bar{\mathbf{10}}_2\,\mathbf{5}_{-1}\,\mathbf{5}_{-1} + c.c.$

The last Yukawa coupling between the $\mathbf{10}_{-2}$- and the $\mathbf{5}_4$-states are located at the point $W \cap \{b_1 = 0\} \cap \{c_2 = 0\}$. Here the enhancement type is E_6 and the invariant coupling is $\mathbf{10}_{-2}\,\mathbf{10}_{-2}\,\mathbf{5}_4 + c.c.$

In addition, three types of Yukawa couplings between the fundamental fields and the singlets occur: At the intersection of the $\mathbf{1}_{\pm 10}$-curve with the GUT divisor W, i.e. at $W \cap \{b_2 = 0\} \cap \{c_3 = 0\}$, the fiber enhances to an $SU(7)$. At this type of points the $\mathbf{5}_{-6}$- and $\mathbf{5}_4$-curve intersect, and by computing the charges of the split curves the Yukawa coupling $\mathbf{1}_{-10}\,\bar{\mathbf{5}}_6\,\mathbf{5}_4 + c.c.$ is found.
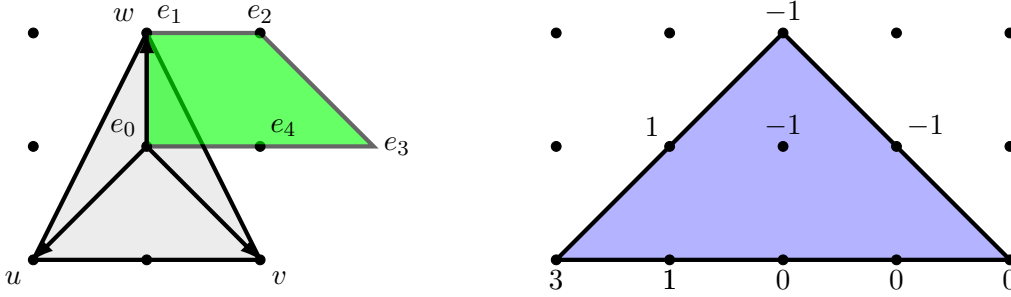
Figure 4.10: $SU(5)$ top over polygon 4 of [19] together with its dual polygon, bounded below by the values z_{min}, shown next to the nodes.

At the intersection of the curves along which the $\mathbf{5}_4$ and $\mathbf{5}_{-1}$ are localised, which corresponds to the points

$$W \cap \{b_1 c_3 = b_2 c_2\} \cap \{b_1^2 c_0 - b_0 b_1 c_1 + c_1^2 = 0\}, \tag{4.6.12}$$

the fiber enhances to $SU(7)$. Here the Yukawa coupling $\mathbf{1}_{-5}\,\mathbf{5}_4\,\bar{\mathbf{5}}_1 + c.c.$ is localised.

At $W \cap \{b_2 = 0\} \cap \{b_1^2 c_0 - b_0 b_1 c_1 + c_1^2 = 0\}$, where the $\mathbf{5}_{-6}$- and the $\bar{\mathbf{5}}_1$-curves intersect, the fiber looks again like an affine $SU(7)$ Dynkin diagram. Thus we have the coupling $\mathbf{1}_5\,\mathbf{5}_{-6}\,\bar{\mathbf{5}}_1 + c.c.$.

Finally, the universal $\mathbf{1}_{10}\mathbf{1}_{-5}\mathbf{1}_{-5} + c.c.$ exists at the intersection of the two singlet curves, as in the model without $SU(5)$ enhancement.

4.6.2 The $SU(5) \times \mathbb{Z}_2$ case

In this subsection we will introduce an $SU(5)$ singularity for the $\mathbb{Z}_2$ model. Since we are interested in studying the relation of the $U(1)$ and the $\mathbb{Z}_2$ model via Higgsing, we will take the top which becomes the top of section 4.6.1 after introducing the point corresponding to s. In the list of $SU(5)$ tops of [20], this is the third top over polygon four, denoted $\tau_{4,3}$. The proper transform of the hypersurface equation after resolving the $SU(5)$ singularity reads

$$
\begin{aligned}
P_2^{SU(5)} =\ & e_1 e_2 w^2 + b_0 u^2 w e_0^2 e_1^2 e_2 e_4 + b_1 uvw + b_2 v^2 w e_2 e_3^2 e_4 \\
& + c_0 u^4 e_0^4 e_1^3 e_2 e_4^2 + c_1 u^3 v e_0^2 e_1 e_4 + c_2 u^2 v^2 e_0 e_3 e_4 + c_3 uv^3 e_0 e_2 e_3^3 e_4^2 + c_4 v^4 e_0 e_2^2 e_3^5 e_4^3 ,
\end{aligned}
\tag{4.6.13}
$$

where we used again b_i and c_k instead of $b_{i,j}$ and $c_{k,l}$. The scaling relations in the ambient space are given in appendix B.3. As in the $U(1)$ case, we work out the fiber components over the divisor W. They are given by

$$
\begin{aligned}
\mathbb{P}_0^1 &= e_0 \cap b_1 u + e_1 e_2 + b_2 e_2 e_3 , & v = w = e_3 = 1 , \\
\mathbb{P}_1^1 &= e_1 \cap b_1 uw + b_2 w e_2 + c_2 u^2 e_0 + c_3 u e_0 e_2 + c_4 e_0 e_2^2 , & v = e_3 = e_4 = 1 , \\
\mathbb{P}_2^1 &= e_2 \cap b_1 w + c_1 e_0^2 e_1 e_4 + c_2 e_0 e_3 e_4 , & u = v = 1 , \\
\mathbb{P}_3^1 &= e_3 \cap b_0 u^2 w e_2 e_4 + b_1 uvw + w^2 e_2 + c_0 u^4 e_2 e_4^2 + c_1 u^3 v e_4 , & e_0 = e_1 = 1 , \\
\mathbb{P}_4^1 &= e_4 \cap b_1 u + e_2 , & v = w = e_1 = 1 ,
\end{aligned}
\tag{4.6.14}
$$

where we used the SR-ideal

$$\text{SR-i}: \quad \{v\,e_0,\ v\,e_1,\ v\,e_2,\ w\,e_0,\ w\,e_4,\ u\,e_3,\ e_0\,e_3,\ e_1\,e_3,\ u\,e_2,\ e_1\,e_4,\ v\,w\,u\} \tag{4.6.15}$$

corresponding to one of the phases of the resolution.
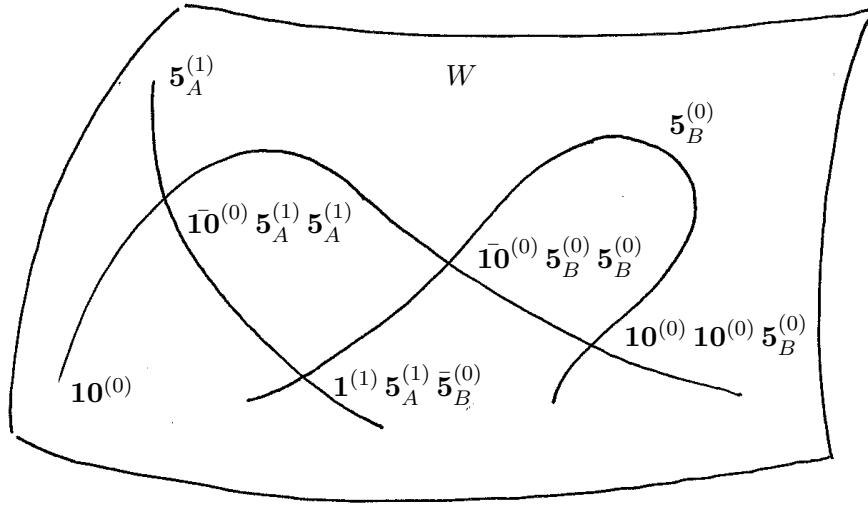
Figure 4.11: The matter curves in $W : \{\theta = 0\}$ and the Yukawa couplings involving the $SU(5)$ charged matter in codimension three.

Matter curves

Calculating again the discriminant of the associate Jacobian fibration to (4.6.13) and expanding it in θ yields

$$\Delta \sim \theta^5 [b_1^4 (b_1^2 c_0 - b_0 b_1 c_1 + c_1^2)(b_2^2 c_2 - b_1 b_2 c_3 + b_1^2 c_4) + \mathcal{O}(\theta)] \,. \tag{4.6.16}$$

Interestingly, this time we only find three matter curves charged under the $SU(5)$. To identify the type of matter along these curves we redo the analysis of the last section.

At $\mathcal{C}_{\mathbf{10}} = W \cap \{b_1 = 0\}$ the following fiber components split,

$$\begin{aligned}
\mathbb{P}_0^1 &= e_0 \cap e_2(e_1 + b_2 e_3) \,, \\
\mathbb{P}_2^1 &= e_2 \cap e_0 e_4 (c_1 e_0 e_1 + c_2 e_3) \,.
\end{aligned} \tag{4.6.17}$$

For the intersection numbers with the exceptional divisors E_i we find

$$\begin{aligned}
\mathbb{P}_{e_0=e_2=0}^1 \cdot (E_1, E_2, E_3, E_4) &= (1, -1, 0, 1) \,, \\
\mathbb{P}_{e_0=e_1+b_2 e_3=0}^1 \cdot (E_1, E_2, E_3, E_4) &= (0, 1, 0, 0) \,,
\end{aligned} \tag{4.6.18}$$

which are weight vectors in the $\overline{\mathbf{10}}$- and the $\mathbf{10}$-representation of $SU(5)$, respectively. The fiber topology is that of the affine $SO(10)$ diagram. For later purposes we also give the intersection with U. The bi-section intersects two of the $\mathbb{P}^1$'s with multiplicity one, specifically $\mathbb{P}_1^1|_{b_1=0}$ and $\mathbb{P}_{e_0=e_1+b_2 e_4=0}^1$.

The first fundamental matter curve, which we will call the A-curve in the following, is $\mathcal{C}_{\mathbf{5}_A} = W \cap \{b_1^2 c_0 - b_0 b_1 c_1 + c_1^2 = 0\}$, because along it $\mathbb{P}_3^1$ factorises as

$$\mathbb{P}_3^1 = e_3 \cap \frac{1}{b_1^2} (b_1 w + c_1 u^2 e_4)\big(b_1(b_1 u v + w e_2 + b_0 u^2 e_2 e_4) - c_1 u^2 e_2 e_4)\big) \,. \tag{4.6.19}$$

We used here that away from $\{b_1 = 0\}$ we may solve for c_0 and resubstitute back into the equations defining the fiber components. The intersection numbers for the two rational curves are

$$\begin{aligned}
\mathbb{P}_{e_3=b_1 w + c_1 u^2 e_4=0}^1 \cdot (E_1, E_2, E_3, E_4) &= (0, 1, -1, 0) \,, \\
\mathbb{P}_{e_3=b_1(b_1 u v + w e_2 + b_0 u^2 e_2 e_4)-c_1 u^2 e_2 e_4=0}^1 \cdot (E_1, E_2, E_3, E_4) &= (0, 0, -1, 1) \,,
\end{aligned} \tag{4.6.20}$$

which correspond to weight vectors associated with two states in the $\bar{\mathbf{5}}$- and the $\mathbf{5}$-representation, respectively. The fiber topology is that of the $SU(6)$ Dynkin diagram. The divisor class of the bi-section U intersects the two adjacent nodes $\mathbb{P}_0^1$ and $\mathbb{P}_1^1$, each with multiplicity one. Note that these are roots.

Solving for c_4 along the third matter curve $\mathcal{C}_{\mathbf{5}_B} = W \cap \{b_2^2 c_2 - b_1 b_2 c_3 + b_1^2 c_4 = 0\}$ we find the factorisation

$$\mathbb{P}_1^1 = e_1 \cap \frac{1}{b_1^2} (b_1 u + b_2 e_2)\big(b_1(b_1 w + c_2 u e_0 + c_3 e_0 e_2) - b_2 c_2 e_0 e_2\big) \tag{4.6.21}$$

and the weights

$$\begin{aligned}
\mathbb{P}_{e_1 = b_1 u + b_2 e_2 = 0}^1 \cdot (E_1, E_2, E_3, E_4) &= (-1, 0, 0, 0) \,, \\
\mathbb{P}_{e_1 = b_1(b_1 w + c_2 u e_0 + c_3 e_0 e_2) - b_2 c_2 e_0 e_2 = 0}^1 \cdot (E_1, E_2, E_3, E_4) &= (-1, 1, 0, 0) \,.
\end{aligned} \tag{4.6.22}$$

These again correspond to states in the $\bar{\mathbf{5}}$- and the $\mathbf{5}$-representation of $SU(5)$, respectively. The fiber forms again an $SU(6)$ structure over $\mathcal{C}_{\mathbf{5}_B}$. The divisor U intersects the irreducible curves $\mathbb{P}_0^1$ and the second curve in (4.6.22). Thus, over the B-curve the bi-section intersects one of the two new effective curves responsible for the fundamental matter at this locus.

The $\mathbb{Z}_2$-charges of the states

As explained already at the end of section 4.2, we can use the divisor U to define a notion of $\mathbb{Z}_2$-charges for the singlets. As in the presence of a $U(1)$ gauge group we demand that the actual divisor whose intersection numbers with the fiber $\mathbb{P}^1$s wrapped by the associated M2-branes give the charges fulfils a suitable of horizontality condition, i.e. the intersection with the bi-section U should vanish. Hence the appropriate divisor before adding the non-abelian singularities is not just U but

$$\mathrm{w}_{\mathbb{Z}_2} = U - [b_2] + \bar{\mathcal{K}} \,. \tag{4.6.23}$$

Similarly to the divisors we usually obtain from sections via the Shioda map, we also demand that the intersections of such a divisor with all $\mathbb{P}^1$ fibers of the fibral divisors vanish, at least modulo two. A divisor with this property is given by

$$\mathrm{w}_{\mathbb{Z}_2} + \tfrac{4}{5} E_1 + \tfrac{3}{5} E_2 + \tfrac{2}{5} E_3 + \tfrac{1}{5} E_4 \,. \tag{4.6.24}$$

For convenience we rescale the above divisor such as to achieve integer intersections with all rational lines and define

$$Q_{\mathbb{Z}_2} := 5 \, \mathrm{w}_{\mathbb{Z}_2} + 4 \, E_1 + 3 \, E_2 + 2 \, E_3 + E_4 \,. \tag{4.6.25}$$

The intersection numbers of this divisor with the five rational fibers of the divisors E_0 to E_4 are given by

$$Q_{\mathbb{Z}_2} \cdot (\mathbb{P}_0^1, \, \mathbb{P}_1^1, \, \mathbb{P}_2^1, \, \mathbb{P}_3^1, \, \mathbb{P}_4^1, \,) = (10, 0, 0, 0, 0) \tag{4.6.26}$$

and thus vanish modulo 2×5, as demanded. Hence, $Q_{\mathbb{Z}_2}$ is a candidate to calculate a $\mathbb{Z}_2$-charge of the matter states. To see this we calculate the intersection of $Q_{\mathbb{Z}_2}$ with the two fibral $\mathbb{P}^1$s over the $\mathbf{10}$-curve defined in (4.6.7) associated with the $\bar{\mathbf{10}}$ and $\mathbf{10}$ representation,

$$Q_{\mathbb{Z}_2} \cdot (\mathbb{P}_{e_0 = e_2 = 0}^1, \mathbb{P}_{e_0 = e_1 + b_2 e_3 = 0}^1) = (2, 8) = (2, -2), \quad \mathrm{mod} \quad 10 \,, \tag{4.6.27}$$

its intersection with anti-fundamental and fundamental fibral $\mathbb{P}^1$s over the $\mathbf{5}_A$-curve,

$$Q_{\mathbb{Z}_2} \cdot (\mathbb{P}_{e_3 = b_1 w + c_1 u^2 e_4 = 0}^1, \, \mathbb{P}_{e_3 = b_1(b_1 u v + w e_2 + b_0 u^2 e_2 e_4) - c_1 u^2 e_2 e_4 = 0}^1) = (1, -1) \,, \tag{4.6.28}$$

the corresponding intersections with the fiber over the $\mathbf{5}_B$-curve,

$$Q_{\mathbb{Z}_2} \cdot (\mathbb{P}^1_{e_1 = b_1 u + b_2 e_2 = 0}, \; \mathbb{P}^1_{e_1 = b_1(b_1 w + c_2 u e_0 + c_3 e_0 e_2) - b_2 c_2 e_0 e_2 = 0}) = (-4, \, 4) \,, \tag{4.6.29}$$

as well as the charges of the states over the singlet curve,

$$Q_{\mathbb{Z}_2} \cdot (\mathbb{P}^1_+, \; \mathbb{P}^1_-) = (5, \, 5) = (-5, \, 5) \quad \text{mod} \quad 10 \,. \tag{4.6.30}$$

As explained in appendix B.1, these charges generate at first sight a $\mathbb{Z}_{10}$ symmetry, which however contains the center of $SU(5)$. To determine the actual discrete symmetry group realised in addition to the non-abelian $SU(5)$ we must correctly divide out this center. Following appendix B.1, we can shift the discrete charges of the fundamentals and antisymmetric states by $2\,n$ and $4\,n$ with $n \in \mathbb{Z}$, respectively, to find a canonical representative of $\mathbb{Z}_{10}/\mathbb{Z}_5$. Choosing $n = -2$ gives

$$\begin{aligned} (\bar{\mathbf{10}}, \mathbf{10}) &: \; (10, -10) = (0, 0) \quad \text{mod} \quad 10 \,, \\ (\bar{\mathbf{5}}_A, \mathbf{5}_A) &: \; (5, -5) \qquad (\bar{\mathbf{5}}_B, \mathbf{5}_B) : (0, 0). \end{aligned} \tag{4.6.31}$$

Recaling these charges by the inverse of the factor relating (4.6.24) and (4.6.25) gives us the co-prime $\mathbb{Z}_2$-charges of the canonical representative of $\mathbb{Z}_{10}/\mathbb{Z}_5$.

Hence, $Q_{\mathbb{Z}_2}$ gives, as expected, well defined $\mathbb{Z}_2$-charges. In the sequel we will denote the $\mathbb{Z}_2$ charges by a superscript (to distinguish them from the $U(1)$ charges prior to Higgsing). The massless spectrum thus consists of the fields $\mathbf{10}^{(0)}$, $\mathbf{5}_A^{(1)}$, $\mathbf{5}_B^{(0)}$ plus conjugates and the singlet $\mathbf{1}^{(1)}$, see Figure 5.1.

Yukawa points

There is only one type of intersection points $W \cap \{b_1 = 0\} \cap \{c_1 = 0\}$ between the $\mathbf{10}^{(0)}$-curve and the fundamental A-curve. Here the fiber takes the form of an affine $SO(12)$ Dynkin diagram. From the fiber topology the coupling $\mathbf{10}^{(0)} \bar{\mathbf{5}}_A^{(1)} \bar{\mathbf{5}}_A^{(1)} + c.c.$ together is deduced. Clearly this is invariant under the assigned $\mathbb{Z}_2$ charges.

By contrast, the fundamental B-curve intersects the $\mathbf{10}^{(0)}$-curve at *two* types of Yukawa points. At $W \cap \{b_1 = 0\} \cap \{b_2 = 0\}$ the fiber takes again the form of an affine $SO(12)$ Dynkin diagram. The Yukawa coupling here is the $\mathbf{10}^{(0)} \bar{\mathbf{5}}_B^{(0)} \bar{\mathbf{5}}_B^{(0)} + c.c.$. At $W \cap \{b_1 = 0\} \cap \{c_2 = 0\}$ the fiber $\mathbb{P}^1$s intersect in the form of the non-affine E_6 Dynkin diagram. As we approach the points $W \cap \{b_1 = 0\} \cap \{c_2 = 0\}$ along the $\mathbf{10}^{(0)}$-curve, the following splitting occurs:

$$\begin{aligned} \mathbb{P}^1_{e_2 = c_1 e_0 e_1 + c_2 e_3 = 0} &\rightarrow & \mathbb{P}^1_{e_2 = e_0 = 0} &+ & \mathbb{P}^1_{e_2 = e_1 = 0} \,, \\ (0, -1, 0, 1) &\rightarrow & (1, -1, 0, 1) &+ & (-1, 0, 0, 0) \,, \\ \mathbf{10} &\rightarrow & \bar{\mathbf{10}} &+ & \bar{\mathbf{5}}_B \,. \end{aligned} \tag{4.6.32}$$

Following the logic of [60] this gives a $\mathbf{10}^{(0)} \mathbf{10}^{(0)} \mathbf{5}_B^{(0)} + c.c.$ Yukawa coupling.

The intersection locus of the singlet locus C with the fundamental matter curves can be shown to take the form $\mathcal{C}_{\mathbf{5}_A^{(1)}} \cap \mathcal{C}_{\mathbf{5}_B^{(0)}} \cap \{b_0 b_2^2 c_1 c_2 - b_1^2 b_2 c_0 c_3 - b_2 c_1^2 c_3 + b_1^3 c_0 c_4 + b_1 c_1^2 c_4\}$ by using the prime ideal decomposition. It may be checked that this is a codimension three point lying in the GUT divisor. Consistently, the fiber over these points degenerates to form an $SU(7)$ Dynkin diagram. This indicates a Yukawa coupling $\mathbf{5}_A^{(1)} \bar{\mathbf{5}}_B^{(0)} \mathbf{1}^{(1)}$.

4.6.3 Interpretation

The observed structure of matter curves and Yukawa interactions is indeed consistent not only with the appearance of a discrete $\mathbb{Z}_2$ selection rule for the $SU(5)$ model of section 4.6.2, but in particular also with the interpretation of this selection rule precisely as the discrete remnant of the $U(1)$ gauge group realised in the $SU(5) \times U(1)$ fibration of section 4.6.1 upon Higgsing along the $\mathbf{1}_{10}$ state. The $\mathbb{Z}_2$ selection rule manifests itself in the appearance of two distinct fundamental matter curves $\mathcal{C}_{\mathbf{5}_A^{(1)}}$ and $\mathcal{C}_{\mathbf{5}_B^{(0)}}$ and the fact that the corresponding states enjoy different couplings: After all, while the coupling $\mathbf{10}^{(0)}\,\mathbf{10}^{(0)}\,\mathbf{5}_B^{(0)} + c.c.$ is realised, an analogous coupling of the form $\mathbf{10}^{(0)}\,\mathbf{10}^{(0)}\,\mathbf{5}_A^{(1)} + c.c.$ is absent from the geometry even though this coupling would be allowed on the basis of the $SU(5)$ symmetry. This and the structure of the remaining Yukawas is consistent with our $\mathbb{Z}_2$ charge assignments.

Moreover, comparing the $SU(5) \times U(1)$ and the $SU(5) \times \mathbb{Z}_2$ models, the curve $\mathcal{C}_{\mathbf{5}_B^{(0)}}$ is the result of recombining the matter curves $\mathcal{C}_{\mathbf{5}_4}$ and $\mathcal{C}_{\mathbf{5}_{-6}}$ upon Higgsing the $\mathbf{1}_{10}$ states, while the curve $\mathcal{C}_{\mathbf{5}_A^{(1)}}$ and $\mathcal{C}_{\mathbf{5}_3}$ are to be identified. Geometrically, if we un-Higgs the $\mathbb{Z}_2$ to $U(1)$ by setting $c_4 = 0$, the curve $\mathcal{C}_{\mathbf{5}_B^{(0)}}$ splits into $\mathcal{C}_{\mathbf{5}_4}$ and $\mathcal{C}_{\mathbf{5}_{-6}}$. The recombination of the two curves upon Higgsing is possible due to the existence of the Yukawa coupling $\mathbf{5}_{-6}\bar{\mathbf{5}}_{-4}\mathbf{1}_{10} + c.c.$. As $\mathbf{1}_{10}$ develops a VEV, a holomorphic off-diagonal mass term for the fields $\mathbf{5}_{-6} + c.c.$ and $\mathbf{5}_4 + c.c.$ is induced such that only a single type of fundamental fields along the recombined locus remains.

Note that naively it might seem that due to the normalization of the $U(1)$ charges in presence of $SU(5)$ charged matter, the remnant discrete selection rule upon Higgsing the singlet field $\mathbf{1}_{10}$ is $\mathbb{Z}_{10}$ and not $\mathbb{Z}_2$. However, a $\mathbb{Z}_5$ subgroup thereof is already accounted for by the center $\mathbb{Z}_5$ of the non-abelian $SU(5)$. In conclusion only an extra $\mathbb{Z}_2$ selection rule remains in addition to the selection rules due to the $SU(5)$ gauge symmetry. The details of the embedding of the center group and how things can change if we go to other gauge groups in the A-series, we refer the reader to appendix B.1.

4.7 R-parity by Higgsing a $U(1)$ in F-theory

As a second example we present, in this section, an $SU(5) \times \mathbb{Z}_2$ GUT model in which the discrete symmetry can be identified with R-parity. In this realisation of the non-abelian gauge symmetry the matter spectrum has different charges under the discrete group. We will see that the spectrum in this model agrees with the embedding of the MSSM with R-parity into the $SU(5)$ GUT model. The model we study here is related via Higgsing to the $SU(5) \times U(1)$ model which has been constructed as top 4 over polygon 6 in [83]. The hypersurface equation of this resolved $SU(5) \times U(1)$ fibration takes the form

$$
\begin{aligned}
& w^2 s e_2 e_3^2 e_4 + b_0 s^2 u^2 w e_0 e_3 e_4 + b_1 s u v w + b_2 v^2 w e_1 e_2 \\
& + c_0 s^3 u^4 e_0^3 e_1 e_3 e_4^2 + c_1 s^2 u^3 v e_0^2 e_1 e_4 + c_2 s u^2 v^2 e_0^2 e_1^2 e_2 e_4 + c_3 u v^3 e_0^2 e_1^3 e_2^2 e_4 = 0 \,.
\end{aligned}
\tag{4.7.1}
$$

The Shioda map of the extra section is

$$
W = 5(S - U - \bar{\mathcal{K}} - [b_2]) + \sum m_i E_i \,, \quad m_i = (2, 4, 6, 3) \,.
\tag{4.7.2}
$$

Since the analysis of the charged matter representations and Yukawa couplings for this model has been performed in [83], we merely restate the results here. Along $W \cap \{b_1 = 0\}$ the antisymmetric $\mathbf{10}_{-1}$ is found. In addition, there are three fundamental matter curves. At $W \cap \{b_2 = 0\}$ the states in the $\mathbf{5}_7 + c.c.$ are located. Along $W \cap \{b_1 c_0 - b_0 c_1 = 0\}$ the $\mathbf{5}_2 + c.c.$ states are found and over the curve $W \cap \{b_2^2 c_1 + b_1 c_2 - b_1^2 c_3 = 0\}$ $\mathbf{5}_{-3} + c.c.$ matter is localised.

There are two types of codimension-three enhancement points giving rise to Yukawa couplings among the $SU(5)$ charged matter. At $W \cap \{b_1 = 0\} \cap \{b_0 = 0\}$ the coupling $\mathbf{10}_{-1}\,\mathbf{10}_{-1}\,\mathbf{5}_2 + c.c.$ is
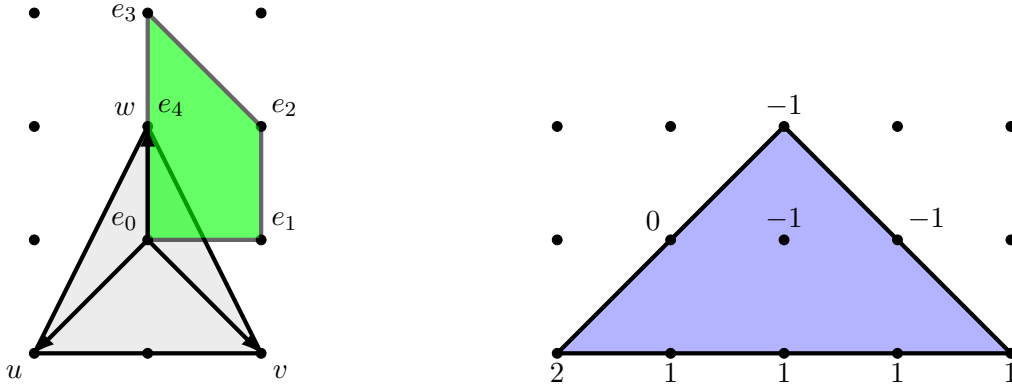
Figure 4.12: $SU(5)$ top over polygon 4 of [19] together with its dual polygon, bounded below by the values z_{min}, shown next to the nodes.
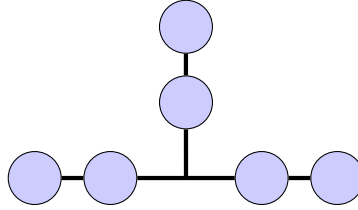
Figure 4.13: fiber topology at the Yukawa point $W \cap \{b_0 = 0\} \cap \{b_1 = 0\}$.

located, and at $W \cap \{b_1 = 0\} \cap \{c_1 = 0\}$ the $\bar{\mathbf{10}}_1 \, \mathbf{5}_{-3} \, \mathbf{5}_2 + c.c.$ is found. There is also a non-flat point at $W \cap \{b_1 = 0\} \cap \{b_2 = 0\}$. The presence of this point has no effect on the following discussion. By an appropriate choice of the base for the fibration this point can be forbidden. In addition, all Yukawa couplings involving the singlets allowed by the $SU(5) \times U(1)$ gauge symmetry are indeed realised, specifically $\mathbf{1}_{-10} \, \mathbf{5}_7 \, \bar{\mathbf{5}}_3$, $\mathbf{1}_{-5} \, \mathbf{5}_7 \, \bar{\mathbf{5}}_{-2}$, $\mathbf{1}_5 \, \mathbf{5}_{-3} \, \bar{\mathbf{5}}_{-2}$ and of course $\mathbf{1}_{10} \, \mathbf{1}_{-5} \, \mathbf{1}_{-5}$, plus their conjugates.

Giving a vacuum expectation value to the states in the $\mathbf{1}_{\pm 10}$ representation breaks the $U(1)$ symmetry again to a remnant $\mathbb{Z}_2$. The Higgsed model is described by the first top over polygon 4, denoted $\tau_{4,1}$ in [20], which gives for the hypersurface equation of the fourfold the following polynomial:

$$
\begin{aligned}
& w^2 e_2 e_3^2 e_4 + b_0 u^2 w e_0 e_3 e_4 + b_1 uvw + b_2 v^2 w e_1 e_2 \\
& + c_0 u^4 e_0^3 e_1 e_3 e_4^2 + c_1 u^3 v e_0^2 e_1 e_4 + c_2 u^2 v^2 e_0^2 e_1^2 e_2 e_4 + c_3 uv^3 e_0^2 e_1^3 e_2^2 e_4 + c_4 v^4 e_0^2 e_1^4 e_2^3 e_4 = 0.
\end{aligned}
\tag{4.7.3}
$$

From the class U of the bi-section we construct the divisor

$$
Q_{\mathbb{Z}_2} = 5w_{\mathbb{Z}_2} + 2E_1 + 4E_2 + 6E_3 + 3E_4, \qquad w_{\mathbb{Z}_2} = U - [b_2] + \bar{\mathcal{K}}, \tag{4.7.4}
$$

which has intersection number zero (modulo ten) with all fiber components in codimension one such that the roots are uncharged under the $\mathbb{Z}_2$ generator.

Along the GUT divisor W we now find only three, as opposed to four, matter curves. At $W \cap \{b_1 = 0\}$ the enhancement is of $SO(10)$ type, and by computing the intersection numbers of the split curves with the exceptional divisors E_i we find weights of the anti-symmetric representation. Computing also the $\mathbb{Z}_2$ charges, which we denote again by a superscript, gives states in the $\mathbf{10}^{(1)}$ and $\bar{\mathbf{10}}^{(1)}$.

Along the two curves at which the fundamental representations are localised the enhancement type is $SU(6)$. Along $W \cap \{b_1 c_0 - b_0 c_1 = 0\}$ we find states in the $\mathbf{5}^{(0)} + c.c.$ These are the only invariant states under the action of $\mathbb{Z}_2$. Along the last matter curve $W \cap \{b_1 b_2^2 c_2 - b_1^2 b_2 c_3 + b_1^3 c_4 - c_1 b_2^3 = 0\}$ there is a $\mathbf{5}^{(1)} + c.c.$

There are altogether three types of enhancement points in codimension three. At $W \cap \{b_0 = 0\} \cap \{b_1 = 0\}$ the $\mathbf{10}_1$- and the $\mathbf{5}_0$- curve intersect. Here the fiber topology is of non-standard, E_6-like, form where the three inner nodes all intersect in one point, see Figure 4.13. At this point the coupling $\mathbf{10}^{(1)} \mathbf{10}^{(1)} \mathbf{5}^{(0)} + c.c.$ is localized. The second Yukawa coupling is found at $W \cap \{b_1 = 0\} \cap \{c_1 = 0\}$, which is a point of $SO(12)$ enhancement. This is where all the three $SU(5)$-charged matter curves meet, and we confirm the coupling $\overline{\mathbf{10}}^{(1)} \mathbf{5}^{(0)} \mathbf{5}^{(1)} + c.c.$ from the fiber topology. Finally, the two distinct $\mathbf{5}$-curves intersect at the point $\mathcal{C}_{\mathbf{5}^{(0)}} \cap \mathcal{C}_{\mathbf{5}^{(1)}} \cap \{b_2^3 c_0 - b_0 b_2^2 c_2 + b_0 b_1 b_2 c_3 - b_0 b_1^2 c_4 = 0\}$. This is computed as the prime ideal decomposition of the intersection of the singlet locus at W with the fundamental matter curves. Here the Yukawa coupling $\mathbf{1}^{(1)} \mathbf{5}^{(0)} \bar{\mathbf{5}}^{(1)} + c.c.$ arises. Note that at the point $W \cap \{b_1 = 0\} \cap \{b_2 = 0\}$ the fiber is again non-flat, and this point must be absent in order for the fibration to give rise to a well-defined F-theory compactification. This can be achieved by choosing a base space $\mathcal{B}$ with specific intersection properties.

The interpretation of this spectrum and the interactions is again consistent with the origin of the $\mathbb{Z}_2$ as a discrete subgroup of the Higgsed $U(1)$. The Higgsing recombines the curves with states $\mathbf{5}_7$ and $\mathbf{5}_{-3}$, which couple to the Higgs field via the Yukawa $\mathbf{1}_{-10} \mathbf{5}_7 \bar{\mathbf{5}}_3$, into a single curve with states of $\mathbb{Z}_2$-charge 1. This is evident by noting that this latter curve factorises accordingly as we un-Higgs the $U(1)$ by setting $c_4 = 0$. All other curves are unaffected (since they do not couple to the Higgs field) and the $\mathbb{Z}_2$ charges of the states after the transition equal the former $U(1)$ charges mod 2. The realised Yukawa couplings respect this $\mathbb{Z}_2$ symmetry and are related to the Yukawa couplings in the $SU(5) \times U(1)$-model as expected upon Higgsing.

Interestingly, the $\mathbb{Z}_2$ selection rule realised in this $SU(5)$ GUT model coincides precisely with matter R-parity: The only field with trivial $\mathbb{Z}_2$ charge is the $\mathbf{5}^{(0)} + c.c.$, which is consequently identified with $\mathbf{5}_{H^u} + \bar{\mathbf{5}}_{H^d}$ field. The non-trivial representations under $\mathbb{Z}_2$ are taken as the GUT matter representations, in particular the $\bar{\mathbf{5}}^{(1)}$ is identified with $\bar{\mathbf{5}}_m$ and the singlet $\mathbf{1}^{(1)}$ corresponds to the right-handed neutrino. The singlet coupling $\mathbf{1}^{(1)} \mathbf{5}^{(0)} \bar{\mathbf{5}}^{(1)}$ thus describes a Dirac mass for the right-handed neutrinos.

4.8 Summary

In this chapter we have studied the realisation of discrete gauge symmetries in F-theory compactifications to four dimensions via Higgsing. In the setup we have considered, a discrete $\mathbb{Z}_2$ symmetry originates as the remnant of a $U(1)$ gauge symmetry upon Higgsing the latter by a field of charge 2. This amounts to a deformation [84] of the generic elliptic fibration with two sections [18] into a bi-section fibration [29]. We have studied this process in detail focusing on aspects which are new to four-dimensional compactifications and in the presence of an additional non-abelian gauge group. We have shown that the Higgsing induces matter curve recombination, and that the resulting curves can be associated a $\mathbb{Z}_2$ charge through a generalisation of the Shioda map for multi-sections. We have further shown that the induced $\mathbb{Z}_2$ charge implies a selection rule on Yukawa couplings which leads to couplings being absent in the geometry even without a $U(1)$ symmetry forbidding them. This is the first implementation of these aspects of discrete symmetries in a semi-realistic F-theory compactification. In particular we have presented an $SU(5)$ model with $\mathbb{Z}_2$ charge assignments which are equivalent to R-parity in the MSSM. It would be very interesting to apply this technology to induce other phenomenologically desirable discrete symmetries.

We have shown an explicit map between a three-dimensional field theory description of the Higgsing and the geometry. This involves an interesting interplay between the Coulomb branch and Kaluza-Klein modes. Further, we have been able to calculate the mixing of the three-dimensional Kaluza-Klein gauge field with the $U(1)$ field by calculating the charges of the Higgsed state. Importantly there are two different M-theory compactifications, or M-theory phases associated with a genus-one fibration

with a bisection. They can be seen as two different blow-downs of the smooth geometry. This is expected to hold generally, in that n different M-theory vacua arise from a four-dimensional Higgs field of charge n. They are associated to Higgsing n different KK modes in the compactification on a circle. The corresponding geometric point of view is that the existence of n vacua correspond to n different blow-downs. We highlight that these vacua are really physically distinct and do not correspond to a different formulation of the same physics.

From the F-theory perspective a $\mathbb{Z}_n$ discrete symmetry is associated with the n isomorphism classes of inequivalent genus-one fibrations with the same Jacobian. These form the Tate-Shafarevich group, of which the Jacobian represents the trivial element. For simplicity we have studied the $n = 2$ case in this work, where there are two different fibrations; P_2 and P_W. The smooth $\mathbb{P}_{112}[4]$-fibration P_2 and its singular Jacobian fibration P_W in Weierstrass form [29]. Compactifications on P_2 have been studied in quite some detail recently in [10, 29, 70, 84, 101, 117].

We have showed in detail how compactification of M-theory on P_2 gives rise to a fibral $U(1)$ gauge symmetry and discussed how this symmetry is lifted to a $\mathbb{Z}_2$ symmetry in the F-theory limit. By contrast, M-theory on P_W yields fibral gauge group $U(1) \times \mathbb{Z}_2$, of which only the $\mathbb{Z}_2$ part survives in the F-theory limit. Consistently with field theoretic expectations based on the different M-theory compactifications on P_2 and P_W, it is only on P_W that torsional homology arises. We have explicitly identified $\mathbb{Z}_2$ torsional 2- and 3-cycles by analyzing a birational blowup-up of P_W. On P_2, on the other hand, torsional homology appears only in the formal sense of a $\mathbb{Z}_2$ torsional fibral 2-cycle *modulo the fiber class*. It would be interesting to explicitly generalize our analysis of the appearance of torsion to fibrations which give rise to higher discrete symmetry groups.

Finally we note that fibrations with Mordell-Weil $\mathbb{Z}_n$ torsion, treated in chapter 3 and fibrations with n-sections are interchanged by mirror symmetry in the fiber [70]. This is observed for the 16 hypersurface representations of tori, where the dual reflexive polygon with $\mathbb{Z}_n$ Mordell-Weil torsion has a $\mathbb{Z}_n$ discrete symmetry group in F-theory. This suggests an intriguing connection between the Tate-Shafarevich group underlying discrete symmetries and the torsion component of the Mordell-Weil group of rational sections, which would be exciting to further study in more detail.

Chapter 5

Gauge fluxes on genus-one fibrations

The discovery that F-theory can be consistently compactified not only on elliptic fibrations but also on genus-one fibrations has significantly enlarged the set of plausible geometries for F-theory models. In the previous chapter we have given a detailed account for the relation between the fiber structure, the duality between F-theory and M-theory and the origin of discrete symmetry in compactifications on genus-one fibrations. The natural next step in the study of F-theory backgrounds without zero section is the inclusion of G_4 flux. As mentioned in section 2.6 the G_4 flux in F-theory unifies the closed string fluxes and the gauge fluxes from the open string sector. In this chapter we will focus on fluxes corresponding to the gauge sector. The study of such fluxes has received a lot of attention in recent F-theory literature, including [31, 46, 47, 59–63, 83, 88, 89, 93, 95, 99, 127–133].

Extending the study of G_4 flux to genus-one compactifications was initiated in [10] by the author and collaborators, followed up by the work [12] on which this chapter is based. In particular we present the explicit examples and calculations from [12]. We discuss in the following which consistent flux solutions that can be turned on in a F-theory model with discrete symmetry. Furthermore we show how to systemize the search for all gauge fluxes in multi-section fibrations as well as elliptic fibrations.

The first question to answer is how to generalise the transversality conditions that ensure a correct uplift from M-theory in three dimensions to the four dimensional F-theory compactification. In section 5.1 we will show how the standard transversality condition is to be modified. The zero-section in (2.6.6) provides an embedding of the base $\mathcal{B}$ into the fibration X while an n-section on the other hand is an embedding of an n-fold cover of $\mathcal{B}$. The essential solution is that the zero section is to be replaced by the n-section in the transversality conditions. This relies on the correct identification of a Kaluza-Klein $U(1)$ associated with the multi-section, as discussed in depth in the previous chapter. In general the divisor class of the embedding multi-section must be corrected such as to single out the KK $U(1)$ relative to the Cartan $U(1)$'s of any additional non-abelian gauge group. The details of this solution are presented in section 5.1 which extends the introduction to F-theory flux in section 2.6. In the subsequent sections our proposal for the generalised consistency conditions is subjected to a number of non-trivial tests.

In section 5.2 we use the generalised transversality conditions to construct all vertical flux solutions for a bisection fibration with F-theory gauge group $SU(5) \times \mathbb{Z}_2$. Here we review the model from section 4.6.2 [10] and use it as an explicit example background. Throughout this chapter we take the fibration to be defined over a generic base space $\mathcal{B}$. This implies that our general solution is spanned by those fluxes that are guaranteed to exist in the fibration for any choice of the base manifold. We show also, in section 5.2.3, that the basis for the vertical fluxes can be written in terms of the $SU(5)$ matter surfaces i.e the 4-cycles given by fibering the split curves in the fiber over the matter loci in the base. In addition we study a certain non-vertical flux which is directly linked to the existence of the

bisection and which turns out to be crucial for a consistent conifold transition. For this set of fluxes we compute the chiral indices of all matter representations in full generality and show that the fluxes that satisfy the generalised transversality condition do not induce any $SU(5)$ anomaly. This serves as a first non-trivial check of our proposal.

Further consistency checks can be obtained from the conifold transition to the model with $SU(5) \times U(1)$ gauge group. In the general setting one expect the gauge fluxes on both sides of the transition to be related such that the induced $D3$ charge and the chiral indices do not change. Therefore we construct also all vertical gauge fluxes in the elliptic $SU(5) \times U(1)$ model in section 5.3. We use the same methods as in the $SU(5) \times \mathbb{Z}_2$ geometry and since the fibration has a zero section the well established standard transversality conditions apply. Under the conifold transition a matching relation between the two sets of fluxes is found which leaves the $D3$ tadpole and the chiral spectrum invariant. This constitutes another consistency check of the flux construction. This kind of matching over the conifold transition has been demonstrated before [59, 89] in the transition between the $SU(5) \times U(1)$ restricted Tate model to a generic $SU(5)$ Tate model.

In the last part of this chapter, in section 5.4, we address two subtle and related issues, the flux quantization condition and the cancellation of discrete gauge anomalies. For the explicit $SU(5) \times \mathbb{Z}_2$ and $SU(5) \times U(1)$ fibrations under consideration the quantization condition can be cast in terms of intersection number of base divisors. In order to have integral chiral indices this amounts to arithmetic constraints on these intersection numbers. These constraints ensure that that the term $\frac{1}{2}c_2(M_4)$ from the quantization condition integrate to an integer on all matter surfaces. We conjecture here that this constraint is satisfied when the considered fibrations are smooth. Furthermore, by assuming that this holds and with our proposed transversality condition, this implies the cancellation of the discrete gauge anomalies associated with the $\mathbb{Z}_2$ symmetry. For the genus-one fibration considered this discrete anomaly must vanish [103, 134] because the discrete symmetry is non-perturbatively exacvt [43, 135]. This provides the final non-trivial test of our construction.

5.1   The transversality condition for fluxes on genus-one fibrations

In this section we propose a generalization of the well-known transversality conditions on G_4-fluxes on elliptic fibrations to fibrations with a multi-section only. The standard consistency conditions were reviewed in section 2.6 and the importance of the divisor class corresponding to the Kaluza-Klein $U(1)$ in three dimensions was stressed. Here we present our proposal for a modified notion of transversality for gauge fluxes in F-theory compactifications without section. The aim will thus be to find a substitute for the zero-section, and re-analyse the lift from M-theory to F-theory. Our construction will apply to a general genus-one fibration X_4 with projection

$$\pi : X_4 \to \mathcal{B} \tag{5.1.1}$$

onto a generic 3-dimensional base space $\mathcal{B}$. The n-section of the fibration is a multi-valued map assigning to each point in the base locally n-points in the fiber which are globally exchanged by monodromies. This defines an n-fold branched cover $\mu_n(\mathcal{B})$ of the base $\mathcal{B}$ inside X_4 together with an embedding

$$\iota_\mu : \mu_n(\mathcal{B}) \hookrightarrow X_4. \tag{5.1.2}$$

We will denote by N the divisor class of the n-section. Recall that in the absence of a zero section the multi-section defines a KK U(1) in three dimensions [10, 11, 101, 117]. The expansion of the M-theory C_3 field will hence contain the term $A_{KK} \wedge N$. The KK $U(1)$ specifies the lift from three to four

dimensions in the F-theory limit and thus transversality of the flux is to be taken with respect to the class N. In terms of the multi-section as an embedding we have that

$$\int_{X_4} G_4 \wedge N \wedge \pi^{-1}D_a = \int_{\mu_n(\mathcal{B})} \iota_n^*(G_4 \wedge \pi^{-1}D_a) \tag{5.1.3}$$

and by comparing to (2.6.6) we see that the analogue condition is

$$\int_{X_4} G_4 \wedge N \wedge \pi^{-1}D_a \stackrel{!}{=} 0. \tag{5.1.4}$$

This guarantees that net flux vanishes through any 4-cycle in $\mathcal{B}$ and thus have zero legs in the fiber. The second condition (2.6.7) must still hold and do not change when considering a genus-one fibration. Bacause the multi-section still defines the notion of a KK $U(1)$ this condition ensures that all elements of the KK tower should have the same chiral index, exactly as in the case of an elliptic fibration.

In general the n-section intersects more than one of the irreducible curves in the Kodaira fiber over a divisor with non-abelian gauge group. This implies that the Cartan fluxes associated with the resolution divisors do not satisfy (5.1.4) in general. One may however construct a linear combination

$$\hat{N} = N + \sum_i a_i E_i \tag{5.1.5}$$

of the the class N and the resolution divisors such that the modified condition

$$\int_{X_4} G_4 \wedge \hat{N} \wedge \pi^{-1}D_a = 0 \tag{5.1.6}$$

is satisfied for all Cartan fluxes $G_4 = E_i \wedge \pi^{-1}F$ and an arbitrary class $F \in H^{1,1}(\mathcal{B})$. Using $\hat{N}$ instead of N amounts to a redefinition of the KK $U(1)$ symmetry such that it does not mix with the Cartan $U(1)$ generators E_i associated with the resolution divisors of the non-abelian singularity. In the case of an elliptic fibration this complication do not arise, as the zero section intersects the affine node of the Kodaira fiber, and thus the Cartan fluxes satisfy (2.6.6) automatically. A similar redefinition has been discussed in a different context in [51].

We conclude this section by outlining the method used in the next section. To construct a transversal flux on a genus-one fibration we single out the n-section class N and determine the shifted class $\hat{N} = N + \sum_i a_i E_i$ such that

$$\int_{X_4} E_i \wedge \hat{N} \wedge \pi^{-1}D_a \wedge \pi^{-1}D_a = 0 \qquad \forall\, D_a, D_b \subset \mathcal{B} \tag{5.1.7}$$

for all resolution divisors E_i. This $\hat{N}$ defines the KK $U(1)$ in the reduction of the 4-dimensional F-theory vacuum to three dimensions and does not mix with the Cartan generators E_i. The transversality conditions on the fluxes are then

$$\int_{X_4} G_4 \wedge \hat{N} \wedge \pi^{-1}D_a \stackrel{!}{=} 0, \tag{5.1.8}$$

$$\int_{X_4} G_4 \wedge \pi^{-1}D_a \wedge \pi^{-1}D_b \stackrel{!}{=} 0. \tag{5.1.9}$$

Furthermore, to preserve the non-abelian gauge symmetries we demand in addition

$$\int_{X_4} G_4 \wedge E_i \wedge \pi^{-1}D_a \stackrel{!}{=} 0. \tag{5.1.10}$$

Here we note that for any flux that satisfy the equations (5.1.10) the first transversality condition in (5.1.8) reduces to the same constraint with $\hat{N}$ replaced by the n-section class N. We will see that this simplifies the calculations, but obscures the fact that $\hat{N}$ is the divisor class identified with the Kaluza-Klein $U(1)$.

5.2   Fluxes on a genus-one fibration with a bisection

We will here briefly review the $\mathbb{P}_{112}[4]$-fibration with gauge group $SU(5) \times \mathbb{Z}_2$ from section 4.6.2. This geometry has all the features needed to test the construction presented in the previous section. The 4-fold X_4 is given by the hypersurface equation

$$P_{\mathbb{Z}_2}^{SU(5)} = e_1 e_2 w^2 + b_{0,2} u^2 w e_0^2 e_1^2 e_2 e_4 + b_1 uvw + b_2 v^2 w e_2 e_3^2 e_4$$
$$+ c_{0,4} u^4 e_0^4 e_1^3 e_2 e_4^2 + c_{1,2} u^3 v e_0^2 e_1 e_4 + c_{2,1} u^2 v^2 e_0 e_3 e_4 + c_{3,1} uv^3 e_0 e_2 e_3^3 e_4^2 + c_{4,1} v^4 e_0 e_2^2 e_3^5 e_4^3$$
(5.2.1)

in the toric ambient space specified in the appendix table B.3.1. The fiber coordinates $[u : v : w]$ are as before homogeneous coordinates of $\mathbb{P}_{1,1,2}$. An $SU(5)$ singularity sits in the fiber over the divisor $\Theta : \{\theta = 0\}$ in $\mathcal{B}$. The hypersurface equation is the proper transform under the resolution of this singularity, with blow-up coordinates e_i, $i = 1, \ldots, 4$ and with e_0 the proper transform of θ. The Calabi-Yau hypersurface comes with the choice of a line bundle on $\mathcal{B}$ with first Chern class $[b_2]$. Given this line bundle on $\mathcal{B}$ the coefficients b_i and c_j transform as sections of the bundles displayed in table 5.2.1, where $\bar{\mathcal{K}}$ is the anti-canonical bundle on the base.

$b_{0,2}$	b_1	b_2	$c_{0,4}$	$c_{1,2}$	$c_{2,1}$	$c_{3,1}$	$c_{4,1}$
$2\bar{\mathcal{K}} - b_2 - 2\Theta$	$\bar{\mathcal{K}}$	b_2	$4\bar{\mathcal{K}} - 2b_2 - 4\Theta$	$3\bar{\mathcal{K}} - b_2 - 2\Theta$	$2\bar{\mathcal{K}} - \Theta$	$\bar{\mathcal{K}} + b_2 - \Theta$	$2b_2 - \Theta$

Table 5.2.1: Classes of the coefficients entering (4.6.13).

The smooth geometry is constructed via a top [19,82], denoted $\tau_{4,3}$ in [20], and the exceptional divisors are $E_i : \{e_i = 0\}$, $i = 1, \ldots, 4$. Furthermore $E_0 = \Theta - \sum_i E_i$. The Stanley-Reisner ideal for our choice of resolution phase is generated by

$$\text{SR-i:} \quad \{v\,e_0,\ v\,e_1,\ v\,e_2,\ w\,e_0,\ w\,e_4,\ u\,e_3,\ e_0\,e_3,\ e_1\,e_3,\ u\,e_2,\ e_1\,e_4,\ v\,w\,u\}. \quad (5.2.2)$$

The intersection of the ambient divisor $U : \{u = 0\}$ with the hypersurface gives a representative of the homology class of the bisection, which intersects each generic fiber in two points exchanged globally by a monodromy. From our previous discussion we would like to associate with U the notion of a KK $U(1)$ in the 3-dimensional M-theory compactification on X_4. It is here that the shift (5.1.5) becomes important because the bisection locally intersects both E_0 and E_1 in one point in the fiber. The (up to normalization) unique solution to the constraints (5.1.7) is given by

$$\hat{U} = U + \frac{1}{5}(4E_1 + 3E_2 + 2E_3 + E_4). \quad (5.2.3)$$

If we fix the (a priori arbitrary) overall normalization such as to achieve integer intersections with all fibral curves by defining

$$\text{w}_{\mathbb{Z}_2} = 5\,\hat{U}, \quad (5.2.4)$$

then the intersection numbers of $\text{w}_{\mathbb{Z}_2}$ with the irreducible split fiber components consistently assign $\mathbb{Z}_2$ charges to the corresponding states modulo 2 in the F-theory limit. Indeed, a $\mathbb{Z}_2$ subgroup of the KK $U(1)$, normalised as in (5.2.4), survives in the F-theory limit as an independent discrete gauge group which we saw in the previous chapter.[1] The discriminant of the hypersurface equation takes the form

$$\Delta \sim \theta^5 [b_1^4 (b_1^2 c_{0,4} - b_0 b_1 c_{1,2} + c_{1,2}^2)(b_2^2 c_{2,1} - b_1 b_2 c_{3,1} + b_1^4 c_{4,1}) + \mathcal{O}(\theta)], \quad (5.2.5)$$

---

[1]Apart from an extra shift in terms of base divisors this agrees with the $\mathbb{Z}_2$ generator as presented in previous chapter (also [10, 70, 101]). This shift does not change the notion of fibral curves and is therefore not of importance for us.
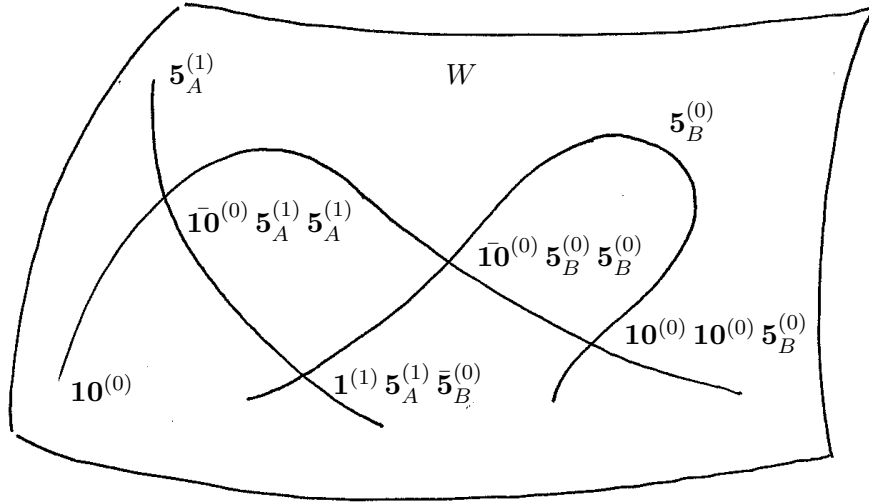
Figure 5.1: The matter curves on the $SU(5)$ divisor $\{\theta = 0\}$ and the Yukawa couplings involving the $SU(5)$ charged matter in codimension three.

which indicates three matter curves on the $SU(5)$ divisor Θ. Away from Θ there is one more matter locus [29], describable as an ideal which defines an irreducible curve on $\mathcal{B}$ [10]. This complicated codimension-two locus C_2 over which the fiber is of type I_2 hosts singlet states that carry $\mathbb{Z}_2$ charge. These states originate from singly charged states in the $SU(5) \times U(1)$ model related to this geometry by a conifold transition. The matter spectrum and the associated $\mathbb{Z}_2$ charges are summarized in table 5.2.2. The intersection structure of the matter curves along the $SU(5)$ divisor Θ is shown in figure 5.1,

locus in base	irrep $SU(5)$	$\mathbb{Z}_2$ charge
$\theta \cap b_1$	$\mathbf{10}, \overline{\mathbf{10}}$	$[0]$
$\theta \cap \{b_1^2 c_{0,4} - b_0 b_1 c_{1,2} + c_{1,2}^2\}$	$\mathbf{5}^A, \overline{\mathbf{5}}^A$	$[1]$
$\theta \cap \{b_2^2 c_{2,1} - b_1 b_2 c_{3,1} + b_1^4 c_{4,1}\}$	$\mathbf{5}^B, \overline{\mathbf{5}}^B$	$[0]$
C_2	$\mathbf{1}$	$[1]$

Table 5.2.2: Matter spectrum in the $SU(5) \times \mathbb{Z}_2$ model.

which we reproduce from [10] for convenience, and the corresponding Yukawa couplings are indicated, all consistent with the $\mathbb{Z}_2$ charges.

5.2.1 A horizontal flux solution

Having reviewed the geometry we now study the proposed transversality conditions,

$$\int_{X_4} G_4 \wedge \hat{U} \wedge \pi^{-1} D_a = 0,$$

$$\int_{X_4} G_4 \wedge \pi^{-1} D_a \wedge \pi^{-1} D_b = 0, \tag{5.2.6}$$

$$\int_{X_4} G_4 \wedge E_i \wedge \pi^{-1} D_a = 0,$$

in the $SU(5) \times \mathbb{Z}_2$ geometry. The last condition only applies if we require the flux solution G_4 to leave a full $SU(5)$ gauge group unbroken in the F-theory limit. As noted before, this eliminates the correction terms in $\hat{U}$ and reduces the system to the usual transversality conditions with respect to the unshifted bisection U.

The first flux solution is an example of a horizontal gauge flux which generalizes the horizontal G_4 flux constructed in [10] for the bisection model without further non-abelian gauge enhancement. The flux is associated with a special algebraic 4-cycle which appears on the sublocus in complex structure moduli space where $c_4 = \rho\tau$. This is modeled after a similar construction in the context of a Tate model [59]. In the presence of an $SU(5)$ singularity the same type of fluxes exists, *mutatis mutandis*, on the sublocus in moduli space where $c_{4,1} = \rho\tau$. In this case the two algebraic 4-cycles described as the complete intersections

$$\sigma_0 \;=\; (u, w, \rho), \tag{5.2.7}$$
$$\sigma_1 \;=\; (u, we_1 + b_2 v^2 e_3^2 e_4, \rho) \tag{5.2.8}$$

in the ambient space X_5 of X_4 automatically lie on X_4. This notation indicates that the 4-cycles should be thought of as the algebraic varieties associated with the ideal generated by the polynomials in brackets.

The two 4-cycles each define one of the two intersection points of the bisection U with the fiber, fibered over the divisor $P : \{\rho = 0\}$ in the base. The dual cohomology classes $[\sigma_0]$ and $[\sigma_1]$ are candidates for a flux. To obtain a well-defined flux we add an ansatz of correction terms $\sum a_i D_i \wedge P$ where D_i runs over a basis of divisors in the 4-fold. Solving for the coefficients a_i yields the flux solutions

$$G_4(P, \sigma_0) \;=\; 5[\sigma_0] + \frac{1}{2}(-5U + (4E_1 + 3E_2 + 2E_3 + E_4) - 2\theta) \wedge P, \tag{5.2.9}$$

$$G_4(P, \sigma_1) \;=\; 5[\sigma_1] - \frac{1}{2}(5U + (4E_1 + 3E_2 + 2E_3 + E_4) - 2\theta) \wedge P, \tag{5.2.10}$$

where, for now, the overall normalization is chosen to give manifestly integral chiral indices as will be discussed later. The two flux solutions are not independent on the hypersurface and for definiteness we choose to consider $G_4(P, \sigma_0)$ in the following.

5.2.2   All vertical fluxes

We next address the problem of describing all independent vertical fluxes on the $SU(5) \times \mathbb{Z}_2$ fibration which exist over a *generic* base $\mathcal{B}$. We follow the strategy in [89], where the first such classification of vertical gauge fluxes has been undertaken for $(U(1)$ restricted) Tate models with gauge groups $SU(N)(\times U(1))$ for $N = 2, 3, 4, 5$ over a generic base $\mathcal{B}$. See [63, 99, 131] for classifications for other types of fibrations. To this end we first compute a basis for the vertical $(2,2)$-forms in the ambient space 'X_5' of X_4. To simplify the notation we will from now on omit the pull-back symbol 'π^{-1}' whenever there is no ambiguity about a divisor coming from the base. Due to relations between the divisors from the Stanley-Reisner ideal SR given in (5.2.2) and from homology relations in the fiber ambient space, not all products of divisors are linearly independent. With the help of `Singular` we can take these relations into account by computing a basis for the quotient ring

$$H^{(*,*)}(X_5) \cong \frac{\mathbb{C}[D_i]}{SR + HOM}, \tag{5.2.11}$$

where $\mathbb{C}[D_i]$ is the formal polynomial ring with all divisors of X_5 as variables.[2] The homology relations HOM, which can be read off from the top, are encoded in the scaling relations in table B.3.1 and take the form

$$W = 2U + 2\bar{\mathcal{K}} - [b_2] - E_1 - 2E_2 - 2E_3 - E_4,$$
$$V = U + \bar{\mathcal{K}} - [b_2] - E_2 - 2E_3 - E_4, \tag{5.2.12}$$
$$\Theta = E_0 + E_1 + E_2 + E_3 + E_4.$$

---

[2]Strictly speaking this construction only gives the vertical part – i.e. linear combinations of products of divisors – of the ambient space cohomology $H^{(*,*)}(X_5)$, which however suffices for all the computations we perform here.

This basis is then used to make an ansatz for the most general flux. The transversality conditions (5.2.6) become a set of equations expressed in intersection numbers on the ambient 5-fold, e.g.

$$\int_{X_4} G_4 \wedge D_a \wedge D_b = \int_{X_5} [P_{\mathbb{Z}_2}^{SU(5)}] \wedge G_4 \wedge D_a \wedge D_b. \tag{5.2.13}$$

Intersection numbers like these can be reduced to intersection numbers on the base by employing the Stanley-Reisner ideal and the homology relations, thereby eliminating redundancies due to the known homology relations in the fiber ambient space. The Stanley-Reisner ideal trivially sets many intersections to zero. Likewise, due to the fibration structure, any intersection number with more than 3 divisor classes pulled back from the base will vanish. Let F_i denote all fibral divisors classes, both the toric classes T_i associated with the homogeneous coordinates of the original fiber ambient space $\mathbb{P}_{1,1,2}$ and exceptional divisors E_i. For i, j, k distinct, and $D_{a,b,c}$ base divisor classes, the non-vanishing intersections (omitting the wedges) are

$$\int_{X_5} T_i T_j D_a D_b D_c = \frac{1}{V(i,j)} \int_{\mathcal{B}} D_a D_b D_c,$$
$$\int_{X_5} E_i F_j F_k D_a D_b = \frac{1}{V(i,j,k)} \int_{\mathcal{B}} \Theta D_a D_b. \tag{5.2.14}$$

Here $V(i,j)$, $(V(i,j,k))$ is the lattice volume of the cell spanned by the fan vectors $f_i, f_j, (f_k)$. For the top used here, all cell volumes are one, except the one spanned by f_u and f_v corresponding to the divisors U and V, which has volume 2. When the i, j, k are non-distinct, we are dealing with a self-intersection of fibral divisor classes. These can be reduced to transversal intersections by using the homology relations in the ambient fiber space. As an example consider the reduction

$$\int_{X_5} W^2 D_a D_b D_c = \int_{X_5} W(2U + 2\bar{\mathcal{K}} - [b_2] - E_1 - 2E_2 - 2E_3 - E_4)D_a D_b D_c$$
$$= \int_{X_5} W(2U + 2\bar{\mathcal{K}} - [b_2] - E_1 - 2E_2 - 2E_3)D_a D_b D_c = 2\int_{\mathcal{B}} D_a D_b D_c. \tag{5.2.15}$$

This way also (self-)intersections of 3,4 or 5 fibral divisor classes may be computed iteratively and reduced to the cases (5.2.14). `Singular` automatically applies this method and reduces the transversality conditions to a system of linear combinations of intersection numbers on the base.

As discussed above, if we demand orthogonality with respect to the Cartan generators, i.e. (5.1.10), this effectively replaces $\hat{U}$ by U in the modified transversality condition (5.1.8). The solution to all transversality conditions, expressed in a chosen basis, takes the form

$$
\begin{aligned}
G_4 = \\
z_1 (5E_1 E_2 + 4E_2^2 + 2E_3 E_4 + \tfrac{1}{2}U\Theta + \Theta^2 + (-1,-3,0,1)E_i[b_2] + (1,8,0,-2)_i E_i \bar{\mathcal{K}} \\
\quad + \tfrac{1}{2}(-4,-19,-2,3)_i E_i \Theta) \\
+ z_2 (5E_1 E_2 + \tfrac{5}{2}E_2^2 + \bar{\mathcal{K}}\Theta + (0,-\tfrac{5}{2},0,0)E_i[b_2] + \tfrac{1}{2}(-4,7,-2,-1)_i E_i \bar{\mathcal{K}} + (0,-5,0,0)_i E_i \Theta) \\
+ z_3 (5E_1 E_2 + 2E_2^2 + E_3 E_4 - U\Theta + [b_2]\Theta + (0,-3,-1,0)E_i[b_2] + (-2,4,0,-1)_i E_i \bar{\mathcal{K}} \\
\quad + (0,-4,0,1)_i E_i \Theta) \\
+ z_4 (E_2 E_4 - E_4 \bar{\mathcal{K}}).
\end{aligned}
\tag{5.2.16}
$$

However, the last term is a trivial solution on the hypersurface as can be verified by wedging it with the hypersurface class and employing the homology relations. Furthermore, the terms with coefficients z_2

and z_3 are identical when restricted to the fourfold, again easily seen using the SR-ideal and homology relations. The most general solution for vertical fluxes is thus expressed as

$$
\begin{aligned}
G_4 = &z_1 G_4^{z_1} + z_2 G_4^{z_2} = \\
&z_1 (5E_1E_2 + 4E_2^2 + 2E_3E_4 + \frac{1}{2}U\Theta + \Theta^2 + (-1,-3,0,1)E_i[b_2] + (1,8,0,-2)_i E_i\bar{\mathcal{K}} \\
&\quad + \frac{1}{2}(-4,-19,-2,3)_i E_i\Theta) \\
+ &z_2 (5E_1E_2 + \frac{5}{2}E_2^2 + \bar{\mathcal{K}}\Theta + (0,-\frac{5}{2},0,0)E_i[b_2] + \frac{1}{2}(-4,7,-2,-1)_i E_i\bar{\mathcal{K}} + (0,-5,0,0)_i E_i\Theta) \, .
\end{aligned}
\tag{5.2.17}
$$

Note again that the normalizations for $G_4^{z_1}$ and $G_4^{z_2}$ is chosen to give manifestly integer chiralities.

5.2.3   Fluxes from matter surfaces

So far we have constructed the most general vertical fluxes by systematically implementing the transversality conditions on a basis of $H^{2,2}_{\text{vert}}(X_5)$ and pulling these fluxes back to X_4. From a conceptual point of view, the gauge data can be encoded in rational equivalence classes of 4-cycles [130] whose homology class is dual to G_4 viewed as an element of $H^{2,2}(X_4)$. The transversality conditions suggest that natural building blocks for the construction of such 4-cycles are the matter surfaces. This approach was, for instance, taken in [83] to construct non-Cartan vertical gauge fluxes. In this section we will analyse the matter surfaces associated with states in the antisymmetric and fundamental representations of $SU(5)$ and relate their cohomology classes to the general vertical flux solution found in the previous section.

As a general remark, recall that the fiber over the **10**-curve in the base – see figure 5.1 – splits into a collection of rational curves intersecting like the nodes of the affine Dynkin diagram of $SO(10)$. Suitable combinations of fibral curves are associated with each of the ten entries of the weight vector of the **10**-representation, and these curves with opposite orientation give rise to the conjugate weights. In the sequel, when we talk about 'the $\overline{\mathbf{10}}$ surface' we have one particular such fibral cycle fibered over the base curve in mind. Since different weights differ only by combinations of simple roots, different such 4-cycles differ by suitable combinations of resolution divisors restricted to the base curve and we will not need to consider all different choices independently. Similar remarks apply to the $\mathbf{5}_A$ and $\mathbf{5}_B$ representations and their associated matter surfaces.

The $\overline{\mathbf{10}}$ Surface

A representative of the matter surface $[\mathcal{C}_{\overline{\mathbf{10}}}]$ is given by the complete ambient intersection (e_0, e_2, b_1). By employing the SR-ideal we find that restricting the hypersurface to (e_0, e_2) implies $b_1 = 0$, and hence we can represent the matter surface by $E_0 \wedge E_2$ in the ambient vertical cohomology. This combination is however not orthogonal to the Cartan divisors, and we have to add correction terms to arrive at a valid flux. An ansatz for the correction term of the form $\sum a_i E_i \bar{\mathcal{K}} + \lambda \bar{\mathcal{K}}\Theta$ turns out to be sufficient. This results in the flux

$$
\begin{aligned}
G_4(\overline{\mathbf{10}}) &= E_0E_2 - \frac{1}{5}\bar{\mathcal{K}}\Theta - \frac{1}{5}(-2,1,-1,-3)_i E_i\bar{\mathcal{K}} \\
&= -E_1E_2 - \frac{1}{2}E_2^2 - \frac{1}{5}\bar{\mathcal{K}}\Theta + \frac{1}{2}E_2[b_2] - \frac{1}{10}(-4,7,-2,-1)_i E_i\bar{\mathcal{K}} + E_2\Theta,
\end{aligned}
\tag{5.2.18}
$$

where we have rewritten the first line in the chosen vertical basis. Up to a factor of -5 the flux agrees exactly with the flux solution with coefficient z_2 in (5.2.17).

The $\bar{\mathbf{5}}^{\mathbf{A}}$ Surface

The homology class of the $\bar{\mathbf{5}}^{\mathbf{A}}$ matter surface is not straightforwardly given. Over the matter curve $\Theta \cap \{b_1^2 c_{0,4} - b_{0,2} b_1 c_{1,2} + c_{1,2}^2 = 0\}$ the rational fiber of the exceptional divisor E_3 splits. This can be seen by solving the second polynomial rationally for $c_{0,4}$ and inserting this together with $e_3 = 0$ into the hypersurface equation. This locally valid approach is enough for computing the weight of the state in the representation, but in order to construct a global flux the homology class of the rationally fibered surface has to be determined. Using `Singular` we compute the intersection of the hypersurface with the exceptional divisor E_3 and the matter curve in the base as the ideal

$$(P_{\mathbb{Z}_2}^{SU(5)}, e_3, b_1^2 c_{0,4} - b_{0,2} b_1 c_{1,2} + c_{1,2}^2). \tag{5.2.19}$$

This ideal prime decomposes into two components, corresponding to states in the fundamental and anti-fundamental representations, respectively. The anti-fundamental surface $\mathcal{C}_{\bar{\mathbf{5}}^{\mathbf{A}}}$ is given as the non-transversal intersection

$$\begin{aligned}
\mathcal{C}_{\bar{\mathbf{5}}^{\mathbf{A}}} = (&e_3, b_1^2 c_{0,4} - b_{0,2} b_1 c_{1,2} + c_{1,2}^2, e_0^2 e_1 e_4 u^2 c_{1,2} + w b_1, \\
&e_0^2 e_1 e_4 u^2 b_1 c_{0,4} + w b_{0,2} b_1 - w c_{1,2}, e_0^4 e_1^2 e_4^2 u^4 c_{0,4} + e_0^2 e_1 e_4 u^2 w b_{0,2} + w^2).
\end{aligned} \tag{5.2.20}$$

To make sense of the matter surface as a transversal intersection of three equations in the ambient 5-fold we employ a trick. By prime decomposing the ideal given by the first three equations $(e_3, b_1^2 c_{0,4} - b_{0,2} b_1 c_{1,2} + c_{1,2}^2, e_0^2 e_1 e_4 u^2 c_{1,2} + w b_1)$ of the above ideal two irreducible components are revealed. The first one is the matter surface (5.2.20) itself, and the second is the ideal $(e_3, b_1, c_{1,2})$ with multiplicity two. In homology we can 'solve' for the matter surface in terms of the two transversal intersections as

$$[\mathcal{C}_{\bar{\mathbf{5}}^{\mathbf{A}}}] = E_3 \wedge 2[c_{1,2}] \wedge (W + [b_1]) - 2 \cdot E_3 \wedge [b_1] \wedge [c_{1,2}]. \tag{5.2.21}$$

Having obtained the homology class we may construct a transversal flux solution by making an ansatz of correction terms. However, to compare with the previously obtained vertical flux solutions we would like to represent the matter surface as a vertical (2,2)-form in the ambient space which, when restricted to the hypersurface, gives the class $[\mathcal{C}_{\bar{\mathbf{5}}^{\mathbf{A}}}]$. To obtain the solution in this form we make the ansatz

$$[\mathcal{C}_{\bar{\mathbf{5}}^{\mathbf{A}}}] = E_3 \wedge \left(\sum_i a_i D_i\right) \wedge [P_{\mathbb{Z}_2}^{SU(5)}] \tag{5.2.22}$$

where the D_i is a basis for the divisors on X_4. By expanding both sides in a basis for $H^{3,3}(X_5)$ in `Singular` we solve for the a_i and obtain that

$$\begin{aligned}
E_3 \left(\sum_i a_i D_i\right) =& E_3(E_3 + 2E_4 - [b_2] + 3\bar{\mathcal{K}} - 3\Theta) \\
=& \frac{1}{2} E_2^2 + E_3 E_4 + (0, \frac{1}{2}, -1, 0)_i E_i [b_2] + (0, -\frac{1}{2}, 3, \frac{1}{2})_i E_i \bar{\mathcal{K}} + (0, 0, -2, 0)_i E_i \Theta
\end{aligned} \tag{5.2.23}$$

restricts to the $\bar{\mathbf{5}}^{\mathbf{A}}$ matter surface on the hypersurface. On the righthand side the solution is given in the chosen basis for $H_{\text{vert}}^{2,2}$.

At this point we are ready to construct a well-defined flux by adding a linear combination of terms with at least one factor coming from the base such that the transversality conditions are satisfied.

The result is

$$
\begin{aligned}
G_4(\mathbf{\bar 5^A}) &= [\mathcal{C}_{\mathbf{\bar 5^A}}] + \{\text{correction terms}\} \\
&= \frac{1}{2}E_2^2 + E_3 E_4 + \frac{1}{5}[b_2]\Theta - \frac{3}{5}\bar{\mathcal{K}}\Theta + \frac{2}{5}\Theta^2 \\
&\quad + \frac{1}{10}(-4,-3,-2,4)_i E_i[b_2] + \frac{1}{10}(12,19,6,-14)_i E_i\bar{\mathcal{K}} + \frac{1}{5}(-4,-8,-2,4)_i E_i\Theta \\
&= \frac{2}{5}(G_4^{z_1} - G_4^{z_2}).
\end{aligned}
$$

(5.2.24)

The last line relates this flux to one combination of vertical fluxes constructed in the previous section.

The $\mathbf{\bar 5^B}$ Surface

By the same technique, we construct a flux from the $\mathbf{\bar 5^B}$ surface. The homology class, obtained by prime decomposition, is

$$
[\mathcal{C}_{\mathbf{\bar 5^B}}] = E_1 \wedge (2[b_2] + [c_{2,1}]) \wedge (\bar{\mathcal{K}} + U) - 2E_1 \wedge \bar{\mathcal{K}} \wedge [b_2].
$$

(5.2.25)

By making a suitable ansatz we find that the element

$$
E_1(E_1 + 2E_2 + [b_2] - \Theta)
$$

(5.2.26)

in the ambient vertical cohomology reproduces $[\mathcal{C}_{\mathbf{\bar 5^B}}]$ when restricted to the hypersurface. Using this representative we construct the transversal flux as

$$
\begin{aligned}
G_4(\mathbf{\bar 5^B}) &= [\mathcal{C}_{\mathbf{\bar 5^B}}] + \{\text{correction terms}\} \\
&= E_1 E_2 - E_2^2 + E_3 E_4 - 2U\Theta + \frac{9}{5}[b_2]\Theta - \frac{6}{5}\bar{\mathcal{K}}\Theta - \frac{2}{5}\Theta^2 \\
&\quad + \frac{1}{5}(2,-6,-9,-2)_i E_i[b_2] + \frac{1}{5}(-8,-1,6,-2)_i E_i\bar{\mathcal{K}} + \frac{1}{5}(4,13,2,6)_i E_i\Theta \\
&= \frac{1}{5}(-2G_4^{z_1} + 3G_4^{z_2}),
\end{aligned}
$$

(5.2.27)

where the second term is expanded in the chosen basis, and the last line gives the flux as a linear combination of the vertical flux solutions in (5.2.17).

5.2.4   Chiralities and non-abelian anomalies

With the explicit flux solutions and also representatives of the homology classes of the matter surfaces at hand, it is straightforward to compute the induced chiralities for all $SU(5)$ representations. The net chirality χ of a state in representation $\mathbf{R}$ of $SU(5)$ induced by a flux G_4 is given by

$$
\chi(\mathbf{R}) = \int_{[\mathcal{C}_{\mathbf{R}}]} G_4 \,.
$$

(5.2.28)

These integrals lift to intersection numbers in the ambient space upon multiplication with the hypersurface class. Using the techniques described above all these intersections are reduced to intersection numbers on the base. The induced chiralities from the three flux solutions described above are, with respect to the general flux combination $G_4 = a\, G_4(P,\sigma_0) + z_1 G_4^{z_1} + z_2 G_4^{z_2}$,

$$
\begin{aligned}
\chi(\mathbf{10}) &= \left[-aP + z_1(-2[b_2] + 12\bar{\mathcal{K}} - 9\Theta) + z_2(6\bar{\mathcal{K}} - 5\Theta)\right]\bar{\mathcal{K}}\Theta, \\
\chi(\mathbf{\bar 5^A}) &= \left[-aP + z_1(-2[b_2] - 8\bar{\mathcal{K}} + \Theta) - 4z_2\bar{\mathcal{K}}\right]([b_2] - 3\bar{\mathcal{K}} + 2\Theta)\Theta, \\
\chi(\mathbf{\bar 5^B}) &= \left[aP([b_2] - 4\bar{\mathcal{K}} + 2\Theta) + z_1(2[b_2]^2 + 3[b_2]\Theta - 2(6\bar{\mathcal{K}}^2 - 5\bar{\mathcal{K}}\Theta + \Theta^2)) \right. \\
&\quad \left. + z_2(4[b_2] - 6\bar{\mathcal{K}} + 3\Theta)\bar{\mathcal{K}}\right]\Theta,
\end{aligned}
$$

(5.2.29)

where we have suppressed integration over the base. It is easily checked that the $SU(5)$ anomaly condition

$$\chi(\mathbf{10}) = \chi(\bar{\mathbf{5}}^{\mathbf{A}}) + \chi(\bar{\mathbf{5}}^{\mathbf{B}}) \tag{5.2.30}$$

is satisfied without further restrictions on a, z_1 and z_2. In fact, this follows directly from the 4-cycle class $[\bar{\mathbf{10}}] + [\bar{\mathbf{5}}^{\mathbf{A}}] + [\bar{\mathbf{5}}^{\mathbf{B}}]$: Due to the homology relations (5.2.12) and SR-ideal (5.2.2) this combination is equal to

$$[P_{SU(5)}] \wedge \left\{ 2[b_2] \wedge (E_1 + E_2) + \bar{\mathcal{K}} \wedge (-E_2 + 3E_3 + E_4) + \Theta \wedge (E_2 - 2E_3 - E_4) - \Theta \wedge [b_2] \right\} . \tag{5.2.31}$$

In this form, it is obvious that *any* valid G_4 yields zero upon integration over this cycle. In particular, the cancellation of the pure $SU(5)$ anomaly only requires conditions (5.1.9) (G_4 does not have two legs along the fiber) and (5.1.10) (G_4 does not break gauge symmetry) since the 4-cycle class (5.2.31) only involves terms of the form $\pi^{-1}D_a \wedge E_i$ and $\pi^{-1}D_a \wedge \pi^{-1}D_b$. The missing condition (5.1.8) will become relevant in the context of the discrete $\mathbb{Z}_2$ anomaly to be discussed in section 5.5.

In addition to the $SU(5)$ charged states, there are localised states with $\mathbb{Z}_2$ charge 1 mod 2 which transform as singlets under $SU(5)$. These states are localised on the curve called C_2 in table 5.2.2, which, as we recall, can be described by an ideal generated by 15 non-transversely intersecting elements [10]. The I_2-fiber over C_2 splits into two rational curves A and B with $[A] = [B]$ in homology. Indeed, both curves are exchanged by a global monodromy over C_2 provided the intersection of the monodromy locus of the bisection with C_2 is non-empty, as is generically the case [10] (see [43, 135] for a discussion of the implications of the absence of this monodromy point on C_2 in non-generic models). The states associated with an M2-brane wrapping A and B have the same quantum numbers. In order to count the number of $\mathcal{N} = 1$ chiral multiplets of the 4-dimensional F-theory vacuum with $\mathbb{Z}_2$ charge 1, we must therefore add the zero modes from M2-branes wrapping both fibral curves [11]. One can separately compute the overlap of G_4 with the 4-cycle $\mathcal{C}_A$ or $\mathcal{C}_B$ given by fibering A or B over C_2, and e.g. the flux $G_4(P, \sigma_0)$ indeed gives a non-zero result for both individual surfaces [11]. However, in total

$$\chi(\mathbf{1}) = \int_{\mathcal{C}_A} G_4 + \int_{\mathcal{C}_B} G_4 = 0 \tag{5.2.32}$$

by the transversality condition (5.1.9) because A and B sum up to the total fiber class. This is the geometric manifestation of the statement that an $SU(5)$ singlet carrying only $\mathbb{Z}_2$ charge does not admit a notion of chirality, of course.

5.3 Fluxes on an elliptic fibration with an extra section

The bisection $\mathbb{P}_{112}[4]$-fibration X_4 is related, via a conifold transition [10, 11, 70, 84, 101, 117], to the elliptic $\mathrm{Bl}^1\mathbb{P}_{112}[4]$-fibration with Mordell-Weil group of rank 1 of [18]. In general, in a conifold transition between F/M-theory 4-folds conservation of M2-brane charge dynamically relates the 4-form fluxes on both sides [59, 89, 136]. For the specific transition between the $\mathbb{P}_{112}[4]$-fibration and the $\mathrm{Bl}^1\mathbb{P}_{112}[4]$-model without extra non-abelian gauge groups, the $U(1)$ flux and the $\mathbb{Z}_2$ flux (5.2.9) have been successfully matched along these lines [10]. In section 5.4 we will extend this match to the full set of fluxes constructed in the previous section. This will serve as an additional non-trivial check on the consistency of our construction. As a preparation we need to construct, in this section, the complete set of vertical fluxes on the $U(1)$ side of the transition with which we will compare the flux solutions in the bisection model.

Let us briefly recap the properties of the $\mathrm{Bl}^1\mathbb{P}_{112}[4]$-fibration of [18], but including an extra $SU(5)$ factor [10] as in the previous chapter. We start from the model (4.6.13) and by a complex structure

deformation set $c_{4,1} \equiv 0$. This introduces a singularity in codimension 2, which is resolved by a blow-up in the ambient space. The proper transform describing an elliptically fibered 4-fold Y_4 reads

$$
\begin{aligned}
P_{U(1)}^{SU(5)} = {} & e_1 e_2 s w^2 + b_{0,2} s^2 u^2 w e_0^2 e_1^2 e_2 e_4 + b_1 suvw + b_2 v^2 w e_2 e_3^2 e_4 \\
& + c_{0,4} u^4 e_0^4 e_1^3 e_2 e_4^2 + c_{1,2} u^3 v e_0^2 e_1 e_4 + c_{2,1} u^2 v^2 e_0 e_3 e_4 + c_{3,1} uv^3 e_0 e_2 e_3^3 e_4^2,
\end{aligned}
\tag{5.3.1}
$$

where s is the blow-up coordinate. The divisor class $S : \{s = 0\}$ is the class of an extra rational section, and $U : \{u = 0\}$ is the holomorphic zero-section of the elliptic fibration. The structure of the exceptional coordinates e_i is identical to its counterpart in the bisection model because the toric description of $\mathbb{P}_{112}$ and $\mathrm{Bl}^1\mathbb{P}_{112}$ admit the construction of the same top [19]. For the chosen triangulation we obtain the Stanley-Reisner ideal generators

$$
\{uw, vs, ve_1, ve_2, we_0, we_4, ue_1, ue_2, ue_3, ue_4, se_2, se_3, se_4, e_0 e_3, e_1 e_3, e_1 e_4\} .
\tag{5.3.2}
$$

The $U(1)$ generator is determined by the Shioda map as

$$
\mathrm{w}_{U(1)} = 5(S - U - \bar{\mathcal{K}} - [b_2]) + 4E_1 + 3E_2 + 2E_3 + E_4.
\tag{5.3.3}
$$

The discriminant

$$
\Delta \sim \theta^5 [\, b_1^4 b_2 (b_1 c_{3,1} - b_2 c_{2,1})(b_1^2 c_{0,4} - b_{0,2} b_1 c_{1,2} + c_{1,2}^2) + \mathcal{O}(\theta)]
\tag{5.3.4}
$$

indicates four matter curves with $SU(5)$ charged matter. In addition there are two singlet curves, not lying completely in the $SU(5)$ divisor Θ. The first one is the curve $C_1 : (b_2, c_{3,1})$ of conifold singularities which got resolved in the conifold transition. M2-branes wrapping the irreducible fiber components give rise to states of $U(1)$ charge ± 10 (in the normalization (5.3.3)), called doubly charged states. The second curve is the more complicated locus, denoted C_2 in (4.1.9) and given explicitly in (B.2.1). Over C_2 the fiber is of type I_2, similarly as in the bisection model. The states localized along this curve have $U(1)$ charge ± 5 and are referred to as singly charged. In table 5.3.1 we summarize the matter spectrum for this model.

The matter curves intersect at a number of loci, giving rise to 6 different Yukawa couplings involving $SU(5)$ charged fields. These are shown in figure 5.2. In addition there is one coupling that is localized outside the GUT divisor. This is the coupling $\mathbf{1}_{-10}\mathbf{1}_5\mathbf{1}_5$ together with its conjugate, and it exists regardless of the $SU(5)$ enhancement.

locus in base	irrep $SU(5)_{U(1)}$
$\theta \cap b_1$	$\mathbf{10}_{-2}, \bar{\mathbf{10}}_2$
$\theta \cap b_2$	$\mathbf{5}_{-6}, \bar{\mathbf{5}}_6$
$\theta \cap \{b_1 c_{3,1} - b_2 c_{2,1}\}$	$\mathbf{5}_4, \bar{\mathbf{5}}_{-4}$
$\theta \cap \{b_1^2 c_{0,4} - b_{0,2} b_1 c_{1,2} + c_{1,2}^2\}$	$\mathbf{5}_{-1}, \bar{\mathbf{5}}_1$
$C_1 = b_2 \cap c_{3,1}$	$\mathbf{1}_{\pm \mathbf{10}}$
C_2	$\mathbf{1}_{\pm \mathbf{5}}$

Table 5.3.1: Matter curves in the $SU(5) \times U(1)$ model.

5.3.1 All vertical fluxes

We now construct all vertical flux solutions to the – in presence of a section standard – transversality conditions

$$
\int_{Y_4} G_4 \wedge U \wedge \pi^{-1} D_a = 0, \quad \int_{Y_4} G_4 \wedge D_a \wedge \pi^{-1} D_b = 0, \quad \int_{Y_4} G_4 \wedge E_i \wedge \pi^{-1} D_a = 0.
\tag{5.3.5}
$$
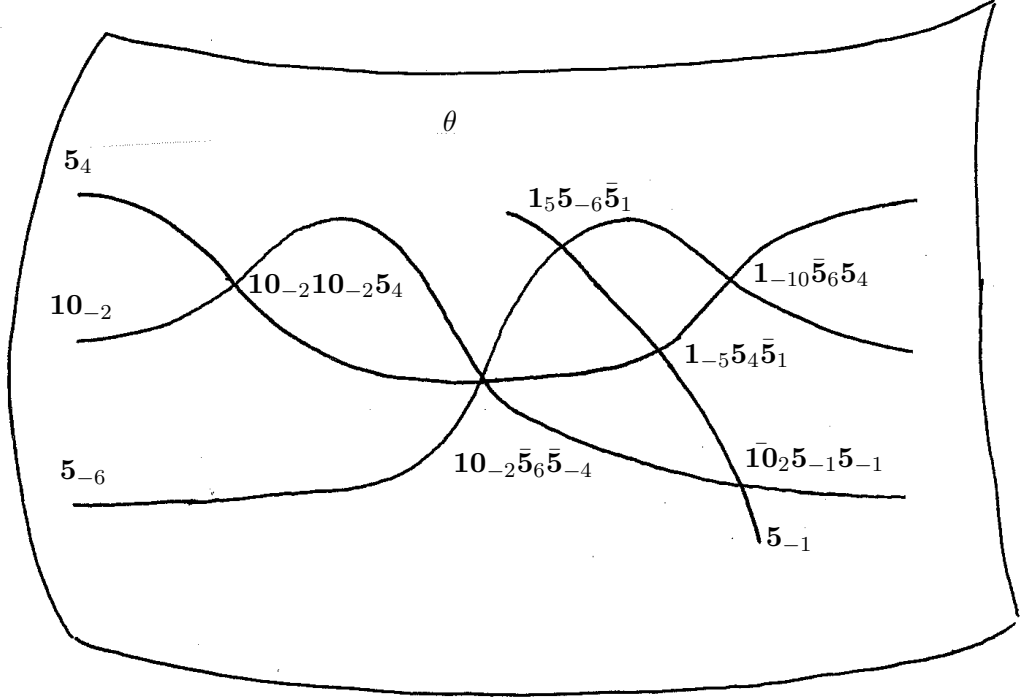
Figure 5.2: The matter curves in the $SU(5)$ divisor $\{\theta = 0\}$ and the Yukawa couplings involving the $SU(5)$ charged matter in codimension three.

As always in the presence of a $U(1)$ gauge group, the $U(1)$ generator $\mathrm{w}_{U(1)}$ in (5.3.3) gives rise to a vertical flux solution

$$G_4(F) = \mathrm{w}_{U(1)} \wedge \pi^{-1}F, \tag{5.3.6}$$

which satisfies the transversality conditions for any choice of base divisor class F.

To find more vertical solutions we make a general ansatz, as in the previous section, expressed in a basis for the vertical cohomology of the ambient space Y_5. Subjecting this ansatz to the transversality conditions and reducing all terms to intersection numbers in the base we find a family of solutions valid over a generic base $\mathcal{B}$,

$$
\begin{aligned}
G_4 =\,& G_4(F) + u_1 G_4^{u_1} + u_2 G_4^{u_2} + u_3 G_4^{u_3} \\
=\,& \mathrm{w}_{U(1)} \wedge F \\
& + u_1(-15E_1E_2 + 5E_2^2 + 25E_3E_4 + (-10, 0, -5, 10)_i E_i[b_2] \\
& \qquad + (36, 37, 18, -16)_i E_i \bar{\mathcal{K}} + (-20, -25, -10, 20)_i) E_i \Theta) \\
& + u_2(-10E_1E_2 - 5E_2^2 + (0, 5, 0, 0)_i E_i[b_2] + (4, -7, 2, 1)_i E_i \bar{\mathcal{K}} + (0, 10, 0, 0)_i E_i \Theta) \\
& + u_3(5E_1E_2 + 5E_2^2 - 5E_3E_4 + 10U\Theta + 10\bar{\mathcal{K}}\Theta + (0, 0, 5, 0)_i E_i[b_2] \\
& \qquad + (-2, 1, -6, 2)_i E_i \bar{\mathcal{K}} + (-4, -13, -2, -6)_i E_i \Theta).
\end{aligned}
\tag{5.3.7}
$$

The normalization is chosen such as to give manifestly integral chiralities, as presented in following sections. By restricting the solution to the hypersurface and expanding it in a basis for $H_{\mathrm{vert}}^{3,3}(Y_5)$, it is shown that the three solutions $G_4^{u_i}$ are independent.

5.3.2 Fluxes from matter surfaces

As in the bisection model, it is possible to express all fluxes originating from $SU(5)$ charged matter surfaces in terms of the general vertical flux solution above. In the sequel we derive the map between

the two representations of the fluxes.

The $\bar{1}0_2$ surface

One possible representative for the matter surface $[\mathcal{C}_{\bar{1}0_2}]$ is given by the complete ambient intersection (e_0, e_2, b_1), which agrees with the corresponding representation of the **10**-surface considered in the $SU(5) \times \mathbb{Z}_2$ model. To find the flux associated with this matter surface, we start from an ansatz $E_0 \wedge E_2$ in the ambient space cohomology and add a linear combination of correction terms of the form $U \wedge D_a, S \wedge D_a, E_i \wedge D_a$ and $D_a \wedge D_b$, for $D_{a,b}$ pullback divisors from the base and solve for the coefficients. Up to the addition of an arbitrary $U(1)$ flux, which we set to zero, the transversality conditions fix the correction terms such that

$$
\begin{aligned}
G_4(\bar{1}0_2) &= E_0 E_2 + \frac{1}{10}(4, -2, 2, 6)_i E_i \bar{\mathcal{K}} \\
&= -E_1 E_2 - \frac{1}{2} E_2^2 + \frac{1}{2} E_2[b_2] + \frac{1}{10}(4, -7, 2, 1)_i E_i \bar{\mathcal{K}} + E_2 \Theta,
\end{aligned}
\tag{5.3.8}
$$

where we have rewritten the first line in the chosen vertical basis. Up to a scaling factor the flux agrees exactly with the flux solution $G_4^{u_2}$ in (5.3.7).

The 5_{-6} surface

A representative of the 5_{-6} surface is given by the complete intersection of (e_0, s) with the hypersurface. Indeed this implies $b_2 = 0$ and thus reproduces the curve in the base over which the 5_{-6} matter is localized. Repeating verbatim the steps performed for the $\bar{1}0_2$-flux we arrive at,

$$
\begin{aligned}
G_4(5_{-6}) &= E_0 S - S\Theta + U\Theta + \bar{\mathcal{K}}\Theta + \frac{1}{5}(4, 3, 2, 1)_i E_i[b_2] - \frac{1}{5}(4, 3, 2, 1)_i E_i \Theta \\
&= -E_1 E_2 + U\Theta + \bar{\mathcal{K}}\Theta + \frac{1}{5}(-1, 3, 2, 1)_i E_i[b_2] + E_1 \bar{\mathcal{K}} - \frac{1}{5}(4, 3, 2, 1)_i E_i \Theta \\
&= \frac{1}{50}(G_4^{u_1} + 6 G_4^{u_2} + 5 G_4^{u_3}).
\end{aligned}
\tag{5.3.9}
$$

In the second line we have used that $E_0 S - S\Theta = -E_1(E_2 - \bar{\mathcal{K}} + [b_2])$ in the ambient cohomology.

The $\bar{5}_{-4}$ surface

The cohomology class of a representative of $\mathcal{C}_{\bar{5}_{-4}}$ can be obtained by an ideal decomposition in `Singular` and is given in the ambient space as

$$
\mathcal{C}_{\bar{5}_{-4}} = E_1(2\bar{\mathcal{K}}^2 + S[b_2] + 2S\bar{\mathcal{K}} - S\Theta - \bar{\mathcal{K}}\Theta).
\tag{5.3.10}
$$

Out of this class a transversal flux may be constructed by adding possible correction terms and solving the transversality conditions. As in the previous chapter we aim at comparing the matter surface to the vertical flux solution. By making the analogous ansatz as in section 5.2.3, we find that

$$
\mathcal{C}_{\bar{5}_{-4}} = E_1 \wedge (E_1 + 2E_2 + [b_2] - \Theta) \wedge [P_{SU(5)}].
\tag{5.3.11}
$$

The factor of E_1 reflects the fact that it is the fiber component of this divisor which splits into weights over the curve. We use this solution to make an ansatz for a well-defined flux as $G_4 = E_1(E_1 + 2E_2 + [b_2] - \Theta) +$ vertical correction terms. As in the previous case, the solution allows

for an arbitrary $U(1)$-flux contribution which can be subtracted. There is also a $U(1)$-flux with fixed coefficient appearing and after rewriting the flux in the chosen vertical basis we find the solution

$$
\begin{aligned}
G_4(\bar{\mathbf{5}}_{-\mathbf{4}}) &= -E_2^2 + E_3 E_4 - 3U\Theta - 3\bar{\mathcal{K}}\Theta \\
&\quad + \frac{1}{5}(1, -3, -7, -1)_i E_i[b_2] + \frac{1}{5}(-3, -1, 6, -2)_i E_i\bar{\mathcal{K}} + \frac{1}{5}(8, 16, 4, 7)_i E_i\Theta - \frac{1}{5}\mathrm{w}_{U(1)}\Theta \quad (5.3.12) \\
&= \frac{1}{50}(-G_4^{u_1} - 6G_4^{u_2} - 15G_4^{u_3}) - \frac{1}{5}\mathrm{w}_{U(1)}\Theta.
\end{aligned}
$$

The $\bar{\mathbf{5}}_{\mathbf{1}}$ surface

By the same method we find that

$$
\mathcal{C}_{\bar{\mathbf{5}}_{\mathbf{1}}} = E_3 \wedge (E_3 + 2E_4 + 3\bar{\mathcal{K}} - [b_2] - 2\Theta) \wedge [P_{SU(5)}]. \tag{5.3.13}
$$

By adding correction terms we get a well-defined, transversal flux which takes the form

$$
\begin{aligned}
G_4(\bar{\mathbf{5}}_{\mathbf{1}}) &= \frac{1}{2}E_2^2 - E_3 E_4 + \frac{1}{10}(-4, -3, -2, 4)_i E_i[b_2] + \frac{1}{10}(12, 19, 6, -7)_i E_i\bar{\mathcal{K}} + \frac{1}{5}(-4, -8, -2, 4)_i E_i\Theta \\
&= \frac{2}{50}(G_4^{u_1} - \frac{3}{2}G_4^{u_2}).
\end{aligned}
$$

$$(5.3.14)$$

We conclude with a summary of the full relation between the vertical flux solutions on one side and the matter surface fluxes on the other,

$$
\begin{aligned}
G_4(\bar{\mathbf{10}}_{\mathbf{2}}) &= \frac{1}{10}G_4^{u_2}, \\
G_4(\bar{\mathbf{5}}_{\mathbf{1}}) &= \frac{2}{50}(G_4^{u_1} - \frac{3}{2}G_4^{u_2}), \\
G_4(\bar{\mathbf{5}}_{-\mathbf{4}}) &= \frac{1}{50}(-G_4^{u_1} - 6G_4^{u_2} - 15G_4^{u_3}) - \frac{1}{5}\mathrm{w}_{U(1)}\Theta, \\
G_4(\mathbf{5}_{-\mathbf{6}}) &= \frac{1}{50}(G_4^{u_1} + 6G_4^{u_2} + 5G_4^{u_3}).
\end{aligned}
\tag{5.3.15}
$$

5.3.3 Chiralities and non-abelian anomalies

The chiralities induced by the general vertical flux solution $G_4(F) + \sum_i G_4^{u_i}$ are computed as

$$
\begin{aligned}
\chi(\mathbf{10}_{-\mathbf{2}}) &= -2[b_1]F\Theta + \left[u_1(-20[b_2] + 42\bar{\mathcal{K}} - 25\Theta) + u_2(-12\bar{\mathcal{K}} + 10\Theta) + u_3(6\bar{\mathcal{K}} - 3\Theta)\right]\bar{\mathcal{K}}\Theta, \\
\chi(\bar{\mathbf{5}}_{\mathbf{1}}) &= 2[c_{1,2}]F\Theta + 2\left[u_1(-10[b_2] - 14\bar{\mathcal{K}} + 5\Theta) + 4u_2\bar{\mathcal{K}} + u_3(-2\bar{\mathcal{K}} + \Theta)\right]([b_2 - 3\bar{\mathcal{K}} + 2\Theta])\Theta, \\
\chi(\bar{\mathbf{5}}_{-\mathbf{4}}) &= [-4([b_2] + [c_{2,1}])F + u_1(10[b_2]^2 - 16[b_2]\bar{\mathcal{K}} - 42\bar{\mathcal{K}}^2 + 10[b_2]\Theta + 61\bar{\mathcal{K}}\Theta - 20\Theta^2) \\
&\quad + 2u_2\bar{\mathcal{K}}(-2[b_2] + 6\bar{\mathcal{K}} - 3\Theta) + u_3(2[b_2]\bar{\mathcal{K}} - 6\bar{\mathcal{K}}^2 + 4[b_2]\Theta + 11\bar{\mathcal{K}}\Theta - 4\Theta^2)]\Theta, \\
\chi(\bar{\mathbf{5}}_{\mathbf{6}}) &= 2\left[3F + u_1(5[b_2] - 18\bar{\mathcal{K}} + 10\Theta) - 2u_2\bar{\mathcal{K}} + u_3(\bar{\mathcal{K}} - 3\Theta)\right][b_2]\Theta,
\end{aligned}
$$

$$(5.3.16)$$

where integration over the base is understood. Consistently, the $SU(5)$ anomaly cancellation condition

$$
\chi(\mathbf{10}_{-\mathbf{2}}) = \chi(\bar{\mathbf{5}}_{\mathbf{1}}) + \chi(\bar{\mathbf{5}}_{-\mathbf{4}}) + \chi(\bar{\mathbf{5}}_{\mathbf{6}}) \tag{5.3.17}
$$

holds for all choices of the coefficients u_i and for arbitrary base class F. As in the $\mathbb{Z}_2$ model, we can directly see the $SU(5)$ anomaly cancellation in the geometry because

$$
\begin{aligned}
&[\bar{\mathbf{10}}_{\mathbf{2}}] + [\bar{\mathbf{5}}_{\mathbf{1}}] + [\bar{\mathbf{5}}_{-\mathbf{4}}] + [\bar{\mathbf{5}}_{\mathbf{6}}] = \\
&[P_{SU(5)}] \wedge \left(2[b_2] \wedge (E_1 + E_2) + \bar{\mathcal{K}} \wedge (-E_2 + 3E_3 + E_4) + \Theta \wedge (-[b_2] + E_2 - E_3 - E_4)\right).
\end{aligned}
\tag{5.3.18}
$$

Again this is of the schematic form $E_i \wedge \pi^{-1}D_a + \pi^{-1}D_a \wedge \pi^{-1}D_b$, which yields zero when integrating a valid G_4-flux over it.

5.4   Comparison over the conifold transition

In this section we compare the flux solutions in the bisection $\mathbb{P}_{112}[4]$-fibration X_4 and in the related elliptic $\mathrm{Bl}^1\mathbb{P}_{112}[4]$-fibration Y_4 upon performing a topological transition between both sides. Since the construction of fluxes in F-theory models on elliptic fibrations is well established, as is the topology change in the conifold transition, we will interpret this as another test of our flux construction for the genus-one fibration. In particular, we will construct an explicit map between the flux solutions in both models and show that all fluxes in the bisection model are accounted for by a corresponding flux in the $U(1)$ model upon performing the conifold transition. This map has already been established in [10] in absence of additional non-abelian gauge data.

In order to find a map between the general flux solutions, we look for quantities that are preserved under the conifold transition. The first such quantity is the total D3-brane charge. Recall that the number of D3-branes is related to the flux and curvature induced D3-charge as [48]

$$n_{D3} = \frac{\chi(X_4)}{24} - \frac{1}{2}\int_{X_4} G_4 \wedge G_4. \tag{5.4.1}$$

We are interested in transitions without explicit participation of D3-branes, and for such transitions n_{D_3} must match on both sides of the transition [137]. We therefore demand that

$$\Delta n_{D3} \equiv n_{D3}|_{X_4} - n_{D3}|_{Y_4} \overset{!}{=} 0. \tag{5.4.2}$$

The topological transition from Y_4 to X_4 proceeds by first creating a conifold singularity in the fiber over the curve $C_1 \subset \mathcal{B}$ given in table 5.3.1 and then deforming [10, 11, 70, 84, 101, 117]. The resulting change [59, 89, 136]

$$\Delta\chi = \chi(X_4) - \chi(Y_4) = -3\chi(C_1) \tag{5.4.3}$$

of Euler numbers allows us to rephrase (5.4.2) in terms of the flux-induced D3 tadpoles as

$$\frac{1}{2}\int_{X_4} G_4 \wedge G_4 \overset{!}{=} -\frac{1}{8}\chi(C_1) + \frac{1}{2}\int_{Y_4} \tilde{G}_4 \wedge \tilde{G}_4. \tag{5.4.4}$$

Here G_4 and $\tilde{G}_4$ denote the fluxes on X_4 and Y_4, respectively.

The chiral spectra of the two models are topological quantities as well and must be conserved under the transition. This applies to the notion of chirality with respect to the unbroken gauge subgroups on both sides of the transition. In the case at hand, this is the non-abelian $SU(5)$ factor. From the field theory perspective this is clear because the Higgsing of the $U(1)$ gauge symmetry to a $\mathbb{Z}_2$ subgroup does not change the $SU(5)$ chiralities of the states. However, the number of individual matter curves as such is not equal. By comparing the discriminants (5.2.5) for $c_{4,1} \neq 0$ and (5.3.4) for $c_{4,1} = 0$, we confirm that the matter curves in the base relate as [10, 101]

$$
\begin{array}{ccc}
X_4 & & Y_4 \\
C_{\mathbf{10}} & \leftrightarrow & C_{\mathbf{10}_{-2}} \\
C_{\mathbf{\bar 5 A}} & \leftrightarrow & C_{\mathbf{\bar 5}_1} \\
C_{\mathbf{\bar 5 B}} & \leftrightarrow & C_{\mathbf{\bar 5}_{-4}} + \mathcal{C}_{\mathbf{\bar 5}_6}.
\end{array} \tag{5.4.5}
$$

Since the chiral indices are linear in the matter surface classes, we arrive at the following matching condition for the chiral spectra,

$$\chi(\mathbf{10}) \overset{!}{=} \chi(\mathbf{10_{-2}}),$$
$$\chi(\mathbf{\bar{5}^A}) \overset{!}{=} \chi(\mathbf{\bar{5}_1}),$$
$$\chi(\mathbf{\bar{5}^B}) \overset{!}{=} \chi(\mathbf{\bar{5}_{-4}}) + \chi(\mathbf{\bar{5}_6}). \tag{5.4.6}$$

To derive the map between the flux solutions recall first that $C_1 = (b_2, c_{3,1})$ is the doubly charged curve along which the Higgsing is performed. The Euler number of this singlet curve is given by

$$\chi(C_1) = \int_{C_1} c_1(C_1) \tag{5.4.7}$$

and with help of the adjunction formula

$$c(C_1) = \frac{c(\mathcal{B})}{1 + [(b_2, c_{3,1})]} \quad \Rightarrow \quad c_1(C_1) = c_1(\mathcal{B}) - [b_2] - [c_{3,1}] = \bar{\mathcal{K}} - [b_2] - ([\bar{\mathcal{K}} + [b_2] - \Theta]) = -[c_{4,1}] \tag{5.4.8}$$

the Euler number contribution is found as

$$-\frac{1}{8}\chi(C_1) = -\frac{1}{8}\int_{\mathcal{B}} c_1(C_1) \wedge [c_{3,1}] \wedge [b_2] = \frac{1}{8}\int_{\mathcal{B}} [b_2] \wedge [c_{3,1}] \wedge [c_{4,1}]. \tag{5.4.9}$$

To gain some intuition, let us first consider the situation in which we switch on only $U(1)$-flux $G_4(F)$ on Y_4 and no further vertical flux solutions. The tadpole contribution on the righthand side of (5.4.4) can then be evaluated as

$$-\frac{1}{8}\chi(C_1) + \frac{1}{2}\int_{Y_4} G_4(F) \wedge G_4(F) = \frac{1}{8}\int_{\mathcal{B}} [b_2] \wedge [c_{3,1}] \wedge [c_{4,1}] - \int_{\mathcal{B}} F \wedge F \wedge (\bar{\mathcal{K}} + [b_2] - \frac{2}{5}\Theta). \tag{5.4.10}$$

From the corresponding transition in [10] without $SU(5)$ gauge factor, and also from the general considerations in [136], we expect that we must allow, possibly amongst other fluxes, for non-vanishing $\mathbb{Z}_2$-flux $a\, G_4(P, \sigma_0)$ on X_4, with a coefficient a to be determined. Part of the contribution of such $a\, G_4(P, \sigma_0)$ to the lefthand side of (5.4.4) is given by the square $\frac{1}{2}\int_{X_4}(a\, G_4(P, \sigma_0))^2$ (in addition to cross-terms with the other fluxes). This expression requires in particular the calculation of the self-intersection of $[\sigma_0]$. The computation proceeds using the normal bundle of σ_0 embedded in the hypersurface [59] and closely follows the steps spelled out in [10]. The intersection numbers of $[\sigma_0]$ with the vertical correction term in (5.2.9) are straightforwardly computed in the ambient space, as is the self-intersection of the vertical correction terms. After reducing everything to base intersection numbers we obtain

$$\frac{1}{2}\int_{X_4}(aG_4(P, \sigma_0))^2 = \frac{25\, a^2}{4}\int_{\mathcal{B}}\left(-P \wedge P \wedge (\bar{\mathcal{K}} + [b_2] - \frac{2}{5}\Theta) + 2P \wedge [b_2] \wedge [c_{3,1}]\right). \tag{5.4.11}$$

Let us first see if it is sufficient to only invoke $a\, G_4(P, \sigma_0)$ in order to reproduce (5.4.10) on the $\mathbb{Z}_2$ side, i.e. whether we can match (5.4.10) and (5.4.11). As seen from (5.4.10), for a general choice of F the $U(1)$-tadpole has a quadratic term in Θ from the singlet curve (hidden in the classes $[c_{3,1}]$ and $[c_{4,1}]$), and a linear term in Θ from the flux contribution. On the other hand, the class P on the $\mathbb{Z}_2$ side may a priori be dependent or independent of Θ. If it carries no multiple of Θ, then the induced tadpole is only linear in the $SU(5)$ divisor class, which can be excluded. If $P = \ldots + k\Theta$ (which we expect, since $c_{4,1} = \rho\,\tau$), then the induced tadpole will have a cubic term in Θ, which has to be cancelled in order to match the $U(1)$-tadpole and the singlet curve term. We thus conclude that some

other flux has to be turned on in order to satisfy the constraint. In order to see what flux contribution is needed we make the general ansatz

$$G_4 = a\, G_4(P, \sigma_0) + \sum_{i=1}^{2} z_i\, G_4^{z_i} \tag{5.4.12}$$

for the flux on the $\mathbb{Z}_2$-side, with i running over the two solutions (5.2.17). We furthermore make an ansatz for the class $P = k\, F + \alpha\,[b_2] + \beta\, \bar{\mathcal{K}} + \gamma\, \Theta$ as a multiple of F plus a correction expanded in the base classes which are *generically* available on any choice of base $\mathcal{B}$. The resulting matching equations of induced tadpoles (5.4.4) and chiral indices (5.4.6) are quite lengthy and we do not display them explicitly here. For our ansatz above and $u_i = 0$, there is one solution given by

$$P = 10F + \frac{1}{2}c_{4,1}, \quad a = \frac{1}{5}, \quad z_1 = -\frac{1}{10}, \quad z_2 = \frac{1}{5}. \tag{5.4.13}$$

This confirms that it is not enough to turn on only $G_4(P, \sigma_0)$, but that it is also required to allow for the other vertical fluxes to find a matching configuration. This is in agreement with similar findings in [31, 89] for a transition from an $SU(5) \times U(1)$ elliptic fibration to an $SU(5)$ elliptic fibration.

Computing the D3-tadpole contributions for a general linear combination of fluxes on both sides of the conifold transition is tedious, but straightforward. We keep the general flux (5.4.12) in the bisection model and since we are searching for the most general solution, we make the ansatz $P = kF + \alpha[b_2] + \beta\bar{\mathcal{K}} + \gamma\Theta$. In the $U(1)$ model we add the linear combination

$$G_4 = G_4(F) + \sum_{i=1}^{3} u_i\, G_4^{u_i} \tag{5.4.14}$$

of all vertical flux solutions. The reduction of all intersection numbers in (5.4.4) and (5.4.6) to intersection numbers of base divisors results in a system of equations for the coefficients $a, z_i, u_i, k, \alpha, \beta$ and γ. The result is that both constraints (5.4.4) and (5.4.6) can be solved by

$$P = 10F + \frac{1}{2}c_{4,1} - 10u_3\Theta, \quad a = \frac{1}{5}, \quad z_1 = \frac{1}{10}(-1 + 100u_1), \quad z_2 = \frac{1}{5}(1 - 65u_1 - 10u_2 + 5u_3) \tag{5.4.15}$$

and we further note the Θ-term contribution to the class $P : \{\rho = 0\}$.

It is reassuring that the possible range $0 \leq P \leq c_{4,1}$ of the divisor class $P = [\rho]$ with $c_{4,1} = \rho\,\tau$ is in beautiful agreement with the observation that fluxes on the $U(1)$ side may obstruct the topological transition provided they induce a purely chiral spectrum of Higgs states [89, 136]. The Higgs fields are the charged singlets localised on the curve C_1. The formalism of [130] suggests that these are counted by the cohomology groups of a line bundle $\mathcal{L} \otimes K_{C_1}^{1/2}$ with $\deg(\mathcal{L}) = \int_{C_1}(10F - 10u_3\Theta)$. This is in agreement with a direct computation of the chiral spectrum of these states, starting from the general flux ansatz (5.4.14). A necessary condition for the existence of vectorlike pairs of Higgs fields, and thus for the existence of a flat direction for the conifold transition, is that $\frac{1}{2}c_1(C_1) \leq \deg(\mathcal{L}) \leq -\frac{1}{2}c_1(C_1)$. With $c_1(C_1) = -c_{4,1}|_{C_1}$ this is in agreement, for the solution $P = 10F + \frac{1}{2}c_{4,1} - 10u_3\Theta$, precisely with the inequality $0 \leq P \leq c_{4,1}$ – see the analogous discussion [10] in absence of an $SU(5)$ factor. For us, this serves as an additional consistency check of the whole construction.

5.5   Flux quantization and discrete anomalies

All results so far have been independent of the overall normalization of the constructed fluxes and tested only the transversality conditions as such. The proper normalization becomes crucial for instance when

it comes to detecting discrete anomalies such as the ones scrutinized in [45, 138]. In particular, the total number of D3-branes as determined by the tadpole equation (5.4.1) must be integer, and this is guaranteed [45] for a flux satisfying the quantization condition (2.6.2). Furthermore the chiral indices must be integer in a consistent theory and this should follow from the quantization condition as well. Indeed, as exemplified in previous sections, we can write the homology classes of all matter surfaces $\mathcal{C}_{\mathbf{R}}$ in terms of complete intersections on the hypersurface and so the $[\mathcal{C}_{\mathbf{R}}]$ are integer classes themselves. Hence

$$\int_{\mathcal{C}_{\mathbf{R}}} \left(G_4 + \frac{1}{2} c_2(M_4) \right) = \chi(\mathbf{R}) + \frac{1}{2} \int_{\mathcal{C}_{\mathbf{R}}} c_2(M_4) \in \mathbb{Z} \tag{5.5.1}$$

if the flux is quantized according to (2.6.2). Thus, as stressed in [47, 89], *if* $\frac{1}{2} \int_{\mathcal{C}_{\mathbf{R}}} c_2(M_4)$ is integer by itself for every matter surface, then the quantization condition ensures integrality of the chiral indices. To the best of our knowledge, it has not been proven from first principles in the literature that $c_2(M_4)$ automatically satisfies these constraints in any smooth Calabi-Yau genus-one fibration. In the sequel will analyze this constraint for the two fibrations X_4 and Y_4, and relate it to the cancellation of $\mathbb{Z}_2$ anomalies.

5.5.1 $c_2(M_4)$ and an arithmetic constraint

To compute $c_2(M_4)$ for M_4 either the $\mathbb{P}_{112}[4]$-fibration X_4 or the $\text{Bl}^1\mathbb{P}_{112}[4]$-fibration Y_4 we use the standard adjunction formula

$$c(M_4) = \frac{c(M_5)}{1 + [P]} \tag{5.5.2}$$

with P the respective hypersurface equation. The answer is expressed in the chosen vertical basis as

$$\begin{aligned}
c_2(X_4) = {}& 5U^2 - E_1 E_2 + \frac{7}{2} E_2^2 - 6 E_3 E_4 + \frac{1}{2}(-4, 9, 20, 4)_i E_i [b_2] + \frac{1}{2}(0, -19, -34, -3)_i E_i \bar{\mathcal{K}} \\
& + (0, -6, 4, -5)_i E_i \theta - 5U[b_2] + 11 U \bar{\mathcal{K}} + 7 U \theta \\
& - 6[b_2]\theta - 5[b_2]\bar{\mathcal{K}} + 7\bar{\mathcal{K}}\theta + [b_2]^2 + 5\bar{\mathcal{K}}^2 + c_2(\mathcal{B}),
\end{aligned} \tag{5.5.3}$$

$$\begin{aligned}
c_2(Y_4) = {}& -7U^2 + E_2^2 - E_3 E_4 + (-1, 2, 5, 2)_i E_i [b_2] + (-1, -7, -12, -4)_i E_i \bar{\mathcal{K}} \\
& + (0, -1, 4, 0)_i E_i \theta + U[b_2] - U\bar{\mathcal{K}} + 2U\theta - S[b_2] + 6S\bar{\mathcal{K}} + S\theta \\
& - [b_2]\theta - 5[b_2]\bar{\mathcal{K}} + 2\bar{\mathcal{K}}\theta + [b_2]^2 + 5\bar{\mathcal{K}}^2 + c_2(\mathcal{B}) .
\end{aligned} \tag{5.5.4}$$

Recall that the change in Euler characteristic between the two geometries is given by the Euler number of the doubly charged singlet curve. This provides a cross-check of the Chern classes computed above. The arithmetic genus $\chi_0 = 1 + h^{1,0} - h^{2,0} + ...$ is given by the integral of the Todd class over the 4-fold,

$$\chi_0 = \int_{M_4} Td(M_4) = \frac{1}{720} \int_{M_4} 3c_2^2 - c_4 = \frac{1}{720} \left[\int_{M_4} 3c_2^2 - \chi(M_4) \right] . \tag{5.5.5}$$

For a Calabi-Yau 4-fold the arithmetic genus is $\chi_0 = 2$, from which one gets a relation between the squared second Chern class and the Euler characteristic. In particular, for the change in Euler characteristic we have

$$\frac{1}{3}\Delta\chi = \int_{X_4} c_2(X_4)^2 - \int_{Y_4} c_2(Y_4)^2 . \tag{5.5.6}$$

In the conifold transition we have the relation (5.4.3), which in terms of the second Chern classes reads

$$\int_{X_4} c_2(X_4)^2 - \int_{Y_4} c_2(Y_4)^2 = -\chi(C_1) = \int_{\mathcal{B}} [b_2] \wedge [c_{3,1}] \wedge [c_{4,1}] . \tag{5.5.7}$$

Given the second Chern classes above it is straightforward to check that (5.5.7) indeed holds.

Note furthermore that for the quantization condition only $c_2(M_4)$ modulo even forms is relevant. In [46] it was shown that $c_2(\mathcal{B}) - \bar{\mathcal{K}}^2$ is an even class for smooth complex threefolds so that the terms $5\bar{\mathcal{K}}^2 + c_2(\mathcal{B})$ in $c_2(X_4)$ and $c_2(Y_4)$ can be eliminated mod 2. In principle the quantization condition can now be checked by demanding that the integral of $G_4 + \frac{1}{2}c_2(M_4)$ over every integer 4-cycle be integer. This requires finding an integral basis of $H^4(M_4)$, which we do not attempt here.

However, we make a curious observation: For the elliptic fibration Y_4, the integral of $c_2(Y_4)$ over the matter surfaces can be evaluated as

$$\frac{1}{2}\int_{\mathcal{C}_{\overline{\mathbf{10}}_2}} c_2(Y_4) \;=\; \frac{1}{2}\int_{\mathcal{B}} \Theta^2 \bar{\mathcal{K}}, \tag{5.5.8}$$

$$\frac{1}{2}\int_{\mathcal{C}_{\mathbf{5}_{-6}}} c_2(Y_4) \;=\; \frac{1}{2}\int_{\mathcal{B}} (-\bar{\mathcal{K}}[b_2]\Theta + [b_2]^2\Theta + [b_2]\Theta^2), \tag{5.5.9}$$

$$\frac{1}{2}\int_{\mathcal{C}_{\bar{\mathbf{5}}_{-4}}} c_2(Y_4) \;=\; \frac{1}{2}\int_{\mathcal{B}} (2\bar{\mathcal{K}}^2\Theta + 3\bar{\mathcal{K}}[b_2]\Theta + [b_2]^2\Theta - \bar{\mathcal{K}}\Theta^2 - [b_2]\Theta^2), \tag{5.5.10}$$

$$\frac{1}{2}\int_{\mathcal{C}_{\bar{\mathbf{5}}_1}} c_2(Y_4) \;=\; \int_{\mathcal{B}} (12\bar{\mathcal{K}}^2\Theta - 10\bar{\mathcal{K}}[b_2]\Theta + 2[b_2]^2\Theta - 12\bar{\mathcal{K}}\Theta^2 + 5[b_2]\Theta^2 + 3\Theta^3). \tag{5.5.11}$$

Note that the first three expressions are *not* automatically integer. However, in this case also the chiral indices would be non-integer as a result of (5.5.1). Similar expressions can be derived for the singlets.[3] A similar problem arises in the bisection model X_4, where the potentially non-integer pairings are

$$\begin{aligned}
\frac{1}{2}\int_{\mathcal{C}_{\overline{\mathbf{10}}}} c_2(X_4) &= \frac{1}{2}\int_{\mathcal{B}} \Theta^2 \bar{\mathcal{K}}\,, \\
\frac{1}{2}\int_{\mathcal{C}_{\bar{\mathbf{5}}\mathbf{A}}} c_2(X_4) &= \int_{\mathcal{B}} 2[b_2]^2 + 2\bar{\mathcal{K}}[b_2]\Theta - [b_2]\Theta^2 + \bar{\mathcal{K}}^2\Theta - \frac{1}{2}\bar{\mathcal{K}}\Theta^2\,.
\end{aligned} \tag{5.5.12}$$

Physical consistency therefore requires the expressions (5.5.8), (5.5.9), (5.5.10) (and also the expressions for the singlet surfaces) as well as (5.5.12) to be integer. Note that integrality of (5.5.8) and (5.5.9) of the $U(1)$ model implies integrality of the other expressions including (5.5.12) on the $\mathbb{Z}_2$ side, but integrality of (5.5.12) alone is not enough to guarantee integrality on the $U(1)$ side. We will resolve this puzzle momentarily.

In principle, the above observation could hint at an additional physical constraint such as a previously unnoticed anomaly which could require this. A more likely option is that these constraints are automatically satisfied for every smooth Calabi-Yau space Y_4 or X_4 described as the respective toric tops. In other words, integrality of the above expressions is most likely a necessary condition for a specific base $\mathcal{B}$, together with a choice of Θ and $[b_2]$, to give rise to a well-defined Calabi-Yau fibration Y_4 or X_4. It would be interesting, but certainly challenging to prove in full generality that in every geometrically consistent fibration $c_2(M_4)$ automatically satisfies these arithmetic properties.

5.5.2   Cancellation of $\mathbb{Z}_2$ anomalies

The quantization condition is also crucial in order investigate possible $\mathbb{Z}_2$ anomalies in the bisection model and their interplay with the G_4-flux. Due to the charge assignments the possible $\mathbb{Z}_2$ anomalies

---

[3]A related puzzle was also observed in [89] for the integral of $\frac{1}{2}c_2$ over the $\mathbf{10}_1$-matter surface in the vanilla $SU(5)\times U(1)$ restricted Tate model. Interestingly, existence of a smooth type IIB limit of the latter model implies that this equation is integer, reproducing the known result that the Freed-Witten anomaly cancellation in Type IIB guarantees integer chiralities [47, 139].

[140] are given by the chiral index of the $\bar{\mathbf{5}}^{\mathbf{A}}$ states modulo 2,

$$\mathcal{A}_{\mathbb{Z}_2^3} = \sum_{\mathbf{R}} (q_{\mathbf{R}}^{\mathbb{Z}_2})^3 \dim(\mathbf{R}) \chi(\mathbf{R}) = \chi(\bar{\mathbf{5}}^{\mathbf{A}}) \bmod 2, \tag{5.5.13}$$

$$\mathcal{A}_{\mathbb{Z}_2 - SU(5)^2} = \sum_{\mathbf{R}} q_{\mathbf{R}}^{\mathbb{Z}_2} c(\mathbf{R}) \chi(\mathbf{R}) = \chi(\bar{\mathbf{5}}^{\mathbf{A}}) \bmod 2, \tag{5.5.14}$$

$$\mathcal{A}_{\mathbb{Z}_2 - \text{grav.}} = \sum_{\mathbf{R}} q_{\mathbf{R}}^{\mathbb{Z}_2} \dim(\mathbf{R}) \chi(\mathbf{R}) = \chi(\bar{\mathbf{5}}^{\mathbf{A}}) \bmod 2 \tag{5.5.15}$$

with $c(\mathbf{R})$ the index of the representation. In general, discrete field theoretic anomalies need not vanish by themselves provided they are cancelled by a suitable discrete version of the Green-Schwarz mechanism [134]. This happens when an anomalous $U(1)$ is Higgsed to a discrete subgroup which is also anomalous. In this case, the anomalous discrete subgroup is not preserved at the non-perturbative level because instantons can violate it. In our case, however, the $\mathbb{Z}_2$ symmetry *is* exact at the non-perturbative level. Potential non-perturbative effects would be M2-brane instantons or fluxed M5-instantons. Their interplay with the discrete symmetry $\mathbb{Z}_2$ has been studied in detail recently [43, 135], and as expected from the general formalism of [74, 103] the discrete symmetry is indeed non-perturbatively exact. Therefore the mixed $\mathbb{Z}_2$ symmetries must vanish by themselves. Consistently, we can adapt the analysis of [62] of the Green-Schwarz mechanism for (mixed) abelian anomalies. The potential Green-Schwarz counter-terms would then be proportional to

$$\int_{X_4} G_4 \wedge \hat{U} \wedge D_a. \tag{5.5.16}$$

As a result of the transversality condition (5.1.8) this vanishes identically, confirming once more that the $\mathbb{Z}_2$ anomalies must vanish by themselves.

We would like to see the manifestation of this field theoretic argument in the geometry. To this end, we use the homology relations (5.2.12) and the SR-ideal (5.2.2) to rewrite the homology class $[\mathcal{C}_{\bar{\mathbf{5}}^{\mathbf{A}}}]$ as

$$[P_{SU(5)}] \wedge \left(2\,E_3 \wedge E_4 - U \wedge \Theta + E_3 \wedge (4\,\bar{\mathcal{K}} - 2\,[b_2]) + \Theta \wedge ([b_2] + E_2 - 2\,E_3 + E_4 - \bar{\mathcal{K}}) \right). \tag{5.5.17}$$

In this representation we see that if we impose the transversality conditions (5.1.8), (5.1.9) and the gauge symmetry condition (5.1.10) on G_4, then we simply have

$$\chi(\bar{\mathbf{5}}^{\mathbf{A}}) = \int_{X_4} G_4 \wedge (2\,E_3 \wedge E_4). \tag{5.5.18}$$

The question now is whether $\int_{X_4} G_4 \wedge E_3 \wedge E_4 \in \mathbb{Z}$ since this would imply that the chirality is even and therefore the discrete $\mathbb{Z}_2$ anomalies vanish. For a well-quantized flux satisfying the quantization condition $G_4 + \frac{1}{2} c_2(X_4) \in H^4(X_4, \mathbb{Z})$, with $c_2(X_4)$ given in (5.5.3), $\mathbb{Z}_2$ cancellation would follow from $1/2 \int_{X_4} c_2 \wedge E_3 \wedge E_4 \in \mathbb{Z}$, since $E_3 \wedge E_4$ is manifestly integer. Direct calculation reveals that

$$\begin{aligned} &\int_{X_4} \frac{c_2(X_4)}{2} \wedge E_3 \wedge E_4 = \\ &\int_{\mathcal{B}} \Theta \wedge \left(\frac{1}{2}(c_2(\mathcal{B}) - \bar{\mathcal{K}}^2) - \bar{\mathcal{K}}^2 - \Theta^2 \right) - \frac{1}{2} \left([b_2]^2\,\Theta - 3\,\bar{\mathcal{K}}\,[b_2]\,\Theta + 3\,[b_2]\Theta^2 - 5\,\bar{\mathcal{K}}\,\Theta^2 \right). \end{aligned} \tag{5.5.19}$$

While the first term is integer (using the result cited above that $c_2(\mathcal{B}) - \bar{\mathcal{K}}^2$ is even), the latter part is not guaranteed to be integer without any further input. However, if we assume integrality of all chiral indices in the $U(1)$ model, i.e. integrality of (5.5.8), (5.5.9) and (5.5.10), then also (5.5.19) is integral and therefore the discrete $\mathbb{Z}_2$-anomalies vanish by themselves. On the other hand, if we impose

integrality of chiral indices (5.5.12) as well as the absence of anomalies in the $\mathbb{Z}_2$ model, the arithmetic constraints on the fibration guarantee a consistent (i.e. integral) chiral spectrum of the $U(1)$ model.

Therefore we see that physical consistency conditions on both the $U(1)$ and the $\mathbb{Z}_2$ model pose *exactly* the same constraints on the geometry. Since the $\mathbb{Z}_2$ and the $U(1)$ model are related by a conifold transition, it is not surprising that cancellation of the $\mathbb{Z}_2$ anomalies requires not only integrality of (5.5.12), but of the corresponding expressions in the $U(1)$ model. We know that any consistent $\mathbb{Z}_2$ fibration defined by $[b_2]$ and Θ on the base $\mathcal{B}$ originates via Higgsing from a $U(1)$ model over the same base with the same fibration data $[b_2]$ and Θ. Now if the $U(1)$ model is consistent, the chiralities and therefore also (5.5.8), (5.5.9) and (5.5.10) must be integer. These intersection properties of $\mathcal{B}$ of course still hold in the $\mathbb{Z}_2$ model and lead to integrality of (5.5.12) as well as the vanishing of the discrete anomaly. From a field theoretic perspective, cancellation of the discrete anomalies is tied to a consistent embedding of the discrete symmetry into a gauged continuous symmetry at high energies. This underlying gauge symmetry is precisely the $U(1)$ symmetry of the model on Y_4 and the relation between consistency of the latter and discrete anomaly cancellation is also expected from this point of view.

Finally, note that the crucial relation (5.5.18) depends not only on the conditions (5.1.9) and (5.1.10), as does the proof for cancellation of the non-abelian cubic anomaly, but also on (5.1.8), where the bisection appears explicitly. This is our final consistency check of the transversality conditions.

5.6   Summary

In this chapter we have systematically studied gauge fluxes in F-theory compactifications on genus-one fibrations. These are F-theory backgrounds without a zero section that provide an embedding of the base manifold into the fibration. Our starting point has been a generalization of the known transversality conditions on 4-form fluxes in F-theory models on elliptic 4-folds to compactifications on genus-one fibrations. The role of the zero-section in these conditions is replaced by the available multi-section which defines an embedding of a multi-cover of the base into the 4-fold. We have then put our proposal for the flux consistency conditions to test by constructing all vertical fluxes available for a bisection fibration including an extra non-abelian gauge factor, which for definiteness we have taken to be $SU(5)$. The total gauge group in F-theory is thus $SU(5) \times \mathbb{Z}_2$. We have focused on those fluxes which exist over a generic base $\mathcal{B}$ without imposing further conditions on the intersection numbers. For a concrete choice of such a base, additional solutions to the transversality conditions may of course arise. We have derived general expressions for the chiral indices of all matter states and confirmed that the transversality conditions automatically imply cancellation of the cubic non-abelian anomalies. As a further test we have dynamically related the constructed fluxes to a basis of vertical fluxes in an F-theory model with gauge group $SU(5) \times U(1)$ which is related to the $SU(5) \times \mathbb{Z}_2$ model via a conifold transition [10, 11, 70, 84, 101, 117]. We have found perfect match between both sets of fluxes in such a way that a dynamical transition implies a change in the flux quantum numbers without changing the induced M2/D3-brane charge and the chiral indices. This parallels earlier studies performed in [10, 59, 89, 136].

A typical challenge in the construction of gauge fluxes is the proper quantization in the sense of [45–47]. We have shown that a smooth fibration of the type considered must necessarily satisfy a set of arithmetic constraints on certain intersection numbers in the base which guarantee that, independently of the concrete choice of fluxes, all chiral indices are integer. It would be very interesting to prove in full generality that these arithmetic constraints automatically hold on smooth fibrations solely based on geometric arguments. With the help of these relations we have been able to exemplify that the discrete $\mathbb{Z}_2$ anomalies vanish by themselves. This is in agreement [103] with the fact in this

geometry non-perturbative effects respect the $\mathbb{Z}_2$-symmetry [43, 135].

An obvious next step would be to apply the same reasoning also to genus-one fibrations with higher-degree multi-sections such as the trisection ($\mathbb{Z}_3$) model studied in [70, 141]. From a phenomenological point of view, discrete symmetries are known to be crucial ingredients in MSSM and GUT model building. A systematic search for 3-generation models e.g. with gauge group $SU(5) \times \mathbb{Z}_2$ (with $\mathbb{Z}_2$ playing the role of R-parity, as exemplified in [10, 101]) can now be undertaken, along the lines of the global 3-generation examples [31, 132] based on elliptic fibrations with other gauge groups.

Finally, recall that in general, the gauge data associated with the 3-form potential C_3 and its 4-form field strength G_4 in F/M-theory is encoded [142, 143] in the Deligne cohomology group $H_{\mathcal{D}}^4(\hat{Y}, \mathbb{Z}(2))$. A useful parametrization of this rather abstract object can be given in terms of algebraic 4-cycles, up to rational equivalence [130]. When speaking of fluxes, it is typically only the cohomology class that one specifies, but one should keep in mind that this data is sufficient only for the computation of topological quantities such as chiral indices or flux-induced charges. A more refined analysis also of the vector-like spectrum, possibly along the lines of [130] (or, alternatively, [30]), would be desirable and important also for fibrations without section. This would be an interesting topic for a future project.

Chapter 6

Summary and outlook

We have studied in this thesis discrete structures in F-theory compactified on elliptic and genus-one fibrations. The central objects of study, sections and multisections are global objects and require a full understanding of the fibrations. This is contrasted to the study of e.g non-abelian gauge symmetries as they are localised along divisors in the base and can be studied in local F-theory models. By representing the torus fiber as a hypersurface in an ambient toric variety the fibrations can be studied in great generality, without having to specify the base of the fibration. This means that the four-dimensional effective gauge theories are in effect large classes of gauge theories which share generic features coming from the fiber structure.

The fact that the F-theory backgrounds are torus-fibered Calabi-Yau varieties has big computational virtues. By using methods and theorems from algebraic geometry the four dimensional gauge theory data may be computed, often with ease. While many of these techniques are well known tools for F-theory compactifactions we have in this work extended the computational reach and enlargened the 'tool box' for F-theory model building. In particular we have utilized the theory of ideals of polynomial rings and prime ideal decomposition in the computation of the singlet curves in section 4.1, and in the systematic computation of gauge fluxes in terms of matter surfaces, e.g in eq. (5.3.15).

As highlighted in the introduction, and discussed in some detail in chapter 2, F-theory can be defined as the generalisation of type IIB string theory at any value of the string coupling. The general characteristics of an F-theory fibration and in particular the computationals methods are independent of whether the dual type IIB theory is weakly coupled. The intuition from type IIB theory with branes can be used as a guiding principle for the physics related to singularities in different codimensions, but is not needed because of the definition through M-theory. All the models studied in this thesis and the results pertaining to torsional sections and discrete selection rules are non-perturbative as they make no reference to the weakly coupled type IIB limit. This is another aspect in which F-theory is a valuable framework for studying generic properties of gauge theories.

In chapter 3 we studied in depth the role of torsional elements in the Mordell-Weil group of an elliptic fibration [9]. Guided by earlier results [69] from eight-dimensional compactifications we showed how the global structure of the gauge group in four dimensions is determined by torsional sections. The foremost difference between two gauge theories whose gauge groups share the same Lie algebra is in the matter representation content. All states in all representations of a Lie algebra are collected in the so called weight lattice. If the Mordell-Weil torsion group is trivial, all these representations lift from the algebra to representations of the gauge group. We showed how the presence of a torsional section forces the weight lattice to be coarser. The remaining states in the lattice are exactly the ones transforming under the gauge group, in this case a finite quotient of the universal covering group. From the representation theory data we derived the change in the center of the gauge group, and the

change of fundamental group relative to the universal cover.

In numerous explicit examples we computed the gauge groups and matter content in four dimensional compactifications with torsional sections. Here we considered three classes of fibrations with Mordell-Weil group $\mathbb{Z}_2$, $\mathbb{Z} \oplus \mathbb{Z}_2$ and $\mathbb{Z}_3$. These are the three generic hypersurface representations of an elliptic fibration with torsion and the class of the torsional section descends from an ambient toric divisor. In each of these geometries we introduced further non-abelian singularities and computed the matter spectrum. The first signs of a non-simply connected gauge groups was noticed through the absence of matter representations which normally would be present. By using the properties of the divisor class of the torsional section we showed how the weight lattice got coarser than what would be that case without torsion. This explained the restricted matter spectrum. By using the representation theoretical data we computed the center and fundamental groups of the gauge groups. This together with the knowledge of the gauge algebra gives the four dimensional gauge group.

It would be interesting to extend this work to bigger torsion groups. By describing the fiber as a complete intersection in a toric variety, as opposed to a hypersurface, further examples could be studied [144]. In particular it would be interesting to study a fibration with Mordell-Weil group $\mathbb{Z} \oplus \mathbb{Z}_6$. By implementing a $\mathfrak{su}(3) \times \mathfrak{su}(2)$ gauge algebra an $(SU(3) \times SU(2) \times U(1))/\mathbb{Z}_6$ gauge theory would be plausible. This would be an interesting starting point for an F-theory realisation of the Standard Model with realistic matter spectrum.

In chapter 4 we changed focus from elliptic fibrations to genus-one fibrations [10, 11]. In general an F-theory compactification on a genus-one fibration with an n-section has a discrete $\mathbb{Z}_n$ symmetry in four dimensions. For definiteness we considered here the case of a bisection. The genus-one fibration is related to an elliptic fibration with an extra $U(1)$ symmetry by a conifold transition. In this topological transition a curve in the fiber shrinks to zero size and introduces a singularity. By deforming the hypersurface equation to a genus-one fibration this singularity is smoothened out. This deformation of the geometry is identified by the higgsing of the $U(1)$ to a $\mathbb{Z}_2$ symmetry in four dimensions. There are two choices in how to shrink a curve in the fiber which, in the M-theory perspective, give rise to two different gauge theories in three dimensions. These two M-theory phases share the same F-theory limit in four dimensions. Important and interesting is how the discrete symmetry in four dimensions arise in two different ways which we adressed in section 4.4.

Discrete symmetries in compactifications of type IIA string theory are known to arise from torsion in the homology of the compactification space. We stress here the difference between torsion homology and torsion in the Mordell-Weil group of elliptic fibrations. The two M-theory phases correspond to compactifications on the genus-one fibration and its associated Jacobian fibration. We show how the torsion homology cycles appear by studying the Jacobian of the genus-one fibration, and explain why no torsion is present in the genus-one fibration. To extend this result and show how the torsion homology cycles appear in genus-one fibrations with trisections or even higher degree multisections would be an interesting subject for future work. We also note here a curious relationship between Mordell-Weil torsion and multi-section fibrations. In the classification of hypersurface representations of tori through reflexive polygons the fibrations with n-sections are dual to fibrations with $\mathbb{Z}_n$ torsional sections. This is an example of mirror symmetry, applied fiberwise. It would be interesting to study this in more detail and for more examples.

From the perspective of model building discrete symmetries are interesting as selection rules. In section 4.6 we introduced an additional $SU(5)$ gauge factor in the models with $\mathbb{Z}_2$ and $U(1)$ symmetries and showed geometrically how to assign $\mathbb{Z}_2$ charges to all matter representations. As expected from the higgsing of the $U(1)$ symmetry by a field of charge 2 the discrete charges was found to correspond to the $U(1)$ charges modulo two. We also demonstrated how the geometrically realised Yukawa couplings are singlets under the discrete symmetry.

In the last chapter we studied gauge fluxes on genus-one fibrations [12]. The introduction of flux in F-theory is essential for having a chiral matter spectrum. The consistent fluxes on elliptic fibrations are solutions to certain transversality conditions. We have shown how these consistency conditions can be generalised to genus-one fibrations. To test our proposal for transversal fluxes in models with discrete symmetries we computed all gauge fluxes in the $SU(5) \times \mathbb{Z}_2$ fibration from chapter 4. In addition we constructed a non-vertical flux solution related to the bisection. By computing all chiral indices we showed that the solutions to our proposed transversality condition induce an anomaly free chiral matter spectrum. To further test our construction we computed all gauge fluxes also in the $SU(5) \times U(1)$ fibration which is related by a conifold transition. The chiral indices and the number of D3 branes are invariants under this transition. We showed that this is indeed that case and how the flux solution on one side of the transition rearrange to preserve the anomaly free chiral spectrum and the total D3 charge. A model with $SU(5) \times \mathbb{Z}_2$ symmetry would be an interesting starting point for an supersymmetric GUT model with R-parity. By the use of the techniques for computing all gauge fluxes a systematic search for 3-generation models could be performed.

In addition to the transversality condition any flux solution in F-theory must be properly quantized. In essence this amounts to finding flux solutions in the integral cohomology of the fibration and is a subtle problem. For the model with discrete symmetry we showed that assuming a properly quantized flux this implies that the discrete gauge anomaly vanishes. This served as a final test of our proposal for consistent fluxes on genus-one fibrations.

Appendix A

In this appendix we present the details of the resolved fibers in the models with additional non-abelian gauge groups in chapter 3. We show the explicit form of the irreducible fiber curves in codimension one and two. The ambient coordinates that can not vanish due to SR-ideal relations are for simplicity set to one.

A.1 $\mathfrak{su}(4)$ top over polygon 13

Here provide the explicit equations for the fiber components of the $(SU(4) \times SU(2))/\mathbb{Z}_2$-model discussed in section 3.3.3.

A.1.1 Codimension one

The equations for the fiber components over $\{w = 0\} \subset \mathcal{B}$ are

$$
\begin{aligned}
e_0 = 0: \quad & e_1 + a_1 tz - e_3 t^4 = 0 & (y = s = e_2 = 1)\,, \\
e_1 = 0: \quad & a_1 styz - e_0 e_2 e_3 st^2 z^2 a_{2,1} - e_0^2 e_3 z^4 a_{4,2} - e_2^2 e_3 s^2 t^4 = 0\,, \\
e_2 = 0: \quad & e_1 - e_3 a_{4,2} + a_1 t = 0 & (y = s = z = e_0 = 1)\,, \\
e_3 = 0: \quad & e_1 + a_1 t = 0 & (y = s = z = 1)\,.
\end{aligned}
\tag{A.1.1}
$$

Here we impose the SR-ideal (3.3.39). The four curves $\mathbb{P}_i^1$ of these divisors intersect like the nodes of the affine Dynkin diagram of A_3.

A.1.2 Codimension two

Over $\{w = a_{4,2} = 0\}$ we obtain:

$$
\begin{aligned}
e_0 = 0: \quad & a_1 tz - e_3 t^4 + e_1 = 0 & (y = s = e_2 = 1)\,, \\
e_1 = 0: \quad & s\,t\,\underbrace{\left(e_0 e_2 e_3 tz^2 a_{2,1} - a_1 yz + e_2^2 e_3 st^3\right)}_{R1} = 0\,, \\
e_2 = 0: \quad & a_1 t + e_1 = 0 & (y = s = z = e_0 = 1)\,, \\
e_3 = 0: \quad & a_1 t + e_1 = 0 & (y = s = z = 1)\,,
\end{aligned}
\tag{A.1.2}
$$

and over $\{w = a_1 = 0\}$:

$$
\begin{aligned}
e_0 = 0: \quad & e_1 - e_3 t^4 = 0 & (y = s = e_2 = 1)\,, \\
e_1 = 0: \quad & e_3 \underbrace{\left(e_0 e_2 s t^2 z^2 a_{2,1} + e_0^2 z^4 a_{4,2} + e_2^2 s^2 t^4\right)}_{R2} = 0\,, \\
e_2 = 0: \quad & e_1 - e_3 a_{4,2} = 0 & (y = s = z = e_0 = 1)\,, \\
e_3 = 0: \quad & e_1 = 0 & (y = s = z = 1)\,.
\end{aligned}
\tag{A.1.3}
$$

Before calculating the weights we analyse the parts $R1$ and $R2$ in detail. For $R1$ one can check that the divisors $\{e_2 = 0\}$, $\{e_3 = 0\}$, $\{t = 0\}$ and $\{z = 0\}$ do not intersect the divisor given by $R1$ in the toric variety given by the projection along e_1. Therefore we can rewrite it as

$$
e_0\, a_{2,1} - y\, a_1 + s = 0
\tag{A.1.4}
$$

with e_0, y and s the homogeneous coordinates of $\mathbb{P}^2$. Since (A.1.4) is a linear equation, we obtain a $\mathbb{P}^1$ for the curve given by $e_1 = 0 = R1$. In the case of $R2$, we find that $\{e_0 = 0\}$, $\{e_2 = 0\}$, $\{z = 0\}$ and $\{t = 0\}$ does not intersect the divisor $R2$ in the toric variety given by the projection along e_1. Hence, we rewrite $R2$ as

$$
s\, a_{2,1} + a_{4,2} + s^2 = 0,
\tag{A.1.5}
$$

where s is now the affine coordinate parametrising $\mathbb{C}$ and the remaining homogeneous coordinates y and e_3 parametrise a $\mathbb{P}^1$. Therefore, we obtain two $\mathbb{P}^1$s from $R2$ which are, however, exchanged when going along the matter curve. Around the branch points $\{w = a_1 = a_{4,2} - \frac{1}{4} a_{2,1}^2 = 0\}$ the solutions of s to (A.1.5) are exchanged.

A.2 $\mathfrak{su}(4)$ top over polygon 15

This appendix contains more information on the $(SU(4) \times SU(2) \times SU(2))/\mathbb{Z}_2 \times U(1)$ fibration presented in section 3.4.3.

A.2.1   Codimension one

The irreducible fiber components over $\{\varpi = 0\}$ are:

$$
\begin{aligned}
e_0 = 0: \quad & e_2 e_3 u^2 + e_1 e_2 w^2 + \gamma_1 u w z = 0 & (c = d = v = 1)\,, \\
e_1 = 0: \quad & e_2 d v^2 + \gamma_1 d v w + \delta_2 e_0 = 0 & (c = u = z = e_3 = 1)\,, \\
e_2 = 0: \quad & \gamma_1 c u v + \gamma_2 e_0 e_1 + \delta_2 e_0 e_3 c u^2 = 0 & (d = w = z = 1)\,, \\
e_3 = 0: \quad & e_2 + \gamma_1 u + \gamma_2 e_0 = 0 & (c = d = v = w = z = e_1 = 1)\,.
\end{aligned}
\tag{A.2.1}
$$

The resolution $\mathbb{P}^1$'s is the intersection of above equations with two generic and independent divisors in the base and they intersect in the pattern of the affine A_3 Dynkin diagram.

A.2.2   Codimension two

Over $\{\varpi = \gamma_1 = 0\}$ the components of the fiber factorizes as

$$
\begin{aligned}
e_0 = 0: \quad & e_2(e_3 u^2 + e_1 w^2) = 0 & (c = d = v = 1)\,, \\
e_1 = 0: \quad & e_2 d v^2 + \delta_2 e_0 = 0 & (c = u = z = e_3 = 1)\,, \\
e_2 = 0: \quad & e_0(\gamma_2 e_1 + \delta_2 e_3 c u^2) = 0 & (d = w = z = 1)\,, \\
e_3 = 0: \quad & e_2 + \gamma_2 e_0 = 0 & (c = d = v = w = z = e_1 = 1)
\end{aligned}
\tag{A.2.2}
$$

and the components intersect as the affine D_4 Dynkin diagram.

Over $\{\varpi = \gamma_2 = 0\}$ the components of the fiber factorizes as

$$
\begin{aligned}
e_0 = 0 : \quad & e_2 e_3 u^2 + e_1 e_2 w^2 + \gamma_1 uwz = 0 && (c = d = v = 1)\,, \\
e_1 = 0 : \quad & e_2 dv^2 + \gamma_1 dvw + \delta_2 e_0 = 0 && (c = u = z = e_3 = 1)\,, \\
e_2 = 0 : \quad & cu(\gamma_1 v + \delta_2 e_0 e_3 u) = 0 && (d = w = z = 1)\,, \\
e_3 = 0 : \quad & e_2 + \gamma_1 u = 0 && (c = d = v = w = z = e_1 = 1)
\end{aligned}
\tag{A.2.3}
$$

with the intersection structure given by the affine A_5 Dynkin diagram.

Over $\{\varpi = \delta_2 = 0\}$ the components of the fiber factorizes as

$$
\begin{aligned}
e_0 = 0 : \quad & e_2 e_3 u^2 + e_1 e_2 w^2 + \gamma_1 uwz = 0 && (c = d = v = 1)\,, \\
e_1 = 0 : \quad & dv(e_2 v + \gamma_1 w = 0) && (c = u = z = e_3 = 1)\,, \\
e_2 = 0 : \quad & \gamma_1 cuv + \gamma_2 e_0 e_1 = 0 && (d = w = z = 1)\,, \\
e_3 = 0 : \quad & e_2 + \gamma_1 u + \gamma_2 e_0 = 0 && (c = d = v = w = z = e_1 = 1)
\end{aligned}
\tag{A.2.4}
$$

intersecting as the affine A_5 Dynkin diagram.

A.3 $\mathfrak{su}(6)$ top over polygon 16

The fiber structure of the $(SU(6) \times SU(3))/\mathbb{Z}_3$-fibration of section 3.5.2 can be summarized as follows:

A.3.1   Codimension one

The irreducible fiber components over $\{w = 0\}$ take the form

$$
\begin{aligned}
e_0 = 0 : \quad & e_1 e_3 p^3 + e_3 e_5 x^3 + a_1 pxz = 0 && (s = q = e_2 = e_4 = 1)\,, \\
e_1 = 0 : \quad & e_3 + a_1 p = 0 && (x = s = q = z = e_4 = e_5 = 1)\,, \\
e_2 = 0 : \quad & a_3 e_1 + a_1 pqsx + e_3 qs^2 x^3 = 0 && (z = e_0 = e_4 = e_5 = 1)\,, \\
e_3 = 0 : \quad & a_3 e_0^2 e_1 e_5 + a_1 x = 0 && (s = q = p = z = 1) \\
e_4 = 0 : \quad & e_3 + a_3 e_5 + a_1 x = 0 && (s = q = p = z = e_0 = e_1 = e_2 = 1) \\
e_5 = 0 : \quad & e_3 + a_1 x = 0 && (s = q = p = z = e_1 = e_2 = 1)\,.
\end{aligned}
\tag{A.3.1}
$$

The resolution $\mathbb{P}^1$'s is the intersection of above equations with two generic and independent divisors in the base and they intersect in the pattern of the affine A_5 Dynkin diagram.

A.3.2   Codimension two

Over $\{w = a_1 = 0\}$ the components of the fiber takes the form

$$
\begin{aligned}
e_0 = 0 : \quad & e_3(e_1 p^3 + e_5 x^3) = 0 && (s = q = e_2 = e_4 = 1)\,, \\
e_1 = 0 : \quad & e_3 = 0 && (x = y = s = q = z = e_4 = e_5 = 1)\,, \\
e_2 = 0 : \quad & a_3 e_1 + e_3 qs^2 x^3 = 0 && (y = z = e_0 = e_4 = e_5 = 1)\,, \\
e_3 = 0 : \quad & a_3 e_0^2 e_1 e_5 = 0 && (y = s = q = p = z = 1) \\
e_4 = 0 : \quad & e_3 + a_3 e_5 = 0 && (y = s = q = p = z = e_0 = e_1 = e_2 = 1) \\
e_5 = 0 : \quad & e_3 = 0 && (y = s = q = p = z = e_1 = e_2 = 1)
\end{aligned}
\tag{A.3.2}
$$

resulting in 6 distinct $\mathbb{P}^1$'s, intersecting as the E_6 Dynkin diagram (*not affine*).

Over $\{w = a_3 = 0\}$ the components of the fiber takes the form

$$
\begin{array}{llr}
e_0 = 0: & e_1 e_3 p^3 + e_3 e_5 x^3 + a_1 pxz = 0 & (s = q = e_2 = e_4 = 1)\,, \\
e_1 = 0: & e_3 + a_1 p = 0 & (x = y = s = q = z = e_4 = e_5 = 1)\,, \\
e_2 = 0: & qsx(a_1 p + e_3 sx^2) = 0 & (y = z = e_0 = e_4 = e_5 = 1)\,, \\
e_3 = 0: & a_1 x = 0 & (y = s = q = p = z = 1) \\
e_4 = 0: & e_3 + a_1 x = 0 & (y = s = q = p = z = e_0 = e_1 = e_2 = 1) \\
e_5 = 0: & e_3 + a_1 x = 0 & (y = s = q = p = z = e_1 = e_2 = 1)
\end{array}
\tag{A.3.3}
$$

resulting in 9 distinct $\mathbb{P}^1$'s, intersecting as the affine A_8 Dynkin diagram.

Appendix B

In this appendix we present some technical details from chapter 4. The scaling relations for the divisor classes in the models with $SU(5) \times \mathbb{Z}_2$ and $SU(5) \times U(1)$ apply to the models in chapter 5 as well.

B.1 Discrete subgroups after Higgsing

In this appendix we derive in detail the remnant discrete subgroup after Higgsing a $U(1)$ in the presence of matter charged under another 'spectator' gauge group. We exemplify our general results for additional $U(1)$ or $SU(N)$ spectator groups as appearing in the recent F-theory literature.

As is well-known, if we give a VEV to a field transforming only under a $U(1)$ with charge q^H, we Higgs the $U(1)$ gauge symmetry to $\mathbb{Z}_{q^H}$. However, this is only true if the $U(1)$-charges of all the fields $\{\varphi_I\}$[1] charged under the $U(1)$ are properly normalised or co-prime[2] , i.e. $\mathrm{GCD}(\{q^I\}) = \mathrm{GCD}(\{q^H, q^i\}) = 1$. Therefore, the actual discrete symmetry is $\mathbb{Z}_{q^H/\mathrm{GCD}(\{q^I\})}$. To prevent cumbersome notation we will use capital letters for co-prime charges, i.e. $Q^I = q^I/\mathrm{GCD}(\{q^I\})$.

Further subtleties can arise if some of the fields $\{\varphi_i\}$ transform in non-trivial representations of other abelian or non-abelian gauge symmetries G_r (with abelian discrete subgroups). This is because a subgroup $\mathbb{Z}_{N_{\mathrm{sub}}}$ of $\mathbb{Z}_{Q^H}$ might be part (or all) of the discrete abelian subgroups $\mathbb{Z}_{N_r}$ of G_r and thus needs to be divided out to avoid double-counting. In such a situation the actual remaining symmetry group after Higgsing is

$$G_r \times \frac{\mathbb{Z}_{Q^H}}{\mathbb{Z}_{N_{\mathrm{sub}}}}.$$

To obtain the subgroup $\mathbb{Z}_{N_{\mathrm{sub}}}$ we first consider the subgroup $\mathbb{Z}_{N_{\mathrm{tsg}}}$ of $\mathbb{Z}_{Q^H}$ which acts trivially on all the fields $\{\varphi_\alpha\} \subset \{\varphi_I\}$ which are uncharged under G_r. The generator of $\mathbb{Z}_{N_{\mathrm{tsg}}}$ is given by taking

$$\mathrm{LCM}\left(\left\{\frac{\mathrm{LCM}(Q^\alpha, Q^H)}{Q^\alpha}\right\}\right)$$

times the generator of $\mathbb{Z}_{Q^H}$, i.e.

$$N_{\mathrm{tsg}} = \frac{Q^H}{\mathrm{LCM}\left(\left\{\frac{\mathrm{LCM}(Q^\alpha, Q^H)}{Q^\alpha}\right\}\right)}.$$

---

[1]Note that this set also includes the Higgs H, i.e. the field which obtains the VEV. In the sequel we will sometimes treat the Higgs field, for presentational purposes, separately. In this case we will use a lower case i to denote all fields different from the Higgs.

[2]Note that in the full theory there are also line operators which define a quantised unit charge independent of matter fields. However in the following analysis we are concerned with discrete symmetries acting on matter fields and with such symmetries there is not a notion of an absolute charge but only a relative one.

If $\text{GCD}(N_{\text{tsg}}, N_r) \neq 1$ then there can be a subgroup $\mathbb{Z}_{N_{\text{sub}}}$ of both $\mathbb{Z}_{N_{\text{tsg}}}$ and $\mathbb{Z}_{N_r}$ such that the elements of the representations of $\mathbb{Z}_{N_{\text{tsg}}}$ and $\mathbb{Z}_{N_r}$ agree on this subgroup $\mathbb{Z}_{N_{\text{sub}}}$. In this case N_{sub} is the order of this subgroup. If $\text{GCD}(N_{\text{tsg}}, N_r) = 1$, there cannot be a common non-trivial subgroup of both $\mathbb{Z}_{N_{\text{tsg}}}$ and $\mathbb{Z}_{N_r}$.

To be more specific about the identification of $\mathbb{Z}_{N_{\text{sub}}}$, we will now consider two explicit examples, given by $G_r = SU(N)$ with $N = 4, 5$ and, respectively, $G_r = U(1)$. For the first example with $G_r = SU(N)$, we specify the matter content, i.e. the set of fields $\{\varphi_I\}$, as appearing in the theories realised (by top constructions) in [83, 92],

$$\mathbf{1}_{2N}, \qquad \mathbf{1}_N, \qquad \boxed{}_{2n}, \qquad \left\{\square_{n+iN}\right\}_{i \in S_i} \tag{B.1.1}$$

with $n = 0, \ldots, N - 1$ for the different tops, S_i some 'integer interval' which has zero as an element, cf. [20], and $\square$ and $\boxed{}$ the fundamental and anti-symmetric representation, respectively. The subscripts next to the states denote the charge under the $U(1)$ which is Higgsed by giving $\mathbf{1}_{2N}$ a VEV. Q^H is therefore

$$Q^H = \begin{cases} 10 & : N = 5, \, n = 1, \ldots, 4 \\ 2 & : N = 5, \, n = 0 \end{cases}, \qquad Q^H = \begin{cases} 8 & : N = 4, \, n = 1, 3 \\ 4 & : N = 4, \, n = 2 \\ 2 & : N = 4, \, n = 0 \end{cases}. \tag{B.1.2}$$

Since there is only one additional $SU(N)$ singlet with half the $U(1)$-charge of the Higgs, one concludes $N_{\text{tsg}} = \frac{1}{2}Q^H$. Hence for $n = 0$, $N_{\text{sub}} = 1$. For the rest we have to work a bit more. The action of $\mathbb{Z}_{N_{\text{tsg}}}$ on the fields can be identified by with a $\mathbb{Z}_{\frac{1}{2}Q^H}$ action with generator

$$e^{2\pi i \frac{2Q^i}{Q^H}} \quad \text{with} \quad \left(2\frac{Q^{\boxed{}}_{2n}}{Q^H}, 2\frac{Q^{\square}_n}{Q^H}\right) \cong \begin{cases} \left(\frac{2n}{N}, \frac{n}{N}\right) = \left(\frac{2n}{5}, \frac{n}{5}\right) & : N = 5, \, n = 1, \ldots, 4 \\ \left(\frac{2n}{N}, \frac{n}{N}\right) = \left(\frac{2n}{4}, \frac{n}{4}\right) & : N = 4, \, n = 1, 3 \\ \left(\frac{2n}{N}, \frac{n}{N}\right) \cong \left(0, \frac{1}{2}\right) & : N = 4, \, n = 2 \end{cases}. \tag{B.1.3}$$

We have given only one generator of $\mathbb{Z}_{N_{\text{tsg}}}$ for the fundamentals because they are the same for all i's. In the first two cases $\mathbb{Z}_{N_{\text{tsg}}}$ agrees with the center of $SU(5)$ and $SU(4)$, respectively. In the last case only the $\mathbb{Z}_2$ subgroup of the $SU(4)$ center is generated. Hence we obtain

$$\frac{\mathbb{Z}_{Q^H}}{\mathbb{Z}_{N_{\text{sub}}}} = \begin{cases} \mathbb{Z}_{10}/\mathbb{Z}_5 & : N = 5, \, n = 1, \ldots, 4 \\ \mathbb{Z}_2 & : N = 5, \, n = 0 \end{cases}, \qquad \frac{\mathbb{Z}_{Q^H}}{\mathbb{Z}_{N_{\text{sub}}}} = \begin{cases} \mathbb{Z}_8/\mathbb{Z}_4 & : N = 4, \, n = 1, 3 \\ \mathbb{Z}_4/\mathbb{Z}_2 & : N = 4, \, n = 2 \\ \mathbb{Z}_2 & : N = 4, \, n = 0 \end{cases}. \tag{B.1.4}$$

We find that the discrete part is for all examples $\mathbb{Z}_2$. Its realisation depends however strongly on the matter content. For $\mathbb{Z}_{10}/\mathbb{Z}_5$ and $\mathbb{Z}_8/\mathbb{Z}_4$ there is a (canonical) representative within the equivalence class generating the $\mathbb{Z}_2$, which acts either with 1 or -1 on all the matter states—like for the $n = 0$ cases where the charges are right from the beginning either zero or one-half. However there is no such representative for $N = 4$ and $n = 1, 3$.[3]

Our second example is a $U(1)_a \times U(1)_b$-model with the matter content

$$\mathbf{1}_{0,2}, \qquad \mathbf{1}_{-1,-2}, \qquad \mathbf{1}_{1,-1}, \qquad \mathbf{1}_{1,0}, \qquad \mathbf{1}_{-1,-1}, \qquad \mathbf{1}_{0,1}. \tag{B.1.5}$$

This theory is realised by F-theory on the elliptic fibrations studied in [52, 63, 83, 92]. We Higgs this model in two different ways. In the first case we will give $\mathbf{1}_{0,2}$ a VEV and in the second case we switch

---

[3]Repeating the same analysis for a spectator $SU(2)$ with charge one modulo two for the fundamentals, one finds a remaining $\mathbb{Z}_4/\mathbb{Z}_2$-symmetry upon switching on a VEV for the singlet of charge four. This situation describes a transition from the $\text{Bl}^1\mathbb{P}_{[1,1,2]}$-fibration to a $\mathbb{P}_{[1,1,2]}$-fibration in the presence of an $SU(2)$. Hence one would naively expect a $\mathbb{Z}_4$ after Higgsing, cf. [70], but as the above analysis shows the actual discrete abelian group is just $\mathbb{Z}_2$.

on a VEV for $\mathbf{1}_{-1,-2}$. For $\langle \mathbf{1}_{0,2} \rangle \neq 0$ the situation is pretty obvious. First of all we note that all the charges are co-prime. Secondly, the Higgs $\mathbf{1}_{0,2}$ is only charged under $U(1)_b$. Hence, $G_r = U(1)_a$ and $\mathbb{Z}_{Q^H} = \mathbb{Z}_2$. There is one other field $\mathbf{1}_{0,1}$ which is only charged under the second factor. Hence, $N_{\text{tsg}} = 1$ and

$$U(1)_a \times \mathbb{Z}_2$$

is the remaining symmetry. This agrees with the model considered in [70].

Alternatively let us consider a Higgsing with $\langle \mathbf{1}_{-1,-2} \rangle \neq 0$. In this case, we have to choose a different basis for the $U(1)$s. For general q_a^H and q_b^H, the direction which leaves φ_H invariant is

$$\phi_a = \frac{\text{LCM}(q_a^H, q_b^H)}{q_a^H} \phi_{a'} , \qquad \phi_b = -\frac{\text{LCM}(q_a^H, q_b^H)}{q_b^H} \phi_{a'} . \tag{B.1.6}$$

The second direction we choose such that it generates together with (B.1.6) the $\mathbb{Z}^2$ charge-lattice of $U(1)_a \times U(1)_b$, i.e.

$$\phi_a = D \, \phi_{b'} , \quad \phi_b = C \, \phi_{b'} \quad \text{with} \quad C \frac{\text{LCM}(q_a^H, q_b^H)}{q_a^H} + D \frac{\text{LCM}(q_a^H, q_b^H)}{q_b^H} = 1 . \tag{B.1.7}$$

Hence, we obtain $(2, -1)$ for the $U(1)_{a'}$ direction and for $U(1)_{b'}$ we choose $(-1, 0)$ out of the possible solutions to (B.1.7). The states (B.1.5) read as follows in the new $U(1)_{a'} \times U(1)_{b'}$ basis:

$$\mathbf{1}_{-2,0}, \qquad \mathbf{1}_{0,1}, \qquad \mathbf{1}_{3,-1}, \qquad \mathbf{1}_{2,-1}, \qquad \mathbf{1}_{-1,1}, \qquad \mathbf{1}_{-1,0} . \tag{B.1.8}$$

Since all the Q^I charges are co-prime and $Q^H = 1$, the remaining symmetry is just $U(1)_{a'}$.

B.2   Singlet matter curves

In this appendix we give the explicit form of the complicated matter curves in the model with an extra $U(1)$ and the model with a bisection. The ideal C_2 in (4.1.9) with 15 generators has the form

$$(c_1 b_2^4 - b_1 c_2 b_2^3 - b_0 c_3 b_2^3 + b_1^2 c_3 b_2^2 + 2c_2 c_3 b_2^2 - 3b_1 c_3^2 b_2 + 2c_3^3,$$
$$4c_0 b_2^4 + b_1 c_1 b_2^3 - 4b_0 c_2 b_2^3 + 4c_2^2 b_2^2 - b_1^2 c_2 b_2^2 + 3b_0 b_1 c_3 b_2^2 - 2c_1 c_3 b_2^2 - 2b_0 c_3^2 b_2 + b_1^3 c_3 b_2$$
$$\quad - 4b_1 c_2 c_3 b_2 - b_1^2 c_3^2 + 4c_2 c_3^2,$$
$$2b_1 c_0 b_2^3 - b_0 c_1 b_2^3 - b_0 b_1 c_2 b_2^2 + 2c_1 c_2 b_2^2 + b_0^2 c_3 b_2^2 - 4c_0 c_3 b_2^2 + b_0 b_1^2 c_3 b_2 - 2b_1 c_1 c_3 b_2 - b_0 b_1 c_3^2 + 2c_1 c_3^2,$$
$$\quad - c_3^2 b_0^2 + b_1 b_2 c_3 b_0 - b_1 b_2^2 c_1 b_0 + b_2^2 c_1^2 + 4c_0 c_3^2 + b_1^2 b_2^2 c_0 - 4b_1 b_2 c_0 c_3,$$
$$b_2 c_3 b_0^3 - b_2^2 c_1 b_0^2 + b_1 b_2 c_2 b_0^2 - 2c_2 c_3 b_0^2 - b_1^2 b_2 c_1 b_0 - 4b_2 c_0 c_3 b_0 + 2b_1 c_1 c_3 b_0 + b_1 b_2 c_1^2 + b_1^3 b_2 c_0 + 4b_2^2 c_0 c_1$$
$$\quad - 4b_1 b_2 c_0 c_2 - 2c_1^2 c_3 - 2b_1^2 c_0 c_3 + 8c_0 c_2 c_3,$$
$$c_0 b_1^4 - b_0 c_1 b_1^3 + c_1^2 b_1^2 + 2b_0 b_2 c_0 b_1^2 + b_0^2 c_2 b_1^2 - 8c_0 c_2 b_1^2 - 3b_0^2 b_2 c_1 b_1 + 4b_2 c_0 c_1 b_1 + 4b_0 c_1 c_2 b_1 - b_0^3 c_3 b_1$$
$$\quad + 4b_0 c_0 c_3 b_1 + 16b_2^2 c_0^2 + 2b_0 b_2 c_1^2 - 4b_0^2 c_2^2 + 16c_0 c_2^2 - 4b_0^2 b_2^2 c_0 - 4c_1^2 c_2 + 4b_0^3 b_2 c_2 - 16b_0 b_2 c_0 c_2$$
$$\quad + 2b_0^2 c_1 c_3 - 8c_0 c_1 c_3,$$
$$\quad - c_3 b_0^4 + b_2 c_1 b_0^3 + b_1 c_2 b_0^3 - 2b_1 b_2 c_0 b_0^2 - b_1^2 c_1 b_0^2 - 2c_1 c_2 b_0^2 + 8c_0 c_3 b_0^2 + 3b_1 c_1^2 b_0 + b_1^3 c_0 b_0 - 4b_2 c_0 c_1 b_0$$
$$\quad - 4b_1 c_0 c_2 b_0 - 2c_1^3 + 8b_1 b_2 c_0^2 - 2b_1^2 c_0 c_1 + 8c_0 c_1 c_2 - 16c_0^2 c_3,$$
$$c_0 c_3^2 b_1^3 - b_0 c_1 c_3^2 b_1^2 + b_2 c_1^2 c_3 b_1^2 - 4b_2 c_0 c_2 c_3 b_1^2 + 4b_2^2 c_0 c_2^2 b_1 + 6b_0 b_2 c_0 c_3^2 b_1 + b_0^2 c_2 c_3^2 b_1 - b_2^2 c_1^2 c_2 b_1$$
$$\quad - 2b_2^2 c_0 c_1 c_3 b_1 + b_2^3 c_1^3 - b_0^3 c_3^3 - b_0^2 b_2 c_1 c_3^2 - 4b_2^3 c_0 c_1 c_2 + 8b_2^3 c_0^2 c_3 + b_0 b_2^2 c_1^2 c_3 - 4b_0 b_2^2 c_0 c_2 c_3,$$
$$b_2 c_1 c_3 b_1^3 - c_1 c_3^2 b_1^2 - b_2^2 c_1 c_2 b_1^2 - 2b_0 b_2 c_2 c_3 b_1^2 + b_2^3 c_1^2 b_1 + 2b_0 b_2^2 c_2^2 b_1 + 4b_0^2 b_2 c_3^2 b_1 - 4b_2 c_0 c_3^2 b_1 + 2b_0 c_2 c_3^2 b_1$$
$$\quad - b_0 b_2^2 c_1 c_3 b_1 - 4b_0^2 c_3^3 + 8c_0 c_3^3 - 2b_0 b_2 c_1 c_3^2 - 2b_0 b_2^3 c_1 c_2 + 2b_2^2 c_1^2 c_3 + 4b_0 b_2^3 c_0 c_3 - 2b_0^2 b_2^2 c_2 c_3,$$
$$b_2 c_3 b_1^4 - c_3^2 b_1^3 - b_2^2 c_2 b_1^3 + b_2^3 c_1 b_1^2 - b_0 b_2^2 c_3 b_1^2 - 4b_2 c_2 c_3 b_1^2 + 4b_2^2 c_2^2 b_1 + 6b_0 b_2 c_3^2 b_1 + 4c_2 c_3^2 b_1 + 2b_2^2 c_1 c_3 b_1$$
$$\quad - 4b_0 c_3^3 - 4b_2 c_1 c_3^2 - 4b_2^3 c_1 c_2 + 8b_2^3 c_0 c_3 - 4b_0 b_2^2 c_2 c_3,$$
$$b_0 b_2 c_3 b_1^3 - b_0 c_3^2 b_1^2 - b_0 b_2^2 c_2 b_1^2 - 2b_2 c_1 c_3 b_1^2 + 2c_1 c_3^2 b_1 + b_0 b_2^3 c_1 b_1 + 2b_2^2 c_1 c_2 b_1 - b_0^2 b_2^2 c_3 b_1 + 4b_2^2 c_0 c_3 b_1$$
$$\quad - 2b_2^3 c_1^2 + 2b_0^2 b_2 c_3^2 - 8b_2 c_0 c_3^2,$$
$$\quad - b_2^2 c_3 b_0^3 - b_1 c_3^2 b_0^2 + b_2^3 c_1 b_0^2 - b_1 b_2^2 c_2 b_0^2 + b_1^2 b_2 c_3 b_0^2 + 2b_2 c_2 c_3 b_0^2 + 4b_2^2 c_0 c_3 b_0 - 2b_1 b_2 c_1 c_3 b_0 + 4b_1 c_0 c_3^2$$
$$\quad - 4b_2^3 c_0 c_1 + 4b_1 b_2^2 c_0 c_2 + 2b_2 c_1^2 c_3 - 2b_1^2 b_2 c_0 c_3 - 8b_2 c_0 c_2 c_3,$$
$$\quad - c_3^2 b_0^3 - 2b_2^2 c_2 b_0^3 + 2b_1 b_2 c_3 b_0^3 + 2b_2 c_2^2 b_0^2 + 2b_2^3 c_0 b_0^2 - b_2 c_1 c_3 b_0^2 - b_1 c_2 c_3 b_0^2 + 4c_0 c_3^2 b_0 + 8b_2^2 c_0 c_2 b_0$$
$$\quad - 2b_1 b_2 c_1 c_2 b_0 - 8b_1 b_2 c_0 c_3 b_0 + b_1^2 c_1 c_3 b_0 - 8b_2^3 c_0^2 - 8b_2 c_0 c_2^2 + 2b_2 c_1^2 c_2 + 2b_1^2 b_2 c_0 c_2 - b_1 c_1^2 c_3$$
$$\quad - b_1^3 c_0 c_3 + 4b_2 c_0 c_1 c_3 + 4b_1 c_0 c_2 c_3,$$
$$b_2 c_3 b_0^4 - b_2^2 c_1 b_0^3 - c_2 c_3 b_0^3 + b_1 b_2^2 c_0 b_0^2 + b_2 c_1 c_2 b_0^2 - 6b_2 c_0 c_3 b_0^2 + b_1 c_1 c_3 b_0^2 - b_1 b_2 c_1^2 b_0 + 4b_2^2 c_0 c_1 b_0$$
$$\quad - c_1^2 c_3 b_0 - b_1^2 c_0 c_3 b_0 + 4c_0 c_2 c_3 b_0 + b_2 c_1^3 - 4b_1 b_2 c_0^2 + b_1^2 b_2 c_0 c_1 - 4b_2 c_0 c_1 c_2 + 8b_2 c_0^2 c_3,$$
$$2b_2 c_2 b_0^4 - 2c_2^2 b_0^3 - 2b_2^2 c_0 b_0^3 - 2b_1 b_2 c_1 b_0^3 + c_1 c_3 b_0^3 + b_2 c_1^2 b_0^2 + 2b_1^2 b_2 c_0 b_0^2 - 8b_2 c_0 c_2 b_0^2 + 3b_1 c_1 c_2 b_0^2$$
$$\quad - 2b_1 c_0 c_3 b_0^2 + 8b_2^2 c_0^2 b_0 - b_1^2 c_1^2 b_0 + 8c_0 c_2^2 b_0 + 4b_1 b_2 c_0 c_1 b_0 - 2c_1^2 c_2 b_0 - 2b_1^2 c_0 c_2 b_0 - 4c_0 c_1 c_3 b_0$$
$$\quad + b_1 c_1^3 - 4b_1^2 b_2 c_0^2 + b_1^3 c_0 c_1 - 4b_1 c_0 c_1 c_2 + 8b_1 c_0^2 c_3).$$

$$(B.2.1)$$

The matter locus in the $\mathbb{Z}_2$ model is given by the ideal C in (4.2.13). The explicit form is

$$(c_4^3 b_1^6 - 3b_2 c_3 c_4^2 b_1^5 - 8c_2 c_4^3 b_1^4 + 3c_3^2 c_4^2 b_1^4 + 2b_2^2 c_2 c_4^2 b_1^4 + 3b_2^2 c_3^2 c_4 b_1^4 - b_2^3 c_3^3 b_1^3 + 16b_2 c_2 c_3 c_4^2 b_1^3 - 6b_2 c_3^3 c_4 b_1^3$$
$$\quad - 4b_2^3 c_2 c_3 c_4 b_1^3 + 3b_2^2 c_3^4 b_1^2 - 64c_0 c_4^4 b_1^2 + 16c_2^2 c_4^2 b_1^2 + 32b_2^2 c_0 c_4^3 b_1^2 + 16c_1 c_3 c_4^3 b_1^2 + 2b_2^4 c_2 c_3^2 b_1^2$$
$$\quad - 8b_2^2 c_2^2 c_4^2 b_1^2 - 16c_2 c_3^2 c_4^2 b_1^2 - 4b_2^4 c_0 c_4^2 b_1^2 - 8b_2^2 c_1 c_3 c_4^2 b_1^2 + 3c_3^4 c_4 b_1^2 + b_2^4 c_2^2 c_4 b_1^2 - 4b_2^2 c_2 c_3^2 c_4 b_1^2$$
$$\quad + b_2^4 c_1 c_3 c_4 b_1^2 - 3b_2 c_3^5 b_1 - 4b_2^3 c_2 c_3^3 b_1 + 64b_2 c_0 c_3 c_4^3 b_1 - b_2^5 c_1 c_3^2 b_1 - 16b_2 c_1 c_3^2 c_4^2 b_1 - 16b_2 c_2^2 c_3 c_4^2 b_1$$
$$\quad - 32b_2^3 c_0 c_3 c_4^2 b_1 - b_2^5 c_2^2 c_3 b_1 + 16b_2 c_2 c_3^3 c_4 b_1 + 8b_2^3 c_1 c_3^2 c_4 b_1 + 8b_2^3 c_2^2 c_3 c_4 b_1 + 4b_2^5 c_0 c_3 c_4 b_1 + c_3^6$$

$$+ 2b_2^2 c_2 c_3^4 + 64 c_1^2 c_4^4 + b_2^4 c_1 c_3^3 - 48 b_2^2 c_1^2 c_3^3 - 64 c_1 c_2 c_3 c_4^3 + b_2^4 c_2^2 c_3^2 - b_2^6 c_0 c_3^2 + 16 c_1 c_3^3 c_4^2 + 12 b_2^4 c_1^2 c_4^2$$
$$+ 16 c_2^2 c_3^2 c_4^2 - 16 b_2^2 c_0 c_3^2 c_4^2 + 48 b_2^2 c_1 c_2 c_3 c_4^2 + b_2^6 c_1 c_2 c_3 - 8 c_2 c_3^4 c_4 - 8 b_2^2 c_1 c_3^3 c_4 - b_2^6 c_1^2 c_4 - 8 b_2^2 c_2^2 c_3^2 c_4$$
$$+ 8 b_2^4 c_0 c_3^2 c_4 - 12 b_2^4 c_1 c_2 c_3 c_4,$$

$$4 c_4^3 b_1^5 - 10 b_2 c_3 c_4^2 b_1^4 - 32 c_2 c_4^3 b_1^3 + 12 c_3^2 c_4^2 b_1^3 + 8 b_2^2 c_2 c_4^2 b_1^3 + 7 b_2^2 c_3^2 c_4 b_1^3 - b_2^3 c_3^3 b_1^2 + 16 b_2 c_1 c_4^3 b_1^2 - 4 b_2^3 c_1 c_4^2 b_1^2$$
$$+ 40 b_2 c_2 c_3 c_4^2 b_1^2 - 16 b_2 c_3^3 c_4 b_1^2 - 10 b_2^3 c_2 c_3 c_4 b_1^2 + 3 b_2^2 c_3^4 b_1 - 256 c_0 c_4^4 b_1 + 64 c_2^2 c_4^3 b_1 + 128 b_2^2 c_0 c_4^3 b_1$$
$$+ 32 c_1 c_3 c_4^3 b_1 + b_2^4 c_2 c_3^2 b_1 - 32 b_2^2 c_2^2 c_4^2 b_1 - 48 c_2 c_3^2 c_4^2 b_1 - 16 b_2^4 c_0 c_4^2 b_1 - 32 b_2^2 c_1 c_3 c_4^2 b_1 + 8 c_3^4 c_4 b_1$$
$$+ 4 b_2^2 c_2^2 c_4 b_1 + 8 b_2^2 c_2 c_3^2 c_4 b_1 + 6 b_2^4 c_1 c_3 c_4 b_1 - 2 b_2 c_3^5 + 128 b_0 c_1 c_4^4 + b_0 b_2^4 c_3^3 - 2 b_2^3 c_2 c_3^3 - 64 b_0 b_2^2 c_1 c_4^3$$
$$- 64 b_2 c_1 c_2 c_4^3 + 128 b_2 c_0 c_3 c_4^3 - 64 b_0 c_2 c_3 c_4^3 - b_2^5 c_1 c_3^2 + 16 b_0 c_3^3 c_4^2 + 8 b_0 b_2^4 c_1 c_4^2 + 32 b_2^3 c_1 c_2 c_4^2$$
$$- 64 b_2^3 c_0 c_3 c_4^2 + 32 b_0 b_2^2 c_2 c_3 c_4^2 - 8 b_0 b_2^2 c_3^3 c_4 + 8 b_2 c_2 c_3^3 c_4 + 4 b_2^3 c_1 c_3^2 c_4 - 4 b_2^5 c_1 c_2 c_4 + 8 b_2^5 c_0 c_3 c_4$$
$$- 4 b_0 b_2^4 c_2 c_3 c_4,$$

$$c_1 b_2^4 - b_1 c_2 b_2^3 - b_0 c_3 b_2^3 + b_1^2 c_3 b_2^2 + 2 c_2 c_3 b_2^2 + 2 b_0 b_1 c_4 b_2^2 - 8 c_1 c_4 b_2^2 - 3 b_1 c_3^2 b_2 - b_1^3 c_4 b_2 + 4 b_1 c_2 c_4 b_2$$
$$+ 4 b_0 c_3 c_4 b_2 + 2 c_3^3 - 8 b_0 b_1 c_4^2 + 16 c_1 c_4^2 + 2 b_1^2 c_3 c_4 - 8 c_2 c_3 c_4,$$

$$2 c_4^2 b_1^5 - 5 b_2 c_3 c_4 b_1^4 + 3 b_2^2 c_3^2 b_1^3 - 16 c_2 c_4^2 b_1^3 + 6 c_3^2 c_4 b_1^3 + 4 b_2^2 c_2 c_4 b_1^3 - 7 b_2 c_3^3 b_1^2 + 8 b_2 c_1 c_4^2 b_1^2 - 5 b_2^3 c_2 c_3 b_1^2$$
$$- 2 b_2^3 c_1 c_4 b_1^2 + 20 b_2 c_2 c_3 c_4 b_1^2 + 4 c_3^4 b_1 - 128 c_0 c_4^3 b_1 + 2 b_2^4 c_2^2 b_1 + b_0 b_2^3 c_3^2 b_1 + 6 b_2^2 c_2 c_3^2 b_1 + 32 c_2^2 c_4^2 b_1$$
$$+ 64 b_2^2 c_0 c_4^2 b_1 + 16 c_1 c_3 c_4^2 b_1 + 3 b_2^4 c_1 c_3 b_1 - 16 b_2^2 c_2^2 c_4 b_1 - 4 b_0 b_2 c_3^2 c_4 b_1 - 24 c_2 c_3^2 c_4 b_1 - 8 b_2^4 c_0 c_4 b_1$$
$$- 16 b_2^2 c_1 c_3 c_4 b_1 - 2 b_0 b_2^2 c_3^3 + 64 b_0 c_1 c_4^3 - 2 b_2^3 c_1 c_3^2 - 32 b_0 b_2^2 c_1 c_4^2 - 32 b_2 c_1 c_2 c_4^2 + 64 b_2 c_0 c_3 c_4^2$$
$$- 32 b_0 c_2 c_3 c_4^2 - 2 b_2^5 c_1 c_2 + 4 b_2^5 c_0 c_3 - 2 b_0 b_2^4 c_2 c_3 + 8 b_0 c_3^3 c_4 + 8 b_2 c_1 c_3^2 c_4 + 4 b_0 b_2^4 c_1 c_4 + 16 b_2^3 c_1 c_2 c_4$$
$$- 32 b_2^3 c_0 c_3 c_4 + 16 b_0 b_2^2 c_2 c_3 c_4,$$

$$- c_3 c_4 b_1^4 + b_2 c_3^2 b_1^3 + 4 b_0 c_4^2 b_1^3 - c_3^3 b_1^2 - 8 c_1 c_4^2 b_1^2 - b_2^2 c_2 c_3 b_1^2 - 6 b_0 b_2 c_3 c_4 b_1^2 + 8 c_2 c_3 c_4 b_1^2 + 3 b_0 b_2^2 c_3^2 b_1$$
$$- 4 b_2 c_2 c_3^2 b_1 + 32 b_2 c_0 c_4^2 b_1 - 16 b_0 c_2 c_4^2 b_1 + b_2^3 c_1 c_3 b_1 - 8 b_2^3 c_0 c_4 b_1 + 4 b_0 b_2^2 c_2 c_4 b_1 + 4 b_2 c_1 c_3 c_4 b_1$$
$$- 2 b_0 b_2 c_3^3 + 4 c_2 c_3^3 - 2 b_2^2 c_1 c_3^2 - 16 b_0 b_2 c_1 c_4^2 + 32 c_1 c_2 c_4^2 + 4 b_2^2 c_2^2 c_3 + 4 b_2^4 c_0 c_3 - 4 b_0 b_2^3 c_2 c_3$$
$$+ 4 b_0 b_2^3 c_1 c_4 - 8 b_2^2 c_1 c_2 c_4 - 16 c_2^2 c_3 c_4 - 16 b_2^2 c_0 c_3 c_4 + 16 b_0 b_2 c_2 c_3 c_4,$$

$$- c_4 b_1^5 + b_2 c_3 b_1^4 - c_3^2 b_1^3 - b_2^2 c_2 b_1^3 + 2 b_0 b_2 c_4 b_1^3 + 8 c_2 c_4 b_1^3 + b_2^3 c_1 b_1^2 - b_0 b_2^2 c_3 b_1^2 - 4 b_2 c_2 c_3 b_1^2 - 8 b_2 c_1 c_4 b_1^2$$
$$- 8 b_0 c_3 c_4 b_1^2 + 4 b_2^2 c_2^2 b_1 + 6 b_0 b_2 c_3^2 b_1 + 4 c_2 c_3^2 b_1 + 64 c_0 c_4^2 b_1 + 2 b_2^2 c_1 c_3 b_1 - 16 c_2^2 c_4 b_1 - 16 b_2^2 c_0 c_4 b_1$$
$$+ 8 c_1 c_3 c_4 b_1 - 4 b_0 c_3^3 - 4 b_2 c_1 c_3^2 - 32 b_0 c_1 c_4^2 - 4 b_2^3 c_1 c_2 + 8 b_2^3 c_0 c_3 - 4 b_0 b_2^2 c_2 c_3 + 8 b_0 b_2^2 c_1 c_4$$
$$+ 16 b_2 c_1 c_2 c_4 - 32 b_2 c_0 c_3 c_4 + 16 b_0 c_2 c_3 c_4,$$

$$- c_4 b_1^4 + b_2 c_3 b_1^3 - c_3^2 b_1^2 - b_2^2 c_2 b_1^2 - 2 b_0 b_2 c_4 b_1^2 + 8 c_2 c_4 b_1^2 + b_2^3 c_1 b_1 + 3 b_0 b_2^2 c_3 b_1 - 4 b_2 c_2 c_3 b_1 - 4 b_2 c_1 c_4 b_1$$
$$- 4 b_0 c_3 c_4 b_1 + 4 b_2^2 c_2^2 - 2 b_0 b_2 c_3^2 + 4 c_2 c_3^2 - 16 b_0^2 c_4^2 + 64 c_0 c_4^2 + 4 b_2^4 c_0 - 4 b_0 b_2^3 c_2 - 2 b_2^2 c_1 c_3 + 4 b_0^2 b_2^2 c_4$$
$$- 16 c_2^2 c_4 - 32 b_2^2 c_0 c_4 + 16 b_0 b_2 c_2 c_4 + 8 c_1 c_3 c_4,$$

$$- b_0 c_4 b_1^3 + b_0 b_2 c_3 b_1^2 + 2 c_1 c_4 b_1^2 - b_0 c_3^2 b_1 + 2 b_2^2 c_0 b_1 - b_0 b_2^2 c_2 b_1 - 2 b_2 c_1 c_3 b_1 - 8 b_2 c_0 c_4 b_1 + 4 b_0 c_2 c_4 b_1$$
$$+ 2 c_1 c_3^2 - b_0 b_2^3 c_1 + 2 b_2^2 c_1 c_2 + b_0^2 b_2^2 c_3 - 4 b_2^2 c_0 c_3 + 4 b_0 b_2 c_1 c_4 - 8 c_1 c_2 c_4 - 4 b_0^2 c_3 c_4 + 16 c_0 c_3 c_4,$$

$$c_3^2 b_0^2 - b_1 b_2 c_3 b_0^2 + b_1^2 c_4 b_0^2 + b_1 b_2^2 c_1 b_0 - 4 b_1 c_1 c_4 b_0 - b_2^2 c_1^2 - 4 c_0 c_3^2 - b_1^2 b_2^2 c_0 + 4 b_1 b_2 c_0 c_3 + 4 c_1^2 c_4,$$

$$c_3^3 b_0^3 + 8 c_1 c_4^2 b_0^3 - 4 c_2 c_3 c_4 b_0^3 + b_2 c_1 c_3^2 b_0^2 - b_1 c_2 c_3^2 b_0^2 - 16 b_1 c_0 c_4^2 b_0^2 + 4 b_1 c_2^2 c_4 b_0^2 - 4 b_2 c_1 c_2 c_4 b_0^2 + 8 b_2 c_0 c_3 c_4 b_0^2$$
$$- 2 b_1 c_1 c_3 c_4 b_0^2 - 6 b_1 b_2 c_0 c_3^2 b_0 + b_1^2 c_1 c_3^2 b_0 - b_2^2 c_1^2 c_3 b_0 + 4 b_2^2 c_0 c_2 c_3 b_0 + 6 b_1 b_2 c_1^2 c_4 b_0 - 8 b_2^2 c_0 c_1 c_4 b_0$$
$$- 4 b_1^2 c_1 c_2 c_4 b_0 + 8 b_1^2 c_0 c_3 c_4 b_0 - b_2^3 c_1^3 - 4 b_1 b_2^2 c_0 c_2^2 - b_1^3 c_0 c_3^2 + b_1 b_2^2 c_1^2 c_2 + 4 b_2^3 c_0 c_1 c_2 - 8 b_2^3 c_0^2 c_3$$
$$- b_1^2 b_2 c_1^2 c_3 + 2 b_1 b_2^2 c_0 c_1 c_3 + 4 b_1^2 b_2 c_0 c_2 c_3 + 16 b_1 b_2^2 c_0^2 c_4 + b_1^3 c_1^2 c_4 - 8 b_1^2 b_2 c_0 c_1 c_4,$$

$$- b_2 c_3 b_0^3 + 2 b_1 c_4 b_0^3 + b_2^2 c_1 b_0^2 - b_1 b_2 c_2 b_0^2 + 2 c_2 c_3 b_0^2 - 4 c_1 c_4 b_0^2 + b_1^2 b_2 c_1 b_0 + 4 b_2 c_0 c_3 b_0 - 2 b_1 c_1 c_3 b_0$$
$$- 8 b_1 c_0 c_4 b_0 - b_1 b_2 c_1^2 - b_1^3 b_2 c_0 - 4 b_2^2 c_0 c_1 + 4 b_1 b_2 c_0 c_2 + 2 c_1^2 c_3 + 2 b_1^2 c_0 c_3 - 8 c_0 c_2 c_3 + 16 c_0 c_1 c_4,$$

$$- c_0 c_3 b_1^4 + 2 b_2 c_0 c_2 b_1^3 + b_0 c_1 c_3 b_1^3 + 4 b_0 c_0 c_4 b_1^3 - 2 b_0 b_2 c_1 c_2 b_1^2 - c_1^2 c_3 b_1^2 - 2 b_0 b_2 c_0 c_3 b_1^2 - b_0^2 c_2 c_3 b_1^2 + 4 c_0 c_2 c_3 b_1^2$$
$$- 4 b_0^2 c_1 c_4 b_1^2 - 8 c_0 c_1 c_4 b_1^2 + 2 b_0^2 b_2 c_2^2 b_1 - 8 b_2 c_0 c_2^2 b_1 + b_0^3 c_3^2 b_1 - 4 b_0 c_0 c_3^2 b_1 + 2 b_2 c_1^2 c_2 b_1 + 3 b_0^2 b_2 c_1 c_3 b_1$$
$$- 4 b_2 c_0 c_1 c_3 b_1 + 32 b_2 c_0^2 c_4 b_1 + 12 b_0 c_1^2 c_4 b_1 - 8 b_0^2 b_2 c_0 c_4 b_1 - 2 b_0^2 c_1 c_3^2 + 8 c_0 c_1 c_3^2 - 2 b_0^2 b_2^2 c_1 c_2$$
$$+ 8 b_2^2 c_0 c_1 c_2 - 16 b_2^2 c_0^2 c_3 - 2 b_0 b_2 c_1^2 c_3 + 4 b_0^2 b_2^2 c_0 c_3 - 2 b_0^3 b_2 c_2 c_3 + 8 b_0 b_2 c_0 c_2 c_3 - 8 c_1^3 c_4 + 4 b_0^3 b_2 c_1 c_4$$
$$- 16 b_0 b_2 c_0 c_1 c_4,$$

$$- b_2 c_0 b_1^4 + b_0 b_2 c_1 b_1^3 + 2 c_0 c_3 b_1^3 - b_2 c_1^2 b_1^2 + 2 b_0 b_2^2 c_0 b_1^2 - b_0^2 b_2 c_2 b_1^2 + 4 b_2 c_0 c_2 b_1^2 - 2 b_0 c_1 c_3 b_1^2 - 8 b_0 c_0 c_4 b_1^2$$
$$- b_0^2 b_2^2 c_1 b_1 - 4 b_2^2 c_0 c_1 b_1 + 2 c_1^2 c_3 b_1 + b_0^3 b_2 c_3 b_1 - 4 b_0 b_2 c_0 c_3 b_1 + 2 b_0^2 c_2 c_3 b_1 - 8 c_0 c_2 c_3 b_1 + 4 b_0^3 c_1 c_4 b_1$$
$$+ 16 c_0 c_1 c_4 b_1 + 2 b_0 b_2^2 c_1^2 - 2 b_0^3 c_3^2 + 8 b_0 c_0 c_3^2 - 8 b_0 c_1^2 c_4,$$

$$- c_0 b_1^5 + b_0 c_1 b_1^4 - c_1^2 b_1^3 + 2 b_0 b_2 c_0 b_1^3 - b_0^2 c_2 b_1^3 + 8 c_0 c_2 b_1^3 - b_0^2 b_2 c_1 b_1^2 - 8 b_2 c_0 c_1 b_1^2 - 4 b_0 c_1 c_2 b_1^2 + b_0^3 c_3 b_1^2$$
$$- 8 b_0 c_0 c_3 b_1^2 + 6 b_0 b_2 c_1^2 b_1 + 4 b_0^2 c_2^2 b_1 - 16 c_0 c_2^2 b_1 + 4 c_1^2 c_2 b_1 + 2 b_0^2 c_1 c_3 b_1 + 8 c_0 c_1 c_3 b_1 + 64 c_0^2 c_4 b_1$$
$$- 16 b_0^2 c_0 c_4 b_1 - 4 b_2 c_1^3 - 4 b_0^2 b_2 c_1 c_2 + 16 b_2 c_0 c_1 c_2 - 32 b_2 c_0^2 c_3 - 4 b_0 c_1^2 c_3 + 8 b_0^2 b_2 c_0 c_3 - 4 b_0^3 c_2 c_3$$
$$+ 16 b_0 c_0 c_2 c_3 + 8 b_0^3 c_1 c_4 - 32 b_0 c_0 c_1 c_4,$$

$$4 c_4 b_0^4 - 4 b_2 c_2 b_0^3 + b_1 c_3 b_0^3 + 4 c_2^2 b_0^2 + 4 b_2^2 c_0 b_0^2 + 3 b_1 b_2 c_1 b_0^2 - b_1^2 c_2 b_0^2 - 2 c_1 c_3 b_0^2 - 32 c_0 c_4 b_0^2 - 2 b_2 c_1^2 b_0$$
$$- 2 b_1^2 b_2 c_0 b_0 + b_1^3 c_1 b_0 + 16 b_2 c_0 c_2 b_0 - 4 b_1 c_1 c_2 b_0 - 4 b_1 c_0 c_3 b_0 - 16 b_2^2 c_0^2 - b_1^2 c_1^2 - 16 c_0 c_2^2 - b_1^4 c_0$$
$$- 4 b_1 b_2 c_0 c_1 + 4 c_1^2 c_2 + 8 b_1^2 c_0 c_2 + 8 c_0 c_1 c_3 + 64 c_0^2 c_4,$$

$$c_3 b_0^4 - b_2 c_1 b_0^3 - b_1 c_2 b_0^3 + 2 b_1 b_2 c_0 b_0^2 + b_1^2 c_1 b_0^2 + 2 c_1 c_2 b_0^2 - 8 c_0 c_3 b_0^2 - 3 b_1 c_1^2 b_0 - b_1^3 c_0 b_0 + 4 b_2 c_0 c_1 b_0$$
$$+ 4 b_1 c_0 c_2 b_0 + 2 c_1^3 - 8 b_1 b_2 c_0^2 + 2 b_1^2 c_0 c_1 - 8 c_0 c_1 c_2 + 16 c_0^2 c_3) \tag{B.2.2}$$

B.3   Scalings and divisor classes

Here we present the scaling relations for the coordinates in the two geometries discussed in chapter 4 and 5. For the bisection model described by the hypersurface equation (4.6.13) (also (5.2.1)) the toric coordinates scale as presented in Table B.3.1. For the model with an extra section with hypersurface equation (4.6.1) (and in (5.3.1)) the scaling relations are collected in Table B.3.2.

	u	v	w	e_0	e_1	e_2	e_3	e_4
$\bar{\mathcal{K}}$	$\cdot$	1	2	$\cdot$	$\cdot$	$\cdot$	$\cdot$	$\cdot$
$[b_2]$	$\cdot$	-1	-1	$\cdot$	$\cdot$	$\cdot$	$\cdot$	$\cdot$
θ	$\cdot$	$\cdot$	$\cdot$	1	$\cdot$	$\cdot$	$\cdot$	$\cdot$
U	1	1	2	$\cdot$	$\cdot$	$\cdot$	$\cdot$	$\cdot$
E_1	$\cdot$	$\cdot$	-1	-1	1	$\cdot$	$\cdot$	$\cdot$
E_2	$\cdot$	-1	-2	-1	$\cdot$	1	$\cdot$	$\cdot$
E_3	$\cdot$	-2	-2	-1	$\cdot$	$\cdot$	1	$\cdot$
E_4	$\cdot$	-1	-1	-1	$\cdot$	$\cdot$	$\cdot$	1

Table B.3.1: *Scaling relations for the toric coordinates in the $\mathbb{Z}_2$-model.*

	u	v	w	s	e_0	e_1	e_2	e_3	e_4
$\bar{\mathcal{K}}$	·	1	2	·	·	·	·	·	·
$[b_2]$	·	−1	−1	·	·	·	·	·	·
θ	·	·	·	·	1	·	·	·	·
U	1	1	2	·	·	·	·	·	·
S	·	1	1	1	·	·	·	·	·
E_1	·	·	−1	·	−1	1	·	·	·
E_2	·	−1	−2	·	−1	·	1	·	·
E_3	·	−2	−2	·	−1	·	·	1	·
E_4	·	−1	−1	·	−1	·	·	·	1

Table B.3.2: *Scaling relations for the toric coordinates in the $U(1)$-model.*

B.4 Blowing up the Matter Locus

As outlined in section 4.5.1, one way to identify the torsional 2-cycles in a smooth geometry is by blowing up the C_2 locus in the base of the fibration [125]. The resulting space is birationally equivalent to the original one and therefore allows one to deduce the torsional cohomology also for the latter [29]. In this appendix we give the technical details of this procedure.

Let us begin with a simple example which we will build up to the final result. Consider the $U(1)$-restricted Tate model presented in [77] given by the hypersurface P_T in $\mathbb{P}_{231}$

$$P_T = y^2 + a_1 xyz + a_3 yz^3 - x^3 - a_2 x^2 z^2 - a_4 xz^4 = 0 \,. \tag{B.4.1}$$

This fibration is a specialization of the Weierstrass model (4.5.3) with no double-charged singlets. It exhibits two independent sections and a set of points with conifold singularities T_2 where matter with charge one with respect to the associated $U(1)$ symmetry resides,

$$T_2 \; : \; a_3 = a_4 = 0 \,. \tag{B.4.2}$$

One can resolve these singularities through a blow-up in the ambient variety, involving the fibre co-ordinates by sending $(x, y) \to (xs, ys)$ and imposing the scaling relation $(x, y, s) \sim \left(\lambda^{-1}x, \lambda^{-1}y, \lambda s\right)$. The blowup divisor $S : \; s = 0$ acts as a rational section, in addition to the zero section $Z : \; z = 0$. The resulting manifold is smooth and over the locus $a_3 = a_4 = 0$ the fibre is of type I_2.

Let us now consider starting from the singular fibration but instead of resolving we blow up the base over the locus T_2 by sending $(a_3, a_4) \to (a_3 t, a_4 t)$ and introducing the relation $(a_3, a_4, t) \sim \left(\lambda^{-1}a_3, \lambda^{-1}a_4, \lambda t\right)$. The resulting geometry now has an $SU(2)$ singularity over the exceptional divisor

$$T \; : \; t = 0. \tag{B.4.3}$$

Note that after this replacement t does not factor from P_T, which means that the proper transform of the hypersurface equation has non-vanishing first Chern class, i.e. is not Calabi-Yau any more. Nonetheless the space is Kähler and we can proceed, though dynamically this configuration is unlikely to be stable due to the absence of supersymmetry. It merely serves as a birational auxiliary geometry which allows us to identify the torsional cycles. We can resolve the $SU(2)$ singularity in the standard way of resolving non-abelian singularities over divisors by performing a second blow-up involving now the fibre coordinates $(x, y, t) \to (xs, ys, ts)$ and identifying $(x, y, t, s) \sim \left(\lambda^{-1}x, \lambda^{-1}y, \lambda^{-1}t, \lambda s\right)$. The resolved fibration takes the form

$$\hat{P}_T = y^2 + a_1 xyz + a_3 tyz^3 - sx^3 - a_2 x^2 z^2 - a_4 txz^4 = 0 \,. \tag{B.4.4}$$

This is a smooth space. The fibre over a generic point on T is of type I_2 with the two components

$$
\begin{aligned}
A_1 &: T \cap \hat{P}_T \cap \{C_{\text{base}}\} \ , \\
B_1 &: S \cap \hat{P}_T \cap \{C_{\text{base}}\} \ ,
\end{aligned}
\tag{B.4.5}
$$

where $\{C_{\text{base}}\}$ is some curve in the base intersecting intersecting T at a generic point. These two components intersect at two points.

Over two sets of special points along the divisor $t = 0$ in the base the fibre changes. The first set D_2 corresponds to the locus $D_2 : \{t = 0\} \cap \{4a_2 + a_1^2 = 0\}$. Over this locus the fibre becomes of Kodaira type III. There is no symmetry enhancement or matter states associated to this locus. The second more interesting locus is given by $\hat{C}_2 : \{t = 0\} \cap \{a_2 a_3^2 - a_1 a_3 a_4 - a_4^2 = 0\}$. Over this locus of points the B components of the fibre splits into 2 components

$$
B_1|_{\hat{C}_2} \to B_{1,1} + B_{1,2}.
\tag{B.4.6}
$$

The fibre becomes type I_3 which signals the presence of matter transforming in the fundamental of $SU(2)$.

There are two important ways that this toy example differs from the singular Weierstraß model we are interested in. The first, quantitative, difference is that the matter point locus T_2 in the example is very simple while the corresponding locus C_2 in the full model (4.5.3) is very complicated. This makes performing the blow-up in the base, though conceptually equivalent, technically difficult. We will return to this later. The second, qualitative, difference is that in the full model there are two rather than one matter loci, C_1 and C_2. We can proceed by blowing up $C_2 \to T$ as in the example above. However the key point is that the resolution $(x, y, t) \to (xs, ys, ts)$ will only resolve the $SU(2)$ singularity over T but not the singularity of C_1.

We will therefore require a further resolution. Importantly this will introduce another independent homology class for the components of the fibre independent of the Cartan of the $SU(2)$. Therefore now in the Kähler cone we will have an additional degeneration possibility where the C_1 locus becomes singular while the T divisor remains smooth. In this limit we can then deform the C_1 locus and reach the smooth geometry with the $\mathbb{Z}_2$ discrete symmetry and torsion. Alternatively we can perform the deformation first and then blow up the base in the deformed model, since the blow-up is localised away from the deformation locus this should lead to the same result.

In the main text we have identified the torsional 2-cycles by studying the intersection numbers of the sections with the resolved Weierstraß model. This is equivalent to looking at their $U(1)$ charges. The intersection of the section with the components of the fibre over the C_1 locus remain unchanged by a blow-up in the base over the C_2 locus. Indeed it is clear that the component B_1 of the fibre over C_1 which shrinks and is then deformed must have vanishing intersection with U, since this remains as the zero section after the deformation; furthermore since the intersection with $S - U$ is the 6-dimensional $U(1)$ charge (of the massless Higgs), it is independentof the resolution. Therefore it must be that the shrinking component intersects S with $+2$ and so the argument for the existence of the 3-chains goes through for the blown-up base geometry as long as we can identify components of the fibre which have the same intersection numbers as B_1 in table 4.3.1. Since this would mean they cannot intersect the Cartan of the $SU(2)$ they can only arise as combinations of the fibre components over the analogue of the matter points $\hat{C}_2$ in the full Weierstrass model P_W. They therefore will induce the 3-chains as described in the main text.

Let us now turn to applying this procedure to the full model P_W (4.5.3). As analysed in [10,70,84], the single-charged locus C_2 is given by a complicated prime ideal. We shall use the particular form

given in [84] where it is given by the (non-transversal) intersection of the 7 polynomials

$$
\begin{aligned}
H_1 =& e_1 b^4 - 2 e_2 e_3 b^2 + 2 e_3^3, \\
H_2 =& 2 e_0 b^4 - 2 e_2^2 b^2 + e_1 e_3 b^2 + 2 e_2 e_3^2, \\
H_3 =& - e_1 e_2 b^2 + 2 e_0 e_3 b^2 + e_1 e_3^2, \\
H_4 =& - e_1^2 b^2 + 4 e_0 e_3^2, \\
H_5 =& 2 e_0 e_1 b^2 + e_1^2 e_3 - 4 e_0 e_2 e_3, \\
H_6 =& 4 e_0^2 b^2 + e_1^2 e_2 - 4 e_0 e_2^2 + 2 e_0 e_1 e_3, \\
H_7 =& e_1^3 - 4 e_0 e_1 e_2 + 8 e_0^2 e_3 \, .
\end{aligned}
\tag{B.4.7}
$$

Here the e_i are as defined below (4.5.3) and we are working with the singular geometry corresponding to $c_4 \equiv 0$, which implies $e_4 = \frac{1}{4} b^2$ (after relabeling $b_2 \to b$). To blow up the zero-locus of this ideal we can introduce new coordinates f_i and t and write the blown-up space as the variety corresponding to the vanishing locus of the ideal

$$
(P_W, f_1 t - H_1, \dots, f_7 t - H_7). \tag{B.4.8}
$$

We further impose the scaling relation associated to the new coordinate t

$$
(f_1, f_2, \dots, t) \sim \left(\lambda f_1, \lambda f_2, \dots, \lambda^{-1} t \right) \, . \tag{B.4.9}
$$

We can then resolve the $SU(2)$ singularity over $T: \; t = 0$ as before by $(x, y, t) \to (xr, yr, tr)$ and by imposing $(x, y, t, r) \sim \left(\lambda^{-1} x, \lambda^{-1} y, \lambda^{-1} t, \lambda r \right)$. The resulting space is now smooth over T with an I_2 fibre over a generic point, while over certain points in T, denoted $\hat{C}_2$, the fibre will factorise to an I_3. The exceptional divisor $R: \; r = 0$ forms the Cartan of the $SU(2)$ on the Coulomb branch.

We can perform this blow-up and resolution in the deformed geometry P_W which directly gives the final smooth space with torsion cycles. This simply amounts to dropping the restriction $e_4 = \frac{1}{4} b^2$. However to identify the torsional 2-cycles using the arguments presented in the main text we need to work with the resolved geometry over C_2. Since the blow-up in the base is localised away from the locus C_1, it does not affect this locus. The crucial information is the intersection numbers of the sections with the fibre components over the points $\hat{C}_2$. These will allow us to identify the 3-chains that will, after the deformation, become the chains with a boundary of twice the torsional two-cycles.

In principle this analysis can be done by using the computer package `Singular` [119], leading to a globally valid blowup and resolution of the singularities over C_2. However, it is more instructive to perform a local analysis of the fibre over the C_2 which will be sufficient to extract the relevant intersection numbers with the sections. Our approach is to consider the locus given by $H_6 = H_7 = 0$. This can be shown, by a prime decomposition, to be composed of the locus C_2 and the separate set of points $e_0 = e_1 = 0$. We will ignore these points in our local analysis though they would lead to $SU(2)$ singularities over points in the base after the blow-up. Indeed since the set of points C_2 does not intersect the curve $e_0 = 0$ [84], we can restrict our attention to the subset $e_0 \neq 0$, where in particular we can allow for functions meromorphic in e_0. We can now explicitly solve the two equations

$$
f_6 t - H_6 = 0 \, , \quad f_7 t - H_7 = 0 \, , \tag{B.4.10}
$$

which gives

$$
\begin{aligned}
e_3 =& \frac{- e_1^3 + 4 e_0 e_1 e_2 + f_7 t}{8 e_0^2}, \\
b^2 =& \frac{e_1^4 - 8 e_0 e_1^2 e_2 + 16 e_0^2 e_2^2 + 4 e_0 f_6 t - e_1 f_7 t}{16 e_0^3} \, .
\end{aligned}
\tag{B.4.11}
$$

Since only b^2 appears in P_W we can plug this back into the equation to analyse the fibre structure explicitly. This solution is valid away from $e_0 = 0$ and also away from $b = 0$, where the coordinate change $(e_3, b) \to (f_6, f_7)$ degenerates. We now redefine

$$x \to x + \frac{\left(-3e_1^2 + 8e_0e_2\right) z^2}{12e_0} \tag{B.4.12}$$

to bring the $SU(2)$ singularity over T to $x = y = 0$. Finally we resolve it by introducing $R : r = 0$ as $(x, y, t) \to (xr, yr, tr)$. There are then two fibre components over the exceptional divisor in the base,

$$\begin{aligned} A_1 &: \quad T \cap \hat{P}_W \cap \{C_{\text{base}}\} \;, \\ B_1 &: \quad R \cap \hat{P}_W \cap \{C_{\text{base}}\} \;. \end{aligned} \tag{B.4.13}$$

The interesting I_3 locus can be identified from the discriminant to lie on

$$\begin{aligned} \hat{C}_2 \;: \quad &\left\{-32e_2f_7^2 - 16e_0^2f_6^2 + 24e_0e_1f_6f_7 + 3e_1^2f_7^2 = 0\right\} \\ &\qquad\qquad\qquad\qquad \cap \{t = 0\} \end{aligned} \tag{B.4.14}$$

(viewed as a locus on the base), and over this locus the fibre component B_1 splits into components

$$\begin{aligned} B_{1,1} &: \quad \{8f_7y - 8f_6xz - 6e_1f_7xz - f_7^2tz^3 = 0\} \cap R \cap P_{\hat{C}_2} \;, \\ B_{1,2} &: \quad \{8f_7y + 8f_6xz + 6e_1f_7xz + f_7^2tz^3 = 0\} \cap R \cap P_{\hat{C}_2} \end{aligned}$$

with $P_{\hat{C}_2}$ the divisor associated to the first polynomial in (B.4.14). Note that we have set $e_0 = -1$ in the above for simplicity, and have given only the important component of the intersecting equations defining the fibre. The other component of the fibre over these points is

$$\begin{aligned} A_1 &: \quad \{16rf_2^2x^3 - 16f_2^2y^2 + 16f_1^2x^2z^2 + 24e_1f_6f_7x^2z^2 \\ &\qquad\qquad +9e_1^2f_7^2x^2z^2 = 0\} \cap T \cap P_{\hat{C}_2} \;. \end{aligned}$$

We can now intersect these components with the proper transform of the sections $U : z = 0$ and $S : [x, y, z] = \left[e_3^2 - \frac{2}{3}b^2e_2, -e_3^3 + b^2e_2e_3 - \frac{1}{2}b^4e_1, ib\right]$ [18], given here on the Weierstraß model before blowup and resolution, which after some calculation eventually yields the intersection numbers

$$\begin{aligned} U \cdot A_1 &= 1 \;, & U \cdot B_{1,1} &= 0 \;, & U \cdot B_{1,2} &= 0 \;, \\ S \cdot A_1 &= 0 \;, & S \cdot B_{1,1} &= 1 \;, & S \cdot B_{1,2} &= 0 \;. \\ R \cdot A_1 &= 2 \;, & R \cdot B_{1,1} &= -1 \;, & R \cdot B_{1,2} &= -1 \;. \end{aligned}$$

This identifies the component of the fibre which becomes the torsional 2-cycle after the deformation as $B_{1,1} - B_{1,2}$.

Bibliography

[1] J. Polchinski, *String theory. Vol. 1: An introduction to the bosonic string*, Cambridge University Press, 2007, ISBN 9780511252273, 9780521672276, 9780521633031.

[2] J. Polchinski, *String theory. Vol. 2: Superstring theory and beyond*, Cambridge University Press, 2007, ISBN 9780511252280, 9780521633048, 9780521672283.

[3] M. B. Green, J. H. Schwarz and E. Witten, *Superstring Theory. Vol. 1: Introduction*, 1988.

[4] M. B. Green, J. H. Schwarz and E. Witten, *Superstring Theory. Vol. 2: Loop Amplitudes, Anomalies and Phenomenology*, 1988.

[5] R. Blumenhagen, D. Lust and S. Theisen, *Basic concepts of string theory*, Heidelberg, Germany: Springer, 2013.

[6] C. Vafa, *Evidence for F-Theory*, Nucl. Phys. **B469** (1996) 403–418, [hep-th/9602022].

[7] D. R. Morrison and C. Vafa, *Compactifications of F theory on Calabi-Yau threefolds. 1*, Nucl.Phys. **B473** (1996) 74–92, [hep-th/9602114].

[8] D. R. Morrison and C. Vafa, *Compactifications of F theory on Calabi-Yau threefolds. 2.*, Nucl.Phys. **B476** (1996) 437–469, [hep-th/9603161].

[9] C. Mayrhofer, D. R. Morrison, O. Till and T. Weigand, *Mordell-Weil Torsion and the Global Structure of Gauge Groups in F-theory*, JHEP **10** (2014) 16, [1405.3656].

[10] C. Mayrhofer, E. Palti, O. Till and T. Weigand, *Discrete Gauge Symmetries by Higgsing in four-dimensional F-Theory Compactifications*, JHEP **12** (2014) 068, [1408.6831].

[11] C. Mayrhofer, E. Palti, O. Till and T. Weigand, *On Discrete Symmetries and Torsion Homology in F-Theory*, JHEP **06** (2015) 029, [1410.7814].

[12] L. Lin, C. Mayrhofer, O. Till and T. Weigand, *Fluxes in F-theory Compactifications on Genus-One Fibrations*, JHEP **01** (2016) 098, [1508.00162].

[13] T. Weigand, *Lectures on F-theory compactifications and model building*, Class.Quant.Grav. **27** (2010) 214004, [1009.3497].

[14] S. Weinberg, *The Quantum theory of fields. Vol. 1: Foundations*, Cambridge University Press, 2005, ISBN 9780521670531, 9780511252044.

[15] F. Denef, *Les Houches Lectures on Constructing String Vacua* pp. 483–610, [0803.1194].

[16] A. Maharana and E. Palti, *Models of Particle Physics from Type IIB String Theory and F-theory: A Review*, Int.J.Mod.Phys. **A28** (2013) 1330005, [1212.0555].

[17] J. H. Silverman, *The Arithmetic of Elliptic Curves*, Springer, 2nd edition, 2008.

[18] D. R. Morrison and D. S. Park, *F-Theory and the Mordell-Weil Group of Elliptically-Fibered Calabi-Yau Threefolds*, *JHEP* **1210** (2012) 128, [`1208.2695`].

[19] V. Bouchard and H. Skarke, *Affine Kac-Moody algebras, CHL strings and the classification of tops*, *Adv.Theor.Math.Phys.* **7** (2003) 205–232, [`hep-th/0303218`].

[20] V. Braun, T. W. Grimm and J. Keitel, *Geometric Engineering in Toric F-Theory and GUTs with U(1) Gauge Factors*, *JHEP* **1312** (2013) 069, [`1306.0577`].

[21] A. Grassi and V. Perduca, *Weierstrass models of elliptic toric K3 hypersurfaces and symplectic cuts* [`1201.0930`].

[22] S. Lang, *Fundamentals of Diophantine geometry*, Springer-Verlag, New York, 1983, xviii+370 pp.

[23] S. Lang and A. Néron, *Rational points of abelian varieties over function fields*, *Amer. J. Math.* **81** (1959) 95–118.

[24] K. Oguiso and T. Shioda, *The Mordell-Weil lattice of a rational elliptic surface*, *Comment. Math. Univ. St. Paul* **40** (1991) 83–99.

[25] R. Kloosterman, *On the classification of degree 1 elliptic threefolds with constant j-invariant*, *Illinois Journal of Math.* **55** (2011) 771–803.

[26] T. Shioda, *Mordell-Weil Lattices and Galois Representation. I*, *Proc. Japan Acad.* **A65** (1989) 268–271.

[27] R. Wazir, *Arithmetic on elliptic threefolds*, *Compos.Math.* **140** (2001) 567–580, [`math.NT/0112259`].

[28] D. S. Park, *Anomaly Equations and Intersection Theory*, *JHEP* **01** (2012) 093, [`1111.2351`].

[29] V. Braun and D. R. Morrison, *F-theory on Genus-One Fibrations*, *JHEP* **1408** (2014) 132, [`1401.7844`].

[30] A. Collinucci and R. Savelli, *F-theory on singular spaces* [`1410.4867`].

[31] S. Krause, C. Mayrhofer and T. Weigand, G_4 *flux, chiral matter and singularity resolution in F-theory compactifications*, *Nucl.Phys.* **B858** (2012) 1–47, [`1109.3454`].

[32] W. Barth, C. Peters and A. Van de Ven, *Compact Complex Surfaces*, Springer Verlag, Berlin, 1984.

[33] K. Kodaira, *On Compact Analytic Surfaces: II*, *Annals of Math.* **77**.

[34] P. S. Aspinwall, *K3 surfaces and string duality* pp. 421–540, [`hep-th/9611137`].

[35] D. A. Cox and S. Zucker, *Intersection Numbers of Sections of Elliptic Surfaces*, *Inv. Mathematicae* **53** (1979) 1–44.

[36] A. Sen, *Orientifold limit of F theory vacua*, *Phys.Rev.* **D55** (1997) 7345–7349, [`hep-th/9702165`].

[37] M. Esole and R. Savelli, *Tate Form and Weak Coupling Limits in F-theory*, *JHEP* **1306** (2013) 027, [`1209.1633`].

[38] A. Clingher, R. Donagi and M. Wijnholt, *The Sen Limit*, *Adv.Theor.Math.Phys.* **18** (2014) 613–658, [1212.4505].

[39] J. Halverson and D. R. Morrison, *The landscape of M-theory compactifications on seven-manifolds with G_2 holonomy*, *JHEP* **04** (2015) 047, [1412.4123].

[40] J. Halverson and D. R. Morrison, *On Gauge Enhancement and Singular Limits in G_2 Compactifications of M-theory* [1507.05965].

[41] A. P. Braun, *Tops as Building Blocks for G2 Manifolds* [1602.03521].

[42] R. Slansky, *Group Theory for Unified Model Building*, *Phys. Rept.* **79** (1981) 1–128.

[43] L. Martucci and T. Weigand, *Non-perturbative selection rules in F-theory* [1506.06764].

[44] K. Becker and M. Becker, *M theory on eight manifolds*, *Nucl.Phys.* **B477** (1996) 155–167, [hep-th/9605053].

[45] E. Witten, *On flux quantization in M theory and the effective action*, *J.Geom.Phys.* **22** (1997) 1–13, [hep-th/9609122].

[46] A. Collinucci and R. Savelli, *On Flux Quantization in F-Theory*, *JHEP* **1202** (2012) 015, [1011.6388].

[47] A. Collinucci and R. Savelli, *On Flux Quantization in F-Theory II: Unitary and Symplectic Gauge Groups*, *JHEP* **1208** (2012) 094, [1203.4542].

[48] S. Sethi, C. Vafa and E. Witten, *Constraints on low dimensional string compactifications*, *Nucl.Phys.* **B480** (1996) 213–224, [hep-th/9606122].

[49] K. Dasgupta, G. Rajesh and S. Sethi, *M theory, orientifolds and G - flux*, *JHEP* **9908** (1999) 023, [hep-th/9908088].

[50] T. W. Grimm, A. Kapfer and J. Keitel, *Effective action of 6D F-Theory with U(1) factors: Rational sections make Chern-Simons terms jump*, *JHEP* **1307** (2013) 115, [1305.1929].

[51] T. W. Grimm and A. Kapfer, *Anomaly Cancelation in Field Theory and F-theory on a Circle* [1502.05398].

[52] M. Cvetič, D. Klevers and H. Piragua, *F-Theory Compactifications with Multiple U(1)-Factors: Constructing Elliptic Fibrations with Rational Sections*, *JHEP* **1306** (2013) 067, [1303.6970].

[53] T. W. Grimm, *The N=1 effective action of F-theory compactifications*, *Nucl.Phys.* **B845** (2011) 48–92, [1008.4133].

[54] E. Witten, *Phase transitions in M theory and F theory*, *Nucl. Phys.* **B471** (1996) 195–216, [hep-th/9603150].

[55] S. H. Katz and C. Vafa, *Matter from geometry*, *Nucl.Phys.* **B497** (1997) 146–154, [hep-th/9606086].

[56] K. A. Intriligator, D. R. Morrison and N. Seiberg, *Five-dimensional supersymmetric gauge theories and degenerations of Calabi-Yau spaces*, *Nucl. Phys.* **B497** (1997) 56–100, [hep-th/9702198].

[57] P. S. Aspinwall, S. Katz and D. R. Morrison, *Lie Groups, Calabi–Yau Threefolds, and F-Theory*, *Adv. Theor. Math. Phys.* **4** (2000) 95–126, [hep-th/0002012].

[58] R. Donagi and M. Wijnholt, *Model Building with F-Theory*, *Adv.Theor.Math.Phys.* **15** (2011) 1237–1318, [0802.2969].

[59] A. P. Braun, A. Collinucci and R. Valandro, *G-flux in F-theory and algebraic cycles*, *Nucl.Phys.* **B856** (2012) 129–179, [1107.5337].

[60] J. Marsano and S. Schafer-Nameki, *Yukawas, G-flux, and Spectral Covers from Resolved Calabi-Yau's*, *JHEP* **11** (2011) 098, [1108.1794].

[61] T. W. Grimm and H. Hayashi, *F-theory fluxes, Chirality and Chern-Simons theories*, *JHEP* **1203** (2012) 027, [1111.1232].

[62] M. Cvetic, T. W. Grimm and D. Klevers, *Anomaly Cancellation And Abelian Gauge Symmetries In F-theory*, *JHEP* **02** (2013) 101, [1210.6034].

[63] M. Cvetič, A. Grassi, D. Klevers and H. Piragua, *Chiral Four-Dimensional F-Theory Compactifications With SU(5) and Multiple U(1)-Factors* [1306.3987].

[64] C. Beasley, J. J. Heckman and C. Vafa, *GUTs and Exceptional Branes in F-theory - II: Experimental Predictions*, *JHEP* **01** (2009) 059, [0806.0102].

[65] R. Donagi and M. Wijnholt, *Breaking GUT Groups in F-Theory*, *Adv.Theor.Math.Phys.* **15** (2011) 1523–1604, [0808.2223].

[66] O. Aharony, N. Seiberg and Y. Tachikawa, *Reading between the lines of four-dimensional gauge theories*, *JHEP* **1308** (2013) 115, [1305.0318].

[67] G. McCabe, *The Structure and Interpretation of the Standard Model*, Elsevier, 1st edition, 2007.

[68] J. C. Baez and J. Huerta, *The Algebra of Grand Unified Theories*, *Bull.Am.Math.Soc.* **47** (2010) 483–552, [0904.1556].

[69] P. S. Aspinwall and D. R. Morrison, *Nonsimply connected gauge groups and rational points on elliptic curves*, *JHEP* **9807** (1998) 012, [hep-th/9805206].

[70] D. Klevers, D. K. Mayorga Pena, P.-K. Oehlmann, H. Piragua and J. Reuter, *F-Theory on all Toric Hypersurface Fibrations and its Higgs Branches*, *JHEP* **01** (2015) 142, [1408.4808].

[71] P. Candelas, E. Perevalov and G. Rajesh, *Comments on A, B, C chains of heterotic and type II vacua*, *Nucl.Phys.* **B502** (1997) 594–612, [hep-th/9703148].

[72] M. Fukae, Y. Yamada and S.-K. Yang, *Mordell-Weil lattice via string junctions*, *Nucl.Phys.* **B572** (2000) 71–94, [hep-th/9909122].

[73] Z. Guralnik, *String junctions and nonsimply connected gauge groups*, *JHEP* **0107** (2001) 002, [hep-th/0102031].

[74] P. G. Camara, L. E. Ibanez and F. Marchesano, *RR photons*, *JHEP* **1109** (2011) 110, [1106.0060].

[75] D. Bump, *Lie Groups*, Springer, 2nd edition, 2013.

[76] P. DiFrancesco, P. Mathieu and D. Senechal, *Conformal Field Theory*, Springer, 1997.

[77] T. W. Grimm and T. Weigand, *On Abelian Gauge Symmetries and Proton Decay in Global F-theory GUTs*, *Phys.Rev.* **D82** (2010) 086009, [1006.0226].

[78] P. Berglund, A. Klemm, P. Mayr and S. Theisen, *On type IIB vacua with varying coupling constant*, *Nucl.Phys.* **B558** (1999) 178–204, [hep-th/9805189].

[79] M. Bershadsky, K. A. Intriligator, S. Kachru, D. R. Morrison, V. Sadov and C. Vafa, *Geometric singularities and enhanced gauge symmetries*, *Nucl.Phys.* **B481** (1996) 215–252, [hep-th/9605200].

[80] A. Grassi and D. R. Morrison, *Anomalies and the Euler characteristic of elliptic Calabi-Yau threefolds*, *Commun.Num.Theor.Phys.* **6** (2012) 51–127, [1109.0042].

[81] S. Katz, D. R. Morrison, S. Schäfer-Nameki and J. Sully, *Tate's algorithm and F-theory*, *JHEP* **1108** (2011) 094, [1106.3854].

[82] P. Candelas and A. Font, *Duality between the webs of heterotic and type II vacua*, *Nucl.Phys.* **B511** (1998) 295–325, [hep-th/9603170].

[83] J. Borchmann, C. Mayrhofer, E. Palti and T. Weigand, *SU(5) Tops with Multiple U(1)s in F-theory*, *Nucl.Phys.* **B882** (2014) 1–69, [1307.2902].

[84] D. R. Morrison and W. Taylor, *Sections, multisections, and U(1) fields in F-theory* [1404.1527].

[85] O. J. Ganor, D. R. Morrison and N. Seiberg, *Branes, Calabi-Yau spaces, and toroidal compactification of the N=1 six-dimensional E(8) theory*, *Nucl.Phys.* **B487** (1997) 93–127, [hep-th/9610251].

[86] R. Donagi and M. Wijnholt, *Higgs Bundles and UV Completion in F-Theory*, *Commun.Math.Phys.* **326** (2014) 287–327, [0904.1218].

[87] S. Krause, C. Mayrhofer and T. Weigand, *Gauge Fluxes in F-theory and Type IIB Orientifolds*, *JHEP* **1208** (2012) 119, [1202.3138].

[88] T. W. Grimm, M. Kerstan, E. Palti and T. Weigand, *Massive Abelian Gauge Symmetries and Fluxes in F-theory*, *JHEP* **1112** (2011) 004, [1107.3842].

[89] S. Krause, C. Mayrhofer and T. Weigand, *Gauge Fluxes in F-theory and Type IIB Orientifolds*, *JHEP* **1208** (2012) 119, [1202.3138].

[90] C. Mayrhofer, E. Palti and T. Weigand, *U(1) symmetries in F-theory GUTs with multiple sections*, *JHEP* **1303** (2013) 098, [1211.6742].

[91] V. Braun, T. W. Grimm and J. Keitel, *New Global F-theory GUTs with U(1) symmetries*, *JHEP* **1309** (2013) 154, [1302.1854].

[92] J. Borchmann, C. Mayrhofer, E. Palti and T. Weigand, *Elliptic fibrations for $SU(5) \times U(1) \times U(1)$ F-theory vacua*, *Phys.Rev.* **D88**, no. 4 (2013) 046005, [1303.5054].

[93] M. Cvetič, D. Klevers and H. Piragua, *F-Theory Compactifications with Multiple U(1)-Factors: Addendum*, *JHEP* **1312** (2013) 056, [1307.6425].

[94] M. Cvetič, D. Klevers, H. Piragua and P. Song, *Elliptic Fibrations with Rank Three Mordell-Weil Group: F-theory with U(1) x U(1) x U(1) Gauge Symmetry* [1310.0463].

[95] C. Mayrhofer, E. Palti and T. Weigand, *Hypercharge Flux in IIB and F-theory: Anomalies and Gauge Coupling Unification* [1303.3589].

[96] S. Krippendorf, D. K. Mayorga Pena, P.-K. Oehlmann and F. Ruehle, *Rational F-Theory GUTs without exotics*, *JHEP* **1407** (2014) 013, [1401.5084].

[97] A. P. Braun, A. Collinucci and R. Valandro, *The fate of U(1)'s at strong coupling in F-theory*, *JHEP* **07** (2014) 028, [1402.4054].

[98] G. Martini and W. Taylor, *6D F-theory models and elliptically fibered Calabi-Yau threefolds over semi-toric base surfaces* [1404.6300].

[99] N. C. Bizet, A. Klemm and D. V. Lopes, *Landscaping with fluxes and the E8 Yukawa Point in F-theory* [1404.7645].

[100] M. Kuntzler and S. Schäfer-Nameki, *Tate Trees for Elliptic Fibrations with Rank one Mordell-Weil group* [1406.5174].

[101] I. García-Etxebarria, T. W. Grimm and J. Keitel, *Yukawas and discrete symmetries in F-theory compactifications without section* [1408.6448].

[102] T. Banks and N. Seiberg, *Symmetries and Strings in Field Theory and Gravity*, *Phys.Rev.* **D83** (2011) 084019, [1011.5120].

[103] M. Berasaluce-Gonzalez, L. E. Ibanez, P. Soler and A. M. Uranga, *Discrete gauge symmetries in D-brane models*, *JHEP* **1112** (2011) 113, [1106.4169].

[104] L. Ibanez, A. Schellekens and A. Uranga, *Discrete Gauge Symmetries in Discrete MSSM-like Orientifolds*, *Nucl.Phys.* **B865** (2012) 509–540, [1205.5364].

[105] M. Berasaluce-Gonzalez, P. Camara, F. Marchesano, D. Regalado and A. Uranga, *Non-Abelian discrete gauge symmetries in 4d string models*, *JHEP* **1209** (2012) 059, [1206.2383].

[106] M. Berasaluce-Gonzalez, P. Camara, F. Marchesano and A. Uranga, *Zp charged branes in flux compactifications*, *JHEP* **1304** (2013) 138, [1211.5317].

[107] F. Marchesano, D. Regalado and L. Vazquez-Mercado, *Discrete flavor symmetries in D-brane models*, *JHEP* **1309** (2013) 028, [1306.1284].

[108] G. Honecker and W. Staessens, *To Tilt or Not To Tilt: Discrete Gauge Symmetries in Global Intersecting D-Brane Models*, *JHEP* **1310** (2013) 146, [1303.4415].

[109] *Antisymmetric tensor Z_p gauge symmetries in field theory and string theory*, *JHEP* **1401** (2014) 059, [1310.5582].

[110] I. Antoniadis and G. Leontaris, *Neutrino mass textures from F-theory*, *Eur.Phys.J.* **C73** (2013) 2670, [1308.1581].

[111] A. Karozas, S. F. King, G. K. Leontaris and A. Meadowcroft, *Discrete Family Symmetry from F-Theory GUTs* [1406.6290].

[112] E. I. Buchbinder, A. Constantin and A. Lukas, *The Moduli Space of Heterotic Line Bundle Models: a Case Study for the Tetra-Quadric*, *JHEP* **1403** (2014) 025, [1311.1941].

[113] E. I. Buchbinder, A. Constantin and A. Lukas, *A heterotic standard model with $B - L$ symmetry and a stable proton*, *JHEP* **1406** (2014) 100, [1404.2767].

[114] E. I. Buchbinder, A. Constantin and A. Lukas, *Non-generic Couplings in Supersymmetric Standard Models* [1409.2412].

[115] A. Grassi, J. Halverson and J. L. Shaneson, *Matter From Geometry Without Resolution* [`1306.1832`].

[116] A. Grassi, J. Halverson and J. L. Shaneson, *Non-Abelian Gauge Symmetry and the Higgs Mechanism in F-theory* [`1402.5962`].

[117] L. B. Anderson, I. Garcia-Etxebarria, T. W. Grimm and J. Keitel, *Physics of F-theory compactifications without section*, *JHEP* **12** (2014) 156, [`1406.5180`].

[118] L. Lin and T. Weigand, *Towards the Standard Model in F-theory*, *Fortsch.Phys.* **63**, no. 2 (2015) 55–104, [`1406.6071`].

[119] W. Decker, G.-M. Greuel, G. Pfister and H. Schoenemann, Singular *3-1-6 — A computer algebra system for polynomial computations*, `http://www.singular.uni-kl.de`, 2012.

[120] E. Witten, *Nonperturbative superpotentials in string theory*, *Nucl.Phys.* **B474** (1996) 343–360, [`hep-th/9604030`].

[121] V. Batyrev and M. Kreuzer, *Intergral cohomology and miror symmetry for Calabi-Yau 3-folds* [`alg-geom/0505432`].

[122] A. Strominger, *Massless black holes and conifolds in string theory*, *Nucl.Phys.* **B451** (1995) 96–108, [`hep-th/9504090`].

[123] B. R. Greene, D. R. Morrison and A. Strominger, *Black hole condensation and the unification of string vacua*, *Nucl.Phys.* **B451** (1995) 109–120, [`hep-th/9504145`].

[124] B. R. Greene, D. R. Morrison and C. Vafa, *A Geometric realization of confinement*, *Nucl.Phys.* **B481** (1996) 513–538, [`hep-th/9608039`].

[125] M. Dolgachev, I. Gross, *Elliptic Three-folds I: Ogg-Shafarevich Theory*, *J. Algebraic Geom.* **3** (1994) 38–80, [`alg-geom/9210009`].

[126] P. S. Aspinwall, D. R. Morrison and M. Gross, *Stable singularities in string theory*, *Commun.Math.Phys.* **178** (1996) 115–134, [`hep-th/9503208`].

[127] R. Tatar and W. Walters, *GUT theories from Calabi-Yau 4-folds with SO(10) Singularities*, *JHEP* **12** (2012) 092, [`1206.5090`].

[128] M. Kuntzler and S. Schafer-Nameki, *G-flux and Spectral Divisors*, *JHEP* **11** (2012) 025, [`1205.5688`].

[129] A. P. Braun, A. Collinucci and R. Valandro, *Hypercharge flux in F-theory and the stable Sen limit*, *JHEP* **1407** (2014) 121, [`1402.4096`].

[130] M. Bies, C. Mayrhofer, C. Pehle and T. Weigand, *Chow groups, Deligne cohomology and massless matter in F-theory* [`1402.5144`].

[131] A. P. Braun and T. Watari, *The Vertical, the Horizontal and the Rest: anatomy of the middle cohomology of Calabi-Yau fourfolds and F-theory applications*, *JHEP* **01** (2015) 047, [`1408.6167`].

[132] M. Cvetic, D. Klevers, D. K. M. Pena, P.-K. Oehlmann and J. Reuter, *Three-Family Particle Physics Models from Global F-theory Compactifications* [`1503.02068`].

[133] T. Watari, *Statistics of Flux Vacua for Particle Physics* [`1506.08433`].

[134] L. E. Ibanez, *More about discrete gauge anomalies*, *Nucl. Phys.* **B398** (1993) 301–318, [`hep-ph/9210211`].

[135] L. Martucci and T. Weigand, *Hidden Selection Rules, M5-instantons and Fluxes in F-theory* [`1507.06999`].

[136] K. Intriligator, H. Jockers, P. Mayr, D. R. Morrison and M. R. Plesser, *Conifold Transitions in M-theory on Calabi-Yau Fourfolds with Background Fluxes* [`1203.6662`].

[137] D. Gaiotto, M. Guica, L. Huang, A. Simons, A. Strominger et al., *D4-D0 branes on the quintic*, *JHEP* **0603** (2006) 019, [`hep-th/0509168`].

[138] D. S. Freed and E. Witten, *Anomalies in string theory with D-branes* [`hep-th/9907189`].

[139] R. Minasian and G. W. Moore, *K theory and Ramond-Ramond charge*, *JHEP* **11** (1997) 002, [`hep-th/9710230`].

[140] L. E. Ibanez and G. G. Ross, *Discrete gauge symmetry anomalies*, *Phys. Lett.* **B260** (1991) 291–295.

[141] M. Cvetič, R. Donagi, D. Klevers, H. Piragua and M. Poretschkin, *F-Theory Vacua with Z_3 Gauge Symmetry* [`1502.06953`].

[142] G. Curio and R. Y. Donagi, *Moduli in N=1 heterotic / F theory duality*, *Nucl.Phys.* **B518** (1998) 603–631, [`hep-th/9801057`].

[143] L. B. Anderson, J. J. Heckman and S. Katz, *T-Branes and Geometry* [`1310.1931`].

[144] V. Braun, T. W. Grimm and J. Keitel, *Complete Intersection Fibers in F-Theory*, *JHEP* **03** (2015) 125, [`1411.2615`]..